DISSERTATION

TRANSITION-METAL NANOCLUSTERS: FUNDAMENTAL STUDIES OF THE FACTORS CONTROLLING FORMATION, STABILIZATION, AND SUBSEQUENT CATALYTIC ACTIVITY

Submitted by

Lisa Starkey Ott

Department of Chemistry

In partial fulfillment of the requirements

For the Degree of Doctorate of Philosophy

Colorado State University

Fort Collins, Colorado

Fall 2006

COLORADO STATE UNIVERSITY

August 15, 2006

WE HEREBY RECOMMEND THAT THE DISSERTATION PREPARED UNDER OUR SUPERVISION BY LISA STARKEY OTT ENTITLED "TRANSITION-METAL NANOCLUSTERS: FUNDAMENTAL STUDIES OF THE FACTORS CONTROLLING FORMATION, STABILIZATION, AND SUBSEQUENT CATALYTIC ACTIVITY" BE ACCEPTED AS FULFILLING IN PART THE REQUIREMENTS FOR THE DEGREE OF DOCTOR OF PHILOSOPHY.

Committee on Graduate Work

Eugene Y.-X. Chen

Bruce A. Parkinson

Dawn Rickey

Laurence Delfiore

Richard G. Finke / Advisor

Anthony K. Rappe / Department Head / Director

ABSTRACT OF DISSERTATION

TRANSITION-METAL NANOCLUSTERS: FUNDAMENTAL STUDIES OF THE FACTORS CONTROLLING FORMATION, STABILIZATION, AND SUBSEQUENT CATALYTIC ACTIVITY

Following a critical review of the relevant nanocluster stabilization literature, the research presented herein primarily studies prototype $Ir(0)_n$ nanoclusters, including: (i) an evaluation of nanoclusters putatively stabilized by solvents plus the effects of weakly coordinating anions, (ii) an evaluation of five common polymeric nanocluster stabilizers, (iii) the first explicity study of the halide series for their individual efficacies in the formation and stabiliztion of nanoclusters, (iv) an investigation into the true source of nanocluster stabilization in imidazolium-based ionic liquids, and (v) a demonstration that added imidazolium-based ionic liquids serve to poison catalytically active $Ir(0)_n$ nanoclusters in the test reaction of acetone hydrogenation at room temperature and mild H_2 pressure.

The broad focus of this dissertation concerns the formation and stabilization of transition-metal nanocluster, specifically Ir nanoclusters. The extant literature in the area of transition-metal nanocluster stabilizers is voluminous and in general not to the level of

precision that modern science requires. The emphasis on compositionally well-defined nanoclusters and careful studies which follow aim to resolve some of the confusion in the nanocluster stabilization literature. Four detailed investigations on claimed stabilizers—solvents, polymers, halides, and imidazolium-based ionic liquids—have been performed with an emphasis on the formation of multiple alternative hypotheses as the most efficient method for scientific investigation. The approach of multiple alternative hypotheses led to the validation of the DLVO theory of colloidal stability for the specific case of BF_4^- in high dielectric constant solvents. Additionally, BF_4^- is shown to be important for nanocluster stabilization even in the presence of polymers or halides. The method of multiple alternative hypotheses also led to the identification of *N*-heterocyclic carbenes as the likely nanocluster stabilizer generated in ionic liquids. Finally, imidazolium-based ionic liquids have also been probed with regard to their role in catalytic acetone hydrogenation reactions, and it was found that these ionic liquids poison previously active $Ir(0)_n$ nanoclusters at room temperature and mild pressure.

Lisa Starkey Ott
Department of Chemistry
Colorado State University
Fort Collins, Colorado 80523
Fall 2006

DEDICATION

I owe thanks to the many people, friends and family alike, who have made this possible. I have been lucky to have such wonderful, supportive, encouraging people in my life–people that went running with me at 5am in the snow with negative wind chills, people that chased me around the house with a bowl of cookie dough, people who believed in me when I was a skinny cross country runner with a head full of curls and a mouthful of braces. The wagging tails and slurping tongues of Artemis and Rhea certainly helped me keep my attitude positive on the tough days, too. My undergraduate experience at Willamette University was another stroke of luck, for without the mentoring and inspiration of Drs. Chapple, Brink, and Williamson, I would not have written this lengthy document, nor would I be off to pursue a career in the world of chemistry. My advisor, Rick Finke, has strengthened me as a chemist in innumerable ways, and I have no doubt that I received the most thorough chemistry education CSU had to offer. Thank you.

Of course, none of this would have been possible without my parents, Jerry and Claudia, and my sister Talia. Mom and Dad, thank you for always believing in me and encouraging my harebrained ideas. I know that I have always had your unconditional love and support. Talia, thank you for not throwing me off a cliff for pestering you mercilessly as a child–I look forward to our continued adventures.

Finally, I couldn't have done this without my fabulous husband Radley. Among countless other things, thank you for listening to me, taking me camping when I didn't know I needed it, and encouraging me to keep at it. I love you babe.

TABLE OF CONTENTS

CHAPTER I

INTRODUCTION

The broad theme of this disseration is the formation and stabilization of transition-metal nanoclusters, with an emphasis on the resultant catalytic activity of the nanoclusters. This dissertation is written in the "journals-format" style (see Appendix A for a discussion of this type of dissertation), and is based on five separate publications and a published literature report. Chapter II is written in the format of Coordination Chemistry Reviews (Elsevier), Chapters III, IV, VI, and VII are written in a format set by the American Chemical Society, and Chapter V is written in a format set by American Scientific Publishers. A level of continuity is achieved herein by (i) this introduction, (ii) the use of bridging paragraphs at the beginning of each chapter, and (iii) a final summary chapter. A concise overview of each chapter's contents is presented below.

Chapter II is a review of the modes of nanocluster stabilization and the methods used to evaluate nanocluster stability. The discussion on different modes of nanocluster stabilizers is illustrated with specific literature examples, including an extensive table of the literature highlighting the need for compositionally well-defined nanocluster systems.

Chapter III is an investigation into putatively "solvent-only" stabilized nanoclusters. Although there are 12 literature reports of "solvent-only" stabilized nanoclusters, these nanoclusters are not expected to be stable based on the two established modes of nanocluster stabilization, electrostatic and steric. The data in Chapter III indicates that even weakly coordinating anions such as BF_4^- can contribute to the stability of $Ir(0)_n$ nanoclusters in high dielectric constant solvents.

Chapter IV examines five common polymeric nanocluster stabilizers, including the most common polymeric stabilizer poly(vinylpyrrolidone). Steric stabilization by these polymers was investigated with respect to both stability and catalytic activity, and compared to anionic stabilizers.

Chapter V presents an investigation into the stabilizing efficacy of halides, which are commonly present in nanocluster syntheses from metal halide precursors. In this Chapter, the transition-metal nanocluster formation and stabilization efficacy of the full halide series, F^-, Cl^-, Br^-, and I^-, is tested herein for the first time for prototype $Ir(0)_n$ nanoclusters. The importance of the traditionally weakly coordinating BF_4^- and high dielectric constant solvents is *again* illustrated.

Chapters VI and VII present investigations into the stability and catalytic activity of $Ir(0)_n$ nanoclusters in the presence of 1,3-substituted imidazolium-based ionic liquids (ILs). In Chapter V, the true mode of nanocluster stabilization in ILs is investigated using ^2H NMR and kinetic studies. In Chapter VI, the role of ILs in the test case of catalytic acetone hydrogenation is probed.

Chapter VIII is a concise summary of the material presented herein.

CHAPTER II

TRANSITION-METAL NANOCLUSTER STABILIZATION: A CRITICAL REVIEW OF RANKING METHODS AND PUTATIVE STABILIZERS

This dissertation chapter contains the manuscript of a review accepted for publication in *Coordination Chemistry Reviews*; a critical review of the transition-metal nanocluster stabilization literature is the essence of this chapter. First, a discussion of methods for evaluating the stabilization of nanoclusters is presented. Then, the common modes of nanocluster stabilization are presented, including an extensive table of relevant examples. The need for compositionally well-defined nanoclusters is emphasized.

This manuscript was prepared by LSO, with assistance and editing from RGF.

Abstract

A significant problem in the burgeoning transition-metal nanocluster literature is the myriad of proposed stabilizers, these stabilizers often being proposed without any firm evidence as to what the true stabilizers actually are. One objective of the present contribution is to provide a critical review of the methods and current rankings that are known of putative transition-metal nanocluster stabilizers, with a focus on catalytically active nanoclusters. Following a brief introduction to the literature methods for evaluating colloidal stabilizers (methods which are 41 and 105 years old), the need for modern methods to measure nanocluster stability via agglomeration kinetics is presented. Discussed next is the one presently available method for evaluating additives (i.e., putative stabilizers) for the formation and stabilization of transition-metal nanoclusters, the so-called 5 criteria method; this is followed by a scheme presenting established nanocluster stabilization modes. Next, a table of 48 prototype examples of established and novel nanocluster stabilizers is presented, followed by a discussion of each stabilization mode with selected, representative examples. One conclusion of this review is that it is clear that reliable, quantitative studies ranking claimed nanocluster stabilizers, and understanding how stabilizers work, are just now appearing. Note that given the lack of quantitative methods to measure stability and thereby rank stabilizers, it follows that much of the information regarding nanocluster stabilization is not on as firm a ground as is desired. Considerable additional effort will be required to achieve the overall goal of simplifying the "dizzying variety" of claimed nanocluster stabilizers into a preferred, small set of solvents and stabilizers yielding stable, high catalytic activity nanoclusters.

1. Introduction to Modern Transition–Metal Nanoclusters.

Transition metal nanoclusters are presently the focus of a great deal of scientific effort [1,2,3,4,5]. This focus derives in part from the sheer novelty of nanoclusters, plus the challenges of understanding their formation [6,7,8], stabilization [9,10,11], agglomeration [12], and size- and shape-dependent properties [13]. Nanoclusters also hold promise for several applications, including (but not limited to) catalysis [14,15,16,17] (including fuel cell catalysts [18]), quantum computers [19], photochemistry [20], optics [21], nanoelectronics [22,23], chemical sensors [24,25] and many others. In support of these claims, a recent book reviewing metal nanoclusters states, "Metal nanoparticles are certain to be the building blocks of the next generation of electronic, optoelectronic, and chemical sensing devices [26]." However, transition-metal nanoclusters remain only kinetically stable, the thermodynamic minimum being bulk metal in all cases to date. Consequently, substantial effort has been centered on *stabilizing* transition-metal nanoclusters, as long-term solution and solid-state (e.g., storage) stability is crucial if practical applications of metal nanoclusters are to be realized.

Modern transition metal nanoclusters are distinguished from traditional colloids by several important factors, initially summarized elsewhere [27]. Specifically, nanoclusters are expected to be smaller (1-10 nm) with near-monodisperse size distributions ($\leq$ 15%), while colloids are often >10 nm with much broader size distributions [27]. Additionally, modern nanoclusters should have reproducible syntheses leading to compositionally well-defined, isolable, and redissolvable nanoclusters [27]. In respect to these characteristics, classic colloids traditionally have less well-defined

compositions (frequently, their surfaces are contaminated with oxide/hydroxide, water, and halides) along with less reproducible syntheses [28]. Modern nanoclusters are typically prepared in dried organic solvents, while traditional colloids (e.g., gold colloids [29]) were prepared in water. (Many preparations of $Au(0)_n$ colloids in organic solvents now exist, however [30]).

There are numerous methods used to prepare transition-metal nanoclusters; synthetic methods have been reviewed recently for the interested reader [4,5,18]. Briefly, there are two general approaches for the formation of metal nanoclusters: a "top-down" and a "bottom-up" approach. The "top-down" approach involves the thermal, chemical, or mechanical [31,32,33,34] decomposition of a larger metal structure (typically either a metal powder [31] or a metal target [32,33,34]) into metal colloids or nanoclusters. For example, Klabunde et al. pioneered a top-down method of deposition of vaporized metal atoms from a solid metal source for the formation of weakly solvated transition-metal nanoclusters; this method, however, yields little size or compositional control [35,36,37]. The more common "bottom-up" approach involves generating the nanocluster by decomposition (usually reduction) of an organometallic precursor. A common preparation method involves reducing metal salts with a suitable reductant such as hydrogen gas or BH_4^- to form neutral $M(0)_n$ nanoclusters [18]. Some additional nanocluster synthesis methods include electrochemical reduction [38,39] or sonochemical decomposition of organometallic precursors [40,41]. Nanocluster *formation* and then *stabilization* are tightly interlinked issues as will become clear in what follows.[1]

[1] For instance, recent work on the preparation of stable $Pt(0)_n$ nanoclusters showed that what was thought to be a *stabilization* issue was in fact a *formation* issue [7]. In that work, ca. 100 experiments done under non-optimum, non-mechanism-based conditions yielded bulk metal. However, knowledge of the four-step mechanism (vide infra) of nanocluster formation and agglomeration, application of the optimized synthetic

2. Past and Present Methods for Ranking the Efficacy of Nanocluster Stabilizers

The stability of colloids has been of interest to researchers for over a century [42]. Most of the earlier work attempting to measure colloidal stability was performed on Au colloids, which have been known since the time of Faraday [43]. In 1901, the stability of Au colloids was studied as a function of added stabilizing agents including glues, gums, and starches [42]. Therein, Zsigmondy established the "gold number", the weight of an added protecting agent that is just incapable of preventing the agglomeration of 10 mL of a gold colloid within 3 minutes after the addition of 1 mL of 10% NaCl [42]. However, in the intervening 105 years, this method of assaying colloidal stability has had very little application; it is also of little relevance to metals other than gold and/or colloids prepared in solvents other than water—that is, to almost all modern transition-metal nanoclusters. Additionally, ill-defined colloidal protecting agents such as glues, gums, and starches are not currently employed, nor desired, for modern transition-metal nanoclusters where determining the composition of the resultant nanocluster is one key to understanding their stability [14]—a little accomplished key, *vide infra.*

A somewhat more recent, but still 41 year old, 1965 study also examined the stability and aggregation of Au colloids, this time by defining "protective value" as "the number of grams of a gold sol which are just protected by 1g of the protective agent against flocculation by 1% NaCl solution [44]." The protective value was evaluated for

---

conditions, and the key solvent change from the low dielectric constant solvent acetone to the high dielectric constant solvent propylene carbonate led to the formation of stable 4.0 ± 1.0 nm $Pt(0)_n$ nanoclusters. Without the application of the mechanistically predicted [7,8] synthesis conditions and the change to propylene carbonate during the *formation* of the nanoclusters, *stabilization* of $Pt(0)_n$ nanoclusters in the absence of bulk metal proved impossible. This is just one case illustrative of the fact that nanocluster formation and stabilization are tightly interlinked issues.

22 protecting agents, and the authors concluded that gelatin and poly(acrylic acid hydrazine) were the most effective at preventing agglomeration for Au colloids. However, the results of this study are difficult to interpret because colloidal stability was studied at different temperatures and for varying amounts of time. Consequently, the stabilizers examined therein [44] should not be rigorously compared either to each other or to prior stabilizers. Like the gold number study discussed above [42], the protective value study has little relevance to colloids of metals other than Au prepared in solvents other than water. Accordingly, the "protective value" is cited mainly either as precedent for stabilizing nanoclusters with polymers [45,46], or as interesting "history" in the literature of modern transition-metal nanoclusters [7,9].

Note, then, that these two, > 105 and > 41 year old methods available in the literature for ranking nanocluster stabilizers have been used *only* used for *Au colloids* and are applicable *only* in *water*. Additionally, these two methods rely on *visual inspection* of a solution (i.e., the color change from red to violet with the agglomeration of the Au colloids) in order to determine the efficacy of the stabilizer. Clearly, these water-soluble, Au colloid-based, qualitative methods are not the desired quantitative method for ranking stabilizers of all metal nanoclusters in a range of solvents. New methods are needed to quantitatively rank nanocluster stabilizers, and have been under development since 2002 [9,12]. In addition, new methods of preparing Au colloids in organic solvents with only the desired stabilizer(s) and solvent present would presumably open up optical methods of following nanocluster stabilization; such methods are under consideration [47].

2.1 Agglomeration-Based Methods of Determining Nanocluster Stability

In a classic study, Enüstün and Turkevich studied pre-formed citrate-stabilized Au colloids and the kinetics of their $NaClO_4$-induced agglomeration [48]. Aliquots of the colloids were taken at predetermined times after the addition of $NaClO_4$, and agglomeration was halted via the addition of a 0.1% gelatin solution. Transmission electron microscopy (TEM) was employed to measure agglomeration. While a valuable, classic study, this paper relies solely on TEM for studying the stability of the colloids. TEM is a useful tool for studying agglomeration, but complications under the harsh conditions of the electron beam are possible, including aggregation [49], charging of the solvent in the electron beam [50], and even nanocluster formation under the TEM beam from nanocluster precursors of especially first row metals [49,51,52]. Additionally, as noted in a TEM textbook, "Certain materials are more susceptible than others, but in the end, you can damage virtually anything you put into the TEM [53]." In short, TEM is an *ex situ* tool and thus not the desired, *in situ / operando* method for studying nanocluster agglomeration.

An alternative and potentially powerful technique for studying the formation and then agglomeration of nanoclusters over time is ultraviolet-visible (UV-visible) spectroscopy. This technique is dependent on (i) the precursor having a measurable absorbance, (ii) the nanocluster having a plasmon absorbance band measurably shifted from the precursor's absorbance band, and (iii) both of these absorbances being in the range of 160-780 nm. UV-visible spectroscopy can be valuable if all three of the above conditions are met, and has yielded information about the timescale of precursor degradation, colloid formation, and subsequent colloidal agglomeration [54,55]. However, the limitations imposed by the necessity of a plasmon absorbance band,

preferably in the visible region (i.e., a band which does not just tail off into the UV) limits the utility of this technique to primarily Au, Ag, and Cu. Confirming the limited utility of a UV-vis method is Mie theory [56], which serves as an accurate predictor of the extinction spectra for a variety of colloids. Creighton et al. have calculated the absorption spectra for 52 metallic colloids [57] and their results show that nanoclusters of several of the important metals in nanocluster science (e.g., Ir, Rh, Ru, Pd, and Pt) have little absorbance in the visible region. Instead, they tail into the UV, making quantitation of nanocluster formation and agglomeration of such metals largely unaccomplished—at least to date—by this otherwise promising method [29,58,59].

Another method used to study the agglomeration of nanoclusters is dynamic light scattering (DLS). DLS appears to be a promising technique for following formation and agglomeration, as measurements can be taken *in situ* and versus the extent of the reaction—that is, be studied in real time. However, measuring nanocluster formation and agglomeration with DLS is fraught with difficulty and its use is contentious at present [60,61]. For instance, the possibility of multiple scattering of particles [60,61] is a challenge, and polydisperse samples may also affect the interpretation of the data [62]. Also, deconvoluting particle sizes from a single autocorrelation function (as in light scattering experiments) is a classic problem in curve fitting of multiple exponentials [63]. Additionally, the use of DLS in studying agglomeration is restricted to relatively small particles that have appreciable Brownian motion [64]. Hence, employing DLS for studying particle agglomeration is not yet widespread.

One recent report details the use of a commercial high-performance particle sizer (HPPS), a modified version of traditional DLS instrumentation, for studying nanocluster

formation and agglomeration [65]. The authors claim that this instrument will offer a high sensitivity, rapid, relatively inexpensive method for studying the *in situ* formation (and agglomeration) of colloids. However, for the discrete "football" shaped polyoxoanion nanoparticle $P_2W_{18}O_{62}^{6-}$ (which is ~1.2 x 1.5 nm), the instrument detected only the long axis [65]. This could lead to an overestimation of the size of some particles, and does not give the accurate shape information that can be gathered with TEM or scanning electron microscopy (SEM). Additionally, HPPS presumably cannot measure the kinetics of the loss of monometallic nanocluster precursors. Moreover, it appears that this instrument is not useful in at least its reported configuration for reactions with gaseous reagents, such as the common reductant H_2. In short, at present there is no *quantitative* measurement of the conversion of precursor to nanocluster or nanocluster to agglomerated material using HPPS.

Other scattering techniques for monitoring nanocluster nucleation, growth, and agglomeration have also been used; the two that appear most promising at present are x-ray absorption fine structure (XAFS) spectroscopy and small angle x-ray scattering (SAXS) spectroscopy [66,67,68,69,70]. Both XAFS and SAXS can yield the highly desirable measurement of nanocluster formation and agglomeration *in situ*, allowing for the real-time monitoring of the kinetics. Furthermore, SAXS can sometimes be used to determine the molecular weight (MW) of nanoclusters [66]. For just one example, XAFS spectroscopy was used to determine that the dehydrogenation catalyst derived from $[(1,5\text{-COD})RhCl]_2$ is a Rh_6 species[2] [71]. Separately, a recent study compared SAXS with the

[2] In recent work at Pacific Northwest National Laboratories (PNNL), the $[Rh_6(\text{unknown stabilizer})]^{n+/0/n-}$ sub-nanometer cluster initially detected by XAFS and XANES [71] is now hypothesized to be a (perhaps more general) "Rh_4" cluster (J. C. Linehan, T. Autrey, private communication). Collaborative studies are in progress to determine (i) the full composition of the cluster; (ii) whether or not it is the true catalyst vs. a

ex situ size characterization techniques TEM and x-ray diffraction (XRD) for the measurement of $CoPt_3$ particle size distributions. This study found that all three techniques were within error for determining nanocluster size—however, SAXS offered the key benefits an *in situ* approach and a much larger sample size than TEM [68]. Currently, the main drawbacks of these techniques are their availability: both XAFS and SAXS require a synchrotron radiation source and the use of a highly specialized reaction apparatus (for example, for typical transmission-mode SAXS measurements, the reaction cell must have a pathlength of ≤1 mm). Broader use of these promising techniques should yield more accurate information on the formation and agglomeration of nanoclusters.

None of the TEM, UV-visible, DLS/HPPS, XAFS, or SAXS methods outlined above currently offers a widely available, *quantitative* method for evaluating agglomeration and stability. Additionally, it is rare [68] for a study to use more the one technique to assay stability: a survey of the literature reveals that a "typical" nanocluster paper often reports stability only through the observation of nanoclusters or colloids *by TEM.* If nanoclusters are seen in the *solid state* by TEM, even if agglomerated and if the state of the remainder of the sample is unknown (i.e., there might be some or even primarily bulk metal present), the nanoclusters are deemed "stable". Hence, developing a quantitative method for following the agglomeration kinetics of transition-metal nanoclusters is of enormous fundamental as well as practical importance in order to efficiently advance the synthesis, isolation, and stability/storage properties of transition-metal nanoclusters with a method that is readily available.

---

catalyst resting state or catalyst precursor; and (iii) the broader generality or not of the "M_4" sub-nanocluster finding: J. C. Linehan, T. Autrey, R. G. Finke, experiments in progress.

2.2 Kinetic Studies: Can the Kinetics of Agglomeration, as a Preferred, Quantitative Way to Assay Transition-Metal Nanocluster Stabilizers, Be Measured by the Catalytic Reporter Reaction Method?

Upon considering the methods discussed in the preceding sections, it is clear that a quantitative method for ranking nanocluster stabilizers is needed. To this end, *kinetic* measurements of agglomeration[3,4] are desirable, for example using the established agglomeration-inducing ligand pyridine [62,72]. However, kinetic probes of agglomeration are relatively rare because the required kinetic methods are also rare [6,7,8,12], as is true for nanocluster nucleation and growth. One kinetic method that has been successfully applied to follow the nucleation and growth of transition-metal nanoclusters [6,14,73], is the cyclohexene hydrogenation catalytic reporter reaction. The reporter reaction as used in the 2-step, autocatalytic nanocluster formation reaction discovered and developed by our group [6,14,73] is shown below in Scheme 1.

---

[3] Difficulties studying nanocluster agglomeration directly reflect its inherent complexity, as stated in a recent review: "Aggregation in most real systems involves a wide range of physical and chemical processes including long- and short-range interactions (van der Waals forces, screened electrostatic interactions, steric effects, hydrodynamic interactions, etc.), adsorption and desorption of ions and neutral species, chemical bond formation, sintering, bridging, etc. In addition, a variety of processes can occur during and after aggregation. These include structural reorganization, reversible aggregation, and chemical processes. In addition, many aggregation processes involve particles with a broad range of sizes, shapes, and compositions. The aggregating particles may also have a surface geometry and large heterogeneities in their surface chemistry. It is clear that incorporation of all these (and many other) effects (such as the change in the solvent structure near to the particle surface) in a single model would be a *formidable undertaking*." (italics have been added) P. Meakin, Adv. Coll. Int. Sci. 28 (1988) 249.

[4] Agglomeration and aggregation are used synonymously in the literature, as they will be in this text. Herein, we use these words to describe irreversible chemical bond formation between one or more clusters, leading eventually to the formation of larger, eventually bulk-type metal.

Scheme 1. The generalized 2-step nanocluster formation reaction mechanism and associated rate constants k_1 and k_2. In this scheme, **A** is the organometallic precursor and **B** is a catalytically active atom on the surface of the nanocluster. The reaction is monitored by the fast cyclohexene reporter reaction [6,73].

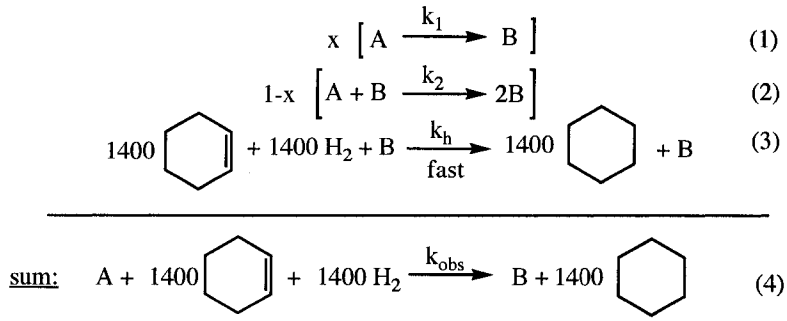

The cyclohexene reporter reaction method allows an indirect but rapid, quantitative, and real-time monitoring of the kinetics of nanocluster nucleation and growth. The cyclohexene hydrogenation must be a "pseudoelementary step" [74] for the catalytic reporter reaction method to accurately amplify the kinetics of nanocluster nucleation and growth—that is, the cyclohexene hydrogenation reaction must be much, much faster than the nanocluster formation steps. Use of the cyclohexene reporter reaction has been well documented for following the 2-step nanocluster nucleation and growth mechanism [6,14,73].

In order to quantitate stability, kinetic methods monitoring nanocluster nucleation, growth, and *agglomeration* are necessary and have recently been developed [7,8,12]. Two mechanisms have been elucidated, the first being a 3-step mechanism describing nanocluster nucleation, growth, and agglomeration where the catalytically *active* species is the nanocluster, **B**, and the agglomerated material, **C**, is catalytically *in*active [7], Scheme 2. The 3-step mechanism follows nanocluster nucleation (rate constant k_1), growth (rate constant k_2) and agglomeration (rate constant k_3) using the cyclohexene reporter-reaction method to amplify the kinetics [6,14,73]. The 3-step mechanism is

effective for modeling the nucleation, growth, and agglomeration of $P_2W_{15}Nb_3O_{62}^{9-}$- and Bu_4N^+-stabilized $Ir(0)_n$ nanoclusters in acetone solvent with two equivalents of the known nanocluster agglomerant pyridine added [12].

Scheme 2. The 3-step mechanism for nanocluster nucleation, surface autocatalytic growth, and bimolecular agglomeration. **A** and **B** are the same species as in Scheme 1; **C** is inactive, agglomerated **B**.

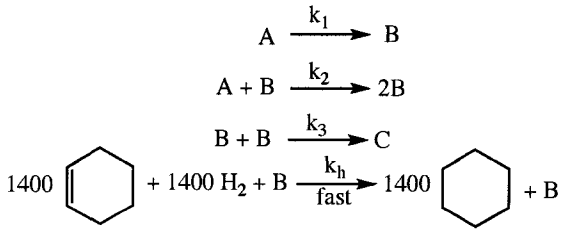

A 4-step, and thus an overall new, mechanism for nanocluster growth and agglomeration has also been recently described, Scheme 3 [7,8]. The 4-step mechanism includes an *autocatalytic* agglomeration step, **B+C→1.5C** (where, as in Scheme 1, **B** is a nanocluster and **C** is agglomerated, bulk-type metal) [7,8]; a more graphic, pictorial representation of what **A**, **B**, and **C** are is available elsewhere for the interested reader [7,8]. In the 4-step mechanism, weakly stabilized nanoclusters aggregate to form bulk-type metal and then this bulk-type metal, **C**, serves as the catalytically active species (for cyclohexene hydrogenation) due to a ligand-poisoning effect especially in the smaller nanoclusters, **B** [7,8]. In addition, and of potentially special significance in developing a quantitative measure of nanocluster stability, is the fact that *the 4-step mechanism defines for the first time the two rate constants for agglomeration, k_3 and k_4, that one wishes to measure.*

Scheme 3. The 4-step mechanism for nanocluster formation and agglomeration. Herein, the nanocluster **B** is catalytically *inactive* while **C**, the bulk-type, agglomerated metal particle, is the active catalyst. Note that the overall mechanism contains two autocatalytic steps.

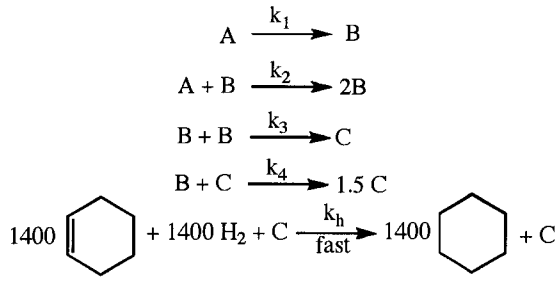

With respect to quantitating agglomeration kinetics and, hence, stability, we have recently shown that we can induce the 4-step mechanism of formation and agglomeration for prototype $P_2W_{15}Nb_3O_{62}^{9-}$–stabilized $Ir(0)_n$ nanoclusters beginning with the organometallic nanocluster precursor $[Bu_4N]_5Na_3[(1,5\text{-COD})Ir{\bullet}P_2W_{15}Nb_3O_{62}]$ and 44 equiv added pyridine [75]. However, with ≥50 equiv added pyridine, the cyclohexene reporter reaction is poisoned and the catalytic reporter reaction method cannot be used to quantitate agglomeration kinetics. We have observed similar results beginning with preformed, isolated, and redispersed $P_2W_{15}Nb_3O_{62}^{9-}$–stabilized $Ir(0)_n$ nanoclusters: ≥20 equiv added pyridine poisons the cyclohexene reporter reaction. Hence, using added pyridine to induce and subsequently quantitate agglomeration kinetics for the 4-step mechanism is not desired/has not been useful [75].

Importantly, we were able to quantitate agglomeration kinetics using the temperature-induced agglomeration of preformed, isolated, and redispersed $P_2W_{15}Nb_3O_{62}^{9-}$–stabilized $Ir(0)_n$ nanoclusters [75]. We measured the rate constants k_3 and k_4 (**B+B→C**, **B+C→1.5C**, respectively, as in Scheme 3) at temperatures from 10-50 °C, and observed an increase in both k_3 and k_4 with increasing temperature. Additionally,

were able to calculate the activation parameters $\Delta H^{\ddagger}$ and $\Delta S^{\ddagger}$ for each step (**B+B→C**, and **B+C→1.5C**). The magnitudes of the two sets of activation parameters support our earlier observation of a particle-size dependent metal-ligand bond energy [8], with larger, bulk-type clusters having lower bond energies. The temperature-induced agglomeration experiments represent, to the best of our knowledge, the first experimental, quantitative measurement of nanocluster agglomeration [75]. While using temperature to induce agglomeration of preformed nanoclusters is an important advance in quantitating nanocluster *stabilization*, it suffers from the limitations that it loses the kinetics of *formation* of the nanoclusters, and that it is only applicable to nanocluster systems that are stable enough to be isolable and redissolvable—that is, to well-stabilized nanoclusters. The initial report of this technique opens the door for future kinetic, quantitative measurements of nanocluster stability.

2.3 The Presently Available Method For Evaluating *Both* the Formation and Stabilization of Modern, Catalytically Active Transition-Metal Nanoclusters.

A 2002 paper reported the development of a method for evaluating both the *formation* and *stabilization* of catalytically active[5] transition-metal nanoclusters [9]. This method relies on 5 criteria for ranking each stabilizer; hence, it is called the 5 criteria method. Its use initially focused on evaluating anionic stabilizers, as anions are known to be key [76] in DLVO-type stabilization (named after its founders Derjaugin, Landau, Verwey, and Overbeek; this and other modes of nanocluster stabilization will be

[5] Often, an inverse correlation between high stability and high catalytic activity is observed [5]—not unexpected, as highly stable nanoclusters often have a large fraction of their otherwise catalytically active surface sites ligated by the stabilizer, Scheme 4. Thus, a *balance* between stability and catalytic activity is key in achieving the goal of nanocluster catalysis [14,15,16,17].

discussed more in a moment). Briefly, the 5 criteria are: (i) a high level of kinetic control during the nanocluster formation reaction, as reflected by a large value of the k_2/k_1 ratio for autocatalytic growth (k_2) to nucleation (k_1), see Scheme 1; (ii) the formation of near-monodisperse nanoclusters (by definition elsewhere [27], nanoclusters with a size distribution of ≤ 15%) as verified by TEM; (iii) the ability to isolate from solution and bottle, without bulk metal formation, the nanoclusters for future use; (iv) the catalytic activity of the redissolved (i.e., from previously isolated) nanoclusters in a chosen solvent with fresh catalytic substrate (typically cyclohexene); and (v) the total turnovers (TTOs) for cyclohexene hydrogenation observed for *in situ* generated nanoclusters in solution. The combination of the above 5 criteria provides an previously unavailable evaluation of the efficacy of a chosen additive for its ability to allow the formation, stabilization, and subsequent catalytic activity of transition-metal nanoclusters, and is not limited to only those nanoclusters that are stable enough to be isolated and redissolved (as is the temperature-induced agglomeration of preformed nanoclusters as a method for ranking stabilizers). Additionally, the 5 criteria method is applicable at least in principle to all metals in a range of solvents. The method and 5 criteria in their current form, while clearly not perfect[6]—for example, the method lacks the desired kinetic measurements of formation and then agglomeration—are nevertheless a welcome advance in an area where modern methods to rank nanocluster stabilizers were previously lacking.

Initially, the 5 criteria were used to rank established anionic nanocluster stabilizers, leading to the first anion stabilization ability series for Ir(0) nanoclusters (shown in Scheme 4) [9]. Use of a balanced reaction stoichiometry plus the 5 criteria

[6] In cases where bulk metal is formed, 4 of the 5 criteria become unavailable, so that the 5 criteria method is applicable in practice only to fairly well-stabilized nanoclusters.

also led to the insight that Proton Sponge™ (PS™; 1,8-bis(dimethylamino)naphthalene) is an effective scavenger for the H^+ product of nanocluster formation reaction when H_2 is the reductant [10]. Hence, PS™ is a common component of our nanocluster formation and stabilization studies using H_2 as the reductant [10,11].

Scheme 4. The anion stabilization series [11].

The Best Anions for the Formation and Stabilization of Ir(0) Nanoclusters in Acetone at 22 °C:
$[P_2W_{15}Nb_3O_{62}]^{9-} \sim [(P_2W_{15}Nb_3O_{61})_2O]^{16-} \sim \{[P_2W_{15}(TiOH)_3O_{59}]^{9-}\}_n$ (n=1,2) > $[SiW_9Nb_3O_{40}]^{7-}$ > HPO_4^{2-} > H_2PO^{4-} > $[C_6H_5O_7]^{3-}$

Poorer Anions for the Formation and Stabilization of Ir(0) Nanoclusters:
$[P_3O_9]^{3-}$ > $[-CH_2-CH(CO_2)-]_n^{n-}$ > Cl^- > OH^-

Insights from the 5 criteria method also led to the development of a "lattice-matching model" [77] that provides an important, molecular-level hypothesis for how tridentate anionic stabilizers may achieve their higher observed level of stabilization, a hypothesis useful for predicting which anions are effective for coordinating the M(111) face of a metal nanocluster [77]. The essence of that model is that the best anionic nanocluster stabilizers present a tridentate, facial array of oxygen atoms for coordination to the $M(0)_n$ surface, and that the preferred tridentate oxoanion stabilizers are those that have the best match between the ligand O-O and metal M-M distances. In addition, the lattice matching model and the 5 criteria have recently been used to uncover a previously unappreciated nanocluster stabilizer, HPO_4^{2-} [11]. Using these insights and applying the 5 criteria, it was predicted—and then demonstrated [11]—that HPO_4^{2-} is a simple,

effective, readily available, and robust stabilizer for at least $Ir(0)_n$ nanoclusters, and probably nanoclusters of other metals such as Rh, Pt, Au, and Cu [77].

In short, the 5 criteria method has been a valuable development in assaying both nanocluster formation and stabilization. It is the lone method currently available in the literature that is applicable, at least in principle, to all metal nanoclusters in a range of solvents. However, a weakness of the method is that for less stabilized systems where bulk metal is readily formed, four of the five criteria become unavailable (however, the fact that four of the five criteria become unavailable in itself is helpful, as it indicates which stabilizers are even *worth ranking*). Hence, evaluating the full 5 criteria method is only possible for better stabilized nanoclusters, such as the $P_2W_{15}Nb_3O_{62}^{9-}$–stabilized $Ir(0)_n$ nanoclusters with which it has been developed [9,10]. Nevertheless, the 5 criteria method is an important advance in both understanding the factors controlling nanocluster formation and stabilization and in ranking stabilizer efficacy. Eventually, improved methods in measuring both the k_1 and k_2 rate constants for formation and k_3 and k_4 rate constants for agglomeration simultaneously (Scheme 3, vide supra) as part of the 5 criteria method should allow refinements in the initial rankings made with the 5 criteria method.

3. On the Modes of Nanocluster Stabilization

There are two historical classes of nanoclusters stabilizers: electrostatic (also known as electronic, or DLVO-type) and steric stabilization. Representative examples are shown in Scheme 5. A third type of nanocluster stabilization, which is frequently presented in the literature but has not been defined precisely in terms of both overall size

and charge requirements [78], is "electrosteric" stabilization (a combination of electrostatic and steric; it is included in Scheme 5 and will be discussed critically later). These three modes of stabilization will be discussed in separate sections below, and then three additional examples of "non-historical" putative stabilization modes will also be discussed—cationic, solvent-only, and ionic liquid stabilization. *Note that given the previously discussed lack of quantitative methods to measure stability and thereby rank stabilizers, it follows that much of the information that follows is not on as firm a ground as is desired.*

Scheme 5. The three nanocluster stabilization modes with selected examples.

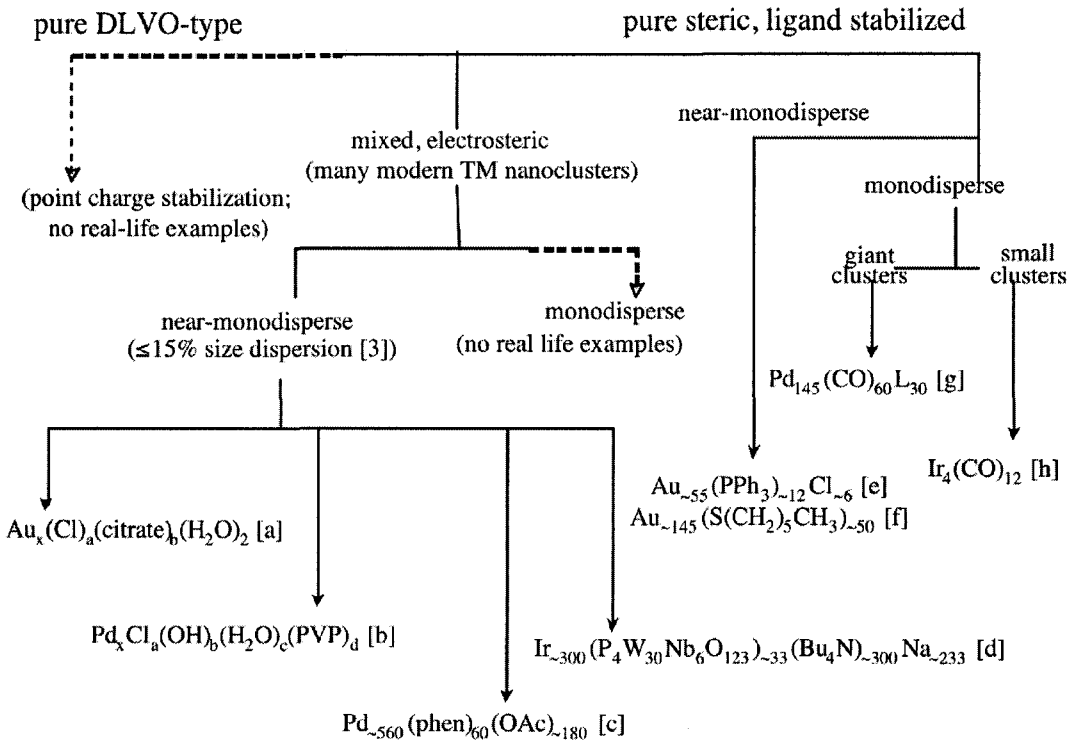

[a] These are early examples of colloids, dating back to the time of Faraday [43].
[b] These sols were first investigated by Hirai in 1979 [110a].
[c] These classic nanoclusters, characterized by TEM, ultracentrifugation, and EXAFS, are catalytically active for oxidative acetoxylation of ethylene with O_2 [87].
[d] Well-defined, catalytically active polyoxoanion-stabilized Ir(0) nanoclusters were first reported in 1994 [14].
[e] These clusters were first reported in 1981 [82].
[f] Clusters of this type were recently reviewed [155]
[g] The structure of this massive cluster was recently established by single-crystal XRD; it is ligand-poisoned, however, and has not been shown to have catalytic activity [87].
[h] Carbonyl clusters, while compositionally well-defined and very stable,are typically not catalytically active until and unless some of the CO ligands are removed.

A general word of caution is necessary before beginning a discussion on the modes of nanocluster stabilization. When evaluating a system, the source of stabilization may seem clear: for example, a coordinating anion or polymer may be present. However, in many systems, there are often multiple possible stabilizers present so that one must carefully consider the contribution of each, as well as the solvent as a possible ligand—

that is, *one must know the precise composition of one's nanoclusters in order to know all the possible alternative hypotheses* [79] *for the true stabilizer in the system.* This is typically almost never done—*and often not even considered*—in the literature. For example, the effects of an anion (often present from the decomposition of a metal salt) are frequently not considered when there is another potential stabilizer present. For instance, when a polymer or surfactant [80] is present and a metal halide precursor is reduced to form a $M(0)_n$ nanocluster, the effects of the halide are often completely ignored and "polymer" or "surfactant" stabilized nanoclusters are claimed. This phenomenon—of interpreting one's data in terms of one's initial, assumed stabilizer hypothesis, without disproof of other, alternative hypotheses—is widespread. It is *the* major conceptual and intellectual error in how nanocluster stabilization science is being done. *Consequently*, the conditions of each system, including the counterions of the precursor complexes, the solvent, the reaction atmosphere (O_2; leading to possible oxide formation), and so on must be taken into account when assigning the stabilizing entity in a nanocluster system. *In short, much of the existing nanocluster stabilization literature is primitive and unrefined—caveat emptor!*

Indeed, a recent report from a collaborative effort of five prestigious groups active in nanocluster research acknowledges the myriad of stabilizers proposed in the literature, noting that in general it is not possible to "understand which (nanocluster) preparation method is the best among those proposed" [109]. The proliferation of claimed stabilizers in the literature may be because the only apparent requirement for claiming novel stabilizers seems to be a TEM of the particles with an associated histogram, and occasionally an accompanying catalytic or other physical property test! Consequently,

the nanocluster/colloid literature has grown at an alarming rate if one has any interest in what really is the stabilizer, or what is the best stabilizer. Accordingly, in the following sections covering nanocluster stabilizers, the focus instead lies on the *mode* of stabilization with a few illustrative examples rather than attempting to review every stabilizer that has appeared in the literature—that is, this review does not portend to cover the recently noted "dizzying variety" [5] of nanocluster stabilizers that are employed in the nanocluster literature. Representative examples of electrostatic/DLVO-type, steric, "solvent-only", and ionic liquid (IL) stabilization modes are covered in Table 1 below. Therein (in chronological order with respect to the first published report), the conditions under which the colloids or nanoclusters were prepared are listed, along with a brief commentary with respect to the key *compositional* information (or lack thereof) and other issues. In cases where more than one paper is referenced, the author (date) column applies to the first report, and the multiple references that follow note systems prepared under closely related conditions that have the same claimed stabilizer, compositional issues, and so on. A main finding from perusing Table 1 is that the *composition of nanoclusters needs to be rigorously established before any reliable discussion of how they are stabilized can ensue, and more in situ measurements of nanoclusters (for example, the MW of the nanoclusters as measured by SAXS and/or analytical ultracentrifugation) need to be undertaken.*

Table 1. A compilation of selected literature examples, highlighting the need for compositional and molecular weight information in many of the systems.

Author (date)	System	Stabilizer Compositions/Related Issues	Ref.
	Electrostatic/ DLVO-*type* Stabilization		
J. Turkevich, P. C. Stevenson, J. Hillier (1951)	An aqueous solution of $HAuCl_4$ was heated to boiling and reduced with an aqueous solution of citric acid	Potential surface contamination and/or contribution to stability from H_2O and Cl^-; citric acid can serve as both a reductant and a stabilizer; size distribution ranges from 100-500 Å *average composition and MW unknown*	81
G. Schmid, R. Pfeil, R. Boese, F. Bandermann, S. Meyer, G. H. M. Calis, J. W. A. ver der Velden (1981)	$AuCl[P(C_6H_5)_3]$ was reduced with B_2H_6 in warm benzene; the dark precipitate is washed with CH_2Cl_2, and precipitated out with pentane	Characterized by TEM, HR-TEM, some STM, ^{31}P NMR, Mössbauer, and secondary ion MS; elemental analysis gives an average composition of $[Au_{9.2}(PPh_3)_2Cl]_n$, while sedimentation MW measurements give an average formula of $[Au_{\sim 55}(PPh_3)_{\sim 12}Cl_{\sim 6}]$ *average composition and MW **known***	82
M. N. Vargaftik, V. P. Sargorodnikov, I. P. Stolarov, I. I. Moiseev, V. A. Likholobov, D. I. Kochubey, A. L. Chuvilin, V. I. Zaikosvsky, K. I. Zamaraev, G. I. Timofeeva (1985)	$Pd(OAc)_2$ was reduced with H_2 in acetic acid in the presence of either 1,10-phenanthroline (phen) or 2,2'-bipyridine (bipy)	Characterized by elemental analysis, TEM, SAXS, ^1H NMR, and EXAFS; workup under oxygen in acetic acid converts the original form of $[Pd_4phen(OAc)_2H_4]_n$ ($n \approx 100$) to the final colloidal composition of $[Pd_{\sim 561}phen_{\sim 60}(OAc)_{\sim 18}]$ *average composition and MW **known***	83
H. Bönnemann, W. Brijoux, R. Brinkmann, E. Dinjus, T. Joußen, B. Korall (1991)	Halide salts of group 6-11 metals are reduced with NR_4BEt_3H in THF	Halides present in 2-4 equivalents per equivalent metal; no halides reported in elemental analysis but other elements only add to 93.4%; proposed coordination of R_4N^+ surfactant is implausible *average composition and MW unknown*	189
M. T. Reetz, W. Helbig, S. A. Quaiser, U. Stimming, N. Breuer, R. Vogel (1995)	Pd colloids prepared electrochemically from Pd sheets in the presence of tetraalkylammonium salts in dried MeCN/THF	Br^- is present in 4% by elemental analysis; proposed coordination of R_4N^+ surfactant is implausible *average composition and MW unknown*	187
J. Rothe, J. Pollmann, R. Franke, J. Hormes, H.	$RhCl_3$ was the precursor for several colloids; reducing agent not stated; solvent not	XPS shows both residual halides and "sample contaminations" (C, O); XPS also shows "a large content of zerovalent Rh-atoms", meaning the colloid is not in the fully reduced state; XANES	84

Bönnemann, W. Brijoux, K. Sipen, J. Richter (1996)	stated; at least 2 different surfactants added	also shows the presence of halides and incomplete reduction of the metal *average composition and MW unknown*	
M. T. Reetz, M. Winter, R. Breinbauer, T. Thurn-Albrecht, W. Vogel (2001)	Pd, Ni, and Pt/Pd colloids were prepared via electrochemical reduction of their corresponding metal sheet in the presence of surfactants in either THF or mixed THF:CH_3CN	Br^- present in surfactant; XRD shows some oxidation of the Pd colloids' surfaces; using short-chain amine surfactants lead to the precipitation of the colloids *average composition and MW unknown*	193
	Steric Stabilization		
H. Hirai, H. Chawanya, N. Toshima (1979)	Fe, Co, Ni, Cu, Ru, Rh, Pd, Pt, Au, Ag, Os, and Ir colloids prepared by refluxing in an alcoholic solvent in the presence of PVP	Alcoholic solvent functions as a reducing agent and possibly also a stabilizer; precursors contain potential stabilizers such as Cl^- and H_2O; oxide surface layer likely after refluxing in air *average composition and MW unknown*	110a
R. H. Terrill, T. A. Postlethwaite, C. Chen, C.-D. Poon, A. Terzis, A. Chen, J. E. Hutchison, M. R. Clark, G. Wignall, J. D. Londono, R. Superfine, M. Falvo, C. S. Johnson, E. T. Samulski, R. W. Murray (1995)	An aqueous solution of $HAuCl_4 \bullet xH_2O$ was extracted into toluene with tetraoctyl-ammonnium bromide, treated with an alkanethiol, and reduced with aqueous $NaBH_4$	Synthesis and nanocluster workup not performed in an inert atmosphere; potential surface contamination and/or contribution to stability from H_2O, Br^- and Cl^-; for two of the samples, elemental analysis of C, H, S, and Au adds to only ~95%, ^1H NMR confirms the absence of free alkanethiol; IR spectra show characteristic stretches of alkane chains; *average composition and MW unknown*	85
M. Antonietti, F. Gröhn, J. Hartmann, L. Bronstein (1997)	$AuCl_3$ and $FeCl_3$ were reduced with N_2H_4 or $NaBH_4$ in aqueous solutions of polystyrene sulfonate microgels	Potential surface contamination and/or contribution to stability from H_2O and Cl^-; TEM shows extensive agglomeration, which the authors call "threads" or "nuggets"; no evidence that Au species are inside the microgels instead of on the sulfonate moieties *average composition and MW unknown*	149
M. Zhao, L. Sun, R. M. Crooks (1998)	$CuSO_4$ was adsorbed into PAMAM dendrimers and reduced with $NaBH_4$ in water; later done with H_2PtCl_6 and H_2PdCl_6	HCl is added to adjust the pH; possible surface contamination and/or contributions to stability from H_2O and Cl^-; an oxide layer may be present due to synthesis under ambient conditions but was not investigated *average composition and MW unknown*	130, 131, 133, 135, 137

L. Balogh, D. A. Tomalia (1998)	$Cu(OAc)_2$ was adsorbed into PAMAM dendrimers and reduced with N_2H_4 in aqueous solution	Potential surface contamination and/or contribution to stability from H_2O and OAc^-; Cu colloids were easily oxidized upon exposure to atmospheric oxygen; no TEM or elemental analysis done *average composition and MW unknown*	138
N. T. Whilton, B. Berton, L. Bronstein, H.-P. Hentze, M. Antonietti (1999)	$(H_3N)_4Pt(NO_3)_2$, $PdCl_2$, $(py)_4RhCl_3$, or Na_2PtCl_6 were reduced with $NaBH_4$ in water or NaOH in solutions of polystyrene sulfonate microgels, then incorporated into a porous silica template	Potential surface contamination and/or contribution to stability from H_2O, OH^- and Cl^-; B incorporation possible; exposure to gaseous HCl during silica templating; potentially stabilizing MeOH produced by templating reaction; final nanocluster in template are heated under O_2 for 12h *average composition and MW unknown*	150
M. Zhao, R. M. Crooks (1999)	$Cu(NO_3)_2 \cdot 2.5H_2O$ was adsorbed into OH-terminated PAMAM dendrimers, the pH was adjusted with NaOH, and then reduced with $NaBH_4$; Cu was later displaced with aqueous solutions of $AgNO_3$, $HAuCl_4$, K_2PdCl_4, or K_2PtCl_4	Potential surface contamination and/or contribution to stability from H_2O, OH^-, Cl^-, NO_3^-; B incorporation possible; no proof that colloids are stabilized only by the dendrimer *average composition and MW unknown*	132
K. B. Stavens, S. V. Pusztay, S. Zou, R. P. Andres, A. Wei (1999)	Au colloids were generated as aerosols and bubbled into mesitylene solutions of resorcinarenes	TEM shows wide size distribution (3-15 nm); colloids precipitate upon removing excess resorcinarene or changing solvents; resorcinarenes are exchanged by added thiols *average composition and MW unknown*	165
L. M. Bronstein, D.M. Chernyshov, P. M. Valetsky, E. A. Wilder, R. J. Spontak (2000)	$H_2PtCl_6 \cdot 6H_2O$, K_2PtCl_4, $AuCl_3$, or Na_2PdCl_4 were reduced with $NaBH_4$ in either a water/acetone or water/ethanol solution in the presence of PODS	Potential surface contamination and/or contribution to stability from H_2O, OH^-, and/or Cl^-; B incorporation possible; colloids not prepared under an inert atmosphere; possible reduction by ethanol and then contribution to stabilization by the resulting alkoxide; possible contribution to stability from silanol moieties *average composition and MW unknown*	126
N. T. Tran, D. R. Powell, L. F. Dahl (2000)	$[Pd(PEt_3)_2Cl_2]$ and $[Au(PPh_3)Cl]$ were stirred under CO for 2 days in a DMF solution containing NaOH pellets, filtered into $[PPh_4]Br$; the dark brown solid was extracted with MeOH, MeCN, and THF	Characterized with single-crystal XRD data with crystals from two separate preparation; no catalytic tests performed (not expected to be catalytic due to strong ligation of ~74% of the surface atoms by CO and PEt_3) ; elemental analysis would compliment the XRD data ***precise composition known*** *to be* $Pd_{145}(CO)_{\sim 60}(PEt_3)_{30}$*; average MW known*	86

R. Wang, J. Yang, Z. Zheng, M. D. Carducci, J. Jiao, S. Seraphin (2001)	$HAuCl_4$ was reduced with an aqueous solution of $NaBH_4$ in the presence of $(n\text{-}C_8H_{17})_4NBr$ and various generations of dendrons	Potential surface contamination and/or contribution to stability from H_2O, Br^-, Cl^-; B incorporation possible; notes that a "significant amount of black precipitate" is generated if the reduction is carried out in the absence of $(n\text{-}C_8H_{17})_4NBr$, indicating a contribution to stability from the surfactant; TEM shows agglomeration; reaction presumably carried out without air-free techniques *average composition and MW unknown*	140
S. V. Pusztay, A. Wei, K. B. Stavens, R. P. Andres (2001)	Au colloids were generated as aerosols and bubbled into mesitylene solutions of resorcinarenes; the resorcinarenes were then crosslinked	Colloids precipitated within hours; TEM showed "clumps rather than isolated particles"; the authors suggest catalytic ability but never test it *average composition and MW unknown*	163
N. Cordente, M. Respaud, F. Senocq, M.-J. Casanove, C. Amiens, B. Chaudret (2001)	$Ni(COD)_2$ was reduced with 3 bar H_2 in THF in the presence of hexadecylamine or trioctylphosphine oxide	No elemental analysis done; TEM shows agglomerated colloids; no controls done with the Ni precursor alone on the TEM grid to check for nanocluster formation under the TEM beam *average composition and MW unknown*	170
Y. Li, M. A. El-Sayed (2001)	$PdCl_2$ or K_2PdCl_4 were reduced by $NaBH_4$ or ethanol in aqueous solutions of either PAMAM dendrimers, PVP, or poly(styrene)-*block*-poly(sodium acrylate)	Potential surface contamination and/or contribution to stability from H_2O, OH^-, Cl^-; B incorporation possible; PAMAM solution acidified with HCl before reduction; PVP and block copolymer solutions were refluxed under air; some precipitation of the colloids is noted after catalysis *average composition and MW unknown*	113
P. N. Floriano, C. O. Noble IV, J. M. Schoonmaker, E. D. Poliakoff, R. L. McCarley (2001)	$Cu(NO_3)_2 \cdot 2.5H_2O$ in methanolic solution was adsorbed into amine-terminated PPI dendrimers with diaminobutane cores and reduced with $NaBH_4$	Potential surface contamination and/or contribution to stability from H_2O, OH^-, MeO^-; NO_3^-; B incorporation possible; TEM shows agglomeration *average composition and MW unknown*	141
B. Kim, S. L. Tripp, A. Wei (2001)	Au colloids stabilized by citrate were treated with a solution of resorcinarenes in THF	Both citrate and the resorcinarene could serve as the stabilizer; possible surface contamination by H_2O; TEM shows near-monodisperse 70 ± 5 nm nanoclusters *average composition and MW unknown*	161, 162,
S. Bucher, J. Hormes, H. Modrow, R. Brinkmann, N. Waldöfner, H.	Pd colloids were prepared by reducing $PdCl_2$ with NR_4BEt_3H in THF	Elemental analysis shows between 1.4-8.1 Cl atoms per Pd (3.1-13.2 Cl per *surface* Pd) and also the presence of the surfactant; XANES, and metastable impact electron spectroscopy (MIES) suggest "that the chlorine is present on the inside of the	190, 191

Bönnemann, L. Beuermann, S. Krischok, W. Maus-Friedrichs, V. Kempter (2002)		protection shell, located between palladium core and $N(alkyl)_4$ groups" *anionic stabilization by halides with a contribution by the countercation is recognized; composition partially determined but average MW unknown*	
Y. Niu, R. M. Crooks (2003)	$CuCl_2•H_2O$ or $Pd(OAc)_2$ was adsorbed into hexanoyl- or palmitoyl-modified PPI dendrimers in $CHCl_3$/MeOH and reduced with $NaBH_4$	Potential surface contamination and/or contribution to stability from H_2O, Cl^-, OH^- and OAc^-; B incorporation possible; nanocluster solution changes color in the presence of atmospheric O_2 *average composition and MW unknown*	136
A. Biffis, N. Orlandi, B. Corain (2003)	$Pd(OAc)_2$ or $PtCl_2(CH_3)CN$ was reduced with either EtOH or $NaHBEt_3$ in the presence of either amine- or pyridine-terminated microgels in CH_2Cl_2 or CH_3CN	Potential surface contamination and/or contribution to stability from H_2O, CH_3CN, OH^- and OAc^-; B incorporation possible *average composition and MW unknown*	152, 153
B. P. S. Chauhan, J. Rathore, M. Chauhan, A. Krawicz (2003)	Reduction of $Pd(OAc)_2$ with PMHS in a benzene/acetic acid solvent; separately done with Ag(OAc)	PMHS can serve as reductant and stabilizer; potential contribution to stability by acetate; TEM shows extensive agglomeration *average composition and MW unknown*	117, 127, 128
E. Ramirez, S. Jansat, K. Philippot, P. Lecante, M. Comez, A. M. Masdeu-Bultó, B. Chaudret (2004)	Pd_2(dibenzylidene acetone)$_3$ or $[Pd(C_3H_5)Cl]_2$ were reduced with 3 bar H_2 in the presence of hexadecylamine, bis-(diphenylphosphino) decane or bis-(diphenylphosphinoethyl)-phenylphosphine in THF or toluene	Potential surface contamination and/or contribution to stability from Cl; TEM shows extensive agglomeration; using THF led to increased stability (as measured by TEM), indicating a contribution to stability from the solvent *average composition and MW unknown*	172
R. Narayanan, M. El-Sayed (2004)	K_2PdCl_4 was reduced with $NaBH_4$ in aqueous solutions of either PVP or PAMAM dendrimers	Potential surface contamination and/or contribution to stability by H_2O, B, and Cl; size distribution monitored by TEM but the presence of bulk metal in the reaction flask means TEM analysis is not representative of the whole sample *average composition and MW unknown*	111
R. Patakfalvi, Z. Virányi, I. Dékány (2004)	$AgNO_3$ was reduced with hydroquinone or sodium citrate in the presence of PVP or PVA in water	Both PVA and citrate can serve as the reducing agent and the stabilizer; potential surface contamination by H_2O; an oxide layer may be present due to synthesis under ambient conditions *average composition and MW unknown*	122

K. Pelzer, B. Laleu, F. Lefebvre, K. Philippot, B. Chaudret, J. P. Candy, J. M. Basset (2004)	$RuCl_3 \cdot 3H_2O$ was used to prepare Ru(COD)(COT), which was reduced with 3 bar H_2 at 193 K in the presence of $H_3SiC_8H_{17}$	Elemental analysis results indicate that "about 0.55 silicon atoms per ruthenium atoms are grafted on the metal surface and about 0.7 octyl chains remain bonded per silicon atom"; TEM shows agglomeration; Ir and ^1H, ^{13}C, and ^{29}Si NMR indicate that organosilane fragments are bonded to the nanocluster surfaces *average composition of surface Ru atoms of $Ru_x[Si(n\text{-}C_8H_{17})_{0.7}]_{1.2}$ is proposed for the $Ru_{\sim 586}$ clusters; average total composition not proposed; average MW not known*	87
	Electrosteric Stabilization		
Y. Lin, R. G. Finke (1994)	$(Bu_4N)_5Na_3Ir \cdot P_2W_{15}Nb_3O_{62}$ was reduced with H_2 in acetone solvent under strict exclusion of O_2 and H_2O	Balanced (average) reaction stoichiometry obtained en route to providing nanocluster composition and stabilization mode; elemental analysis and **ultracentrifugation MW measurements** determine the average composition of $[Ir(0)_{\sim 300}(P_4W_{30}Nb_6O_{123}^{16-})_{\sim 33}](Bu_4N)_{\sim 300}Na_{\sim 233}$. *average composition and MW **known***	6, 9, 10, 11, 12, 14, 76, 77, 88, 176,
J. D. Aiken III, R. G. Finke (1999)	$(Bu_4N)_5Na_3Rh \cdot P_2W_{15}Nb_3O_{62}$ was reduced with H_2 in acetone solvent under strict exclusion of O_2 and H_2O	Ion-exchange resin studies demand that the polyoxoanion is the stabilizing entity; elemental analysis and EDS establishes the average composition as $[Rh(0)_{\sim 7}(P_4W_{30}Nb_6O_{123})(Bu_4N)_{\sim 5.5}Na_{\sim 10.5}]_{\sim 340}$ *average composition **known**, but not MW*	15, 50, 147
	Putative "Solvent-only" Stabilization		
K. J. Klabunde, H. F. Efner, T. O. Murdock, R. Ropple (1976)	Ni•solvent (hexane, toluene, or THF) slurries were prepared by co-condensation of vaporized Ni atoms and the solvent	SEM shows agglomeration and μm sized particles; solvent:metal ratio determined by desorption of organics upon pyrolysis, but no elemental analysis was done *average composition and MW unknown*	35
G. Cardenas-Trivino, K. J. Klabunde, E. B. Dale (1987)	Pd atoms were prepared by metal atom vaporization, followed by condensation with a non-aqueous solvent to form Pd colloids	Size dispersion not given; TEM shows aggregation; electrophoresis proves charge is scavenged from the reaction environment *average composition and MW unknown*	202
H. Bönneman, B. Korall (1992)	$TiCl_4$ in THF was reduced with $K[BEt_3H]$ to form "Ti·0.5 THF"	Elemental analysis shows the presence of B, K and Cl; XRD analysis shows the presence of KCl; XPS data indicates that the colloids formed are "almost as reduced as titanium metal"; oxides (TiO_x) seem likely *average composition and MW unknown*	84, 196a

M. T. Reetz, G. Lohmer (1996)	decomposition of Pd electrode or thermal decomposition of $Pd(OAc)_2$, both in propylene carbonate	In the electrode preparation, both Cl^- and ethanol are present as potential stabilizers; In the thermal decomposition preparation, OAc^- is a potential stabilizer: TEM on both systems shows wide size distributions and marked aggregation *average composition and MW unknown*	39
R. Franke, J. Rothe, J. Pollmann, J. Hormes, H. Bönnemann, W. Brijoux, Th. Hindenburg (1996)	$TiBr_4$•2THF was reduced with $K[BEt_3H]$ in THF	Elemental analysis shows 5.5% K and 0.7% Br; no B analysis reported; XPS shows evidence of surface oxidation; most observations interpreted in terms of Ti-THF coordination (Ti 2p BE shift in XPS, energy shift in XANES analysis, etc) could also be attributed to surface oxidation; also applied to colloids of Zr, V, Nb, and Mn *average composition and MW unknown*	196b
N. A. Dhas, H. Cohen, A. Gedanken (1997)	Pd_2(dibenzylidene-acetonate)$_3$ in mesitylene was subjected to ultrasound irradiation under Ar	Elemental analysis shows > 41% carbon and < 1.5% hydrogen; authors claim a "carbon-activated palladium powder"; no powder XRD peaks until heating to 300-400 °C; XPS C 1s spectrum is consistent with graphitic carbon *average composition and MW unknown*	89
O. Vidoni, K. Philippot, C. Amiens, B. Chaudret, O. Balmes, J.-O. Malm, J.-O. Bovin, F. Senocq, M.-J. Casanove (1999)	Ru(COD)(COT) was reduced with 3 bar H_2 in various ratios of MeOH:THF	Possible methoxide stabilizer; passivating oxide layer present by XRD and XPS; TEM shows aggregation of particles; particles isolated by precipitation cannot be redissolved *average composition and MW unknown*	197
P. J. Collier, J. A. Iggo, R. Whyman (1999)	Pd and Pt atoms were prepared by metal atom vaporization followed by condensation with organic solvents; in some cases, proprietary stabilizing agents "KD1" and "KD2" were used	No TEM shown; histograms from TEM data show bimodal size distribution; TEM is noted to look like "frogspawn" or "raspberries," indicating aggregation; not "solvent-only" stabilized given the added stabilizing agents (also, no evidence that KD1 and KD2 are superior stabilizing agents—or even information on what they are!) *average composition and MW unknown*	198
Y. Wang, J. Ren, K. Den, L. Gui, Y. Tang (2000)	$H_2PtCl_6 \cdot 6H_20$ was heated in a 0.5M NaOH solution in ethylene glycol; aqueous solutions of either $RhCl_3 \cdot 3H_20$ or $RuCl_3 \cdot 6H_20$ were heated in a 0.5M NaOH solution in water	Possible surface contamination and/or contribution to stability by OH^-, Cl^-, and H_20; preparations at pH<12 form bulk metal instead of colloids; TEM shows agglomeration; XPS and elemental analysis measurements were taken only after repeated washings in HCl and acetone *average composition and MW unknown*	199
K. Pelzer, O.	$RuCl_3$•$3H_2O$ was used	Possible surface contamination and/or contribution	201

Vidoni, K. Philippot, B. Chaudret, V. Collière (2003)	to prepare Ru(COD)(COT), which was reduced with 3 bar H_2 in either a pure alcohol or an alcohol/THF mixture	to stability by alcohols; alcoholic solvents can serve as the reductant and the stabilizer; THF may coordinate to the nanocluster surface; no elemental analysis performed; TEM shows agglomeration *average composition and MW unknown*	
K. Pelzer, K. Philippot, B. Chaudret (2003)	$RuCl_3 \cdot 3H_2O$ was used to prepare Ru(COD)(COT), which was reduced with 3 bar H_2 in heptanol	Alcoholic solvents can serve as the reductant and the stabilizer; ^1H and ^{13}C NMR indicate coordination of heptoxy molecules on the nanocluster surface; TEM shows some agglomeration; elemental analysis "indicate[s] the presence of *ca.* 70% Ru and *ca.* 1 heptanol : 7.5 Ru." *estimated composition proposed; no MW information additional evidence desirable for this interesting system*	90
	Ionic Liquid (IL) Stabilization		
J. Dupont, G. S. Fonseca, A. P. Umpierre, P. F. P. Fichtner, S. R. Teixeira (2002)	$[(1,5\text{-COD})IrCl]_2$ or [(1,5-COD)Ir(py)(PCy_3)]-$[PF_6]$ was reduced under 4 atm H_2 at 75 °C in [bmim][PF_6]	Cl^- present; TEM shows extensive agglomeration; IL not predicted to stabilize by DLVO theory or through steric stabilization—i.e., unknown stabilization mechanism *average composition and MW unknown*	214
C. W. Scheeren, G. Machado, J. Dupont, P. F. P. Fichtner, S. R. Texeira (2003)	Pt_2(bis-dibenzylidene acetone) was reduced with 4 atm H_2 in [bmim][PF_6]	Cl^- present in IL in ~1.4 mg/L levels as synthetic impurity; TEM shows extensive agglomeration; EDS was not able to determine the constituent elements of the colloids in IL *average composition and MW unknown*	216
H. Itoh, K. Naka, Y. Chujo (2004)	$HAuCl_4$ was reduced with $NaBH_4$ in the presence of an imidazolium-based dichloride IL	Cl^- present from precursor and IL; all colloids are in an aqueous solution with IL present; TEM shows a wide size distribution (no size distribution given); particles agglomerated with anion exchange *average composition and MW unknown*	218
C. C. Cassol, A. P. Umpierre, G. Machado, S. I. Wolke, J. Dupont (2005)	Chloropalladated propargyl amine was reacted with a large excess of dimethylallene in CH_2Cl_2	One equiv Cl^- present per equiv Pd; TEM shows agglomeration; no elemental analysis done *average composition and MW unknown*	219
L. S. Ott, M. L. Cline, M. Deetlefs, K. R. Seddon, R. G. Finke (2005)	$[(1,5\text{-COD})Ir(CH_3CN)_2][BF_4]$ was reduced in acetone with varying equivalents of imidazolium-based ILs	Increased solution stability observed with increasing equivalents of IL; ^2H NMR evidence of *N*-heterocyclic carbene formation from the imidazolium cation; carbene implicated as stabilizer *average composition and MW unknown, but nature of stabilizer from ILs elucidated*	239
L. S. Ott, S.	$[(1,5\text{-COD})IrCl]_2$ was	1 equiv IL poisons previously active nanocluster	91

Campbell, K. R. Seddon, R. G. Finke (2006)	reduced with H_2 in acetone, neat IL, or acetone plus 0-5 equiv IL	catalysts in acetone *average composition and MW unknown, but nature of poison from ILs implicated*

3.1 Electrostatic/DLVO-type stabilization

The classic theory of electrostatic colloidal stabilization was developed by Derjaugin, Landau, Verwey, and Overbeek, and is commonly referred to as DLVO theory [92]. Concisely stated, DLVO theory predicts that nanocluster stabilization is based on a delicate balance in interparticle forces between repulsive Coloumbic forces opposing attractive van der Waals forces. This theory was developed in the 1940s, is the most commonly used for, and seems to be the most accurate predictor of, the stability of so-called lyophobic colloids—colloids that are defined as having weak or no interactions between the colloid and the solvent [92] (the antithesis of lyophilic, putatively "solvent-only" stabilized colloids). Indeed, it was recently stated that "For colloid science the theory of DLVO stands at the same level of importance as does Darwin's theory of the origin of the species in Biology [93]" (with the understanding that the overall importance of DLVO theory is not being claimed to be at the same level as Darwin's theory of evolution!).

In DLVO-type electrostatic stabilization, the stabilizer of initial if not primary interest is the anion [76], as shown pictorially in Figure 1. Anions, whether added to the solution separately or present from reduction of a metal salt precursor, will be bonded to any previously coordinatively unsaturated, electrophilic nanocluster surface [27]. Hence, anions form a layer immediately adjacent to the nanocluster, providing the Columbic repulsion component of DLVO-type stabilization between two now anionically charged particles, Figure 1. Countercations are also present, to provide charge balance and

complete the electronic multi-layer. DLVO theory treats counterions as point charges, so small monoanions such as halides are among the closest "real-life", albeit still imperfect, examples of DLVO-type stabilization.

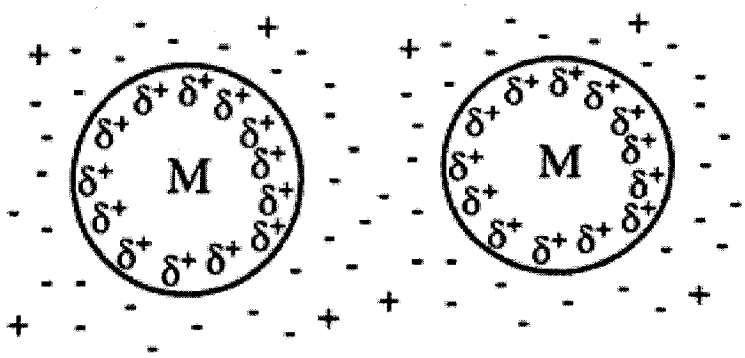

Figure 1. Pictorial representation of two electrostatic/DLVO-type stabilized nanoclusters. The partial positive charge shown on the surface of the nanoclusters results from the electrostatic charge mirror generated from the attraction of anions to the coordinatively unsaturated, electrophilic nanocluster surfaces. Note that this cartoon, initially published elsewhere [9], has an exaggerated, non-charge-balanced emphasis on the anions to illustrate their importance. Reprinted with permission from reference [9]. Copyright 2002 American Chemical Society.

In the DLVO picture of colloidal stability, another important factor is the thickness of the Debye layer ($1/\kappa$). The Debye layer refers to the layer(s) of counterions surrounding the colloid, these ions being separated by solvent molecules. The thickness of the Debye layer affects the stability of the nanoclusters—generally, thicker Debye layers provide greater interparticle distances, reducing potentially agglomerative attractive van der Waals forces between the particles and increasing the nanocluster stability. The equation for the thickness (calculated in m; however, $1/\kappa$ values are typically on the order of nm) of the Debye layer, $1/\kappa$, is as follows (see equation 3.8.13a on p. 134 of reference [94];).

$$1/\kappa = ((\varepsilon_0 \times \varepsilon_R \times k \times T)/\sum_i (z_i e)^2 \times c_{i_0}))^{0.5}$$

Above, ε_0 is the permittivity of free space, ε_R is the dielectric constant of the medium (the solvent), k is the Boltzmann constant, T is the temperature, z_i is the ion valency, e is the charge on an electron, and c_{i0} is the concentration of the ion species, *i*, in the bulk solution [94]. Of note with regard to the Debye layer is the prediction that a thicker diffuse layer—and consequently better stabilization—will be achieved in the presence of *high dielectric constant* solvents. This DLVO theory prediction has been investigated elsewhere [95] using solvents of varying ε. It was found that the DLVO theory prediction generally follows even for the case of the traditionally weakly coordinating anion BF_4^-, with polar, high ε solvents like *N*-methylacetamide (ε=165) and propylene carbonate (ε=69) [39] providing considerably more stable nanoclusters than lower ε solvents such as acetone (ε=20) [95] even though BF_4^- is far from the idealized point charge.

Care must be taken to apply DLVO theory only to appropriate nanocluster systems [93,96]. DLVO theory was not designed to account for counterions with multiple charge or sterically stabilized systems. Additionally, DLVO theory does not appear to work well in more concentrated systems (> 5 $x10^{-2}$ M), where dispersion forces (induced dipole-induced dipole interactions) may dominate electrostatic forces [96]. It is also not possible to find "real-life" examples of ideal, exactly DLVO-type *point charge* electrostatic stabilization since no such ions actually exist. Perhaps for these reasons, DLVO theory continues to be widely discussed and somewhat controversial [97,98,99], including, for example, the addition of so-called "extra-DLVO" forces [96] (including hydrogen bonding and the hydrophobic effect, hydration pressure, non charge-transfer Lewis acid/base interactions, and steric interactions [99]). In spite of the limitations discussed above, DLVO theory (i) is the first place one should turn in thinking about

electrostatic colloidal/nanocluster stability, and (ii) does correctly predict that discussions of nanocluster stability should start with coordinating *anions plus high dielectric constant solvents* [95,103,180].

3.2 Steric Stabilization

As mentioned earlier, one mode of nanocluster stabilization not a component of DLVO theory is steric stabilization. In some sterically stabilized systems, the surfaces of the nanoclusters may be ligated (e.g., in one limit by strong ligands such as thiols [100] or carbonyls [101]). Very small ligand-stabilized clusters, such as $Ir_4(CO)_{12}$, can be considered ligand–stabilized as well as ligand–*poisoned* clusters—that is, they possess coordinatively saturated, 18 electron metal centers and are not catalytically active. However, larger nanoclusters or colloids with surface bound ligands may still be catalytically active provided some fraction of the surface sites remain coordinatively unsaturated.

3.2.1 Polymers

One of the most frequently studied types of steric stabilization is stabilization by polymers. Polymers stabilize at least in part by ligation of nanocluster surface atoms, but also by physically occupying space around the nanoclusters, thereby sterically discouraging direct contact between the nanoclusters. *However, there is little direct evidence for the latter mode of polymer stabilization.* Nanoclusters of many transition metals (including Au, Ag, Pd, Pt, and Ir, among others) have been prepared with a variety of polymeric additives, the two most frequently employed polymers being

poly(vinylpyrrolidone) and poly(vinyl alcohol) (*vide infra*). A survey of the literature indicates that above a "critical" amount of polymer, the stabilization is independent of the quantity of polymer used; however, it has been shown that the polymer chain *length* does have some influence on the stability of Ni colloids [102]. However, many polymers contain adventitious water [103], leading to compositionally ill-defined nanoclusters that may contain surface H_2), OH^-, or O^{2-} ligands. Studies elsewhere show that the amount of H_2O in the polymer influences both the formation and stabilization of prototype $Ir(0)_n$ nanoclusters [103,104], but also that this water can be effectively removed by drying the polymer over activated molecular sieves for ≥12 h [103]. In addition, metal halide nanocluster precursors are often used, raising the issue of a coordinated halide, DLVO-type contribution to stability rather than the assumed polymeric (steric) stabilization. A drawback of polymer-stabilized nanoclusters is that polymeric coordination (for example, with the strongly coordinating polymer poly(vinylpyridine) [105,106,107,108]) or steric blocking of the surface atoms may compromise the catalytic activity.

Another little studied or even cited issue is that polymer stabilization is typically written as if one polymer chain stabilizes one nanocluster. In fact, *one would expect longer polymers to attach to more than one nanocluster*, and Taylor dispersion measurements (of the hydrodynamic radius of the nanoclusters in solution) indicate that one polymer chain can in fact attach to multiple nanoclusters [109], as illustrated pictorially in Figure 2 below. The nanocluster science community would be well served if Taylor dispersion measurements on nanoclusters [109] were much more common.

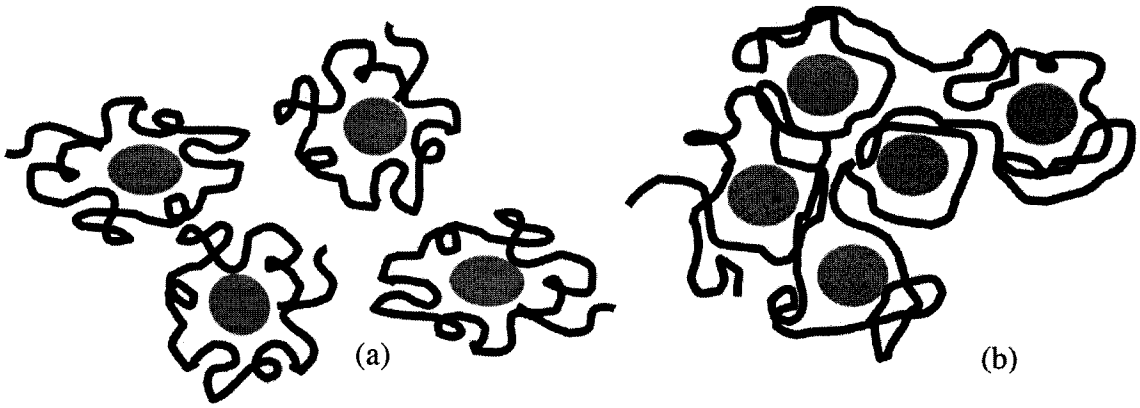

Figure 2. A cartoon of two possible polymeric stabilization modes. Part (a) shows stabilization of nanoclusters with individual polymer chains as often assumed in the literature, while part (b) shows stabilization of multiple nanoclusters by a single polymer chain as supported by Taylor dispersion measurements [109].

The most commonly used polymeric nanocluster stabilizer is poly(vinyl pyrrolidone) (PVP). There is an extensive literature documenting the use of PVP as a nanocluster stabilizer [110], including a classic study of colloids of several metals stabilized with PVP by Hirai et al in 1979 [110a]. PVP-stabilized nanoclusters have been shown to be active in several catalytic reactions, including hydrogenation [105,110a,111], the Suzuki reaction [112,113], and the Heck reaction [114]. However, these PVP-protected nanoclusters are frequently prepared in water beginning with chlorinated precursors (such as $RhCl_3 \bullet H_2O$ [110a] and $HAuCl_4$ [115]), leading, once again, to the possibility of halide stabilization and compositionally ill-defined colloidal surfaces. Additionally, as in prototype PVP-stabilized nanoclusters [110a], an alcohol is frequently used as both solvent and reducing agent. Again, this leads to compositionally ill-defined colloid surfaces which may be coordinated by alkoxy molecules or possibly the resultant oxidized carbonyl product (e.g., H_2CO from CH_3OH or oligomers of H_2CO).

The 5 criteria method outlined earlier has also been employed to test PVP for its ability to stabilize $Ir(0)_n$ nanoclusters [104]. PVP was tested as a steric stabilizer (but in

the presence of BF_4^- from the decomposition of the organometallic precursor [(1,5-COD)Ir($CH_3CN)_2$][BF_4]), and in combination with the $P_2W_{15}Nb_3O_{62}^{9-}$ polyoxoanion (electrostatic) stabilizer (Figure 2, *vide supra*). Additionally, four other polymeric nanocluster stabilizers reported previously were investigated with the 5 criteria method, specifically poly(methyl methacrylate) (PMMA) [116], poly(styrene) (PS) [117], poly(methylhydrosiloxane) (PMHS) [118], and poly(bis(ethoxy)phosphazene) (PBEP) [119], all of which have been implied to be excellent nanocluster stabilizers [116,117,118,119]. The main findings are that : (i) using dried polymers is important for preparing transition-metal nanoclusters in (dry) organic solvents; (ii) 1 equiv of BF_4^- plus the high dielectric constant solvent propylene carbonate provides at least as much nanocluster formation and stabilization ability as does 1 equiv of dried PVP; (iii) adding 40 equivs of dried PVP plus having 1 equiv BF_4^- present is necessary to achieve isolable and redissolvable $Ir(0)_n$ nanoclusters; (iv) 40 equiv dried MW_{ave}=10,000 g/mol PVP plus 1 equiv BF_4^- is inferior for *both* nanocluster *formation and stabilization* when compared to then current "Gold Standard" (poly)anion of 1 equiv $P_2W_{15}Nb_3O_{62}^{9-}$, at least for $Ir(0)_n$ nanoclusters and under the conditions of 22 °C and 40 psig H_2 in propylene carbonate; (v) 40 equiv dried PVP added to nanoclusters stabilized by 1 equiv $P_2W_{15}Nb_3O_{62}^{9-}$ *slows* the catalytic activity and total catalytic lifetime by ca. 50%; and (vi) of the four other polymers, PMMA was the most similar to PVP in providing a modest level of stabilization as measured by the 5 criteria—PS, PMHS, and PBEP were all found to be ineffective for the formation and stabilization of catalytically active $Ir(0)_n$ nanoclusters.

Separately, poly(vinyl alcohol) (PVA) has also been studied as a steric stabilizer, beginning with the work of Rampino and Nord in 1941 on Pd and Pt colloids [120,121].

Since then, PVA has been used to stabilize nanoclusters of many different metals, including for example Ag [122,123] and Au [124]. Grätzel studied PVA-stabilized Pt colloids for their efficacy in oxidizing methyl viologen during the light-induced H_2 evolution from water as part of photo redox processes for solar cells [125]. PVA polymers in nanocluster systems have the potential to serve as both the reductant of the organometallic complex *and* the nanocluster stabilizer. Again, compositionally poorly defined nanoclusters are the rule to date in putative "PVA-stabilized" nanoclusters.

3.2.2 Siloxane Polymers

Recently, siloxane polymers (such as poly(octadecylsiloxane) (PODS) or poly(methylhydrosiloxane) (PMHS as above)) have been used to stabilize transition-metal nanoclusters [117,126,127,128]. In the first report of siloxane stabilized nanoclusters, PODS was used to stabilize Au, Pd, and Pt nanoclusters [126]. The silanol moieties on the partially condensed siloxane polymer were capable of reducing the Pd and Pt precursors, offering the advantage of simple reaction conditions. Though the condensed polymer is expected to provide some steric stabilization, TEM micrographs show *extensively agglomerated nanoclusters.* Additionally, the presence of H_2O, Cl^-, and in some cases EtOH complicates assignment of the true stabilizer and leads to compositionally ill-defined clusters [126]. In a series of other papers [117,127,128], PMHS was used to generate and stabilize Pd and Ag nanoclusters. The authors claimed that reduction of the organometallic precursor by the Si-H bonds present simplifies the reaction conditions; however, this possible advantage is overshadowed by the ill-characterized nature of the oxidized product/stabilizer as well as by the extensive

nanocluster agglomeration shown by TEM [117]. Additionally, after the nanoclusters were isolated from the solution, SEM showed that the average size of the nanoclusters had grown 6-8 fold from 6 ± 1 nm in solution to 40-50 nm in the solid state. Given the above evidence, it does not appear that siloxane polymers are superior steric stabilizers for transition-metal nanoclusters as claimed by others [117,127,128]. At the minimum, siloxane polymers are untested stabilizers, for example versus the alternative hypothesis that other common stabilizers are actually superior.

3.2.3 Dendrimers

Dendrimers have also been recently explored as structurally well-defined steric stabilizers. Most dendrimers employed for nanocluster synthesis and stabilization are nitrogen-based, such as poly(amidoamine) (PAMAM) and poly(propylene imine) (PPI) [129]. Dendrimers have been well-studied as nanocluster stabilizers, beginning with the pioneering work of Crooks et al. Crooks first reported the preparation of Cu nanoclusters in PAMAM dendrimers [130] in 1998, and this work has been expanded upon by his group [131,132,133,134,135,136,137,138] and others [139,140,141,142]. Dendrimers have a precisely branched, well controlled structure (with correspondingly difficult syntheses). It has been demonstrated by spectrophotometric titration [130] that the number of metal atoms adsorbed into the dendrimer interior corresponds to the number of interior tertiary amines. Adsorption of the metal ion on the *surface* amine groups of the dendrimer is usually undesirable, as the nanoclusters then formed on the exterior of the dendrimer are susceptible to aggregation via intermolecular collisions. Adjusting the pH of the dendrimer solution with HCl is a common method for protonating the exterior

amine groups and assuring the organometallic precursor is selectively adsorbed in the interior of the dendrimer [135]. Using dendrimers has the advantage of good size control of the nanoclusters by selecting the dendrimer with the precise number of interior tertiary amines (= desired number of nanocluster precursor atoms). Thus, the metal atoms are in the interior of the dendrimer before reduction and the newly formed nanocluster has a dendritic stabilizer already in place [129], as in Figure 3. Dendrimers have, therefore, some very nice architectural features useful in preparing nanoclusters.

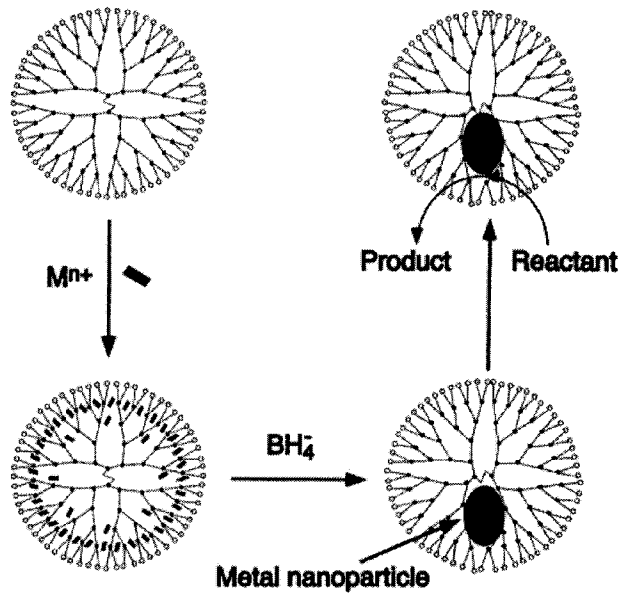

Figure 3. Formation of dendrimer-encapsulated nanoparticles. Reprinted with permission from reference [129]. Copyright 2001 American Chemical Society.

However, there are also limitations when using dendrimers as steric stabilizers. The major drawback of at least early dendrimers was their limited solubility. Dendrimers such as the most commonly used PAMAM dendrimer are typically soluble in only a few solvents (such as water, alcohols, and weak acids, and usually only as a 1% solution after tumbling for 24 hours [143]), which greatly limits their utility. Preparing nanoclusters with well-defined surface compositions in alcoholic or weakly acidic solvents can be

problematic, as these solvent molecules may adsorb to the surface of the nanocluster leading to compositionally ill-defined clusters. Through the functionalization of the terminal groups of PAMAM, it is now possible to prepare dendrimer-encapsulated nanoclusters in organic solvents [138]. Although the method of preparation leading to intra-dendrimer nanoclusters has been shown to lead to stable nanoclusters [130,131,132,133,134,135,136,137,139,140,141,142] (including bimetallic nanoclusters [144,145]), their utility as catalysts may be diminished due to low substrate access caused by a dense layer of terminal groups in high generation dendrimers [146]. Additionally, the CS_2 poisoning method [147] to titrate the number of catalytically active sites has not been, but needs to be, performed for dendrimer-stabilized nanoclusters. A limited permeability of the dendrimer surface (and hence access for catalytic substrates) has been demonstrated by showing that thiols can extract Pd nanoclusters from the interior of PAMAM dendrimers [148]. Overall, the useful architectural features of dendrimers seem well established, but their utility as nanocluster stabilizers is diminished by their extremely limited solubility in common organic solvents [143] and their uncertain, perhaps sterically hindered, level of catalytic activity.

3.2.4 Microgels

Transition metal nanoclusters have also been suspended in sterically stabilizing microgels [149,150,151,152,153]. These cross-linked globular macromolecules have been shown to be competent nanocluster stabilizers, yielding in one case Pd nanoclusters of 2.3 ± 0.8 nm which serve as catalysts (or possibly catalyst precursors [154]) for the Suzuki reaction [152]. Similar Pd nanoclusters suspended in functionalized microgels

were shown to be catalytically active for the Heck reaction of activated aryl bromides [153]. However, microgels have a less precisely controlled structure than dendrimers, offering reduced control over the size and, presumably, also the desired properties of the nanoclusters. Hence, microgels do not appear to be preferred stabilizers for modern transition-metal nanoclusters where determining the composition of the resultant nanocluster is one key to understanding their stability.

3.2.5 Alkanethiol (and other) Surfactants

Of the surfactant stabilizers employed in the literature, alkanethiols are perhaps the most frequently employed (as recently discussed by Murray et al. [155]). Due to strong bonding between the RS^- group and the electrophilic nanocluster surface, alkanethiols become covalently linked to the nanocluster surface, making these *ligand* stabilized nanoclusters [155]. This coordination decreases the number of surface atoms available for catalysis. Thiol-stabilized Ag nanoclusters recently have been prepared using supercritical CO_2 as solvent; however, some of these nanoclusters had a wide size distribution of ± 92% [156]. It is not known if oxidation and RS-SR coordination to the surface of the nanocluster occurs as has been postulated for RS^-/Au self-assembled monolayers [157]. Additionally, catalytic conversion of thiols to disulfides has recently been reported for Ru nanoclusters [158]. Although some surfactant stabilized nanoclusters are catalytically active [159], surfactants are generally not preferred stabilizers for nanoclusters in catalysis as strong binding to the nanocluster surface may instead lead to ligand-*poisoned* nanoclusters (see Scheme 5).

3.2.6 Resorcinarenes

Resorcinarene molecules have recently been employed as stabilizers for metal nanoclusters [160,161,162,163,164,165,166,167,168]. Resorcinarenes, also called calix[4]resorcinarenes or resorcinol-derived calix[4]arenes [169], are surfactants with electrophilic macrocyclic headgroups, Figure 4. Often, resorcinarenes have either thiols (as in Figure 4) or hydroxy groups incorporated into the headgroup, and hence in their deprotonated form can be classified as steric (really, ligand) stabilizers. These resorcinarenes, with multiple adsorption points on the nanocluster surface, are believed to be more effective stabilizers than other surfactants with small, monodentate headgroups [161,165,166]. Little direct evidence exists, however, to validate this supposition. Resorcinarenes do display increased spacing between hydrocarbon chains relative to long, single hydrocarbon chain surfactants, resulting in improved steric repulsion between particles and reduced entropic cost of nanocluster stabilization through the need for fewer large resorcinarene molecules per nanocluster [160]. Nanoclusters with resorcinarene stabilizers are prepared by generation as aerosols [160,165], citrate reduction of the organometallic precursor [161,166] or thermolysis [164] followed by extraction into organic solutions containing resorcinarene molecules. In some cases, near-monodisperse 34 ± 2 nm Au nanoclusters were observed by TEM [160]. When chloride-containing organometallic precursors are used [161,166] it is again likely that the nanoclusters surface is passivated by at least some Cl^- as well as resorcinarene molecules, a point which remains to be experimentally investigated.

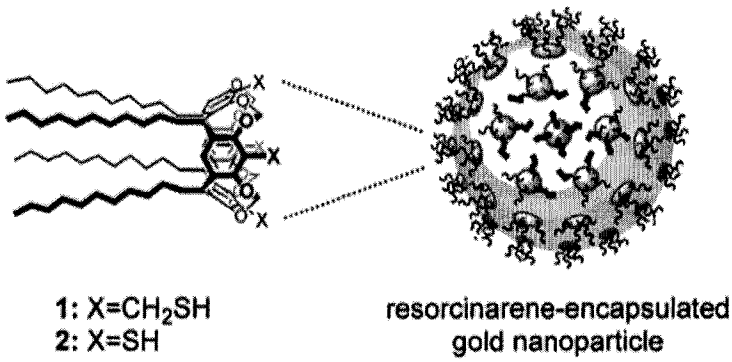

Figure 4. An example of a tetrathiolated resorcinarene, and a model for their ligation of an Au nanoparticle. Reprinted with permission from reference [166]. Copyright 2002 American Chemical Society.

However, to date stabilization by resorcinarenes has only been demonstrated for Au and Co nanoclusters. Additionally, resorcinarene stabilization is insufficient to allow complete redissolution of isolated nanoclusters [163,166] indicating a failure in one of the key goals of nanocluster science [26], the synthesis of "bottleable" nanoclusters that can be made, stored in the solid state, then weighed out at any desired time later in any desired amount like other, well-established, optimum chemicals. Although one of the claimed benefits of using resorcinarenes as stabilizers is increased availability of catalytically active surface atoms, there are no reports of catalytically active nanoclusters stabilized by resorcinarenes. Accordingly, again missing is the needed comparison of the catalytic activity *per exposed metal* [147] to the most active nanoclusters, for example by the previously cited CS_2 poisoning method [147]. Comparisons of catalytic activity per exposed metal atom are needed for all future claims of high catalytic activity of all nanoclusters [147].

3.2.7 Amines and Phosphines

Long-chain amines and phosphines provide another example of steric ("ligand") stabilization of nanoclusters. For example, amines and phosphines have been used in the preparation of Au [82], Ni [170], Ru [158], Co [171], and Pd [172] colloids. However, these stabilizers do not appear to be superior, since "superstructures" of colloids are often formed [158,172]. These "superstructures," upon inspection of the TEM micrographs, are really just agglomerates of smaller clusters. This extensive agglomeration indicates ineffective stabilization. Additionally, *none* of these studies performed the needed TEM controls of examining the precursor under the electron beam to check for colloidal formation and/or agglomeration during TEM analysis [49,51,52], especially important for lighter metals such as Ni and Co. Direct, *in situ* molecular weight measurements using ultracentrifugation [14] are needed to confirm or refute the presence of such "superstructures" in solution vs. as an artifact of the TEM preparation or observation.

3.2.8 Branched Polymers

Yet other examples of steric stabilization can be found in hyperbranched polymers such as aramids [173,174] and polyglycerols [175]. However, hyperbranched polymers such as polyglycerols have a less well-defined (e.g., when compared to dendrimers), and usually uncontrolled, structure. Nonetheless, polyglycerols stabilizers yielded Pd nanoclusters that were stable in solution for months and capable of catalyzing the hydrogenation of cyclohexene at a rate claimed faster than a commercial supported Pd/activated charcoal catalyst [175]. Unfortunately, again the needed catalytic rate *per exposed Pd* for each system, as required for a rigorous comparison of their activities, is not available [147]. Hence, the claim of a superior rate to the commercial Pd catalyst

remains undocumented. Polyaramids were also used to stabilize Pd nanoclusters, yielding nanoclusters with an average diameter of 3.2 nm (no size distribution was given). Though catalytically active for the hydrogenation of a wide variety of olefins, TEM micrographs show that these nanoclusters are agglomerated [173]. Hence, branched polymers do not appear to be superior steric stabilizers.

3.2.9 Summary

In summary, steric stabilization of colloids and nanoclusters has proved useful since the 1940s [120,121], and will likely find continued utility in the future. However, finding the *optimum* steric stabilizer that yields compositionally well-defined, highly stable, isolable and redissolvable nanoclusters that retain high catalytic activity remains an important, unsolved problem.

3.3 "Electrosteric" Stabilization

In the literature, many authors have combined the two well-precedented modes of nanocluster stabilization into so-called "electrosteric" stabilization. Tracking down the origin and a clear definition of this term proved difficult. It is mentioned in a 1983 text [78] on the polymeric stabilization of colloids: however, in that text there are also several vague references to earlier use of "electrosteric" stabilization in biological systems. As the term "electrosteric" implies, this mode of stabilization is actually a combination of electrostatic stabilization (as described in DLVO theory) and steric stabilization. Electrosteric stabilizers have the potential to be superior for catalytic applications, as the combination of electrostatic and steric stabilization *may* mean that fewer equivalents of

stabilizer per nanocluster are necessary for stabilization, *possibly* leaving more coordinatively unsaturated surface atoms available for catalysis. Note, however, that one weakness in the description of "electrosteric" is that there is neither a clear definition of an "electrosteric" stabilizer nor a cut-off as to when a stabilizer is large enough to be "electrosteric" *vs.* a DLVO-type stabilizer.

The first report on polyoxoanion-stabilized nanoclusters noted that the $P_2W_{15}Nb_3O_{62}^{9-}$ and associated $(Bu_4N)_9^{9+}$ stabilization of $Ir(0)_{\sim 300}$ nanoclusters was of apparently a novel type— a "combined high charge plus significant steric bulk present intrinsically" [14] within the (large, ca.15 Å by 12 Å [27]) polyoxoanion and nine (large) Bu_4N^+ countercations (see p. 8342 elsewhere [14]), recall Figure 2 (vide supra); $P_2W_{15}Nb_3O_{62}^{9-}$ has now been used to stabilize both Ir [6,9,10,11,12,14,76,176,77] and Rh [15,50,147] nanoclusters. Hence, it would be tempting to term these highly charged, sterically massive stabilizers as prototype "electrosteric" stabilizers.

A 2002 study employing the 5 criteria method found that these potentially "electrosteric" $P_2W_{15}Nb_3O_{62}^{9-}$ stabilizing anions (with Bu_4N^+ countercations, Figure 5) were superior for the *formation and stabilization* of $Ir(0)_{\sim 300}$ nanoclusters, in comparison to $SiW_9Nb_3O_{40}^{7-}$, $C_6H_5O_7^{3-}$ (citrate), $[-CH_2-CH(CO_2^-)-]_n^{n-}$ (poly(acrylate)), OAc^-, $P_3O_9^{3-}$ (trimetaphosphate), Cl^-, and OH^-. Specifically, the results of the 5 criteria methods for $P_2W_{15}Nb_3O_{62}^{9-}$ were: (i) a high level of kinetic control during the nanocluster formation reaction, as reflected by a large value of $\sim 10^5$ for the k_2/k_1 ratio for autocatalytic growth (k_2) to nucleation (k_1); (ii) the formation of near-monodisperse nanoclusters as verified by TEM (often displaying a size dispersion of <14%, impressive for a self-assembly reaction involving > 300 steps; for more details on nanocluster formation see reference [8] and

earlier references therein); (iii) the ability to isolate (from solution) and bottle the nanoclusters for future use, the $P_2W_{15}Nb_3O_{62}^{9-}$ stabilized nanoclusters being taken to dryness and redissolved with no discernable agglomeration by TEM;[7] (iv) the catalytic activity of 2.2 mmol H_2/hr at 22 °C and 40 psig H_2[8] of the isolated nanoclusters once redissolving them in solution with fresh substrate (in a separate preparation of $P_2W_{15}Nb_3O_{62}^{9-}$ stabilized, isolated, bottled, and redispersed $Ir_{\sim 2000}$ nanoclusters, 65% of the initial hydrogenation activity was retained [176]); and (v) a total catalytic lifetime in solution of 68,000 total turnovers (TTOs) of cyclohexene hydrogenation without the formation of visible bulk metal). A pictorial representation of $P_2W_{15}Nb_3O_{62}^{9-}$ polyoxoanion-stabilized nanoclusters is shown in Figure 5.

[7] The fact that these nanoclusters can be taken to dryness and subsequently redispersed indicates that they lack a so-called critical coagulation constant (ccc). Classical colloids possess a ccc: upon adding electrolyte (thus compacting the protective electrical double layer), the colloids become unstable and precipitate from solution. The lack of a ccc in the case of selected nanoclusters, for example the above-mentioned $P_2W_{15}Nb_3O_{62}^{9-}$- and tetrabutylammonium-stabilized nanoclusters, indicates that they possess an unusual stability with respect to most classical colloids [9].

[8] This cited initial hydrogenation rate has not been corrected for the number of *active* surface sites on the nanoclusters. However, the percentage of active surface atoms with respect to the total number of atoms has recently been shown to be ca. 2.4% for larger, $Ir(0)_{\sim 2000}$ $P_2W_{15}Nb_3O_{62}^{9-}$- and tetrabutylammonium-stabilized Ir(0) nanoclusters [176].

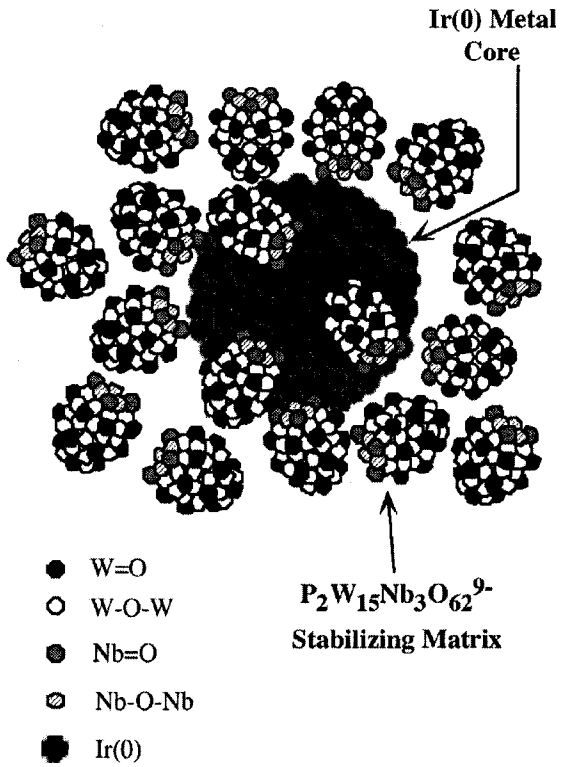

Figure 5. Idealized, roughly to scale representation of a $P_2W_{15}Nb_3O_{62}^{9-}$ polyoxoanion and Bu_4N^+ stabilized $Ir(0)_{\sim 300}$ nanocluster. For the sake of clarity, only 17 polyoxoanions are shown and the Bu_4N^+ cations have been omitted. The polyoxoanions are of course actually coordinated to the $Ir(0)_{\sim 300}$ nanoclusters, although this is not illustrated in this particular representation. Reprinted with permission from reference [15]. Copyright 2001 American Chemical Society.

The case of $P_2W_{15}Nb_3O_{62}^{9-}$– and Bu_4N^+–stabilized Ir(0) nanoclusters is of special note as this system is one of the few *compositionally well-defined* nanocluster systems. The nanocluster composition was established by full elemental analysis and analytical ultracentrifugation molecular weight measurements [14]. Additionally, electrophoresis measurements demand that the 9^- anions are on the surface of the neutral Ir(0) core [14]. These nanoclusters have a balanced stoichiometry of formation [14], have been scaled up [176], are isolable and "bottleable" [9,10], and have had the number of active sites determined by CS_2 poisoning [176]. More compositionally well-defined nanocluster

systems such as this system and the others listed in Table 1 are needed for nanocluster science to proceed more efficiently.

Other groups have also picked up the idea of "electrosteric" polyoxoanion stabilizers [177,178,179]. However, there remains confusion about claims whether or not non-basic polyoxoanions such as $PW_{12}O_{40}^{3-}$, $SiW_{12}O_{40}^{4-}$, or $P_2W_{18}O_{62}^{3-}$ are stabilizers (as their Bu_4N^+ salts) [14]. Note that these classic types of polyoxoanions are non-basic (they formally have zero surface-charge density as rewriting these anions as $(PO_4^{3-})(W_{12}O_{36}^{0})$, (SiO_4^{4-}) $(W_{12}O_{36}^{0})$, and $(PO_4^{3-})_2(W_{18}O_{54}^{0})$ shows). Hence, these classic types of polyoxoanions have little surface anionic charge density at least formally, and they have been tested and found not to stabilize $Ir(0)_n$ nanoclusters [14]. This "non-stabilization" result has been repeated recently for $PW_{12}O_{40}^{3-}$ and $P_2W_{18}O_{62}^{3-}$ in acetone with the known nanocluster precursors $[(1,5\text{-COD})Ir(CH_3CN)_2][BF_4]$ and Pd_2(bis-dibenzylidene acetonate)$_3$ with the finding that the original result [14] is repeatable: bulk metal, not well-stabilized nanoclusters, are the end result [14,180]. It is not clear why others continue to claim that these nonbasic polyoxoanions are good stabilizers [79]. Studies of potentially tetradentate-oxygen ligand stabilizers $PW_{11}O_{39}^{7-}$ and $P_2W_{17}O_{61}^{10-}$ have been reported [181,182,183,184,185] and are being extended by the 5 criteria method [186], as these polyoxoanions do have surface oxygen basicity and should be decent, perhaps superior, stabilizers.

Returning to the subject of what is an "electrosteric" stabilizer and what is not, and also given that DLVO theory treats anions as point charges, anything larger than a point charge (i.e., *everything*) would be classified as an electrosteric stabilizer. The main problem with the term "electrosteric," then, is its ill-defined nature and seemingly too-

broad definition. Whether or not the term "electrosteric" should remain in the literature as a mode of nanocluster stabilization remains to be seen—however, due to the widespread use of the term, we felt it prudent to give some examples of why the term "electrosteric" remains in use and our recommendations for its use. On reflection, we do recommend the use of "electrosteric stabilizers" but suggest that the term be reserved for examples that have both multiple charge (> 1^-) and steric bulk in one dimension at minimum of one quarter the size of the nanocluster (for example, a 5 nm nanocluster would require an "electrosteric" stabilizer of $\geq 2^-$ with one dimension of the stabilizer being ≥1.25 nm).

4. On Novel Modes of Nanocluster Stabilization

In the literature, there are several postulated mechanisms for nanocluster stabilization that are not addressed by electrostatic, steric, or electrosteric stabilization. Most of these claimed stabilization schemes need to be more carefully evaluated, as will be detailed below. A recurring theme in the following examples— indeed, in almost all of the nanocluster stabilization literature except for a handful of important papers (see for example references [14], [15], [82], [83], [86] in Table 1)— is the need for *compositionally well-defined* nanoclusters so that the putative stabilizers *that are actually present* are known. Additionally, and as noted earlier, *in situ* nanocluster solution "stability" is often assessed only by TEM, an *ex situ,* solid state technique. Much greater use of (i) the 5 criteria method of evaluating stabilizers [9,10], (ii) an agglomeration-based, quantitative kinetic method for evaluating stabilizers [75], and (iii) *in situ*

techniques such as XAFS and SAXS are needed prior to any claim that a superior stabilizer has been invented and/or discovered.

4.1 Putative Cationic Stabilization

A literature hypothesis is that modern transition-metal nanoclusters can be stabilized by tetraalkylammonium *cations*[9] [38, 159,187]. Notably, a widely cited *Science* paper [187] assumes that R_4N^+ cations are directly coordinated to Ag particle surfaces.[9] However, cationic stabilization is counterintuitive, given that positively charged cations (with no free electron pair to serve as a ligand) should not be attracted to the *electrophilic* nanocluster surfaces (as posited and pictorially shown in reference [188], reproduced in Figure 6 below), a point that has been corrected in the literature [27]. Despite this correction, there are many reports of nanoclusters prepared in the presence of tetraalkylammonium halides wherein the nanoclusters are judged to be stable and the *cation* is claimed as the stabilizer [38,39,187,188,189]. In many of these studies [38,39,187,189], the authors fail to consider the effects of the *halide* (present in 5-6% by elemental analysis of the nanoclusters after being taken to dryness [38]) which DLVO theory predicts will be drawn to the (electrophilic) nanocluster surface [92]. Following a correction of this [9,27], in more recent contributions, it has been recognized that in the

[9] The belief that the cationic component of a surfactant is the stabilizer appears to have some roots in a 1979 *J. Am. Chem. Soc.* paper [125]. In that paper, the authors report "for the first time that a surfactant acts as a protective agent for metal platinum". However, significant sources of Cl^- exist therein from both $PtCl_4$ and the cetyltrimethylammonium chloride surfactant employed. The myth that R_4N^+ cations may be directly coordinated to the nanocluster surface is traceable to a 1988 paper employing surface enhanced Raman scattering on poorly characterized Ag colloids (J. Weisner, A. Wokaun, H. Hoffmann, Prog. Colloid Poly. Sci. 76 (1988) 271). While that paper implies that the long-chain amines are present on the Ag surface, the authors recognize that the binding of a *cationic* amine to a *cationic* Ag^+ surface "must imply the intermediacy of...the Br^- counteranion." Unfortunately, others [187] incorrectly cite this paper as providing evidence for R_4N^+ coordination to a nanocluster surface, apparently since they just refer to the misleading figure (Figure 3 of the Prog. Colloid Poly. Sci. paper cited above) rather than carefully reading the text noted above.

case of Pd colloids prepared in the presence of long-chain $[R_4N][Cl]$ compounds that Cl^- is "the more appropriate stabilization mode" [190,191] as detailed in the right-hand side of Figure 6.

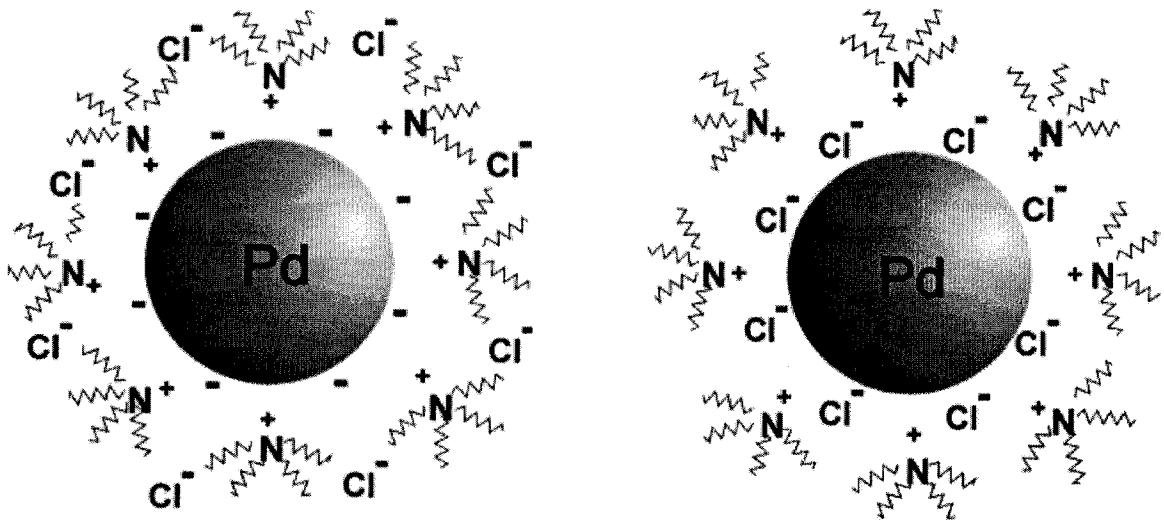

Figure 6. Two literature representations of nanocluster stabilization by bound anions plus surrounding R_4N^+ surfactant [190]. In the figure on the left, the nanocluster is assumed to bear negative charge [190]. In the figure on the right, the neutral metal core is surrounded by Cl^- anions that provide DLVO-type stabilization [190]. Also of note in this figure and others by the same group is the incorrect, square-pyramidal representation of the four alkyl ligands on the ammonium cation and the incomplete charge balance. Reprinted from reference [190] with permission from Elsevier.

In another similar case, the hypothesis that the cation is the nanocluster stabilizer is paired with an *assumption* that the surface of Group 6-11 nanoclusters bore negative charge after being reduced by tetraalkylammonium hydrotriorganoborates [38]. However, elemental analysis of a sample of a putatively tetraoctylammonium-stabilized palladium nanoclusters shows 3.98% Br^- is present [38]. With a mean particle size of 4.8 nm [38], approximately 26% of the Pd atoms are on the surface [192]. Back-of-the-envelope calculations indicate this particle size and Br^- content would yield

approximately 1 Br^- atom for every 3 Pd surface atoms, which is probably sufficient to provide electrostatic stabilization. The evidence (NMR, MS, and elemental analysis) indicating of the presence of the tetraoctylammonium cation in the isolated material is consistent with the multilayer of anions surrounding the nanocluster as *predicted by DLVO theory* [92]. In later papers by the same group, post the correction provided elsewhere [9,27], the stabilizers is assigned as "$R_4N^+X^-$", thereby acknowledging the role of the halide [193].

DLVO theory predicts that large cations, such as tetraalkylammoniums, should have a contribution to the stability of electrostatically stabilized systems by expanding the diffuse layer of ions around the colloid and hence increasing the thickness of the Debye layer [92]. However, and again as DLVO theory predicts, the *anions* should be the primary source of stabilization for the electrophilic nanoclusters. The cationic stabilizer assumption has been propagated through the literature from its apparent beginning with the miscited Ag surface-enhanced Raman scattering (SERS) paper [187], even appearing in electrochemistry textbooks [194]. As argued elsewhere, "propagation of this apparent myth should be stopped until, and unless, direct, compelling evidence for a non-anion-mediated, direct R_4N^+ nanocluster interaction is forthcoming" [195].

4.2 Putative Solvent-Only Stabilization

Another putative type of stabilization in the recent literature is "solvent-only" stabilization [39,196,197,198,199,200,201,202,203,204]. This type of stabilization is in theory attractive, with *potential* benefits including availability of surface sites for catalysis in the absence of strongly coordinated ligands, simplicity of reaction conditions,

and avoidance of surface contamination. However, there is no clear source of stabilization in claimed "solvent-only" stabilized systems, as by definition such "solvent-only" systems must lack the ions necessary for DLVO-type stabilization and also have no bulky, tightly bound ligands that would qualify as steric stabilizers. As in the case of claimed cationic stabilization discussed above, in "solvent-only" stabilization *halides are often present* [196,199] so that the alternative hypothesis of halide-mediated DLVO-type stabilization has, again and unfortunately, not been disproved or, often, *even considered.* Additionally, there are frequently other nanocluster stabilizers and/or contaminants present, such as acetate [200], hydroxide [199], alcohols [197,200], water [200], and others [198,203].[10] In fact, in one study it was noted that a "passivating oxide layer" was detected by both x-ray diffraction (XRD) and x-ray photoelectron spectroscopy (XPS) [197], this oxide layer in our view likely being the main source of nanocluster stability.[11] Hence, it is likely that the nanoclusters are not solely "solvent-only" stabilized. They are likely often anion, oxide coating [205,206,207,208,209,210,211], or otherwise stabilized. Note in this regard, at least for small organometallic clusters, "solvent-only" clusters are unknown: that is, "$Ir_4(solvent)_{12}$", analogous to the well-known, stable, and soluble

[10] In these final two cases, the only solvents that yielded nanoclusters were ketones. These ketones may participate in a limited stabilization by undergoing keto-enol tautomerism followed by deprotonation to yield, initially, an alkoxide stabilizer which may then undergo further conversion as in Scheme 6 below for the specific example of acetone. Interestingly, an impurity in acetone has been shown to lead to an increased rate of hydrogenation catalytic activity for $Ir(0)_n$ nanoclusters, but remains unidentified despite considerable effort to uncover its identity (see p. 10-13 of the Supporting Information elsewhere [14]).

Scheme 6. Potential stabilization of M(0) species by ketones.

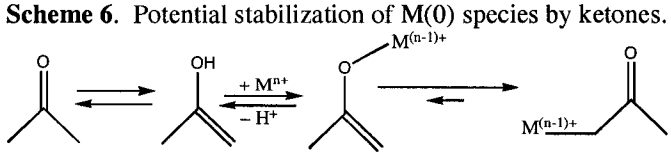

[11] The O_2 sensitivity of nanoclusters has been little studied. However, recent work in showed that Ir(0) nanoclusters stored in the drybox display a greater-than-expected, *apparent* oxygen sensitivity, losing almost 90% of their activity during the course of a year [176]. Of note is that nanoclusters of all metals are expected to show much more air sensitivity than their bulk metal counterparts due to the nanoclusters' higher surface area, their higher energetic nature (i.e., their less negative $\Delta H_{formation}$), and, hence, their greater reactivity towards ligands such as O_2 [176].

$Ir_4(CO)_{12}$, does not exist at least as present as even a meta-stable molecule—although $M_4(stabilizer)_n^{x-}$ clusters may be a new, control target in (sub) nanocluster chemistry and catalysis [71].

As an example of "solvent-only" stabilization, putatively THF-stabilized "$Ti(0)_n$" nanoclusters were prepared by $K[BEt_3H]$ reduction [196]. However, the possibility of stabilization by Cl^- was not considered despite a Cl content of 8.5% by elemental analysis [196]. Also, KCl was observed in the X-ray diffraction pattern of the isolated metal colloid. In addition, the use of BH_4^- as a reductant invariably leads to the presence of a few percent of B in the resultant nanoclusters (for example, Zr colloids prepared as part of the abovementioned study contained 3.7% B [196]). Despite this evidence, the authors concluded that stabilization of the Ti nanoclusters resulted from a combination of coordinated THF and surface hydrides. Again, the problematic trend of interpreting one's data only in terms of one's original hypothesis is apparent, as well as the pattern of a lack of disproof of alternative hypotheses that is required for good, efficient science [79]. Also, the need for *compositionally well-defined* nanoclusters is once again re-emphasized: a complete understanding of the composition of one's nanoclusters *must* be in hand before one can postulate all possible alternative hypotheses [79] on how the nanoclusters might be stabilized, followed by the necessary attempts at disproof of each of those alternative hypotheses. What's left, often necessarily interpreted with the aid of the conditional exclusion we call "Ockham's Razor" [212] is, then, the experimentally supported stabilization modes(s).

Chaudret and co-workers have also reported several cases of "solvent-only" stabilized nanoclusters [197,201]. One clever design feature in these systems is that they

are prepared with the anion-free precursor [Ru(COD)(COT)] (where COT=cyclooctatriene) in THF plus varying but predetermined equivalents of MeOH. The use of this precursor excludes from the start the alternative hypothesis that anions are contributing to the stability of the system. However, employing alcoholic solvents such as methanol leads to the possibility that the alcohol can serve as both the reductant and subsequently as at least the possible stabilizer in their deprotonated, alkoxy form. Instead, ill-defined stabilizing "nanoreactors", "vesicles", or "pockets" are hypothesized to be formed with cyclooctane (as a byproduct of the decomposition of the precursor) in mixed ROH/THF solvents, all without compelling evidence [197,201]—the primary evidence based on TEM and other *ex situ* solid state techniques. Note also here that another alternative hypothesis not ruled out is that the solvent has reacted, for example through a ring-opening of THF at the active metal surface which could at least conceivably yield an oligomeric/polymeric THF-product based stabilizer (i.e., and then polymer rather than "solvent-only" stabilized nanoclusters). Other alternative hypotheses as to the source of the stabilization may be possible as well.

Another precursor that appears ideal for studying solvent-only stabilization is $Pd_2(dba)_3$ (where dba is dibenzylidene acetonate) [213]. However, elemental analysis of isolated nanoclusters prepared from this precursor shows >41% C (relative to the entire mass of the sample) and the XPS C 1s spectrum indicates the presence of "amorphous (graphitic) carbon" on the surface of the nanoclusters [213]—a potential if not obvious stabilizer. In any event, the surface layer of carbon means the nanoclusters prepared in this study, too, are not truly "solvent-only" stabilized.

One paper testing seven alternative hypotheses for solvent-only stabilized nanoclusters has appeared [95]. By using the system $[(1,5\text{-COD})Ir(CH_3CN)_2][BF_4]$ with only the weakly coordinating BF_4^- anion in 5 different solvents, and by ensuring the absence of O_2, H_2O, ROH, and Cl^-, the "solvent-only" stabilization hypothesis was subjected to its first more rigorous test via the 5 criteria method. The main findings of that study are that: (i) even high donor number solvents alone do not provide enough stabilization to allow for the formation of nanoclusters; (ii) traditionally weakly coordinating anions such as BF_4^- obey DLVO theory and yield to transiently solution stable nanoclusters in high dielectric constant solvents; (iii) exposure to O_2 or the strong ligand pyridine were needed to attain long-term (>2 weeks) solution stability. In short, putative "solvent-only" stabilized nanoclusters appear to be another, now de-bunked [95] myth of the nanocluster area.

4.3 Room-Temperature Ionic Liquid Stabilization

Another mode of postulated nanocluster stabilization is room-temperature ionic liquid (IL) stabilization [214,215,216,217,218,219]. These negligible vapor pressure (but distillable [220]), highly polar, viscous solvents have received much recent attention in the literature [221,222,223,224], with a plethora of reactions having been carried out in IL media as covered in several review articles [225,226,227]. Recently, there have been reports of catalytically active nanoclusters suspended in ionic liquids [214,215,216,217,218,219]. However, as in the organic "solvent-only" stabilized cases above, these nanocluster/IL systems are frequently contaminated by halides (not only from halogenated nanocluster precursors [214] but from the preparation of the ILs

themselves from imidazolium *halide* precursors [228]), thus leading to the possibility of halide stabilization when IL stabilization is claimed. The amount of halide present in ILs and on the resultant nanoclusters is rarely quantified, and these halide impurities can have detrimental effects on the ILs themselves (such as increasing the IL density and /or viscosity, or poisoning heterogeneous catalysts suspended in ILs [229]). The present best method used to quantitate halide concentration in ILs, ion chromatography [229], showed that the difference in Cl^- concentration in two [bmim][BF_4] samples from different sources to be 12.6 ppm vs. 228 ppm: note the 18 fold difference in Cl^- concentration [230]. A Cl^- content of 228 ppm corresponds to approximately $8.4x10^{-3}$ M. For a nanocluster sample such as $Ir_{\sim 300}$ nanoclusters [14] which have ~50% of their atoms on the surface, a 228 ppm Cl^- contamination of the IL leads to *approximately 12 Cl^- atoms per surface Ir atom*! Such high concentrations of chloride indicate that DLVO-type stabilization by chloride is a plausible—but untested—alternative hypothesis to that of the IL being the nanocluster stabilizer. In addition, hygroscopic ILs have to be carefully dried before use to avoid surface contamination of the nanoclusters by water, hydroxides or oxides.

As is the case for "solvent-only" stabilized nanoclusters, there is no precedented mode of stabilization for transition metal nanoclusters in ILs unless the weakly coordinating anions [231] that comprise half the composition of the IL are involved. Those anions are typically BF_4^-, PF_6^-, and $N(SO_2CF_3)^-$, chosen to ensure the preparation of a room-temperature IL instead of a solid salt. Contributions to stability by one of these anions is consistent with the finding that BF_4^- can contribute to the stability of transition-metal nanoclusters in high dielectric constant solvents [95,180,103] (the dielectric

constant of ILs remains somewhat controversial, however [232]). Additionally, Dupont et al. recently reported that PF_6^- from [bmim][PF_6] was found on a Pt(0) nanocluster surface by XPS [233]. This further supports the hypothesis that even weakly coordinating anions can contribute to the stability of transition-metal nanoclusters [95].

The literature also suggests the "non-innocence" of ILs in the presence of transition metals. Specifically, there is growing precedent for oxidative addition to the C(2)–H bond of imidazolium cations to form a M(H)(*N*-heterocyclic carbene) [234,235,236,237,238]. The "non-innocence" of ILs in *nanocluster* formation and stabilization was recently investigated [239]. It was found that even under the mild conditions of 22 °C and 40 psig H_2, the oxidative addition and formation of *N*-heterocyclic carbenes from the imidazolium component of the IL was detectable under D_2 by H/D exchange studies, Figure 7. There *N*-heterocyclic carbenes are, then and in addition to the BF_4^-, another source of nanocluster stabilization in IL solvents [239]. Additionally, the *N*-heterocyclic carbenes derived from just one equivalent of imidazolium-based IL have been shown to poison the catalytic activity of $Ir(0)_n$ in acetone [91].

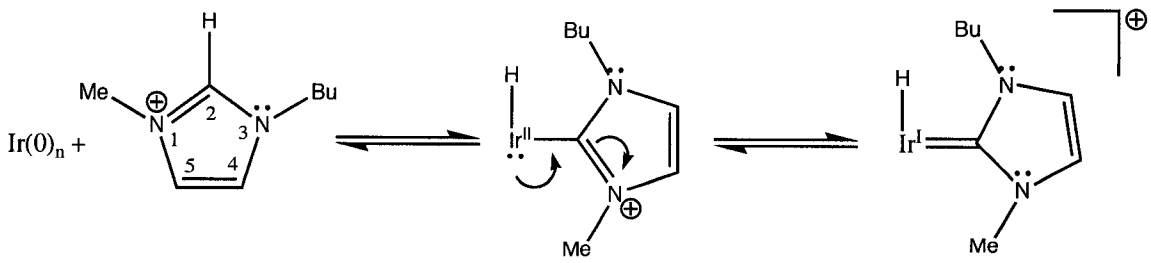

Figure 7. Mechanism for the formation of *N*-heterocyclic carbenes in the presence of nanoclusters (showing only one resonance form explicitly), supported by H/D exchange studies which show D exchange in the C_2-H (and other [239]) positions of the imidazolium cation.

5. Summary and Conclusions

The major findings of this review are as follows:

- Historical literature methods for ranking nanocluster stabilizers are inadequate. These studies are 41 and 105 years old [42,44] and apply only to gold colloids prepared in water. Additionally, they are far too qualitative to be useful to modern nanocluster science. A plasmon-resonance method for the properly chosen and prepared Au, Ag, or Cu nanoclusters is conceivable, however, and is under a collaborative investigation [47].

- A method of ranking nanocluster stability by quantitating the nanocluster agglomeration rate constants k_3 and k_4 (Schemes 2 and 3) is now available for the temperature-induced agglomeration of preformed, isolated, and redispersed nanoclusters [75]. However, a method quantitating both nanocluster *formation* and *agglomeration* is still needed.

- The 5 criteria developed in 2002 [9] represent an imperfect, but presently best available stride towards quantitating both nanocluster formation and stabilization. Of these 5 criteria, 4 are quantitative. The 5 criteria are applicable at least in theory to all metal nanoclusters in all solvents. In practice, however, application of the 5 criteria is possible only for relatively stable nanoclusters, since 4 of the 5 criteria—and all of the criteria that measure stability—are non-quantifiable for unstable, non-isolable nanoclusters. However, this feature in itself is useful as it makes clear which stabilizers are even *worth ranking* en route to identifying the top stabilizer. The 5 criteria have led to a ranking of anions [9,10,11], including the halides [180], testing of the effects of solvent and weakly coordinating anions [95], five different polymers [103], and 1,3-substituted imidazolium ionic liquids [239].

- There are two fundamental modes of nanocluster stabilization: electrostatic and steric. Additionally, the term "electrosteric" stabilization is commonly used to describe what authors consider a combination of the two main stabilization modes. Herein, we propose the first *quantitative* definition for an "electrosteric" stabilizer: those entities which possess both multiple charge ($> 1^-$) and steric bulk at minimum of one quarter the size of the nanocluster.

- Failure to determine the true nanocluster composition is a common denominator in the literature—*the* primary problem in identifying even which potential stabilizers are present, much less which is the dominant, true source of the stabilization. For example, in a recent review with 668 references [5], *the composition of each class of nanoclusters was never mentioned.* Instead, the claimed stabilizing agents were tacitly assumed to be correct without consideration of other stabilizing entities present in the solution. Note that given the lack of quantitative methods to measure stability and thereby rank stabilizers, it follows that much of the information regarding the nature of the stabilizer is not on as firm a ground as is desired.

- Hence, there exists a great deal of confusion in the nanocluster literature with respect to the nature of the true stabilizer in a given system. "Stability" is far too often claimed based on a few *ex situ* methods such as TEM images, images of course of the solid state, not of the desired solution sample. Several "non-classical" types of stabilization have been proposed based on such initial TEM evidence, although many of these claims can be traced back to not knowing the *composition* of the nanocluster system. The lack of even formation of, much less disproof of, alternative hypotheses as to the true mode of stabilization is rampant in the nanocluster literature—a literature

propelled too fast, too far, by a single, "too-sensitive" technique, TEM. Much greater use of *in situ/operando* methods of assaying nanocluster stability are needed (i.e., determination of the rate constants k_3 and k_4 [75], use of XAFS [71], etc.). Better science, consisting of the disproof of multiple alternative hypotheses [79], is needed in this area with more than a TEM image to support the claims of stabilized nanoclusters. At a minimum, seeing if the nanoclusters are stable enough to be taken to dryness, then redissolved without forming bulk metal, is a recommended test of stability and a key part of the 5 criteria method.

- Nanocluster science will not be able to move forward efficiently until stabilization is better understood and more often quantitated. Doing so will greatly simplify the current "dizzying variety" [5] of claimed nanocluster stabilizers into a few preferred anions, solvents (e.g., propylene carbonate [39,95]) and steric stabilizers.

In short, it would be fair to say that reliable, quantitative studies of how nanoclusters of known composition are stabilized are just beginning. It is hoped that the present critical review will serve to expedite the needed studies.

Acknowledgements. This work was supported by DOE grant DE-FG02-03ER15453.

References

[1] G. Schmid, L. Chi, Adv. Mater. 10 (1998) 515.
[2] G. Schmid, M. Baumle, M. Geerkens, I. Heim, C. Osemann, T. Sawitowski, Chem. Soc. Rev. 28 (1999) 179.
[3] J. D. Aiken III, R. G. Finke, J. Mol. Cat. A 145 (1999) 1.
[4] A. Roucoux, J. Schulz, H. Patin, Chem. Rev. 102 (2002) 3757.
[5] B. L. Cushing, V. L. Kolesnichenko, C. J. O'Connor, Chem. Rev. 104 (2004) 3893.
[6] M. A. Watzky, R. G. Finke, J. Am. Chem. Soc. 119 (1997) 10382.

[7] C. Besson, E. E. Finney, R. G. Finke, J. Am. Chem. Soc. 127 (2005) 8179.
[8]C. Besson, E. E. Finney, R. G. Finke, Chem. Mater. 17 (2005) 4925.
[9] S. Özkar, R. G. Finke, J. Am. Chem. Soc. 124 (2002) 5796.
[10] S. Özkar, R. G. Finke, Langmuir 18 (2002) 7653.
[11] S. Özkar, R. G. Finke, Langmuir, 19 (2003) 6247.
[12] B. J. Hornstein, R. G. Finke, Chem. Mater. 1 (2004) 139.
[13] For a recent review, see: C. Burda, X. Chen, R. Narayanan, M. A. El-Sayed, Chem. Rev. 105 (2005) 1025.
[14] Y. Lin, R. G. Finke, J. Am. Chem. Soc. 116 (1994) 8335.
[15] J. D. Aiken III, R. G. Finke, Chem. Mater. 11 (1999) 1035.
[16] G. A. Somorjai, Y. G. Borodko, Catal. Lett. 76 (2001) 1.
[17] A. Roucoux, J. Schulz, H. Patin, Chem. Rev. 102 (2002) 3757.
[18] H. Bönneman, R. M. Richards, Eur. J. Inorg. Chem. 10 (2001) 2445.
[19] J. Glanz, Science 269 (1995) 1363.
[20] A. Henglein, Chem. Rev. 89 (1989) 1861.
[21] W. Caseri, Macromol. Rapid Commun. 21 (2000) 705.
[22] G. Schmid, U. Simon. Chem. Commun. 6 (2005) 697.
[23] G. Schmid, Adv. Eng. Mater. 3 (2001) 737.
[24] A. P. Alivisatos, K. P. Johnson, X. Peng, T. E. Wilson, C. J. Loweth, M. P. Bruchez Jr., P. G. Schultz, Nature, 382 (1996) 609.
[25] R. Elghanian, J. J. Storhoff, R. C. Mucic, R. L. Letsinger, C. A. Mirkin, Science, 277 (1997) 1078.
[26] *Metal Nanoparticles: Synthesis, Characterization, and Applications*; D. L. Feldheim, C. A. Foss Jr., Eds., Marcel Dekker, New York, 2002.
[27] R. G. Finke, in *Metal Nanoparticles: Synthesis, Characterization, and Applications*; D. L. Feldheim, C. A. Foss Jr., Eds., Marcel Dekker, New York, 2002, chapter 2.
[28] J. U. Köhler and J. S. Bradley, Catal. Lett. 45 (1997) 203.
[29] J. Turkevich, Gold Bull. 18 (1985) 86, J. Turkevich, Gold Bull. 18 (1985) 125, and references therein.
[30] M.-C. Daniel, D. Astruc, Chem. Rev. 104 (2004) 293.
[31] J. Zhang, J. Worley, S. Dénommée, C. Kingston, Z. J. Jakubek, Y. Deslandes, M. [Post, B. Simard, N. Braidy, G. A. Botton, J. Phys. Chem. B. 107 (2003) 6920.
[32] J. Nedersen, G. Chumanov, T. M. Cotton, Appl. Spectr. 47 (1993) 1959.
[33] M. S. Sibbald, G. Chumanov, T. M. Cotton, J. Phys. Chem. 100 (1996) 4672.
[34] M.-S. Yeh, Y.-S. Yang, Y.-P. Lee, H.-F. Lee, Y.-H. Yeh, C.-S. Yeh, J. Phys. Chem. B. 103 (1999) 6851.
[35] K. J. Klabunde, H. F. Efner, L. Satek, W. Donely, J. Organomet. Chem. 71 (1974) 309.
[36] K. J. Klabunde, H. F. Efner, T. O. Murdock, R. Ropple, J. Am. Chem. Soc. 98 (1976) 1021.
[37] T. O. Murdock, K. J. Klabunde, J. Org. Chem. 41 (1976) 1077.
[38] M. T. Reetz, W. Helbig, J. Am. Chem. Soc. 116 (1994) 7401.
[39] M. T. Reetz, G. Lohmer, Chem. Commun. 16 (1996) 1921.
[40] K. S. Suslick, S.-B. Choe, A. A. Cichowias, M. W Grinstaff, Nature 353 (1991) 414.
[41] N. A. Dhas, K. S. Suslick, J. Am. Chem. Soc. 127 (2005) 2368.

[42] R. Zsigmondy, Z. Anal. Chem. (1901) 697.
[43] M. Faraday, Phil. Trans. Roy. Soc. 147 (1857) 145.
[44] H. Thiele, H. S. von Levern, J. Coll. Sci. 20 (1965) 679.
[45] F. Bensebaa, N. Patrito, Y. Le Page, P. L'Ecuyer, P. S. Wang, J. Mater. Chem. 14 (2004) 3378.
[46] P. L. Kuo, C. C. Chen, M. W. Jao, J. Phys. Chem. B 109 (2005) 9445.
[47] R. G. Finke, W. E. Buhro, experiments under consideration.
[48] B. V. Enüstün, J. Turkevich, J. Am. Chem. Soc. 85 (1963) 3317.
[49] C. M. Hagen, P. M. Maitlis, R. G. Finke, J. Am. Chem. Soc. 127 (2005) 4423.
[50] J. A. Widegren, R. G. Finke, Inorg. Chem. 41 (2002) 1558.
[51] C. A. Jaska, I. Manners, J. Am. Chem. Soc. 126 (2004) 1334.
[52] C. A. Jaska, I. Manners, J. Am. Chem. Soc. 126 (2004) 9776.
[53] D. B. Williams, C. B. Carter, In *Transmission Electron Microscopy*, Plenum Press, New York, 1996.
[54] C.-C. Huang, Y.-F. Huang, H.-T. Chang, J. Nanosci. Nanotech. 4 (2003) 622.
[55] R. Patakfalvi, Z. Virányi, I. Dékány, Colloid Polym. Sci. 283 (2004) 299.
[56] G. Mie, Ann. Phys. 25 (1908) 377.
[57] J. A. Creighton, D. G. Eadon, J. Chem. Soc. Faraday Trans. 87 (1991) 3881.
[58] N. Yanagihara, Chem. Lett. (1998) 305.
[59] D. L. Van Hyning, W. G. Klemperer, C. F. Zukoski, Langmuir, 17 (2001) 3128.
[60] J. P. Wilcoxon, J. E. Martin, D. W. Schaefer, Phys. Rev. Lett. 58 (1987) 1051.
[61] D. A. Weitz, M. Y. Lin, H. M. Lindsay, J. S. Huang, Phys. Rev. Lett. 58 (1987) 1052.
[62] D. A. Weitz, J. S. Huang, M. Y. Lin, J. Sung, Phys. Rev. Lett. 54 (1985) 1416.
[63] J. G. Reich, *C Curve Fitting and Modeling for Scientists and Engineers*, McGraw-Hill, Inc., New York, 1992.
[64] J. Gregory, In *Nanoparticles in Solids and Solutions*, J. H. Fendler, I. Dékány, Eds., Kluwer Academic Publishers, Dordrecht, 1996.
[65] L. D'Souza, A. Suchopar, R. M. Richards, J. Coll. Int. Sci. 279 (2004) 458.
[66] B. Chu, T. Liu, J. Nanopart. Res. 2 (2000) 29.
[67] F. Meneau, G. Sankar, N. Morgante, R. Winter, C. R. A. Catlow, G. N. Greavews, J. M. Thomas, Faraday Discuss. 122 (2002) 203.
[68] H. Borchert, E. V. Shevchenko, A. Robert, I. Mekis, A. Kornowski, G. Grübel, H. Weller, Langmuir 21 (2005) 1931.
[69] Y. Mori, M. Furukawa, T. Hayashi, K. Nakamura, Part. Sci. Tech. 24 (2006) 97.
[70] G. S. Fonseca, G. Machado, S. R. Teixeira, G. H. Fecher, J. Morais, M. C. M. Alves, J. Dupont, J. Coll. Int. Sci. 301 (2006) 193.
[71] Y. Chen, J. L. Fulton, J. C. Linehan, T. Autry, J. Am. Chem. Soc. 127 (2005) 3245.
[72] C. G. Blatchford, J. R. Campbell, J. A. Creighton, Surf. Sci. 120 (1982) 435.
[73] J. A. Widegren, J. D. Aiken III, S. Özkar, R. G. Finke Chem. Mater. 13 (2001) 312.
[74] The catalytic reporter reaction relies on the pseduelementary step concept (R. M. Noyes, R. J. Field, Acc. Chem. Res. 10 (1977) 214; R. M.Noyes, R. J. Field, Acc. Chem. Res. 10 (1977) 273) used extensively in our previous work (for example, see references [6] and [73]).

[75] L. S. Ott, R. G. Finke, "Nanocluster Formation, Stabilization, and Agglomeration Fundamental Studies: Can the Kinetics of Agglomeration, as a Preferred, Quantitative Way to Assay Transition-Metal Nanocluster Stabilizers, Be Measured by the Catalytic Reporter Reaction Method?" Manuscript in preparation.
[76] J. D. Aiken III, Y. Lin, R. G. Finke, J. Mol. Cat. A. 114 (1996) 29.
[77] S. Özkar, R. G. Finke, Coord. Chem. Rev. 248 (2004) 135.
[78] D. H. Napper, *Polymeric Stabilization of Colloidal Dispersions*, Academic Press, New York, 1983.
[79] J. Platt, Science 146 (1964) 347.
[80] J. Yang, J. Y. Lee, T. C. Deivaraj, H.-P. Too, Coll. Surf. A 240 (2004) 131.
[81] J. Turkevich, P. C. Stevenson, J. Hillier, Disscus. Faraday Soc. 11 (1951) 55.
[82] G. Schmid, R. Pfeil, R. Boese, F. Bandermann, S. Meyer, G. H. M. Calis, J. W. A. van der Velden, Chem. Ber. 114 (1981) 3634.
[83] M. N. Vargaftik, V. P. Sargorodnikov, I. P. Stolarov, I. I. Moiseev, V. A. Likholobov, D. I. Kochubey, A. L. Chuvilin, V. I. Zaikosvsky, K. I. Zamaraev, G. I. Timofeeva, J. Chem. Soc. Chem. Commun. (1985) 937.
[84] J. Rothe, J. Pollmann, R. Franke, J. Hormes, H. Bönnemann, W. Brijoux, K. Siepen, J. Richter, Fresenius J. Anal. Chem. 335 (1996) 372.
[85] R. H. Terrill, T. A. Postlethwaite, C.-h. Chen, C.-D. Poon, A. Terzis, A. Chen, J. E. Hutchison, M. R. Clark, G. Wignall, J. D. Londono, R. Superfine, M. Falvo, C. S. Johson Jr., E. T. Samulski, R. W. Murray, J. Am. Chem. Soc. 117 (1995) 12537.
[86] N. T. Tran, D. R. Powell, L. F. Dahl, Angew. Chem. Int. Ed. 39 (2000) 4121.
[87] K. Pelzer, B. Laleu, F. Lefebvre, K. Philippot, B. Chaudret, J. P. Candy, J. M. Basset, Chem. Mater. 16 (2004) 4937.
[88] M. Watzky, R. G. Finke, Chem. Mater. 9 (1997) 3083.
[89] N. A. Dhas, H. Cohen, A. Gedanken, J. Am. Chem. Soc. 101 (1997) 6834.
[90] K. Pelzer, K. Philippot, B. Chaudret, Z. Phys. Chem. 217 (2003) 1539.
[91] L. S. Ott, S. Campbell, K. R. Seddon, R. G. Finke. "Are Imidazolium-Based Ionic Liquids a Preferred Medium for Nanocluster Catalysts? The Test Case of Acetone Hydrogenation by Iridium(0) Nanoclusters." Inorg. Chem., submitted.
[92] E. J. W. Verwey, J. T. G. Overbeek, *Theory of the Stability of Lyophobic Colloids*; 2nd ed., Dover Publications, Inc., Mineola, New York, 1999.
[93] B. W. Ninham, Adv. Coll. Int. Sci. 83 (1999) 1.
[94] D. F. Evans, H. Wennerström, *The Colloidal Domain*, 2nd ed., Wiley-VCH, New York, 1999.
[95] L. S. Ott, R. G. Finke. "Nanocluster Formation and Stabilization Fundamental Studies: Investigating "Solvent-Only" Stabilization En Route to Discovering Stabilization by the Traditionally Weakly Coordinating Anion BF_4^- Plus High Dielectric Constant Solvents." Inorg. Chem., in press.
[96] M. Boström, D. R. W. Williams, B. W. Ninham, Phys. Rev. Lett. 87 (2001) 168103.
[97] J. Czarnecki, Z. Phys. Chemie (Leipzig) 6 (1985) 1116.
[98] F. J. Rubio-Hernandez, J. Non.-Equilib. Thermodyn. 24 (1999) 75.
[99] D. Grasso, K. Subramaniam, M. Butkus, K. Strevett, J. Bergendahl, Re/Views Env. Sci. & Bio/Tech. 1 (2002) 17.

[100] M. Brust, M. Walker, D. Bethell, D. J. Schiffrin, R. Whyman, J. Chem. Soc., Chem. Commun. (1994) 801.
[101] N. T. Tran, D. R. Powell, L. F. Dahl, Angew. Chem. Int. Ed. 39 (2000) 4121.
[102] T. O. Ely, C. Amiens, B. Chaudret, E. Snoeck, M. Verelst, M. Respaud, J.-M. Broto, Chem. Mater. 11 (1999) 526.
[103] L. S. Ott, B. J. Hornstein, R. G. Finke, "A Test of the Transition-Metal Nanocluster Formation and Stabilization Ability of the Most Common Polymeric Stabilizer, Poly(vinylpyrrolidone), As Well As Four Other Polymeric Protectants." Langmuir, in press.
[104] Y. Lin, R. G. Finke, Inorg. Chem. 33 (1994) 4891.
[105] H. Hirai, H. Chawanya, N. Toshima, Reactive Polymers 3 (1985) 127.
[106] W. Hoogsteen, L. G. J. Fokkink, J. Coll. Int. Sci. 175 (1995) 12.
[107] J. Ramos, A. Millán, F. Palacio, Polymer 41 (2000) 8461.
[108] I. Gilbert, A. Millán, F. Palacio, A. Falqui, E. Snoeck, V. Serin, Polyhedron 22 (2002) 2457.
[109] N. Toshima, Y. Shiraishi, T. Teranishi, M. Miyake, T. Tominaga, H. Watanabe, W. Brijoux, H. Bönnemann, G. Schmid, Appl. Organomet. Chem. 15 (2001) 178.
[110] Lead references to the extensive literature of PVP stabilization of colloids and nanoclusters are: (a) H. Hirai, Y. Nakao, N. Toshima, J. Macromol. Sci.–Chem. A13 (1979) 727;
(b) J. U. Köhler, J. S. Bradley, Langmuir, 14 (1998) 2730;
(c) Y. Huang, J. Chen, H. Chem, R. Li, Y. Li, L. Min, X. Li, J. Mol. Catal. A: Chem. 170 (2001) 143;
(d) W.-Y. Yu, H.-F. Liu, Q. Tao, Chem. Comm. (1996) 1773;
(e) H. Hiria, H. Chawanya, N. Toshima, Makromol. Chem., Rapid Comm. 2 (1981) 99;
(f) H. Hiria, N. Yakura, Y. Seta, S. Hodoshima, React. Funct. Polym. 37 (1998) 121;
(g) W.-Y. Yu, M. Liu, H. Liu, J. Zheng, J. Colloid Interf. Sci. 210 (1999) 218;
(h) W.-Y. Yu, H. Liu, M. Liu, Q. Tao, J. Mol. Catal. A: Chemical 138 (1999) 273;
(i) Y. Shiraishi, M. Nakayama, E. Takagi, T. Tominaga, N. Toshima, Inorg. Chim. Acta. 300-302 (2000) 964;
(j) Y. Li, X. M. Hong, D. M. Collard, M. A. El-Sayed, Org. Lett. 2 (2000) 2385;
(k) N. Toshima, T. Yonezawa, New J. Chem. (1998) 1179 (A Review of PVP-stabilized bimetallic nanoparticles);
(l) T. Hashimoto, K. Saijo, M. Harada, N. Toshima, J. Chem. Phys. 109 (1998) 5627;
(m) B.-S. Wan, S.-J. Liao, Y. Xu, .-R. Yu, D J. Mol. Catal. A: Chemical 136 (1998) 263;
(n) Pd/Cu, PVP-protected bimetallic nanoclusters: J. S. Bradley, E. W. Hill, C. Klein, B. Chaudret, A. Duteil, Chem. Mater. 5 (1993) 254;
(o) W. Yu, Y. Wang, H. Liu, W. Zheng, J. Mol. Catal. A: Chemical 112 (1996) 105;
(p) N. Toshima, K. Kushihashi, T. Yonezawa, H. Kirai, Chem. Lett. (1989) 1769;
(q) N. Toshima, M. Harada, T. Yonezawa, K. Kushihashi, K. Asakura, J. Phys. Chem. 95 (1991) 7448;
(r) M. Harada, K. Asakura, Y. Ueki, N. Toshima, J. Phys. Chem. 96 (1992) 9730.
[111] Y. Huang, Y. Li, J. Hu, P. Cheng, H. Chen, R. Li, X. Li, C. W. Yip, S. C. A. Chan, J. Mol. Cat. A.: Chem. 189 (2002) 219.
[112] R. Narayanan, M. A. El-Sayed, J. Phys. Chem. B 108 (2004) 8572.

[113] R. Narayanan, M. A. El-Sayed, J. Am. Chem. Soc. 125 (2003) 8340.
[114] J. L. Bars, U. Specht, J. S. Bradley, D. G. Blackmond, Langmuir, 15 (1999) 7621.
[115] I. Pastoriza-Santos, L. M. Liz-Marzán, Langmuir 18 (2002) 2888.
[116] S. King, K. Hyunh, R. Tannenbaum, J. Phys. Chem. B 107 (2003) 12097.
[117] B. P. S. Chauhan, J. S. Rathore, M. Chauhan, A. Krawicz, J. Am. Chem. Soc. 125 (2003) 2876.
[118] E. Tadd, A. Zeno, M. Zubris, N. Dan, R. Tannenbaum, Macromolecules 36 (2003) 6497.
[119]A. Spitaleri, P. Pertici, N. Scalera, G. Vitulli, M. Hoang, T. W. Turney, M. Gleria, Inorg. Chem. Acta. 352 (2003) 61.
[120] L. D. Rampino, F. F. Nord, J. Am. Chem. Soc. 63 (1941) 2745.
[121] L. D. Rampino, F. F. Nord, J. Am. Chem. Soc. 63 (1941) 3268.
[122] R. Patakfalvi, Z. Virányi, I. Dékány, Colloid Polym. Sci. 283 (2004) 299.
[123] Y. Zhou, S. H. Yu, C. Y. Wang, X. G. Li, Y. R. Zhu, Z. Y. Chen, Adv. Mater. 11 (1999) 850.
[124] C.-C. Huang, Y.-F. Huang, H.-T. Chang, J. Nanosci. Nanotech. 4 (2003) 622.
[125] J. Kiwi, M. Grätzel, J. Am. Chem. Soc. 101 (1979) 7214.
[126] L. M. Bronstein, D. M. Chernyshov, P. M. Valetsky, E. A. Wilder, R. J. Spontak, Langmuir 16 (2000) 8221.
[127] B. P. S. Chauhan, J. S. Rathore, T. Bandoo, J. Am. Chem. Soc. 126 (2004) 8493.
[128] B. P. S. Chauhan, R. Sardar, Macromolecules 37 (2004) 5136.
[129] R. M. Crooks, M. Zhao, L. Sun, V. Chechik, L. K. Yeung, Acc. Chem. Res. 34 (2001) 181.
[130] M. Zhao, L. Sun, R. M. Crooks, J. Am. Chem. Soc. 120 (1998) 4877.
[131] M. Zhao, R. M. Crooks, Adv. Mater. 11 (1999) 217.
[132] M. Zhao, R. M. Crooks. Chem. Mater. 11 (1999) 3379.
[133] M. Zhao, R. M. Crooks, Angew. Chem. Int. Ed. 38 (1999) 364.
[134] V. Chechik, R. M. Crooks, J. Am. Chem. Soc. 122 (2000) 1243.
[135] R. W. J. Scott, H. Ye, R. R. Henriquez, R. M. Crooks, Chem. Mater. 15 (2003) 3873.
[136] Y. Niu, R. M. Crooks, Chem. Mater. 15 (2003) 3463.
[137] J. C. Garcia-Martinez, R. W. J. Scott, R. M. Crooks, J. Am. Chem. Soc. 125 (2003) 11190.
[138] R. W. J. Scott, O. M. Wilson, R. M. Crooks, J. Phys. Chem. B, 109 (2005) 692.
[139] L. Balogh, D. A. Tomalia, J. Am. Chem. Soc. 120 (1998) 7355.
[140] R. Wang, J. Yang, Z. Zheng, M. D. Carducci, J. Jiao, S. Seraphin, Angew. Chem. Int. Ed. 40 (2001) 549.
[141] P. N. Floriano, C. O. Noble IV, J. M. Schoonmaker, E. D. Poliakoff, R. L. McCarley, J. Am. Chem. Soc. 123 (2001) 10545.
[142] Y. Luo, Y. Li, X. Jia, H. Yang, L. Yang, Q. Zhou, Y. Wei, J. Appl. Polym. Sci. 89 (2003) 1515.
[143] Dr. Emery Scheibert, personal communication. Additional information can be found at www.dendritech.com.
[144] R. W. J. Scott, A. K. Dayte, R. M. Crooks, J. Am. Chem. Soc. 125 (2003) 3708.

[145] R. W. J. Scott, C. Sivadinarayana, O. M. Wilson, Z. Yan, W. Goodman, R. M. Crooks, J. Am. Chem. Soc. 127 (2005) 1380.
[146] Y. Niu, R. M. Crooks, C. R. Chimie 6 (2003) 1049.
[147] B. J. Hornstein, J. D. Aiken III, R. G. Finke, Inorg. Chem. 41 (2002) 1625.
[148] J. C. Garcia-Martinez, R. W. J. Scott, R. M. Crooks, J. Am. Chem. Soc. 125 (2003) 11190.
[149] M. Antonietti, F. Gröhn, J. Hartmann, L. Bronstein, Angew. Chem. Int. Ed. 36 (1997) 2080.
[150] N. T. Whilton, B. Berton, L. Bronstein, H. Henze, M. Antonetti, Adv. Mater. 11 (1999) 1014.
[151] A. Biffis, J. Mol. Cat. A.: Chem. 165 (2001) 303.
[152] A. Biffis, E. Speretto, Langmuir 19 (2003) 9548.
[153] A. Biffis, N. Orlandi, B. Corain, Adv. Mater. 15 (2003) 1551.
[154] N. T. S. Phan, M. Van Der Sluys, C. W. Jones, Adv. Synth. Catal. 348 (2006) 609.
[155] A. C. Templeton, W. P. Wuelfing, R. M. Murray, Acc. Chem. Res. 33 (2000) 27.
[156] P. S. Shah, S. Husain, K. P. Johnston, B. A. Korgel, J. Phys. Chem. B 106 (2002) 12178.
[157] J. C. Love, L. A. Estroff, J. K. Kriebel, R. G. Nuzzo, G. M. Whitesides, Chem. Rev. 105 (2005) 1103.
[158] C. Pan, K. Pelzer, K. Philippot, B. Chaudret, F. Dassenoy, P. Lecante, M.-J.Casanove, J. Am. Chem. Soc. 123 (2001) 7584.
[159] V. Mévellec, A. Roucoux, E. Ramirez, K. Philippot, B. Chaudret, Adv. Synth. Catal. 346 (2004) 72.
[160] A. Wie, B. Kim, S. V. Pusztay, S. L. Tripp, R. Balasubramanian, J. Inclus. Phenom. Macrocyclic Chem. 41 (2001) 83.
[161] R. Balasubramanian, J. Xu, B. Kim, B. Sadtler, A. Wei, J. Disp. Sci. Tech. 22 (2001) 485.
[162] B. Kim, S. L. Tripp, A. Wei, J. Am. Chem. Soc. 123 (2001) 7955.
[163] S. V. Pusztay, A. Wei, K. B. Stavens, R. P. Andres, Supramolecular Chem. 14 (2002) 291.
[164] S. L. Tripp, S. V. Pusztay, A. E. Ribbe, A. Wei, J. Am. Chem. Soc. 124 (2002) 7914.
[165] K. B. Stavens, S. V. Pusztay, S. Zou, R. P. Andres, A. Wei, Langmuir, 15 (1999) 8337.
[166] R. Balasubramanian, B. Kim, S. L. Tripp, X. Wang, M. Lieberman, A. Wei, Langmuir 18 (2002) 3676.
[167] B. Kim, M. A. Carignano, S. L. Tripp, A. Wei, Langmuir 20 (2004) 9360.
[168] B. Kim, R. Balasubramanian, W. Perez-Segarra, A. Wei, B. Decker, J. Mattay, Supramol. Chem. 17 (2005) 173.
[169] P. Timmerman, W. Verboom, D. N. Reinhoudt, Tetrahedron 52 (1996) 2663.
[170] N. Cordente, M. Respaud, F. Senocq, M.-J. Casanove, C. Amiens, B. Chaudret, Nano Lett. 1 (2001) 565.
[171] F. Dumestre, B. Chaudret, C. Amiens, M.-C. Fromen, M.-J. Casanove, P. Renaud, P. Zurcher, Angew. Chem. Int. Ed. 41 (2002) 4286.

[172] E. Ramirez, S. Jansat, K. Philippot, P. Lecante, M. Gomez, A. M. Masdeu-Bultó, B. Chaudret, J. Organomet. Chem. 689 (2004) 4601.
[173] D. Tabuani, O. Monticelli, A. Chincarini, C. Bianchini, F. Vizza, S. Moneti, S. Russo, Macromolecules 36 (2003) 4294.
[174] D. Tabuani, O. Monticelli, H. Komber, S. Russo, Marcromol. Chem. Phys. 204 (2003) 1576.
[175] S. Mecking, R. Thomann, H. Frey, A. Sunder, Macromolecules 33 (2000) 3958.
[176] B. J. Hornstein, R. G. Finke, Chem. Mater. 15 (2003) 899.
[177] (a) S. Mandal, P. Selvakannan, R. Pasricha, M. Sastry, J. Am. Chem. Soc. 125 (2003) 8440;
(b) A. Sanyal, M. Sastry, Chem. Commun. 11 (2003) 1236;
(c) S. Mandal, D. Rautaray, M. Sastry, J. Mater. Chem. 13 (2003) 3002;
(d) S. Mandal, A. Das, R. Srivastava, M. Sastry, Langmuir 21 (2005) 2408.
[178] A. Troupis, A. Hiskia, E. Papaconstantinou, Angew. Chem. Int. Ed. 41 (2002) 1911.
[179] (a) A. V. Gordeev, B. G. Ershov, High Energy Chem. 33 (1999) 218;
(b) B. G. Ershov, A. V. Gordeev, Mendeleev Commun. (2001) 147;
(c) A. V. Gordeev, N. I. Kartashev, B. G. Ershov, High Energy Chem. 36 (2002) 75.
[180] L. S. Ott, M. L. Cline, R. G. Finke, "Nanocluster Formation and Stabilization Fundamental Studies: Ranking the Nanocluster Stabilizing Ability of Halides." J. Nanosci. Nanotech., submitted.
[181] V. Kogan, Z. Aizenshtat, R. Popovitz-Biro, R. Neumann, Org. Lett. 4 (2002), 3529.
[182] B. G. Ershov, A. V. Gordeev, Medeleev Commun. 11 (2001) 147.
[183] A. V. Gordeev, B. G. Ershov, Rad. Chem. 33 (1999) 218.
[184] A. V. Gordeev, N. I. Kartashev, B. G. Ershov, Rad. Chem. 36 (2002) 75.
[185] G. M. Maksimov, V. I. Zaikovski, K. I. Matveev, V. A. Likholobov, Kinetics and Catalysis 41 (2000) 844.
[186] C. R. Graham, L. S. Ott, R. G. Finke. Studies in progress.
[187] M. T. Reetz, W. Helbig, S. A. Quaiser, U. Stimming, N. Breur, R. Vogel, Science, 267 (1995) 367.
[188] J. A. Becker, R. Schäfer, R. Festag, W. Ruland, J. H. Wendoff, J. Pebler, S. A. Quaiser, W. Helbig, M. T. Reetz, J. Chem. Phys. 103 (1995) 2520.
[189] H. Bönnemann, W. Brijoux, R. Brinkmann, E. Dinjus, T. Joußen, B. Korall, Angew. Chem. Int. Ed. 30 (1991) 1312.
[190] S. Bucher, J. Hormes, H. Modrow, R. Brinkman, N. Waldöfner, H. Bönneman, L. Beuermann, S. Krischok, W. Maus-Friedrichs, V. Kempter, Surf. Sci. 497 (2002) 321.
[191] H. Modrow, S. Bucher, J. Hormes, R. Brinkmann, H. Bönnemann, J. Phys. Chem. B. 107 (2003) 3684.
[192] The approximate number of surface atoms was calculated with the formula based on the "magic number" nanoclusters [14]. A 4.8 nm cluster contains approximately 3937 Pd atoms, which is close to the 10-shell magic number of 3871 atoms. The number of surface atoms is calculated using the equation $y=10n2+2$ (where y is the number of surface atoms and n is the number of shells in the cluster). From this equation, 10 shells have 1002 surface atoms and 1002/3871= 26% surface atoms.

[193] M. T. Reetz, M. Winter, R. Brienbauer, T. Thurn-Albrecht, W. Vogel, Chem. Eur. J. 7 (2001) 1084.
[194] A. J. Bard, L. R. Fulkner, *Electrochemical Methods: Fundamentals and Applications*, 2nd ed., Wiley Interscience, New York, 2001, p. 545.
[195] See p. 26 of reference [27].
[196] (a) H. Bönneman, B. Korall, Angew. Chem. Int. Ed. 31 (1992) 1490;
(b) R. Franke, J. Rothe, J. Pollman, J. Hormes, H. Bonneman, W. Brijoux, T. Hindenburg, J. Am. Chem. Soc. 118 (1996) 12090.
[197] O. Vidoni, K. Philippot, C. Amiens, B. Chaudret, O. Balmes, J.-O. Malam, J.-O. Bovin, F. Senocq, M.-J. Casanove, Angew. Chem. Int. Ed. 38 (1999) 3736.
[198] P. J. Collier, J. A. Iggo, R. Whyman, J. Mol. Cat. A 146 (1999) 149.
[199] Y. Wang, J. Ren, K. Deng, L. Gi, Y. Tang, Chem. Mater. 12 (2000) 1622.
[200] A. C. Curtis, D. G. Duff, P. P. Edwards, D. A. Jefferson, B. F. G. Johnson, A. I. Kirkland, A. S. Wallace, J. Phys. Chem. 92 (1987) 2270.
[201] K. Pelzer, O. Vidoni, K. Philippot, B. Chaudret, V. Colliere, Adv. Func. Mater. 13 (2003) 118.
[202] G. Cardenas-Trivino, K. J. Klabunde, E. B. Dale, Langmuir 3 (1987) 986.
[203] K. Esumi, T. Tano, K. Meguro, Langmuir, 5 (1989) 268.
[204] B. He, Y. Chen, H. Liu, Y. Liu, J. Nanosci. Nanotech. 5 (2005) 266.
[205] Freas, R. B. *J. Am. Chem. Soc.* **1986**, *108*, 4659.
[206] M. T. Reetz, S. A. Quaiser, M. Winter, J. A. Becker, R. Schäfer, U. Stimming, A. Marmann, R. Vogel, T. Konno, Angew. Chem. Int. Ed. 35 (1996) 2092.
[207] J. Rothe, J. Pollmann, R. Franke, J. Hormes, H. Bönnemann, W. Brijoux, K. Siepen, J. Richter, Fresenius J Anal. Chem. 355 (1996) 372.
[208] U. Kolb, S. A. Quaiser, M. Winter, M. T. Reetz, Chem. Mater. 8 (1996) 1889.
[209] J. Stein, L. N. Lewis, Y. Gao, R. A. Scott, J. Am. Chem. Soc. 121 (1999) 3693.
[210] K. Siepen, H. Bönnemann, W. Brijoux, J. Rothe, J. Hormes, Appl. Organomet. Chem. 14 (2000) 549.
[211] K. Ebitani, K.-M. Choi, T. Mizugaki, K. Kaneda, Langmuir, 18 (2002) 1849.
[212] As cited in E. A. Moody *The Encyclopedia of Philosophy*, McMillan, 1967, vol 7.
[213] N. A. Dhas, H. Cohen, A. Gedanken, J. Phys. Chem. B 101 (1997) 6834.
[214] J. Dupont, G. S. Fonseca, A. P. Umpierre, P. F. P. Fichtner, S. R. Teixeira, J. Am. Chem. Soc. 124 (2002) 4228.
[215] G. S. Fonseca, A. P. Umpierre, P. F. P. Fichtner, S. R. Teixeira, J. Dupont, Chem. Eur. J. 9 (2003) 3263.
[216] C. W. Scheeren, G. Machado, J. Dupont, P. F. P. Fichtner, S. R. Teixeria, Inorg. Chem. 42 (2003) 4738.
[217] L. M. Rossi, G. Machado, P. F. P. Fichtner, S. R. Teixeira, J. Dupont, Catal. Lett. 92 (2004) 149.
[218] H. Itoh, K. Naka, Y. Chujo, J. Am. Chem. Soc. 126 (2004) 3026.
[219] C. C. Cassol, A. P. Umpierre, G. Machado, S. I. Wolke, J. Dupont, J. Am. Chem. Soc. 127 (2005) 3298.
[220] M. J. Earle, J. M. S. S. Esperança, M. A. Gilea, J. N. C. Lopes, L. P. N. Rebelo, J. W. Magee, K. R. Seddon, J. A. Widegren, Nature 439 (2006) 831.
[221] T. Welton, Chem. Rev. 99 (1999) 2071.

[222] M. J. Earle, K. R. Seddon, Pure Appl. Chem. 72 (2000) 1391.
[223] P. Wasserscheid, W. Keim, Angew. Chem. Int. Ed. 39 (2000) 3772.
[224] J. Dupont, R. F. de Souza, P. A. Z. Suarez, Chem. Rev. 102 (2002) 3667.
[225] T. Welton, Chem. Rev. 99 (1999) 2071.
[226] P. Wassercheid, W. Keim, Angew. Chem. Int. Ed. 39 (2000) 3772.
[227] J. Dupont, R. F. de Souza, P. A. Z. Suarez, Chem. Rev. 102 (2002) 3667.
[228] K. R. Seddon, A. Stark, M.-J. Torres, Pure Appl. Chem. 72 (2000) 2275.
[229] C. Villagrán, M. Deetlefs, W. R. Pitner, C. Hardacre, Anal. Chem. 76 (2004) 2118.
[230] L. S. Ott, M. L. Cline, M. Deetlefs, K. R. Seddon, R. G. Finke, Unpublished results.
[231] S. H. Strauss, Chem. Rev. 93 (1993) 927.
[232] For just one example, see the controversy contained in: F. V. Bright, G. A. Baker, J. Phys. Chem. B 110 (2006) 5822 and C. Wakai, A. Oleinikova, H. Weingärtner, J. Phys. Chem. B 110 (2006) 5824 and references therein.
[233] A. P. Umpierre, G. Machado, G. H. Fecher, J. Morais, J. Dupont, Adv. Synth. Catal. 347 (2005) 1404.
[234] D. S. McGuiness, K. J. Cavell, B. F. Yates, B. W. Skelton, A. H. White, J. Am. Chem. Soc. 123 (2001) 8317.
[235] J. Dupont, J. Spencer, Angew. Chem. Int. Ed. 43 (2004) 5296.
[236] H. Lebel, M. K. Janes, A. B. Charette, S. P. Nolan, J. Am. Chem. Soc. 126 (2004) 5046.
[237] N. D. Clement, K. J. Cavell, C. Jones, C. J. Elsevier, Angew. Chem. Int. Ed. 43 (2004) 1277.
[238] N. D. Clement, K. J. Cavell, Angew. Chem. Int. Ed. 43 (2004) 3845.
[239] L. S. Ott, M. L. Cline, M. Deetlefs, K. R. Seddon, R. G. Finke, J. Am. Chem. Soc. 127 (2005) 5758.

CHAPTER III

NANOCLUSTER FORMATION AND STABILIZATION FUNDAMENTAL STUDIES: INVESTIGATING "SOLVENT-ONLY" STABILIZATION EN ROUTE TO DISCOVERING STABILIZATION BY THE TRADITIONALLY WEAKLY COORDINATING ANION BF_4^- PLUS HIGH DIELECTRIC CONSTANT SOLVENTS.

This dissertation chapter contains the manuscript of a full paper in press in *Inorganic Chemistry* and describes studies investigating the true nature of the stabilizer in putatively "solvent-only" stabilized nanocluster systems. Overall, it was found that the "solvent-only" stabilization hypothesis was not supported, even with high donor number solvents. Importantly, we found that even the traditionally weakly coordinating anion BF_4^- contributes to the stability of $Ir(0)_n$ nanoclusters in high dielectric constant solvents. Additionally, five alternative hypotheses for the source of nanocluster stability were examined and ruled out. Next, surface coordination of the nanoclusters was investigated by exposing the nanoclusters to oxygen and the strong ligand pyridine. Finally, the stabilization provided by BF_4^- in high dielectric constant solvents was compared to the strong anionic stabilizer $P_2W_{15}Nb_3O_{62}^{9-}$.

The experiments in this chapter were performed by LSO. The manuscript was prepared by LSO with assistance and editing by RGF.

Abstract.

The nanocluster literature contains a wide variety of nanocluster stabilizing agents. In addition to the plethora of stabilizing additives, multiple claims appear of "solvent-only" stabilization of transition-metal nanoclusters—a hypothesis that is tested for the first time as part of the present studies. When considering the two main modes of nanocluster stabilization, electrostatic and steric, "solvent-only" stabilization can only be steric (i.e., is not electrostatic) in nature. "Solvent-only" stabilization would require that strongly coordinated, perhaps even kinetically non-labile solvent be present on the nanocluster surface. Hence, an investigation has been conducted into potential sources for the stabilization of prototype $Ir(0)_n$ transition-metal nanoclusters prepared from [(1,5-COD)Ir($CH_3CN)_2$][BF_4] in five different solvents, with a special focus on the formulation and testing of alternative hypotheses regarding the true source of the nanocluster stabilization in putative "solvent only" stabilization conditions. Seven total hypotheses are tested with five being initially ruled out, namely stabilization by: (i) trace chloride (ii), surface hydrides, (iii) scavenged charge, (iv) solvent oxidative addition reactions with the nanocluster surface, or (v) polymerized solvent. This led in turn to two additional, main alternative hypotheses: (vi) nanocluster surface ligation by high donor number solvents (i.e., in the absence of anions), and (vii) nanocluster stabilization by surface-coordination by the traditionally weakly coordinating anion BF_4^-. Our results show that the contribution to nanocluster stability from the traditionally weakly coordinating BF_4^- in high dielectric constant solvents such as propylene carbonate is a significant source of nanocluster stabilization. Literature claims of "solvent-only" nanocluster stabilization are not supported by our findings. Overall, DLVO (Derjaugin-

Landau-Verwey-Overbeek) theory of colloidal stability is supported and found to apply to even traditionally weakly coordinating anions.

Introduction

Transition-metal nanoclusters have received a great deal of interest due to their perceived importance in several areas of science, including but not limited to catalysis,[1] chemical sensors,[2] and quantum computers,[3] to name just a few. In order to realize these and other potential applications, the requisite nanoclusters should ideally be "bottleable" and redissolvable—that is, one should be able to prepare, isolate, weigh out, and fully redisperse identical samples of reproducible nanoclusters.[4] This in turn means that understanding the topic of transition-metal nanocluster *stabilizers* is of considerable, fundamental importance.

However, as recently stated, "the (nanocluster) literature contains a dizzying variety of stabilizing agents."[1f] Additionally, there are at least 11 claims of nanoclusters prepared *without* added stabilizing agents—that is, "solvent-only" stabilized nanoclusters.[5,6,7,8,9,10,11,12,13,14] Separately, others have noted that, for transition-metal nanoclusters, "people in general cannot understand...which preparation method is the best among those proposed."[15] In short, the myriad of claimed stabilizers appearing in the literature is hindering the progress of nanocluster science. For this reason, we have been engaged for some time now in evaluating the efficacy of putative nanocluster stabilizers,[16,17] with an emphasis on catalytically active nanoclusters.[18]

DLVO Theory and Nanocluster Stabilization. DLVO (Derjaugin-Landau-Verwey-Overbeek) theory[19] was developed in the 1940s to describe how colloids are stabilized.[20] DLVO theory relies on anions adsorbed to the coordinatively unsaturated,

electrophilic surface of nano-colloids to achieve Columbic repulsion between particles.[21] The electrostatic repulsion opposes van der Waals attractions that would otherwise lead to particle agglomeration and precipitation. Hence, DLVO-type stabilization is also commonly referred to as *electrostatic stabilization.* Anions in excess of those that can adsorb onto the nanocluster surface comprise the diffuse multi-layer of ions surrounding the nanoclusters; this diffuse layer is referred to as the Debye layer (denoted by $1/\kappa$; values are typically in nm) depicted in Equation 1 below.

$$1/\kappa = ((\varepsilon_0 \times \varepsilon_R \times k \times T)/\sum_i (z_i e)^2 \times c_{i_0}))^{0.5} \quad (1)$$

In eq. 1, ε_0 is the permittivity of free space, ε_R is the dielectric constant of the medium (the solvent), k is the Boltzman constant, T is the temperature, z_i is the ion valency, e is the charge on an electron, and c_{i0} is the concentration of the ion species, *i*, in the bulk solution.[22] Two predictions of DLVO theory and eq. 1, are especially important for the studies herein,: (i) that *ions* are necessary for the stability of nanocluster systems and in the absence of steric stabilizers, and (ii) that a thicker Debye layer (and hence more stable nanoclusters) will be formed in *high dielectric constant* solvents if a layer of adsorbed anions is present along with an excess of anions available for the diffuse layer. The other general source of colloidal stabilization is steric stabilization,[23] that is, repulsion between sterically bulky ligands coordinated to the nanocluster surfaces[24] (see Scheme 4 elsewhere[62]).

The Current Status of Methods for Measuring Nanocluster Stability. A general problem in the area of transition-metal nanocluster stabilization is that no standard method exists to assay "stability". Indeed, nanocluster "stability" is not even an operationally well-defined term, so that an assessment of "stability" is presently at the

discretion of individual research groups. A survey of the nanocluster literature reveals that "stability" is often declared based on a (ex situ, solid state) transmission electron microscopy (TEM) image alone! Even then it is not clear if the images shown are representative; as a specific example, of 60 preparations of $Pt(0)_n$ nanoclusters, examined elsewhere, only 4 report a yield of nanoclusters, and fewer report whether or not bulk metal was formed (as was found in control experiments reported subsequently[25]).

Examination of the colloidal/nanocluster literature reveals that only two methods are available for evaluating classical water-soluble colloidal stability:[27,28] these methods, which were used for gums, other ill-defined additives or polymers, are 41 and 105 years old, are qualitative, and are applicable only to Au colloids in water.[27,28] Additionally, these two methods only visually assay stability qualitatively based on the color change observed upon agglomeration of Au colloids in water. Hence, a modern operational definition of nanocluster stability, plus a method for assaying relative stabilities, is needed.

Reflection on the above point and the relevant literature[26,27,28] teaches that the preferred method and thereby operational definition is a kinetic measurement of stability based on the *quantitative rates of agglomeration* of nanoclusters. Noteworthy is that nanocluster agglomeration is expected to be a complex, subtle interplay of multiple phenomena such as chemical bond formation, structural reorganization, and sometimes reversible agglomeration.[29] Efforts have been underway in our labs to provide the needed, kinetic methods to measure agglomeration rates, studies that are still in progress.[30]

In the absence of general kinetic method to assay nanocluster agglomeration under any solvent, temperature, or other conditions, the one method available in the literature at present for ranking the *formation and stabilization* of transition-metal nanoclusters is the 5 criteria method developed in our labs in 2002.[16,17] The 5 criteria are: (i) the level of kinetic control during the nanocluster formation reaction as measured by the k_2/k_1 ratio of autocatalytic surface growth (k_2) to nucleation (k_1)—larger values indicating a high level of kinetic control; (ii) the nanoclusters' size distribution as determined by TEM ($\leq\pm$10–15% being defined as "near-monodisperse" nanoclusters[4]); (iii) the ability to isolate from solution and ideally bottle the nanoclusters for future use without their agglomeration to bulk metal; (iv) the catalytic activity of the isolated nanoclusters once redissolved in solution with fresh cyclohexene substrate; and (v) the total catalytic lifetime for cyclohexene hydrogenation observed for the nanoclusters in solution. The perhaps single most stringent test of claimed nanocluster stabilizers is criteria (iii), the formation of isolable and subsequently redissolvable nanoclusters while seeing whether or not bulk metal is formed.

We first used the 5 criteria method to rank anionic stabilizers, anions being expected to be a key by DLVO theory (recall eq. 1) for stabilizing otherwise coordinatively unsaturated, electrophilic transition-metal nanoclusters. This method and the 5 criteria, while admittedly not perfect (e.g., lacking a kinetic measurement of agglomeration), are nevertheless a welcome advance in an area where no modern methods previously existed to rank nanocluster stabilizers.

Claims of "Solvent-Only" Stabilized Nanoclusters. A belief in the literature of modern transition-metal nanoclusters directly relevant to the present work is that *solvent-only*

stabilized nanoclusters exist.[5,6,7,8,9,10,11,12,13,14] The concept of "solvent-only" nanocluster stabilization is attractive since such nanoclusters, if they exist, would have their surfaces sites ready for catalysis via only a dissociation of weakly coordinated solvent—a perhaps ideal solution to what we have coined as the "naked nanocluster problem" of nanocluster catalysis.[31] By definition, such putatively "solvent-only" stabilized nanoclusters should not possess surface-coordinated anions[19]—that is, putative "solvent-only" stabilization is, in its essence, little precedented "anti-DLVO theory" stabilization.

The "solvent-only" stabilization hypothesis has not been previously subjected to attempts to disprove it[32], despite at least 12 papers making the claim of solvent-only stabilized nanoclusters. For example, an early paper claims to have prepared "$Ti(0)_n$•THF" and "$Zr(0)_m$•THF" colloids[5a]—however, the authors ignore the 8.5% Cl^- present by elemental analysis that is expected to provide electrostatic, DLVO-type stabilization. (Later contributions by the same group preparing alkylammonium halide stabilized nanoclusters do, however, recognize the role of anions, and specifically Cl^-, as stabilizers.[33,34]) Hypothetical "$Ti(0)_n$•THF" and "$Zr(0)_m$•THF" colloids would also be highly air-sensitive[35] with, therefore, and expected oxide coating as a stabilizer on their surface.

As a second example of putative solvent-only stabilization, propylene carbonate is the claimed stabilizer in a system of electrochemically generated Pd colloids.[11] However, those authors did not consider two key alternative hypotheses for stabilization, namely: (i) that Cl^- from the NaCl electrolyte is probably contributing to the stability via electrostatic, DLVO-type stabilization, nor (ii) that the 5% ethanol in the PC solution

might be contributing to the stability by ligating the nanocluster surface, possibly in its deprotonated, alkoxide form.[11]

There are some isolated reports of nanoclusters prepared in the absence of anions, where truly solvent-only stabilized nanoclusters are at least conceivable. Chaudret et al. have reported a well-designed, halide-free precursor, Ru(COD)(COT) (COD = 1,5-cyclooctadinee; COT = cyclooctatriene), to prepare $Ru(0)_n$ nanoclusters. However, frequently there are other potentially stabilizing entities present such as alcohols,[6,10] long chain amines,[36] or polymers.[37] Consequently, these systems, too, cannot be considered strictly "solvent-only" stabilized. Another precursor that appears ideal for studying solvent-only stabilization is $Pd_2(dba)_3$[38] (where dba is dibenzylidene acetonate). However, elemental analysis of isolated nanoclusters prepared from this precursor shows >41% C (relative to the entire mass of the sample) and the XPS C 1s spectrum indicates the presence of "amorphous (graphitic) carbon" on the surface of the nanoclusters[38]—a potential if not obvious stabilizer. In any event, the surface layer of carbon means the nanoclusters prepared in this study, too, are not truly "solvent-only" stabilized. Therefore, *even with these two seemingly ideal nanocluster precursors, there is confusion as to whether solvent-only stabilized nanoclusters actually exist.* Note also here that "solvent" may be either a nanocluster ligand, or have more general solvent effects (e.g. on the $1/\kappa$ of DLVO theory as noted in eq. 1, or both). Table S1 of the Supporting Information provides further details on the literature's 12 claims of "solvent-only" stabilized nanoclusters. In short, testing whether or not solvent-only stabilized nanoclusters truly exist is an important goal towards understanding the factors that stabilize modern transition-metal nanoclusters.

The Present Study. Herein, using the 5 criteria method, along with the scientific method of multiple alternative hypotheses and attempted disproof of each hypothesis,[32] we evaluate the formation and stabilization of $Ir(0)_n$ nanoclusters prepared from [(1,5-COD)Ir($CH_3CN)_2$][BF_4] in five solvents[39] (see Table 1). Five alternative hypotheses for "solvent-only" stabilization have been investigated and ruled out en route to the main two alternative hypotheses investigated of: (i) stabilization by solvent ligation of the nanocluster surface by high donor number[40] (DN) solvents, and (ii) DLVO-type stabilization by the BF_4^- anion plus high dielectric constant solvent. These main two alternative hypotheses will be reported first in what follows.

Table 1. The five solvents studied herein,[41] their dielectric constants (ε), and donor numbers (DN), the solvent donor number being a measure of Lewis basicity.[40]

Solvent (abbreviation)	ε	DN
N-methylacetamide (NMA)	165	(27.8) [a]
Propylene carbonate (PC)	69	15.1
Acetonitrile (CH_3CN)	39	14.1
N-methylpyrrolidinone (NMP)	30	27.1
Acetone	20	17.0

[a] This value is the donor number from the structurally similar dimethylacetamide, since a donor number for NMA itself is not yet available in the literature.

Results and Discussion

Testing the Solvent-Only Stabilized Nanoclusters Hypothesis. *Preparation of $Ir(0)_n$ Nanoclusters in the Absence of Anionic Stabilizers.* As an initial test of the "solvent-only" stabilization hypothesis, we prepared $Ir(0)_n$ nanoclusters as before[17] from the precursor $[(1,5\text{-COD})Ir(CH_3CN)_2][BF_4]$, but this time without Proton Sponge™ (PS™, 1,8-bis(dimethylamino)naphthalene) so that no potentially stabilizing anion would be present, Scheme 1. This follows since without a base like PS™, the conjugate acid is formed, $H^+BF_4^-$ (or more generally H^+Y^-), rather than the potentially stabilizing anion BF_4^- with a PS™–H^+ counter cation (or, more generally, Y^- / PS™–H^+). Relevant here is that PS™ has been shown to be a preferred H^+ scavenger in nanocluster syntheses,[17] Scheme 2,[17] yet itself not serve as a good ligand due to its steric bulk.

Scheme 1. A generalized $Ir(0)_n$ nanocluster formation reaction without PS™.

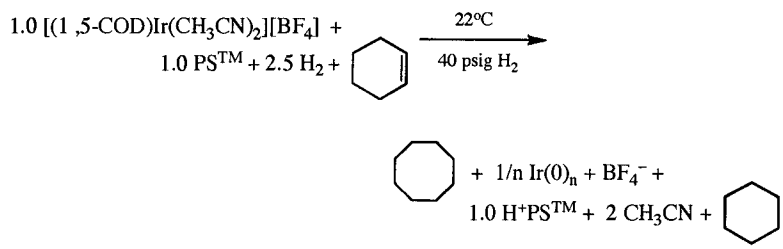

To follow the kinetics of nanocluster formation (to obtain the k_1 and k_2 parameters that are part of the 5 criteria method[16,17]), we again used the cyclohexene reporter-reaction kinetic method.[42,43] This method exploits the fact that the cyclohexene hydrogenation reaction is much faster than the nanocluster formation reaction and, hence, can be used to indirectly—but powerfully and in real time—monitor the kinetics of nanocluster formation.[42] The hydrogen uptake curves for nanocluster formation are

converted to cyclohexene consumption curves using the known 1:1 H_2 to cyclohexene stoichiometry and the kinetic data are then fit by the established 2-step mechanism for nucleation (k_1) and autocatalytic surface-growth (k_2) kinetic parameters for transition-metal nanocluster formation[42,43] (see the Experimental Section for further details).

Any stabilization observed under the conditions and resultant reaction in Scheme 1 would, therefore, have to come from strong, presumably approaching kinetically non-labile solvent coordinated to the nanocluster surface. Since the coordinatively unsaturated, electrophilic nanocluster surface is Lewis acidic, one expects that higher donor number solvents would, therefore, be preferred for preparing "solvent-only" stabilized nanoclusters.

We attempted 3 nanocluster syntheses under the conditions in Scheme 1 in *N*-methylacetamide (NMA), *N*-methylpyrrolidinone (NMP), and propylene carbonate (PC) (entries 1-3 in Table 2); note that the donor number changes by a factor of ~2 in this series. However, reduction of $[(1,5\text{-COD})Ir(CH_3CN)_2][BF_4]$ in all three solvents yielded clear and colorless solutions—that is, instead of nanoclusters, bulk metal. Hence, "solvent-only" stabilization through solvent ligation of the nanocluster surface by high donor number solvents does not afford stable $Ir(0)_n$ nanoclusters. These experiments, the first carefully designed to remove the stabilization effect of any coordinating anion while different donor number solvents are tested as putative stabilizers, do not support the claims of "solvent-only" stabilized nanoclusters.

Table 2. The 5 criteria Evaluated for $Ir(0)_n$ Nanoclusters in Five Solvents for $H^+BF_4^-$, BF_4^-, and 1-$MeCB_{11}F_{11}^-$.

	solvent	ε	counterion	k_1 (h^{-1})	$k_2 \times 10^{-3}$ (h^{-1} M^{-1})[a]	$k_2/k_1 \times 10^{-5}$ (M^{-1})	d_m (Å)	appearance	redisp	cat. act.[b]	TTO[c]
1	NMA	165	$H^+BF_4^-$	---	---	poor fit	---	clear, metal[e]	no	---	---
2	NMP	36	$H^+BF_4^-$	---	---	poor fit	---	clear, metal[e]	no	---	---
3	PC	69	$H^+BF_4^-$	---	---	poor fit	---	clear, metal	no	---	---
4	NMA	165	BF_4^-	0.98(8)	7.9(4)	0.081(8)	agg.[f]	brown	part	0.88(5)	[62,500]
5	PC	69	BF_4^-	1.1(1)	7(1)	0.070(4)	agg.[f]	brown	part	0.083(5)	[45,600]
6	CH_3CN	39	BF_4^-	0.11(1)	3.6(2)	0.34(5)	----	clear, metal	no	---	---
7	NMP	36	BF_4^-	0.18(1)	8.9(4)	0.49(3)	----	brown, metal	no	---	---
8	acetone	20	BF_4^-	0.052(5)	12.1(2)	2.4(2)	----	clear, metal	no	---	---
9	PC	69	1-$MeCB_{11}F_{11}^-$	0.46(5)	6.0(5)	0.20(3)	---	clear, metal	no	---	---

(a) The values for k_2/k_1 have been corrected by the mathematically required stoichiometry factor of 1400 as detailed elsewhere.[42] (b) mmol H_2/h (c) total turnovers of cyclohexene hydrogenation (mol product/mol catalyst); square brackets indicated that bulk metal was formed during the course of these experiments, so these values are necessarily an upper limit on the true nanoparticle TTOs. (d) A poor fit to the 2-step mechanism was observed for the indicated data. (e) These solutions initially appear black, but close inspection reveals a clear solution with finely divided particles plus bulk metal on the stir bar and culture tube. (f) agg=aggregated

Investigating Contributions to Nanocluster Stabilization from the Traditionally Weakly Coordinating Anion BF_4^-.

Preparation of $Ir(0)_n$ Nanoclusters in the Presence of the Traditionally Weakly Coordinating Anion BF_4^-. In the next series of experiments, PS™ was added to [(1,5-COD)Ir(CH_3CN)$_2$][BF_4] such that the *BF_4^- anion* is formed instead of the conjugate acid $H^+BF_4^-$, Scheme 2.

Scheme 2. A generalized $Ir(0)_n$ nanocluster formation reaction in which the only anion present is BF_4^-.

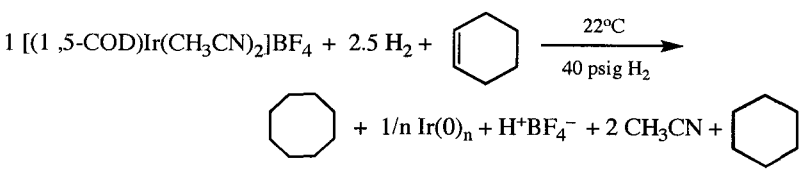

Examination of entries 4-8 in Table 2 reveals that, with BF_4^- present as the only possible anionic stabilizer, only the two solvents with the highest dielectric constants studied, NMA and PC (ε=165 and 69, respectively), afforded homogeneous brown solutions characteristic of $Ir(0)_n$ nanoclusters.[44] The other three lower ε solvents yielded clear solutions with bulk metal present instead of nanoclusters (see the Supporting Information for details). The resulting implication, then, is that the traditionally weakly coordinating BF_4^- plus high ε solvents is sufficient to provide meta-stable nanoclusters. Recent XPS evidence from Dupont and co-workers confirms that the traditionally weakly coordinating PF_6^- anion is present on the surface of a sample of dried nanoclusters (the PF_6^- being the anionic component of the ionic liquid 1-butyl 3-methylimidazolium hexafluorophosphate that is employed in that particular study).[45] A specific hypothesis for how BF_4^- and PF_6^- can coordinate to, and thereby stabilize, transition-metal nanoclusters is the tridentate surface-binding mode postulated elsewhere.[46] Also probably key in how even traditionally weakly coordinating anions such as BF_4^- or PF_6^- can provide nanocluster stabilization in polar solvents, is the *up to 2-fold stronger metal-ligand bond dissociation energies in nanoclusters than the corresponding bulk metal,* thermodynamic effects identified elsewhere[25,47] which result in a particle-size-dependent fractional ligand coverage of nanocluster surfaces.[25]

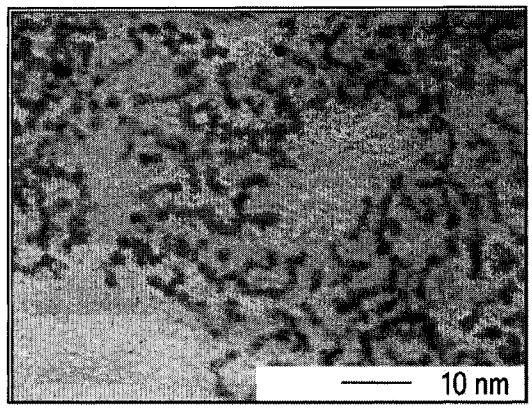

Figure 1. TEM micrograph (580k magnification) of agglomerated $Ir(0)_n$ nanoclusters prepared in PC in the presence of 1 eqv BF_4^-.

Nanoclusters prepared in NMA and PC (entries 4 and 5 in Table 2) were examined using TEM, criteria (ii) of the 5 criteria method. A representative image of nanoclusters prepared in PC is shown in Figure 1. This micrograph is qualitatively useful, allowing the direct observation of agglomerated nanoclusters, but the extensive agglomeration eliminates any hope of quantitating the size and size distribution of the nanoclusters. Attempts to isolate nanoclusters prepared under the conditions of Scheme 2 in NMA or PC by precipitation with anhydrous diethyl ether yielded bulk metal. This important observation means that these BF_4^- / high ε solvent stabilized, meta-stable nanoclusters are, however, not sufficiently stable to pass the stringent test of isolability and redissolvability without the formation of bulk metal. Nanoclusters prepared under the conditions of Scheme 2 with 1 equiv BF_4^- present in NMA or PC precipitate out of solution ~5 hours after complete nanocluster formation. Additionally, bulk metal was formed during TTO experiments. These data again indicate that 1 equiv BF_4^- plus polar solvents provides, at best, meta-stable transition-metal nanoclusters, at least in the test case of $Ir(0)_n$ nanoclusters.

Increased Solution Stability in PC with 50 or 100 Eqv BF_4^-. We performed three nanocluster formation and stabilization experiments with excess, added $[Bu_4N][BF_4]$ so as to increase the amount of BF_4^- over and above the 1 eqv BF_4^- present from reduction of $[(1,5\text{-COD})Ir(CH_3CN)_2][BF_4]$, Scheme 2. While adding just a 10-fold excess of $[Bu_4N][BF_4]$ at the beginning of the nanocluster formation reaction had no apparent effect on the solution stability of the resultant nanoclusters in PC, adding 50 equivalents of $[Bu_4N][BF_4]$ increased the solution stability of the nanoclusters from ~5 hours *to* ≥*2 months* under a N_2. Adding 100 equivs $[Bu_4N][BF_4]$ gave indistinguishable results. This corresponds to a ≥288 fold increase in the solution stability. Nanoclusters prepared with 50 eqv added $[Bu_4N][BF_4]$ are not obviously agglomerated by TEM, but they do show a somewhat broad size distribution of 36±12 Å (see Figure S3 of the Supporting Information). However, despite the increased solution stability of the systems with 50 or 100 eqv added $[Bu_4N][BF_4]$, neither solution of nanoclusters were isolable and/or redissolvable—that is, BF_4^- / high ε solvent stabilized nanoclusters again fail the isolability test of stability.

Reflection upon the improved solution stability and decreased agglomeration with 50 to 100 eqv added $[Bu_4N][BF_4]$ yields further insights. Normally, added salts yield a *collapse* of the Debye layer[19,22] (recall eq.1, where the concentration of ions in the bulk solution is in the denominator), typically resulting in precipitation of traditional colloids. This phenomenon is the critical coagulation concentration (ccc) of colloidal stability, described in the literature as a "rather abrupt change from stability to instability on changing the salt concentration".[22] It follows that the *increased stability* seen with 50 to 100 equivalents of $[Bu_4N][BF_4]$ demands a different explanation. The obvious one is

given in equation 2 below in which we hypothesize an equilibrium between free and surface-bound BF_4^- to account for the increased solution stability with 50 or 100 eqv $[Bu_4N][BF_4]$. Increasing the concentration of $[Bu_4N][BF_4]$ should shift the equilibrium to the right, increasing the concentration of surface bound BF_4^-, thereby providing more of DLVO-type anionic (Coulombic repulsion) stability between $[Ir(0)_n\bullet(BF_4^-)_x(solvent)_y]^{x-}$ nanoclusters.

$$Ir(0)_n + xBu_4N^+BF_4^- \rightleftharpoons Ir(0)_n\bullet xBF_4^- + xBu_4N^+ \qquad (2)$$

Consistent with more surface-coordinated BF_4^-, the nanoclusters with 50 or 100 eqv added $[Bu_4N][BF_4]$ were proved to be *half* as catalytically active for cyclohexene hydrogenation.

Interestingly, adding 480 eqv $[Bu_4N][BF_4]$ and then monitoring the formation reaction in PC resulted in bulk metal. This is an important finding, one that: (i) supports strongly DLVO theory as directly applicable to nanocluster stability since the additional $[Bu_4N][BF_4]$ salt appears to have collapsed the Debye layer; (ii) documents, therefore, the dual effects of added salt stabilizers; and (iii) means that in the future nanocluster stability needs to be reported, as well as tested, as a function of the amount of added salt(s) present.

X-ray Photoelectron Spectroscopy (XPS) of Dried Nanoclusters Prepared with 1 Eqv BF_4^-. The presence of BF_4^- in a film of dried nanoclusters, prepared under the conditions of Scheme 2 in PC, was confirmed by XPS.[48] A high-resolution XPS spectrum showed that 5% of the total surface composition was attributable to F (see Figure S2 of the Supporting Information), at least in a *solid state* sample of the (dried) nanoclusters.

Electrophoretic Mobility Experiment Providing Evidence for BF_4^- Coordination in Solution. To provide addition evidence for the coordination of BF_4^- to the $Ir(0)_n$ nanoclusters, we performed an electrophoretic mobility experiment analogous to those we have done before[49] (see Figure S4 for a drawing of the electrophoretic mechanism apparatus, and see the Experimental Section for details). First, however, a control experiment was done repeating the electrophoretic mobility demonstrated before for a brown solution of $P_2W_{15}Nb_3O_{62}^{9-}$-stabilized $Ir(0)_n$ nanoclusters (done before in acetone):[49] in PC a brown band migrated toward the positive electrode while the solution on the negative side of the apparatus remained clear and colorless, providing good evidence that the proven neutral[49] $Ir(0)_n$ nanocluster core has acquired a net anion charge by coordinating the 9– polyoxoanion stabilizer.[49] In a separate experiment a brown solution of $Ir(0)_n$ nanoclusters prepared with 50 eqv added $[Bu_4N][BF_4]$ also migrated toward the positive electrode while the solution on the negative electrode side of the apparatus remained clear and colorless. This indicates that the surfaces of the nanoclusters prepared with 50 eqv BF_4^- have an overall negative charge. A separate H_2 uptake experiment confirmed that these specific $Ir(0)_n$ nanoclusters are neutral (as we have demonstrated for the polyoxoanion-stabilized nanoclusters[49]); the H_2 uptake experiment performed confirms the stoichiometry in Scheme 2 in which precisely 2.5 eqv H_2 per eqv $[(1,5\text{-COD})Ir(CH_3CN)_2][BF_4]$ is taken up, so that the resultant $Ir(0)_n$ nanoclusters must be are neutral (see the section titled "Stabilization by Surface Hydrides" for more details). Given that the $Ir(0)_n$ core is neutral, yet the nanoclusters migrate to the positive electrode of an electrophoretic mobility experiment, and given that BF_4^- is the only anion present, this experiment *confirms that BF_4^- is adsorbed on the*

nanocluster surface in solution, $[Ir(0)_n(BF_{4-})_x]^{x-}$. This, in turn, provides further compelling evidence for DLVO-type, electrostatic stabilization, but in this case with the novel insight being that such stabilization is provided by even the traditionally weakly coordinating BF_4^- anion.

^{19}F NMR Attempts to Detect Coordinated BF_4^-. We used ^{19}F NMR spectroscopy as a direct, *solution* method to detect surface-bound BF_4^- on separate nanocluster solutions with either 1 or 50 eqv BF_4^- present.[50] However, no significant shift in the ^{19}F NMR signal was observed for either nanocluster solution compared to a reference solution of $[Bu_4N][BF_4]$, Figure S5 of the Supporting Information. Recalling our compelling evidence that BF_4^- coordinates to the nanocluster surface (i.e., the increased stability when 1 equiv BF_4^- is present, the increased stability with 50-100 equiv BF_4^-, the decreased catalytic activity with increasing equiv BF_4^-, and the electrophoretic mobility to the positive electrode directly traceable to coordinated equiv BF_4^- as the only anion present), our inability to detect Ir•BF_4^- formation by ^{19}F NMR can be rationalized by one or more of: (i) being below the detection limit at the concentrations employed, (ii) rapid exchange of the BF_4^- anion, or (iii) slow tumbling of the nanoclusters in solution.[51]

Carborane Control Experiment: Further Evidence Supporting BF_4^- as a Nanocluster Surface-Ligating Anion.

In light of the negative ^{19}F NMR experiment above, we designed one more experiment to provide additional evidence for (or against) the coordination of traditionally weakly coordinating anions to electrophilic transition-metal nanocluster surfaces. Specifically, we prepared and used the novel organometallic precursor [(1,5-

COD)Ir($CH_3CN)_2$][1-$MeCB_{11}F_{11}$] under the otherwise identical nanocluster synthesis conditions shown in Scheme 2 (see Figure S6 for ^1H, ^{11}B, and ^{19}F NMR spectra and the Experimental Section for assignment of the spectra characterizing this new complex). This nanocluster precursor contains an even more weakly coordinating (than BF_4^-) carborane anion;[52] the resultant nanoclusters should, therefore, be even less stabilized than those with BF_4^-.[53] Indeed, reduction of [(1,5-COD)Ir($CH_3CN)_2$][1-$MeCB_{11}F_{11}$] under H_2 in PC resulted in a clear and colorless solution with bulk metal present (entry 9, Table 2)—the resultant, transient Ir(0)n nanoclusters were not even meta-stable. This result provides further confirmation that BF_4^- coordination is an important contribution to $Ir(0)_n$ nanocluster stability—and by implication the stability of nanoclusters of other transition-metals—in solutions of high ε solvents.

Ruling Out Five Alternative Hypotheses for Contributions to Nanocluster Stabilization.

We have also considered 5 other (7 total) alternative hypotheses as to the source of nanocluster stability, such fundamental studies not having been reported before as well as being necessary to confirm the conclusion of this work that "BF_4^- coordination in polar solvents is key to the nanocluster stability."

Possible Stabilization by Trace Chloride: The organometallic precursor [(1,5-COD)Ir($CH_3CN)_2$][BF_4] is, ostensibly, halide-free, an important point since Cl^- is an established nanocluster stabilizer.[16,17,54] However, since this precursor is prepared from the halide-containing dimer, [(1,5-COD)IrCl]$_2$, this leaves open the possibility that trace chloride may be present in the system as a result of a non-stoichiometric reaction with

$Ag^+BF_4^-$. Elemental analysis of dried nanoclusters prepared in PC under the conditions of Scheme 2 did, indeed, confirm a trace chloride content of 0.15(2)% (corresponding to 0.008 eqv of Cl^- per Ir). Consequently, an attempt to increase the solution stability of the nanoclusters was made by the addition of Cl^- in the form of added $[Bu_4N][Cl]$. The addition of up to 1 equivalent $[Bu_4N][Cl]$ per Ir (which allows for >1 Cl^- atom per *surface* Ir atom in the nanoclusters) had no effect on the resultant solution stability of the nanoclusters prepared in PC from $[(1,5\text{-COD})Ir(CH_3CN)_2][BF_4]$. The nanoclusters still precipitated out of solution after ~5 hours. Hence, the hypothesis that trace chloride was responsible for the observed solution stability of nanoclusters prepared from $[(1,5\text{-COD})Ir(CH_3CN)_2][BF_4]$ is not supported.

Possible Stabilization by Reaction of the Solvent with the Nanocluster Surface. One alternative hypothesis is that solvents plus reactive nanocluster surfaces could undergo reactions such as oxidative addition of a C–H bond[55] to form (in this case) surface Ir-R and Ir-H bonds that might serve as steric stabilizers. To test this alternative hypothesis, we carried out the reaction shown in Scheme 2 under both H_2 and D_2 in both PC and NMP. If the solvent reacted with the nanocluster surface (e.g., in a series of oxidative addition and reductive elimination steps), deuterium incorporation is expected. However, GC-MS showed identical elution times and fragmentation patterns under H_2 and D_2 for both PC and NMP; hence, the structure and composition of the solvent appeared unchanged. The hypothesis of solvent reaction with the nanocluster surface is, therefore, not supported, the caveat here being that the only reversible reaction[55] would have been detected by our precedented D_2 exchange method.[55]

Possible Stabilization by Surface Hydrides: Under the conditions of relatively high hydrogen pressure that we employ (40 psig), another hypothesis was that surface hydrides could be formed on the surface of the electrophilic, coordinatively unsaturated nanoclusters, thereby potentially (sterically?) stabilizing the nanoclusters. Consequently, we performed hydrogen uptake studies in PC in the *absence* of cyclohexene with a sensitive pressure transducer (±0.1 Torr). From Scheme 2, the reaction stoichiometry predicts 2.5 equivalents of H_2 should be consumed per equivalent of [(1,5-COD)Ir($CH_3CN)_2$][BF_4]. Experimentally, we observe that 2.6 ± 0.4 equivalents are consumed, a result which confirms an analogus finding for polyoxoanion-stabilized $Ir(0)_n$ nanoclusters.[49] Hence, the hypothesis that surface hydrides are a source of the observed solution stability is not supported.

Possible Stabilization by Scavenged Charge: It has been shown in the literature that $Pd(0)_n$ nanoclusters are capable of scavenging charge from a W/Al_2O_3 crucible that was part of the reaction apparatus.[12] Consequently, we tested the perhaps remote hypothesis that our $Ir(0)_n$ nanoclusters might also be capable of scavenging charge from the reaction apparatus by performing an electrophoretic mobility experiment analogous to the one described earlier with 50 eqv [Bu_4N][BF_4] (see the apparatus in Figure S4), but now on nanoclusters prepared under the conditions of Scheme 2 with 1 eqv [Bu_4N][BF_4] present. The resultant $Ir(0)_n$ nanoclusters were not drawn toward the positive or negative electrode in ~5 hours, after which the nanoclusters precipitated out of solution ending the experiment. This experiment indicates that any putative scavenged charge on the nanoclusters is less than that provided by 50 equiv BF_4^- (which did cause the migration of the nanoclusters, *vide supra*). In short, this control experiment argues against the

formulation of the nanoclusters as intrinsically anionically charged, "$Ir(0)_n^{x-}$", as a conceivable, but unlikely, source of the observed solution stability.

Possible Stabilization by Polymerized Solvent. A fifth alternative hypothesis builds off the plethora of literature examples of nanoclusters stabilized by polymers, including investigations more than 60 years old.[56] While it seems unlikely,[57] it is still conceivable that propylene carbonate could be polymerizing under the reaction conditions to form the known polymer poly(propylene carbonate)[58,59] as a nanocluster stabilizer. Electrospray ionization mass spectrometry (ESI-MS), a technique of demonstrated utility in determining polymeric molecular weights,[60] was employed to test this hypothesis. However, no detectable poly(propylene carbonate) is formed under our reaction conditions, Figure S7 of the Supporting Information. Therefore, the hypothesis that $Ir(0)_n$ nanoclusters are stabilized by polymerized solvent is also not supported.

In summary, none of the additional five hypotheses that we could conceive of as to the source of solution meta-stability observed for $[Ir(0)_n \bullet (BF_4^-)_x(PC)_y]^{x-}$ nanoclusters in PC are supported. Our prior conclusion, that these nanoclusters are stabilized by surface-adsorbed BF_4^- plus PC, along with a Debye multi-layer expanded by the polar solvent PC, is therefore further supported.

O_2/Surface Oxide and Pyridine Ligated Nanoclusters: Enhanced Solution Stability. One expects that surfaces of the nanoclusters prepared with 1 eqv BF_4^- have weakly coordinated BF_4^- that, therefore, should be readily replaceable. To test this hypothesis, we exposed a solution of fully formed nanoclusters in PC to oxygen by stirring the nanoclusters under atmospheric O_2 for 15 minutes.[61] After exposing nanoclusters

prepared under the conditions in Scheme 2 to atmospheric oxygen, *the nanoclusters attained long-term solution stability* (>2 weeks, compared to ~5 hours for nanoclusters that had not been exposed to O_2), a ≥67 fold improvement in their solution stability. This experiment is important in at least three respects: (i) it confirms[49,61b] that the as-prepared $Ir(0)_n$ nanoclusters are O_2 sensitive; (ii) it demonstrates that the previously coordinated BF_4^- and solvent are easily displaced by oxidation; and most significantly (iii) it demonstrates that uncontrolled surface oxygenation of putative "solvent-only stabilized" nanoclusters may well be a significant source of any observed stability.

A separate test of the displaceability of the surface ligand of $Ir(0)_n$ nanoclusters prepared with 1 eqv BF_4^- in PC was performed by adding the strong ligand pyridine to a solution of the nanoclusters. The solution of nanoclusters with added pyridine again attained enhanced solution-stability (>2 weeks). This experiment further demonstrates: (i) that the BF_4^- plus PC ligands of $[Ir(0)_n\bullet(BF_4^-)_x(PC)_y]^{x-}$ are readily replaced (and thus relatively weakly coordinated); and (ii) that (neutral) strong *ligand coordination and stabilization* is another mode of nanocluster stabilization.[62] As expected, however, the nanocluster solution with added pyridine was catalytically *inactive* towards cyclohexene hydrogenation, indicating pyridine coordination to the previously catalytically active surface atoms of the nanoclusters.

How Does BF_4^- Compare to the "Gold Standard" $Ir(0)_n$ Nanocluster Stabilizer $P_2W_{15}Nb_3O_{62}^{9-}$? The present "Gold Standard" (poly)anion for nanocluster high stabilization, in comparison to 11 anions studied so far[16,17] is the 9– charged, Brønstead basic $P_2W_{15}Nb_3O_{62}^{9-}$ polyoxoanion and according to the 5 criteria method, even in the

lower ε solvent acetone.[16,17,,63] As such, the $P_2W_{15}Nb_3O_{62}^{9-}$ polyoxoanion is a valuable reference point for ranking other stabilizers, at least for the prototype $Ir(0)_n$ nanocluster system.

Scheme 3. The generalized $Ir(0)_n$ nanocluster formation reaction in the presence of added anions, $Bu_4N^+Y^-$,[64] such as $[Bu_4N]_9[P_2W_{15}Nb_3O_{62}]$.

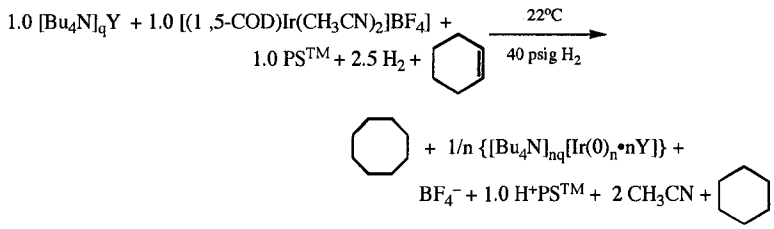

Five sets of experiments are reported in the Supporting Information comparing BF_4^- to $P_2W_{15}Nb_3O_{62}^{9-}$ for all five solvents listed in Table 1. The essence of our findings is that $P_2W_{15}Nb_3O_{62}^{9-}$ is a considerably superior stabilizer compared to BF_4^- in all five solvents, as measured by the 5 criteria method.

Further Tests of DLVO Theory: Do Increasingly High ε Solvents Increase the Stability of $Ir(0)_n$ Nanoclusters in the Presence of $P_2W_{15}Nb_3O_{62}^{9-}$? We examined the five solvents shown in Table 1 for the reaction in Scheme 3. A detailed discussion appears in the Supporting Information; the interesting, key result is that solvent ε *does not appear* to influence the stability of $P_2W_{15}Nb_3O_{62}^{9-}$-stabilized nanoclusters as measured by the 5 criteria. It is not clear at present if this result is a reflection of a break-down of DLVO theory when non-point charge, non-unit charge (poly)anions like $P_2W_{15}Nb_3O_{62}^{9-}$ are present or an insensitivity of the 5 criteria method. This does, therefore, set up an important target to restudy if and when an agglomeration kinetic method becomes available for assaying nanocluster stability.

Summary and Conclusions

The highlights of the present work can be summarized as follows:

- Literature claims of "solvent-only" stabilized nanoclusters are not supported by our findings, at least in the case of $Ir(0)_n$ nanoclusters. Instead and in accordance with DLVO theory, surface-coordinated anions yield repulsive, electrostatic stabilization between nanoclusters.

- Hence, anion coordination and electrostatic stabilization is *the first hypothesis* one should test and support or refute when it comes to claims of how transition-metal nanoclusters are stabilized and prior to postulating unprecedented "solvent-only" or other new stabilization modes.

- Even the traditionally weakly coordinating anions such as BF_4^- *contribute significantly to the stability of prototype* $Ir(0)_n$ *nanoclusters in high* ε *solvents.* This is a major, previously unappreciated finding from this study.

- Two sub-hypotheses for the observed nanocluster meta–stability in the presence of BF_4^- are a possible tridentate, facial coordination of BF_4^- on the metal surface[46] and the probability of a particle-size dependent fractional ligand coverage of the nanocluster surface, with a recently identified up to 2-fold stronger metal-ligand bond dissociation energies in nanoclusters in comparison to the corresponding bulk metal.[25]

- The stability of $[Ir(0)_n \bullet (BF_4^-)_x(PC)_y]^{x-}$ nanoclusters is enhanced by adding 50-100 equivs of $[Bu_4N][BF_4]$, but is then decreased when larger amounts (480 equivs) of $[Bu_4N][BF_4]$ are added. This was rationalized by the competition of opposing effects: the increase of surface-coordinated of BF_4^- due to the operation of the equilibrium in eq. 2

(vide supra), vs. the collapse of the Debye layer in accordance with DLVO theory and the concept of a ccc (critical coagulation concentration) salt effect.[19,22]

- Nanocluster stability, then, really makes sense only as function of the amount and specifics of the types of salt and solvent present. Hereafter, each claim and report of "nanocluster stability" should test the stability *in solution* as a function of the salt concentration and in various dielectric constant solvents.

- The solution stability time is improved significantly by exposing the nanoclusters to atmospheric O_2 or pyridine. Hence, the presence or absence of surface oxides needs to be carefully considered and ruled out or supported in each claim of nanocluster stability where the nanoclusters have been exposed to O_2. Nanocluster oxides have received some investigation,[65,66] but deserve additional systematic study.

- As measured by the 5 criteria, nanoclusters prepared in the presence of 1 equiv BF_4^- are much less stabilized (and, for example, are not isolable) in comparison to the highly stabilized, isolable nanoclusters with the $P_2W_{15}Nb_3O_{62}^{9-}$ 'Gold Standard" (poly)anionic stabilizer. Nevertheless, the findings of weak, meta-stabilization by anions such as BF_4^- in high ε solvents may have applications towards solving the "naked nanocluster" (really "ligand-labile") problem[31].

Experimental Section

Materials and Instrumentation. All commercially obtained reagents were used as received unless otherwise noted. All solvents were stored in the drybox prior to use. N-methylacetamide (Aldrich, 99+%) was purified according to literature procedure.[67] Propylene carbonate (Aldrich, 99.7%) was evacuated under vacuum (≤100 mgHg) for at

least four hours and stored over activated 4Å molecular sieves. Acetonitrile (Aldrich, 99.93+%) and acetone (Burdick and Jackson, 99.9+% by GC) were purged with argon for a minimum of 20 minutes. Nitromethane (Aldrich, 99+%) was purified according to literature procedures.[68] N-methylpyrrolidinone (Aldrich, 99.5%) was bubbled with Ar for 20 min and stored over activated 4Å molecular sieves. Cyclohexene (Aldrich, 99%) was freshly distilled over Na metal under argon and stored in the drybox prior to use. Pyridine (Aldrich, 99%) was vacuum distilled and stored over activated 4Å molecular sieves. CH_2Cl_2 (Aldrich, 99%) was distilled over P_2O_5 and stored in the drybox. The crystalline iridium solvate complex, $[(1,5\text{-COD})Ir(CH_3CN)_2][BF_4]$, was prepared following the procedure for the corresponding hexafluorophosphate salt.[69] The purity of the solvate complex was verified by ^1H NMR (CD_2Cl_2: s (δ 4.3), s (δ 2.6), m (δ 2.3), m (δ 1.8)). Proton Sponge™ (1,8-bis(dimethylamino)naphthalene, Aldrich, 99%) was stored in the drybox prior to use. The polyoxoanion $[Bu_4N]_9[P_2W_{15}Nb_3O_{62}]$ used in control reactions was prepared according to our most recent literature procedure.[70] The purity of the polyoxoanion was checked by ^{31}P NMR (CD_3CN: δ -6.5, -13.6 relative to 85% H_3PO_4, with small impurity peaks at -8.7 and -13.2). $AgBF_4$ (Aldrich, 99%), $[Bu_4N][BF_4]$ (Aldrich, 99%), and C_6F_6 (Aldrich, 99.5+%) were used as received and stored in the drybox.

Gas chromatography was performed using a Hewlett-Packard 5890 Series II GC with a FID detector equipped with a Supelcowax 10 column coupled to a Hewlett-Packard 3395 integrator. Parameters were as follows: T_1=50 °C, t_1=3 min, ramp=10 °C/min, T_2=180 °C, t_2=14 min, injection volume 2 μL. Negative-ion electrospray mass spectrometry (ESI-MS) was performed on a Finnigan LCQ Duo MS directly coupled

with a syringe pump. ^{1}H, ^{11}B, and ^{19}F NMR experiments were carried out on a Varian Inova 300 spectrometer. Spectra were obtained in 5.0 mm o.d. oven dried (≥24h at 160 °C) NMR tubes at 22 °C in either CD_2Cl_2 or CD_3CN. ^{19}F NMR spectroscopy for this study was carried out using a Varian 400MHz NMR with the following spectral parameters: acquisition time, 0.599 s; relaxation delay, 4.0 s; sweep width, 34965.0 Hz; scan repetitions, 84. An internal reference of C_6F_6 (set to δ=–165.00) was used. XPS spectra were collected using a Physical Electronics (PHI) Model 5800XPS system equipped with a monochromator (Al Kα source operating at 1486.8 eV; system pressure ≤ $1x10^{-9}$ Torr) and a hemispherical analyzer to detect the ejected electrons.

Hydrogenations. The nanoclusters studied herein were prepared based on our "Standard Conditions" reaction conditions.[71,72] Experiments were carried out in an in-house constructed, previously well-described[71,72] hydrogenation apparatus for continuously monitoring the loss of H_2 pressure via an Omega PX621 pressure transducer interfaced to a PC through an Omega D1131 A/D converter. For reactions prepared under the conditions in Scheme 1, 1.7 mg (3.6 μmol) $[(1,5\text{-COD})Ir(CH_3CN)_2][BF_4]$ was weighed into a 2–dram glass vial. For reactions prepared under the conditions in Scheme 2 and 3, 1 eqv (0.8 mg, 3.6 μmol) Proton Sponge™ was also added. For reactions prepared under the conditions in Scheme 3, 22.6 mg (3.6 mmol) $[Bu_4N]_9[P_2W_{12}Nb_3O_{62}]$ was added.[64] The solvent under study (2.5 mL) was added with a gas-tight syringe. This solution was mixed with a disposable polyethylene pipet until the solution was homogenous. Next, the solution was transferred using the pipet to a new 22 x 175 mm Pyrex culture tube with a new 5/8 x 5/16 in Teflon-coated stir bar. Then, freshly distilled cyclohexene (0.5 mL) was added with a 1.0 mL gas–tight syringe.

The culture tube containing the reaction solution was then placed in a Fischer-Porter (F-P) bottle. The F-P bottle was sealed and brought out of the drybox. Next, the F-P bottle was placed in a jacketed reaction flask with temperature control at 22.0 ± 0.1 °C by means of a constant temperature circulating water bath. The F-P bottle was attached to the hydrogenation apparatus with Swagelok TFE-sealed Quick-Connects. Stirring was initiated at ≥ 600 rpm,[73] and the F-P bottle was purged 13 times (once every 15 s x 13 repetitions = 3 min and 15 s total) with 40 ± 1 psig H_2 gas. After five minutes, t=0 was set and data collection began. Pressure uptake data was fitted to the analytical form for autocatalysis[42] using ORIGIN 7.0. Formation of the nanoclusters was monitored directly by the evolution of cyclooctane by GLC as previously documented.[42]

Catalytic Activity, Nanocluster Isolation, and Redispersability Experiments. After the minimum time required for the complete formation of nanoclusters as judged by a separate cyclooctane evolution experiment,[42] the F-P bottle was disconnected, vented, sealed, and brought into the drybox. There, three aliquots of the reaction solution (0.5 mL each) were removed from the culture tube using a 1.0 mL gas-tight syringe. The first aliquot was placed in a new culture tube with a new stir bar, and diluted to 2.5 mL with the solvent under study. Next, freshly distilled cyclohexene (0.5 mL) was added to the culture tube with a 1.0 mL gas-tight syringe. Last, the culture tube was sealed in the F-P bottle, brought out of the drybox, and hydrogenation was initiated as described herein.

The other two 0.5 mL aliquots taken were used for transmission electron microscopy (TEM) analysis (see "Transmission Electron Microscopy" section below) and nanocluster redispersability experiments. Neither NMA nor PC is sufficiently volatile to allow for simple solvent removal under vacuum (NMA boils at ca. 204-206 °C, PC at

240 °C). Accordingly, nanoclusters prepared in these solvents were precipitated with diethyl ether following a procedure established elsewhere.[74] The isolated nanoclusters were then redispersed by adding the solvent under study (2.5 mL) to the dried nanocluster film, and agitated with a polyethylene pipet until the solution was a homogeneous light brown (NB: this was only possible for $P_2W_{15}Nb_3O_{62}^{9-}$-stabilized nanoclusters, as none of the nanoclusters prepared with BF_4^- were redispersable without the formation of bulk metal). Using the polyethylene pipet, the redispersed nanocluster solution was transferred into a new culture tube with a new stir bar, and freshly distilled cyclohexene (0.5 mL) was added. The culture tube was placed in the F-P bottle, which was subsequently sealed, removed from the drybox, and attached to the hydrogenation apparatus. Hydrogenation was initiated exactly as described in the section titled "Hydrogenations".

Transmission Electron Microscopy (TEM). TEM analysis was carried out with the expert assistance of Dr. JoAn Hudson at either the University of Oregon or Clemson University. As described previously,[16] micrographs were obtained with a Phillips CM-12 microscope operating at 100 keV. Size measurements were obtained from micrographs with 430k magnification or higher. Size distributions of nanoclusters were determined by counting > 100 nanoclusters. Since propylene carbonate is not a suitable solvent for preparing TEM grids[74] if prepared by a "standard" method (by placing two drops of the diluted reaction solution onto TEM grids), the reaction solutions were sprayed onto TEM grids using an asthmatic's nebulizer (PulmoAide, model 5610D). In the drybox, the reaction solution (0.5 mL) was syringed into a new disposable medicine cup. 300 mesh silicon monoxide TEM grids (Ted Pella, Inc.) were carefully held with tweezers in front

of the nebulizer mouthpiece while the reaction solution was nebulized. After trials with 5, 10, 15, and 30 s of nebulization time, it was determined that 5 s exposure time was sufficient to visualize the nanoclusters. Control TEM images of $P_2W_{15}Nb_3O_{62}^{9-}$–stabilized $Ir(0)_n$ nanoclusters in acetone prepared either by the "standard" method or the nebulizer method confirmed that both techniques yield statistically indistinguishable results. Dark field TEM images were inverted and then enlarged using Adobe Photoshop 7.0.

Total Turnover (TTO) experiments. The total turnover experiments were carried out exactly as reported previously.[16,17]

XPS of Dried Nanoclusters Prepared with 50 eqv added $[Bu_4N][BF_4]$. A nanocluster formation reaction was carried out exactly as described in the section titled "Hydrogenations". Then, the nanoclusters were precipitated from solution in a scintillation vial following our literature procedure.[74] In the drybox, the scintillation vial was broken with a hammer. A portion of the vial with metal visible to the naked eye plated out on it was sealed in a separate oven-dried glass scintillation vial, which was subsequently sealed with electrical tape. The vial was removed from the drybox. Then, under flowing N_2, a portion of the metal-coated vial was mounted onto a XPS sample holder with Scotch tape. After thoroughly evacuating the sample chamber ($\leq 10^{-9}$ Torr), sample analysis was initiated.

Hydrogenations with excess $[Bu_4N][BF_4]$. These experiments were carried out as described in the section titled "Hydrogenations" with the following modification: to the glass vial containing $[(1,5\text{-COD})Ir(CH_3CN)_2][BF_4]$ and PS™, 10, 50 or 100 equivalents

of $[Bu_4N][BF_4]$ (36, 180, or 360 μmol) were added. The rest of the hydrogenation procedure was carried out exactly as reported.

Electrophoretic Mobility Experiments. The apparatus used herein was a modification of a previously used[49] glass U-Tube with an addition arm. For the experiments herein, a glass tube in a W shape with an addition arm and two fine glass frits was used (see Figure S4 in the Supporting Information). An electrolyte solution (40 mL) of 2mM $[Bu_4N][BF_4]$ in PC was prepared and used to fill both arms of the W-Tube. Then, a solution of fully formed nanoclusters in PC was added to the addition arm with the stopcock closed. Two Pt wire electrodes were immersed in the electrolyte solution in the arms of the W-tube. After opening the stopcock and allowing the nanocluster solution into the center of the W-tube, a voltage of 21V was applied with a Keithley 2400 SourceMeter. An analogous experiment was carried out with nanoclusters prepared under the conditions of Scheme 1 but with 50 eqv added $[Bu_4N][[BF_4]$. Two control experiments, with either $P_2W_{15}Nb_3O_{62}^{9-}$- or Cl^--stabilized nanoclusters, were also performed to confirm the expected migration of the negatively charged nanoclusters toward the positive electrode.

^{19}F NMR Spectroscopy. As a control to establish the spectrum of "free" BF_4^-, $[Bu_4N][BF_4]$ (1.0 mg, 3.0 μmol) was dissolved in propylene carbonate (0.75 mL) with two drops C_6F_6. An aliquot of this solution (100 μL) was dissolved in CD_2Cl_2 for analysis. For the two reaction solutions, 100 μL of either a nanocluster solution prepared under the conditions of Scheme 1 or a nanocluster solution with 50 eqv added $[Bu_4N][BF_4]$ was diluted in 0.5 mL CD_2Cl_2 with two drops C_6F_6.

Preparation of the Carborane Complex $[(1,5\text{-COD})Ir(CH_3CN)_2][1\text{-Me-}CB_{11}F_{11}]$. The carborane solvate complex was prepared by a modification of literature procedures.[69]

All glassware used was oven-dried for ≥12h at 160 °C. In a 25 mL Erlenmeyer flask, freshly prepared[75] Cs[1-Me-$CB_{11}F_{11}$] (51.1 mg, 0.105 mmol) was dissolved in 10 mL CH_2Cl_2. $AgBF_4$ (20.4 mg, 0.105 mmol) was added to the carborane solution, precipitating $CsBF_4$ as a white powder. The solution was gravity filtered through a Whatman No. 2 filter, yielding a clear and colorless Ag[1-Me-$CB_{11}F_{11}$] solution. Separately, in a 25 mL Erlenmeyer flask, $[(1,5\text{-COD})IrCl]_2$ (35.6mg, 0.053 mmol) was dissolved in ~10 mL CH_2Cl_2 with stirring, yielding a clear, bright red solution. Next, CH_3CN (1.0 mL) was added with a gas-tight syringe to the $[(1,5\text{-COD})IrCl]_2$ solution, immediately producing a clear, bright-yellow solution. Then, the Ir solution was added to the Ag[1-Me-$CB_{11}F_{11}$] solution with a polyethylene pipet. This addition yielded a bright-yellow solution and precipitated AgCl as a white solid. The solution was gravity filtered through a Whatman No. 2 filter into a 50 mL Erlenmeyer flask which contained ~10 mL anhydrous diethyl ether. The flask was covered with a KimWipe and the solvent was allowed to slowly evaporate over a period of three days. $[(1,5\text{-COD})Ir(CH_3CN)_2]$[1-Me-$CB_{11}F_{11}$] (45.3 mg, 58% yield) was collected as a brilliant-yellow powder and characterized by ^1H, ^{11}B, and ^{19}F NMR spectroscopy (Figure S4 in the Supporting Information). ^1H: s (δ 4.3), s (δ 2.6), s (δ 2.3), m (δ 2.0), m (δ 1.8), s (δ 1.6), m (δ 1.3), corresponding to the expected proton peaks for the Ir solvate complex (vide infra) plus the protons from the carborane methyl group. ^{11}B NMR spectroscopy showed two broad peaks centered at δ=⁻10 and ⁻18, corresponding to the terminal and belt boron atoms of the icosahedral carborane, respectively. Boron-decoupled ^{19}F NR spectroscopy showed the following peaks: s (δ -253), s (δ -258), s(δ -260), corresponding to the terminal fluorine atom and the two belts

of fluorine atoms, respectively. Literature ^{11}B and ^{19}F NMR spectra for the Cs[1-Me-$CB_{11}F_{11}$] complex are available.[75]

Nanocluster Formation under H_2 and D_2 for GC-MS. These experiments were carried out exactly as described in the section titled "Hydrogenations" with the exception that D_2 was substituted for H_2 in two of the reactions. After complete nanocluster formation, the F-P bottle was vented, sealed, and brought into the drybox. Aliquots (0.5 mL) of each of the four reaction solutions were placed in pre-dried 1.0 mL GC vials and capped with PTFE-lined crimp top caps. Prior to ESI-MS, the solutions were diluted 10 fold in CH_3CN.

Elemental analysis. The nanocluster material was isolated from PC by precipitation with diethyl ether following a literature procedure.[74] The samples were sealed under nitrogen, double-bottled, and sent to Galbraith Laboratories for analysis (Knoxville, TN). The Cl^- content of the samples was determined by ICP.

Hydrogen uptake experiment. The hydrogen uptake was monitored using the same apparatus and technique previously described.[43] Briefly, in a nitrogen-atmosphere drybox, [(1,5-COD)Ir(CH_3CN)$_2$][BF_4] (10.1 mg, 21.5 μmol) was weighed into a pre-dried two-dram glass vial, and propylene carbonate (5 mL) was added with a 10.0 mL gas-tight syringe. This bright-yellow solution was agitated with a disposable polyethylene pipet until it was homogeneous, and transferred to a pre-dried 50 mL Pyrex reaction bulb which contained a 1 x 3 mm Teflon-coated stir bar. The two-dram vial was rinsed with an additional 5 mL PC, and the rinse solution was also added to the reaction bulb. A final 5 mL PC was added, bringing the final reaction volume to 15 mL. The reaction bulb was sealed, brought out of the drybox, and attached to the vacuum line

apparatus as shown in Figure A of the Supporting Information elsewhere.[43] The solution was degassed via three freeze-pump-thaw cycles, and then vortex stirred for ≥1 hour to attain a stable temperature. With the reaction flask isolated and under vacuum, the manifold was pressurized to ~640 Torr with H_2 (approximately 1 atm pressure at our mile-high altitude). Next, the reaction flask was opened to the manifold, t=0 was set and an initial pressure was noted. Pressure was monitored every five minutes with an MKS Baratron Pressure Gauge.

ESI-MS. Nanoclusters were prepared in PC as described in the section titled "Hydrogenations". Samples were prepared by diluting 1 μL of the reaction solution or control solution in 1 mL 50/50 MeOH/H_2O.

Exposure of Fully Formed Nanoclusters to Oxygen or the Strong Ligand Pyridine. *O_2*: After complete nanocluster formation as judged by a separate cyclooctane evolution experiment, the F-P bottle was disconnected from the hydrogenation apparatus and opened outside the drybox. The dark brown nanocluster solution was stirred for 15 minutes. Then, the nanocluster solution was decanted into a pre-dried glass scintillation vial which was first evacuated and then placed in the drybox.

Pyridine: After complete nanocluster formation as judged by a separate cyclooctane evolution experiment,[42] the F-P bottle was disconnected from the hydrogenation apparatus, vented, sealed, and brought into the drybox. With a polyethylene pipet, the dark-brown nanocluster solution was transferred into a pre-dried glass scintillation vial containing a Teflon-coated magnetic stir bar. Pyridine (1 mL, 12.4 mmol, ~3000 equivs vs. Ir) was added to the scintillation vial with a gas-tight syringe with stirring. Then, the nanocluster solution was vortex stirred for 15 minutes to ensure complete mixing of the

pyridine. The nanocluster solution was kept sealed in the drybox while the solution stability was monitored.

Supporting Information Available: Table S1, examining the "solvent-only" stabilized nanocluster literature; Figure S1, possible reaction of nitromethane with Proton Sponge™; a discussion of stabilization by BF_4^- in low ε solvents plus a structural comparison of NMP and poly(vinylpyrrolidone); Figure S2, XPS spectrum of dried nanoclusters prepared under the conditions of Scheme 1; Figure S3, TEM image of nanoclusters prepared with 50 eqv added $[Bu_4N][BF_4]$; Figure S4, cartoon of the apparatus for the electrophoretic mechanism experiment; Figure S5, ^{19}F NMR spectra investigating the coordination of BF_4^-; Figure S6, ^1H, ^{11}B, and ^{19}F NMR spectra of [(1,5-COD)Ir($CH_3CN)_2$][1-Me-$CB_{11}F_{11}$]; Figure S7, ESI-MS spectra of neat PC and of the reaction solution in PC; Figure S8, the difference in kinetic control[76] of the nanocluster formation reaction in propylene carbonate for nanoclusters prepared with and without added $P_2W_{15}Nb_3O_{62}^{9-}$; and a discussion of $P_2W_{15}Nb_3O_{62}^{9-}$-stabilized $Ir(0)_n$ nanocluster stability in solvents of varying ε.

Acknowledgements. We thank Prof. S. H. Strauss for the use of his high vacuum line for the H_2 uptake experiments and for the generous donation of Cs[1-Me$CB_{11}F_{11}$]. The authors would like to thank Dr. C. D. Rithner for his help with the ^{19}F NMR spectra, Dr. P. McCurdy for collecting the XPS spectra, and Mr. D. Dick for collecting the mass spectral data. This work was funded by DOE grant DE-FG02-03ER15453.

References.

[1] Reviews of nanoclusters: (a) Astruc, D.; Lu, F.; Aranzes, J. R. *Angew Chem. Int. Ed.* **2005**, *44*, 7852. (b) Burda, C.; Chen, X.; Narayanan, R.; El-Sayed, M. A. *Chem. Rev.* **2005**, *105*, 1025. (c) Murphy, C. J.; Sau, T. K.; Gole, A. M.; Orendorff, C. J.; Gao, J.; Gou, L.; Hunyadi, S. E.; Li, T. *J. Phys. Chem. B* **2005**, *109*, 13857. (d) Green, M. *Chem. Commuun.* **2005**, *24*, 3002. (e) Narayanan, R.; El-Sayed, M. A. *J. Phys. Chem. B* **2005**, *109*, 12663. (f) Cushing, B. L.; Kolesnichenko, V. L.; O'Connor, C. J. *Chem. Rev.* **2004**, *104*, 3893. (g) Shenhar, R.; Rotello, V. M. *Acc. Chem. Res.* **2003**, *36*, 549. (h) Roucoux, A.; Schulz, J.; Patin, H. *Chem. Rev.* **2002**, *102*, 3757. (i) Králik, M.; Biffis, A. *J. Mol. Cat. A* **2001**, *177*, 113. (j) Rao, C. N. R.; Kulkarni, G. U.; Thomas, P. J.; Edwards, P. P. *Chem. Soc. Rev.* **2000**, *29*, 27. (k) Schmid, G.; Baumle, M.; Geerkens, M.; Heim, I.; Osemann, C.; Sawitowski, T. *Chem. Soc. Rev.* **1999**, *28*, 179. (l) Schmid, G.; Chi, L. F. *Adv. Mater.* **1998**, *10*, 515. (m) Fendler, J. H., Ed. *Nanoparticles and Nanostructured Films*; Wiley-VCH: Weinheim, 1998. (n) Fürstner, A., Ed. *Active Metals: Preparation, Characterization, and Applications*, VCH: Weinheim, 1996. (o) Bradley, J. S. in *Clusters and Colloids. From Theory to Applications*; Schmid, G., Ed.; VCH: New York, 1994; p. 459-544. (p) Schmid, G. *Chem. Rev.* **1992**, *92*, 1709. (q) A superb series of papers, complete with a record of the insightful comments by the experts attending the conference, is available in: *Faraday Discussions* **1991**, *92*, 1-300. (r) Schmid, G. in *Aspects of Homogeneous Catalysis*; Ugo, R., Ed.; Kluwer: Dordrecht, 1990; Chapter 1. (s) Andres, R. P.; Averback, R. S.; Brown, W. L.; Brus, L. E.; Goddard, W. A. III; Kaldor, A.; Louie S. G.; Moscovits, M.; Peercy, P. S.; Riley, S. J.; Siegel, R. W.; Spaepen, F.; Wang, Y.; *J. Mater. Res.* **1989**, *4*, 704. (t) Henglein, A. *Chem. Rev.* **1989**, *89*, 1861. (u) Thomas, J. M. *Pure Appl. Chem.* **1988**, *60*, 1517. (v) Jena, P.; Rao B. K.; Khanna, S. N; *Physics and Chemistry of Small Clusters*; Plenum: New York, 1987.

[2] Elghanian, R.; Storhoff, J. J.; Mucic, R. C.; Letsinger, R. L.; Mirkin, C. A. *Science* **1997**, *277*, 1078.

[3] Glanz, J. *Science*, **1995**, *269*, 1363.

[4] Finke, R. G. in *Metal Nanoparticles: Synthesis, Characterization, and Applications*; Feldheim, D. L., Foss, C. A., Jr., Eds.; Marcel Dekker: New York, 2002; Chapter 2, p 17-54.

[5] (a) Bönneman, H.; Korall, B. *Agnew. Chem. Int. Ed.* **1992**, *31*, 1490. (b) Franke, R.; Rothe, J.; Pollman, J.; Hormes, J.; Bonneman, H.; Brijoux, W.; Hindenburg, T. *J. Am. Chem. Soc.* **1996**, *118*, 12090.

[6] Chaudret, B.; Vidoni, O.; Philippot, K.; Amiens, C.; Balmes, O.; Malam, J.-O.; Bovin, J.-O.; Senocq, F.; Casanove, M.-J. *Angew. Chem. Int. Ed.* **1999**, *38*, 3736.

[7] Collier, P. J.; Iggo, J. A.; Whyman, R. *J. Mol. Cat. A* **1999**, *146*, 149.

[8] Wang, Y.; Ren, J.; Deng, K.; Gi, L.; Tang, Y. *Chem. Mater.* **2000**, *12*, 1622.

[9] Curtis, A. C.; Duff, D. G.; Edwards, P. P.; Jefferson, D. A.; Johnson, B. F. G.; Kirkland, A. I.; Wallace, A. S. *J. Phys. Chem.* **1987**, *92*, 2270.

[10] Pelzer, K.; Vidoni, O.; Philippot, K.; Chaudret, B.; Colliere, V. *Adv. Func. Mater.* **2003**, *13*, 118.

[11] Reetz, M. T.; Lohmer, G. *Chem. Commun.* **1996**, *16*, 1921.

[12] Cardenas-Trivino, G.; Klabunde, K. J.; Dale, E. B. *Langmuir* **1987**, *3*, 986.
[13] Esumi, K.; Tano, T.; Meguro, K. *Langmuir*, **1989**, *5*, 268.
[14] He, B.; Chen, Y.; Liu, H.; Liu, Y. *J. Nanosci. Nanotech.* **2005**, *5*, 266.
[15] Toshima, N.; Shiraishi, Y.; Teranishi, T.; Miyake, M.; Tominaga, T.; Watanabe, H.; Brijoux, W.; Bönnemann, H.; Schmid, G. *Appl. Organometal. Chem.* **2001**, *15*, 178.
[16] Özkar, S.; Finke, R. G. *J. Am. Chem. Soc.* **2002**, *124*, 5796.
[17] Özkar, S.; Finke, R. G. *Langmuir*, **2002**, *18*, 7653.
[18] Aiken, J. D., III; Finke, R. G. *J. Mol. Cat. A-Chem.* **1999**, *145*, 1.
[19] Verwey, E. J. W.; Overbeek, J. T. G. *Theory of the Stability of Lyophobic Colloids*; 2 ed.; Dover Publications, Inc.: Mineola, New York, 1999.
[20] Ninham, B. W. *Adv. Coll. Int. Sci.* **1999**, *83*, 1.
[21] In a neutral metal nanoclusters, anions are attracted to the coordinatively unsaturated, electrophilic nanocluster surfaces. Adsorption of these anions induces an electrostatic charge mirror, resulting in a partial positive charge (mirror) on the nanocluster surface.[19,22] The resulting particles with surface-bound anions are then anionic in nature and repel each other, this Coulombic repulsion being a key component of DLVO-type, electrostatic stabilization.[19]
[22] Evans, D. F.; Wennerström, H. *The Colloidal Domain*, 2nd ed.; Wiley-VCH: New York, 1999.
[23] Some authors claim "non-DLVO" forces, such as hydration, structural, oscillatory, hydrophobic, depletion, fluctuation, and protrusion forces. However, these forces are generally believed insufficient to be the sole source of stabilization.[20]
[24] Ott, L. S.; Hornstein, B. J.; Finke, R. G. "A Test of the Transition-Metal Nanocluster Formation and Stabilization Ability of the Most Common Polymeric Stabilizer, Poly(vinylpyrrolidone), As Well As Four Other Polymeric Protectants". *Langmuir*, submitted.
[25] Besson, C.; Finney, E. E.; Finke, R. G. *J. Am. Chem. Soc.* **2005**, *127*, 8179.
[26] Enüstün, B. V. ; Turkevich, J. *J. Am. Chem. Soc.* **1963**, *85*, 3317.
[27] Zsigmondy, R. *Z. Anal. Chem.* **1901**, 697.
[28] Theile, H.; von Levern, H. S. *J. Coll. Sci.* **1965**, *20*, 3378.
[29] Meakin, P. *Adv. Coll. Int. Sci.* **1988**, *28*, 249.
[30] Ott, L. S.; Finke, R. G. "Nanocluster Stabilization Fundamental Studies: Kinetic Studies En Route to Developing an Agglomeration-Based Method for Assaying Nanocluster Stabilizers." Manuscript in preparation.
[31] (a) The "naked nanocluster problem,"[31b,c] perhaps more accurately called the "ligand-labile nanocluster problem" is the need for efficient, high yield syntheses of metastable nanoclusters that have relatively easily removed ligands so that they can be used for low-temperature syntheses of novel heterogeneous catalysts or other applications of clean, ideally naked-surface nanoclusters. In practice, completely naked nanoclusters will likely not be achievable (since even alkane metal-ligand bond energies can be 10±3 kcal/mol)[31d] so that approaches that parallel precedent such as Wilke's "naked nickel",[31e] $Ni(1,5\text{-}COD)_2$, with stabilizing but displaceable ligands are what is envisaged here. (b) Özkar, S.; Graham, C. R.; Finke, R. G. Unpublished results and experiments in progress. (c) Recent efforts to completely remove polymeric poly(vinylpyrrolidone) stabilizers from $Pt(0)_n$ nanoclusters with heat

treatments, e^- beams, O-atom beams, or H_2/O_2 treatments were unsucessful: Kim, F.; Connor, S.; Song, H.; Kuykendall, T.; Yang, P. *Angew. Chem. Int. Ed.* **2004**, *43*, 3673; Song, H.; Kim, F.; Connor. S.; Somorjai, G. A.; Yang, P. *J. Phys. Chem. B* **2005**, *109*, 188; Rioux, R. M.; Song, H.; Hoefelmeyer, J. D.; Yang, P.; Somorjai, G. A. *J. Phys. Chem.* **2005**, *109*, 2192; Song, H.; Rioux, R. M.; Hoefelmeyer, J. D.; Komor, R.; Niesz, K.; Grass, M.; Yang, P.; Somorjai, G. A. *J. Am. Chem. Soc.* **2006**, *128*, 3027. (d) Yang, G. K.; Peters, K. S.; Vaida, V. *Chem. Phys. Lett.* **1986**, *125*, 566; Simon, J. D.; Xie, X. *J. Phys. Chem.* **1989**, *93*, 291-293; Morse, J. M., Jr.; Parker, G. H.; Burkey, T. J. *Organometallics* **1989**, *8*, 2471; (e) Fischer, K.; Jonas, K.; Misbach, P.; Stabba, R.; Wilke, G. *Angew. Chem. Int. Ed.* **1973**, *12*, 943; Wilke, G. *Angew. Chem. Int. Ed.* **1988**, *27*, 185.

[32] Platt, J. *Science* **1965**, *146*, 347.

[33] Bucher, S.; Hormes, J.; Modrow, H.; Brinkman, R.; Waldöfner, N.; Bönnemann, H.; Beuermann, L.; Krischok, S.; Maus-Friedrichs, W.; Kempter, V. *Surf. Sci.* **2002**, *497*, 321.

[34] Modrow, H.; Bucher, S.; Hormes, J.; Brinkmann, R.; Bönnemann, H. *J. Phys. Chem. B.* **2003**, *107*, 3684.

[35] Pez, G. P.; Armor, J. N. *Adv. Organomet. Chem.* **1981**, *19*, 1.

[36] Pery, T.; Pelzer, K.; Buntkowsky, G.; Philippot, K.; Limbach, H.-H.; Chaudret, B. *ChemPhysChem* **2005**, *6*, 605.

[37] Pan, C.; Pelzer, K.; Philippot, K.; Chaudret, B.; Dassenoy, F.; Lecante, P.; Casanove, M.-J. *J. Am. Chem. Soc.* **2001**, *123*, 7584.

[38] Dhas, N. A.; Cohen, H.; Gedanken, A. *J. Phys. Chem. B* **1997**, *101*, 6834.

[39] Since DLVO theory[19] remains the only predictive tool for colloidal stability (and predicts solvent effects based solely on ε), we initially chose the solvents studied herein based on their widely variant dielectric constants.

[40] Gutmann, V. *Coord. Chem. Rev.* **1976**, *18*, 225.

[41] We intended to study nitromethane (ε=36) but it appears to be deprotonated by PS™, leading, in turn, to an undetermined, inactive, brown species in the reaction solution before the solution was exposed to H_2 (see Figure S1 of the Supporting Information).

[42] Watzky, M. A.; Finke, R. G. *J. Am. Chem. Soc.* **1997**, *119*, 10382.

[43] Widegren, J. A.; Aiken, J. D., III; Özkar, S.; Finke, R. G. *Chem. Mater.* **2001**, *13*, 312.

[44] Creighton, J. A.; Eadon, D. G. *J. Chem. Soc., Faraday Trans.* **1991**, *87*, 3881.

[45] Umpierre, A. P.; Machado, G.; Fecher, G. H.; Morais, J.; Dupont, J. *Adv. Synth. Catal.* **2005**, *347*, 1404.

[46] Özkar, S.; Finke, R. G. *Coord. Chem. Rev.* **2004**, *248*, 135.

[47] Parks, E. K.; Nieman, G. C.; Kerns, K. P.; Riley, S. J. *J. Chem. Phys.* **1998**, *108*, 3731.

[48] All of the BF_4^- stability studies were carried out in PC. Since PC and NMA provided similar results for the 5 criteria as judged by the k_2/k_1 ratio, TEM, and visual observation, and since PC is more amenable to work with than NMA (NMA has an inconveniently high melting point of 28 °C and thus frequently crystallizes in syringe needles).

[49] Lin, Y.; Finke, R. G. *J. Am. Chem. Soc.* **1994**, *116*, 8335.

[50] An Ir-F a signal should appear significantly downfield in the ^{19}F NMR spectrum. For a homogeneous Ir-F complex, the Ir-F bond was observed at δ -219.3 ppm: Gorol, M.;

Mösch-Zaetti, N. C.; Roesky, H. W.; Noltemeyer, M.; Schmidt, H.-D. *Eur. J. Inorg. Chem.* **2004**, *13*, 2678

[51] Pelzer, K.; Laleu, B.; Lefebvre, F.; Philippot, K.; Chaudret, B.; Candy, J. P.; Basset, J. M. *Chem. Mater.* **2004**, *16*, 4937.

[52] Reed, C. A. *Acc. Chem. Res.* **1998**, *31*, 133.

[53] Strauss, S. H. *Chem. Rev.* **1993**, *93*, 927.

[54] Köhler, J. U.; Bradley, J. S. *Catal. Lett.* **1997**, *45*, 203.

[55] Ott, L. S.; Cline, M. L.; Deetlefs, M.; Seddon, K. R.; Finke, R. G. *J. Am. Chem. Soc.* **2005**, *127*, 5758.

[56] (a) Rampino, L. D.; Nord, F. F.; *J. Am. Chem. Soc.* **1941**, 63, 2745. (b) Rampino, L. D.; Nord, F. F.; *J. Am. Chem. Soc.* **1941**, 63, 3268.

[57] Poly(propylene carbonate) is usually formed by the copolymerization of CO_2 and propylene oxide under the rather harsh reaction conditions (i.e., compared to those of the work reported in the main text) of 50 atm CO_2, 60 °C and 40 h in the presence of a metal catalyst.[59]

[58] Chisholm, M. H.; Navarro-Llobet, D.; Zhou, Z. *Macromolecules* **2002**, *35*, 6494.

[59] Zhu, Q.; Meng, Y. Z.; Tjong, S. C.; Zhao, X. S.; Chen, Y. L. *Polym. Int.* **2002**, *51*, 1079.

[60] Hanton, S. D. *Chem. Rev.* **2001**, *101*, 527.

[61] Although the oxidation of bulk Ir normally only occurs at high temperatures,[61a] we have recently shown that $Ir(0)_n$ nanoclusters appear to be capable of titrating some contaminant, presumably oxygen, from our $\leq$5 ppm O_2 drybox.[61b] Consequently, the Ir nanocluster surfaces appear to be more susceptible to oxygenation than bulk metal, as expected for the higher surface area and more energetic nanoclusters (the heat of vaporization of $Ir(0)_n$ to nIr(0) atoms requires 159 kcal/mol[4] demonstrating the higher energetic nature of small metal(0) nanoclusters). (a) Cheetham, A. K.; Day, P. *Solid State Chemistry Techniques*; Clarendon Press: Oxford, 1987. (b) Hornstein, B. J.; Finke, R. G. *Chem. Mater.* **2003**, *15*, 899.

[62] Ott, L. S.; Finke, R. G. *Coord. Chem. Rev.* **2006**, accepted pending revisions.

[63] Özkar, S.; Finke, R. G. *Langmuir* **2003**, *19*, 6247.

[64] In nanocluster formation reactions with added $[Bu_4N][P_2W_{15}Nb_3O_{62}]$, the order of mixing $[Bu_4N][P_2W_{15}Nb_3O_{62}]$, and $[(1,5\text{-COD})Ir(CH_3CN)_2][BF_4]$ has an effect on the nanocluster formation reaction and, hence, the products. It is preferable to make two separate solutions, one containing $[Bu_4N][P_2W_{15}Nb_3O_{62}]$ and one containing $[(1,5\text{-COD})Ir(CH_3CN)_2][BF_4]$ and PS™, and then add the solution containing $[(1,5\text{-COD})Ir(CH_3CN)_2][BF_4]$ and PS™ dropwise to a rapidly stirring solution of $[Bu_4N][P_2W_{15}Nb_3O_{62}]$. This order of addition leads to reproducible kinetics of nanocluster formation, well-fit by the 2-step autocatalytic nanocluster formation mechanism, and to reproducible, near-monodisperse $Ir(0)_n$ nanoclusters. This order of mixing, which promotes the formation of a 1:1 metal:polyanion complex, is also corroborated by our earlier work on supported organometallics: see for example Pohl, M.; Lyon, D. K.; Mizuno, N.; Nomiya, K.; Finke, R. G. *Inorg. Chem.* **1995**, *34*, 1413 and references therein.

[65] (a) Freas, R. B. *J. Am. Chem. Soc.* **1986**, *108*, 4659. (b) Reetz, M. T.; Quaiser, S. A.; Winter, M.; Becker, J. A.; Schäfer, R.; Stimming, U.; Marmann, A.; Vogel, R.;

Konno, T. *Angew. Chem. Int. Ed.* **1996**, *35*, 2092. (c) Rothe, J.; Pollmann, J.; Franke, R.; Hormes, J.; Bönnemann, H.; Brijoux, W.; Siepen, K.; Richter, J. *Fresenius J Anal. Chem.* **1996**, *355*, 372. (d) Kolb, U.; Quaiser, S. A.; Winter, M.; Reetz, M. T. *Chem. Mater.* **1996**, *8*, 1889. (e) Stein, J.; Lewis, L. N.; Gao, Y.; Scott, R. A. *J. Am. Chem. Soc.* **1999**, *121*, 3693. (f) Aiken, J. D., III; Finke, R. G. *J. Mol. Cat. A: Chem.* **1999**, *145*, 1. (g) Siepen, K.; Bönnemann, H.; Brijoux, W.; Rothe, J.; Hormes, J. *Appl. Organomet. Chem.* **2000**, *14*, 549. (h) Ebitani, K.; Choi, K.-M.; Mizugaki, T.; Kaneda, K. *Langmuir*, **2002**, *18*, 1849.

[66] Catalysis by heterogeneous metal oxide catalysts is well-known: (a) Maxted, E. B. *Adv. Catal.* **1951**, *3*, 129. (b) Kiwi, J. *Isreal J. Chem.* **1979**, *18*, 369. (c) Shannon, R. D.; Gier, T. E.; Carcia, P. F.; Bierstedt, P. E.; Flippen, R. B.; Vega, A. J. *Inorg. Chem.* **1982**, *21*, 3372. (d) Lamber, R.; Romanowski, W. *J. Catal.* **1987**, *105*, 213. (e) Naito, S.; Tanimoto, M. *J. Chem. Soc., Chem. Commun.* **1988**, 832. (f) Logan, A. D.; Sharoudi, K.; Datye, A. K. *J. Phys. Chem.* **1991**, *95*, 5568. (g) Gai-Boyes, P. L. *Catal. Rev.–Sci. Eng.* **1992**, *34*, 1. (h) Guo, X.-C.; Madix, R. J. *J. Am. Chem. Soc.* **1995**, *117*, 5523. (i) Pal, T.; Sau, T. K.; Jana, N. R. *Langmuir*, **1997**, *13*, 1481. (j) Fuente, A. M.; Pulgar, G.; González, F.; Pesquera, C.; Blanco, C. *Appl. Catal. A* **2001**, *208*, 35.

[67] Knecht, L. A.; Kolthoff, I. M. *Inorg. Chem.* **1962**, *1*, 195.

[68] Perrin, D. D., Armargo, W. L. F., Perrin, D. R. *Purification of Laboratory Chemicals*; 2 ed.; Pergamon Press: Elmsford, New York, 1980.

[69] Day, V. W.; Klemperer, W. G.; Main, D. J. *Inorg. Chem.* **1990**, *29*, 2345.

[70] Hornstein, B. J., Finke, R. G. *Inorg. Chem.* **2002**, *41*, 2720.

[71] Watzky, M. A.; Finke, R. G. *Chem. Mater.* **1997**, *9*, 3083.

[72] Aiken, J. D., III; Finke, R. G. *Chem. Mater.* **1999**, *11*, 1035.

[73] Aiken, J. D., III; Finke, R. G. *J. Am. Chem. Soc.* **1998**, *120*, 9545.

[74] Widegren, J. A.; Finke, R. G. *Inorg. Chem.* **2002**, *41*, 1558.

[75] Ivanov, S. V.; Rockwell, J. J.; Polyakov, O. G.; Gaudinski, C. M.; Anderson, O. P.; Solntsev, K. A.; Strauss, S. H. *J. Am. Chem. Soc.* **1998**, *120*, 4224.

[76] Formation and stabilization of nanoclusters are tightly interlinked issues. This has been illustrated for the case of Pt(0) nanoclusters.[25] See also Besson, C.; Finney, E. E.; Finke, R. G. *Chem. Mater.* **2005**, *17*, 4925.

SUPPORTING INFORMATION

Nanocluster Formation and Stabilization Fundamental Studies: Investigating "Solvent-Only" Stabilization En Route to Discovering Stabilization by the Traditionally Weakly Coordinating Anion BF_4^- Plus High Dielectric Constant Solvents.

Lisa Starkey Ott and Richard G. Finke

Department of Chemistry, Colorado State University, Fort Collins, Colorado 80523

Table S1. A compilation of the "solvent-only" nanocluster stabilization literature.

	author (date)	system	comments
1	K. J. Klabunde, H. F. Efner, T. O. Murdock, R. Ropple (1976)	Ni•solvent (hexane, toluene, or THF) slurries were prepared by co-condensation of vaporized Ni atoms and the solvent	SEM shows agglomeration and μm sized particles; solvent:metal ratio determined by desorption of organics upon pyrolysis, but no elemental analysis was done
2	G. Cardenas-Trivino, K. J. Klabunde, E. B. Dale (1987)	Pd atoms were prepared by metal atom vaporization, followed by condensation with a nonaqueous solvent to form Pd colloids	Size dispersion not given; TEM shows aggregation; electrophoresis proves charge is scavenged from the reaction environment
3	P. P. Edwards, D. A. Jefferson, B. F. G. Johnson, et. al (1987)	$Cu(OAc)(H_20)$ was reduced with hydrazine hydrate while refluxing in methanol	TEM shows a wide size distribution and significant aggregation; acetate, water, and methoxide are potential stabilizers
4	K. Esumi, T. Tano, K. Meguro (1989)	$Pd(acac)_2$ was refluxed in each of 10 organic solvents	Refluxing carried out under air; TEM shows almost complete aggregation; conjugate bases of acid solvents are potential stabilizers
5	H. Bönneman, B. Korall (1992)	$TiCl_4$ in THF was reduced with $K[BEt_3H]$ to form "Ti·0.5 THF"	Elemental analysis shows the presence of B, K and Cl; a later paper with a $TiBr_4$ precursor has lower levels of the alkali metal and halide impurities, but the B level was not reported
6	M. T. Reetz, G. Lohmer (1996)	decomposition of Pd electrode or thermal decomposition of $Pd(OAc)_2$; both in propylene carbonate	In the electrode preparation, both Cl^- and ethanol are present as potential stabilizers; in the thermal decomposition preparation, OAc^- is a potential stabilizer: TEM on both systems shows wide size distributions and marked aggregation
7	N. A. Dhas, H. Cohen, A. Gedanken (1997)	$Pd_2(dba)_3$ was ultrasonically irradiated in mesitylene solvent under Ar while with the sonication cell in a dry ice/acetone bath	Elemental analysis of isolated nanoclusters prepared from this precursor shows >41% C and <1.5% H; XPS C 1s spectrum indicates the presence of "amorphous (graphitic) carbon" on the surface of the nanoclusters

[1] Klabunde, K. J.; Efner, H. F.; Murdock, T. O.; Ropple, R. *J. Am. Chem. Soc.* **1976**, *98*, 1021.
[2] Cardenas-Trivino, G.; Klabunde, K. J.; Dale, E. B. *Langmuir* **1987**, *3*, 986.
[3] Curtis, A. C.; Duff, D. G.; Edwards, P. P.; Jefferson, D. A.; Johnson, B. F. G.; Kirkland, A. I.; Wallace, A. S. *J. Phys. Chem.* **1987**, *92*, 2270.
[4] Esumi, K.; Tano, T.; Meguro, K. *Langmuir*, **1989**, *5*, 268.
[5] Bönneman, H.; Korall, B. *Angew. Chem. Int. Ed.* **1992**, *31*, 1490.
[6] Reetz, M. T.; Lohmer, G. *Chem. Commun.* **1996**, *16*, 1921.
[7] Dhas, N. A.; Cohen, H.; Gedanken, A. *J. Phys. Chem. B* **1997**, *101*, 6834.

8	P. J. Collier, J. A. Iggo, R. Whyman (1999)	Pd and Pt atoms were prepared by metal atom vaporization followed by condensation with organic solvents; in some cases, proprietary stabilizating agents "KD1" and "KD2" were used	No TEM shown; histograms from TEM data show bimodal size distribution; TEM is noted to look like "frogspawn" or "rasperries," indicating aggregation; not "solvent-only" stabilized, as added stabilizing agents KD1 and KD2 were employed
9	Y. Wang, J. Ren, K. Den, L. Gui, Y. Tang (2000)	$H_2PtCl_6 \cdot 6H_20$ was heated in a 0.5M NaOH solution in ethylene glycol; aqueous solutions of either $RhCl_3 \cdot 3H_20$ or $RuCl_3 \cdot 6H_20$ were heated in a 0.5M NaOH solution in water	OH^-, Cl^-, and H_20 could all serve as stabilizers; preparations at pH<12 form bulk metal instead of colloids; TEM shows agglomeration; XPS and elemental analysis measurements were taken only after repeated washings in HCl and acetone
10	K. Pelzer, O. Vidoni, K. Philippot, B. Chaudret, V. Collièr (2003)	Ru(COD)(COT) was reduced with 3 bar H_2; the solvent was either a pure alcohol or a mixture of alcohol/THF	Possible methoxide stabilizer; TEM shows aggregation; XPS shows passivating oxide layer; no size distributions given
11	K. Pelzer, K. Philippot, B. Chaudret (2003)	$RuCl_3 \bullet 3H_2O$ was used to prepare Ru(COD)(COT), which was reduced with 3 bar H_2 in heptanol	Alcoholic solvents can serve as the reductant and the stabilizer; ^1H and ^{13}C NMR indicate coordination of heptoxy molecules on the nanocluster surface; TEM shows some agglomeration; elemental analysis "indicate[s] the presence of *ca.* 70% Ru and *ca.* 1 heptanol : 7.5 Ru."
12	B. He,; Y. Chen, H. Liu, Y. Liu (2005)	$H_2PtCl_6 \bullet 6H_2O$, $RhCl_3 \bullet 3H_2O$, or $RuCl_3 \bullet 3H_2O$ were dissolved in glycol with added NaOH and microwave irradiated	Alcoholic solvents can serve as the reductant and the stabilizer, Cl^-, OH^-, and H_2O present

[8] Collier, P. J.; Iggo, J. A.; Whyman, R. *J. Mol. Cat. A* **1999**, *146*, 149.
[9] Wang, Y.; Ren, J.; Deng, K.; Gi, L.; Tang, Y. *Chem. Mater.* **2000**, *12*, 1622.
[10] Pelzer, K.; Vidoni, O.; Philippot, K.; Chaudret, B.; Colliere, V. *Adv. Func. Mater.* **2003**, *13*, 118.
[11] Pelzer, K.; Philippot, K.; Chaudret, B. *Z. Phys. Chem.* **2003**, *217*, 1539.
[12] He, B.; Chen, Y.; Liu, H.; Liu, Y. *J. Nanosci. Nanotech.* **2005**, *5*, 266.

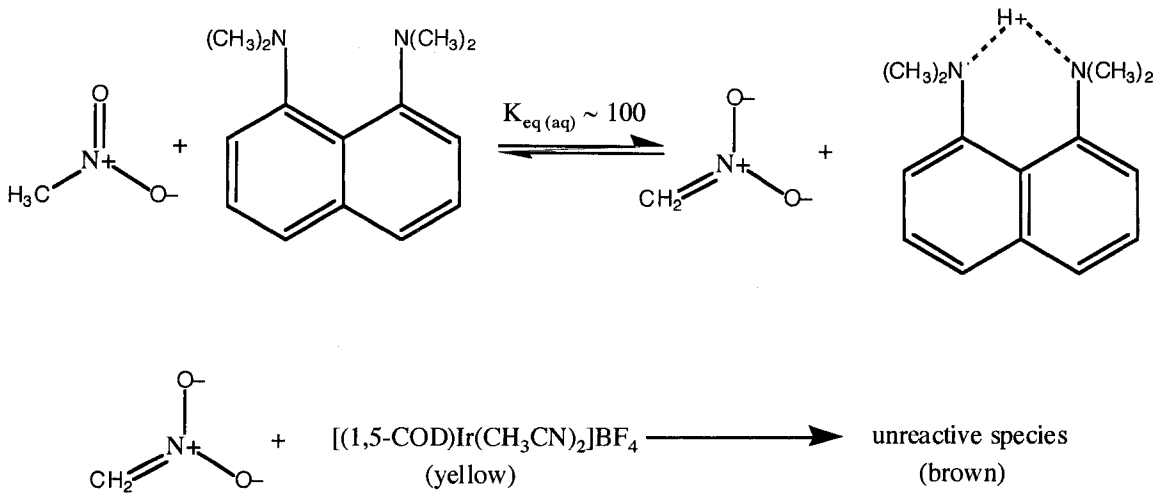

Figure S1. Proposed reaction of NM with Proton Sponge™, followed by the reaction of the conjugate base with the $[(1,5\text{-COD})Ir(CH_3CN)_2][BF_4]$ precursor. The $K_{eq\,(aq)}$ was estimated from the difference in pKa values between nitromethane (pKa=10.2) and Proton Sponge™ (pKa=12.4).[13]

[13] Gordon, A. J.; Ford, R. F. *The Chemist's Companion: A Handbook of Practical Data, Techniques, and References*; Wiley-Interscience: New York, 1972.

Evidence for Nanocluster Instability with 1 Eqv of BF_4^- in Low Dielectric Constant Solvents. Two lower ε solvents, acetonitrile and acetone (ε=39 and 20, respectively), did not yield a brown nanocluster solution (entries 6 and 8 of Table 2 in the main text).[14] Instead, reduction of $[(1,5\text{-COD})Ir(CH_3CN)_2][BF_4]$ yielded only bulk metal in a clear and colorless solution, revealing that nanoclusters prepared in the presence of lower ε solvents and BF_4^- are not well stabilized. The absence of a brown solution indicative of $Ir(0)_n$ nanoclusters in these lower ε solvents again supports the DLVO theory prediction that anions and high ε solvents are important for the formation of stable nanoclusters.

N-methylpyrrolidinone (NMP), also a lower ε solvent (ε=30), was studied based on its structural similarity to the common, seemingly effective nanocluster stabilizer poly(vinylpyrrolidone)[15] (see below). However, NMP did not yield long-term solution stability for nanoclusters (entry 7 of Table 2 in the main text), a finding supported by separate experiments testing the effects of PVP vs. NMP as stabilizers for $Pt(0)_n$ nanoclusters.[16] Although a brown solution characteristic of $Ir(0)_n$ nanoclusters was formed, the solution contained particles of bulk metal visible to the naked eye.

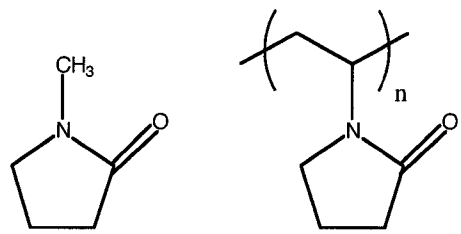

N-methyl pyrrolidinone poly(vinyl pyrrolidone)

Structural comparison of N-methylpyrrolidinone and poly(vinyl pyrrolidone).

[14] The experiment in neat acetonitrile also disproves the alternative hypothesis that the 2 eqv of coordinating CH_3CN present from reduction of $[(1,5\text{-COD})Ir(CH_3CN)_2][BF_4]$ is responsible for nanocluster stability through coordination of the electrophilic nanocluster surfaces, since neat acetonitrile yields only bulk metal, not stable nanoclusters.

[15] Hirai, H.; Nakao, Y.; Toshima, N. *J. Macromol. Sci.–Chem.* **1979**, *A13*, 727.

[16] Duff, D. G.; Edwards, P. P.; Johnson, B. F. G. *J. Phys. Chem.* **1995**, *99*, 15934.

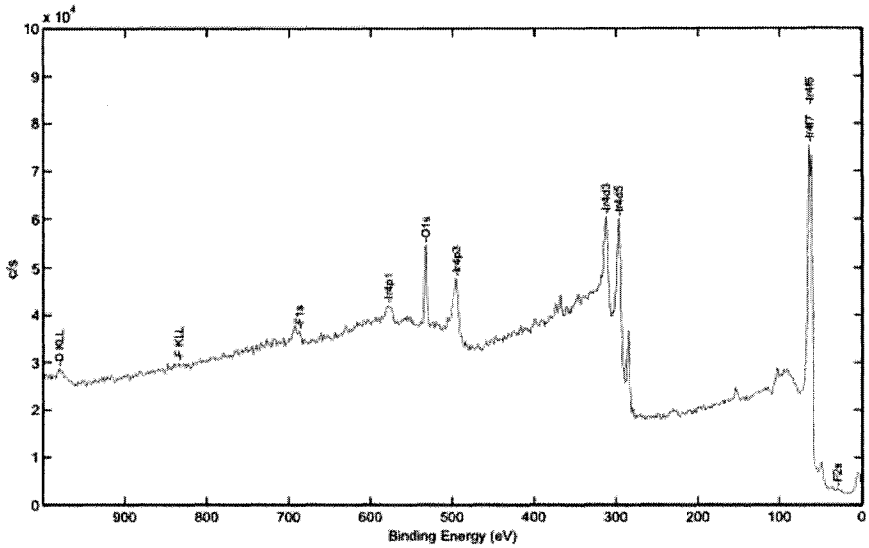

Figure S2. XPS spectrum of dried $Ir(0)_n$ nanoclusters prepared under the conditions of Scheme 1. Peaks for O are due to oxygen exposure upon introduction of the sample into the XPS chamber. The peaks for F are seen, in turn attributable to BF_4^- on the surface of the nanoclusters.

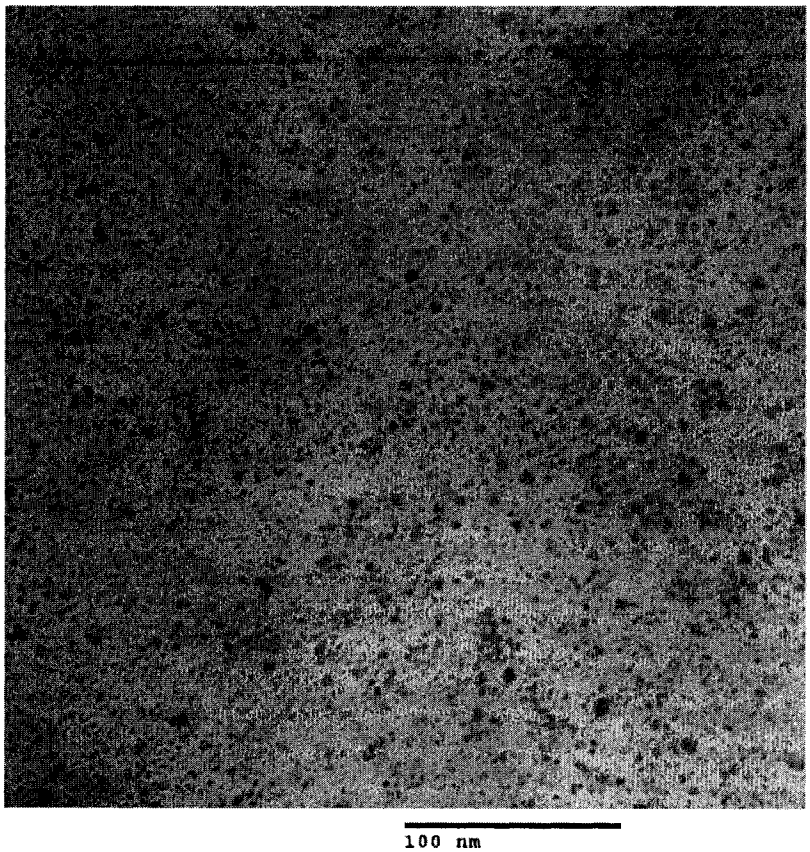

Figure S3. TEM image (400k magnification) of $Ir(0)_n$ nanoclusters prepared in PC from $[(1,5\text{-COD})Ir(CH_3CN)_2][BF_4]$ plus PS™ and 50 eqv $[Bu_4N][BF_4]$. The nanoclusters show a wide, ±33% size distribution of 36±12 Å.

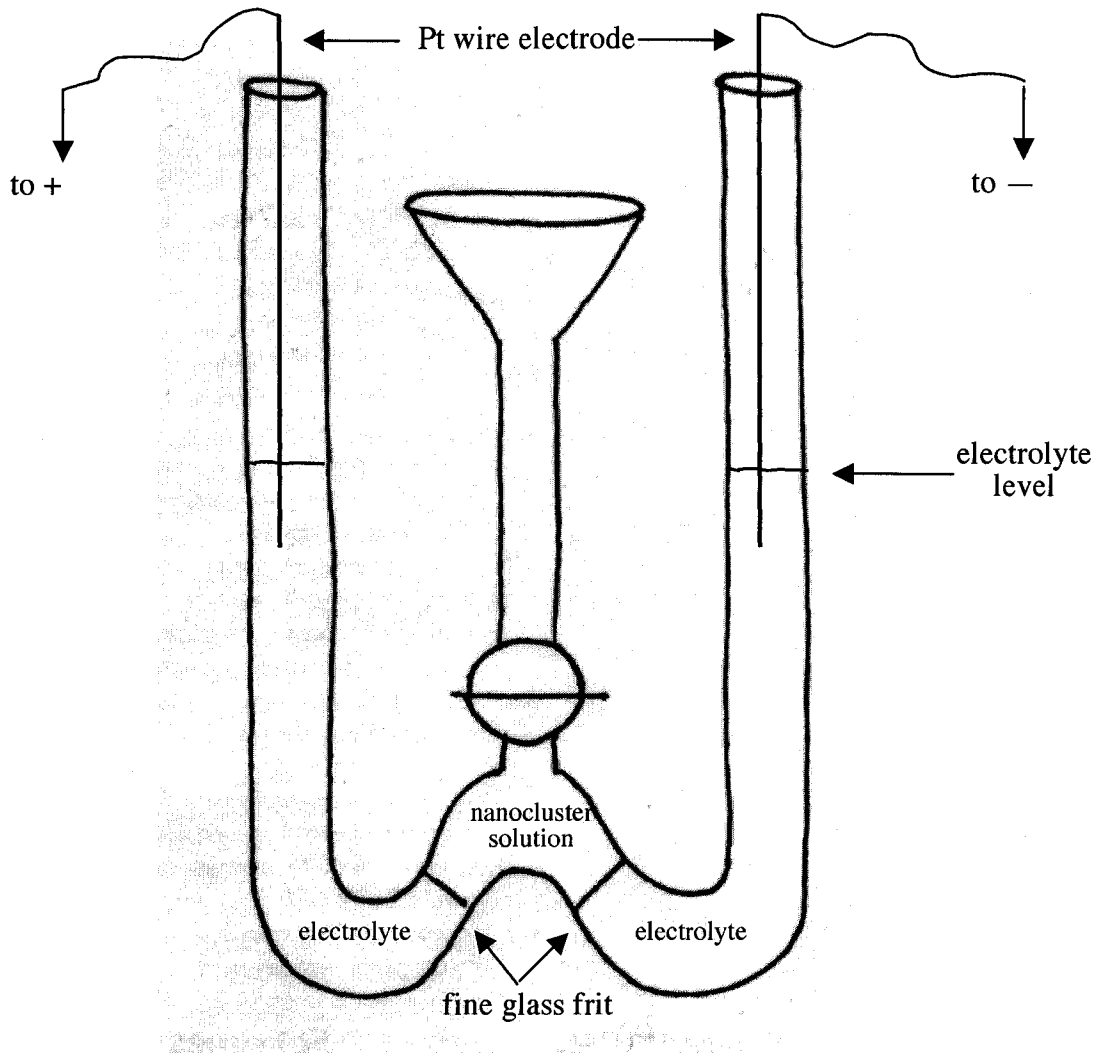

Figure S4. A drawing of the apparatus used for the electrophoretic mobility experiment. The addition arm (with funnel) initially contains the nanocluster solution. The propylene carbonate/$[Bu_4N][BF_4]$ electrolyte solution is added on either side of the fine frits. The frits initially block the migration of electrolyte solution, but after several minutes the frits become saturated with the solution, allowing the electrolyte solution to pass into the center of the W shaped apparatus and the nanocluster solution to pass into the "arms." This also allows for a contiguous salt solution through which charge can be passed. The $P_2W_{15}Nb_3O_{62}^{9-}$ and 50 eqv added $[Bu_4N][BF_4]$ stabilized nanoclusters migrate toward the positive electrode, indicating a negatively charged nanocluster surface from surface-adsorbed anions. However, nanoclusters prepared with just 1 eqv BF_4^- nanoclusters do not migrate prior to their precipitation as bulk metal.

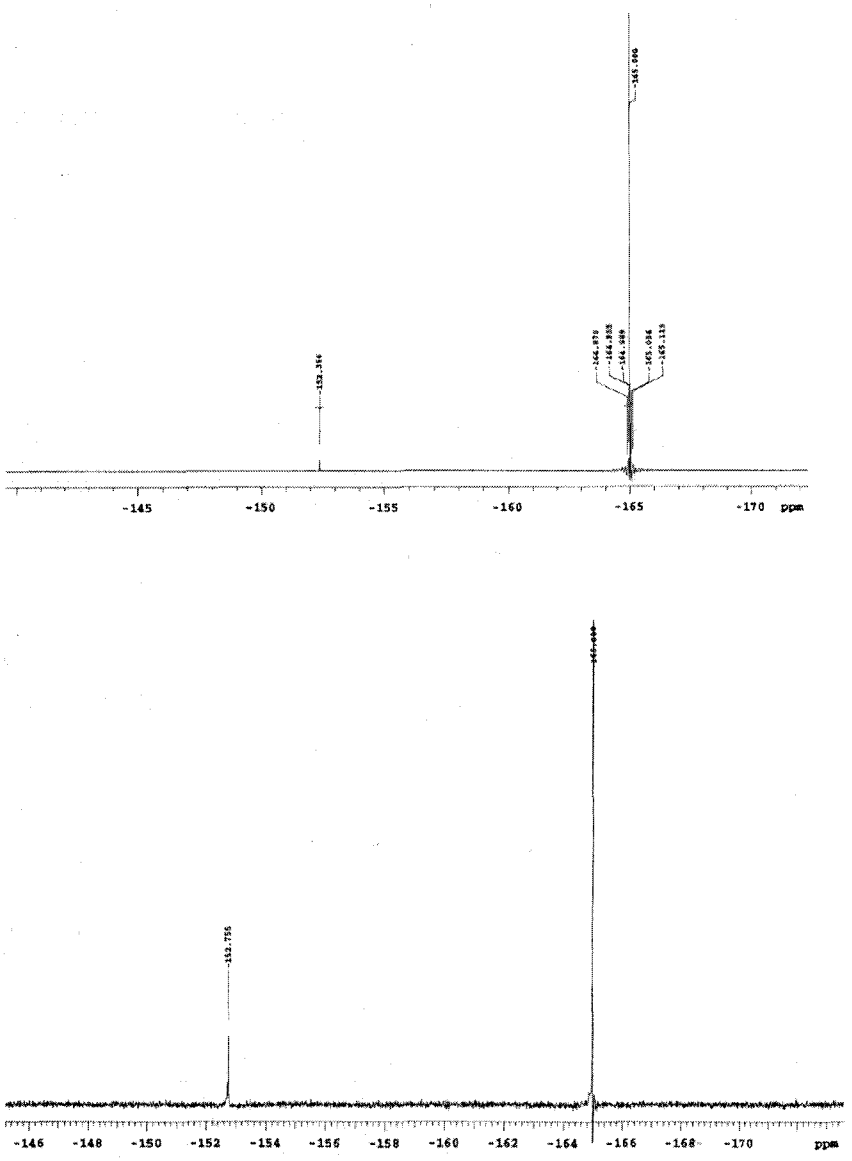

Figure S5. 400 MHz ^{19}F NMR of (a) $[Bu_4N][BF_4]$ in PC and (b) the nanocluster reaction solution, both referenced to C_6F_6 (δ=-165.0). The peak for "free" BF_4^- from $[Bu_4N][BF_4]$ at δ=-152.4(2) is within experimental error of the peak observed in the reaction solution, δ=-152.8(2). Neither peak is near the value of δ=-213.9 observed for an Ir-F bond in a homogeneous complex.[17] Hence, Ir-F bonds on the nanocluster surface are not detectable by ^{19}F NMR spectroscopy, at least under the stated conditions.

[17] Gorol, M.; Mösch-Zaetti, N. C.; Roesky, H. W.; Noltemeyer, M.; Schmidt, H.-D. *Eur. J. Inorg. Chem.* **2004**, *13*, 2678.

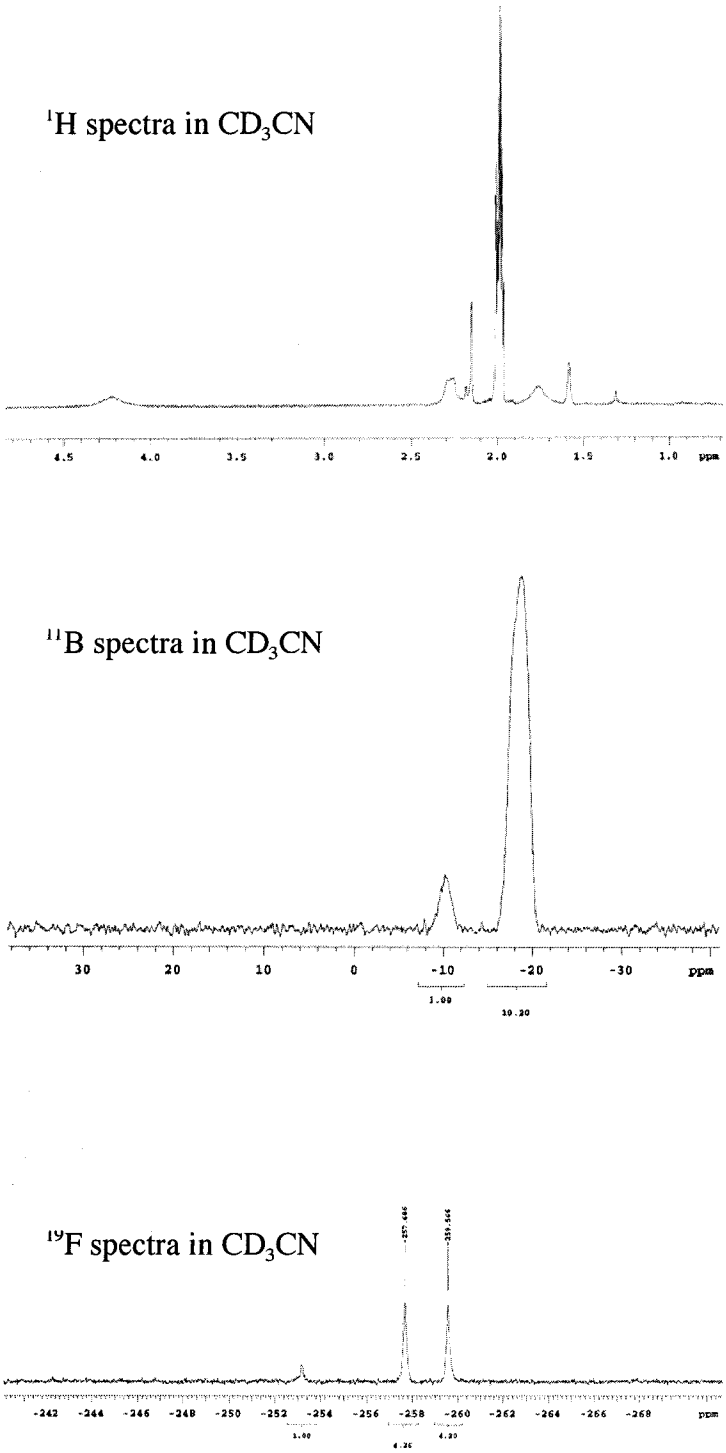

Figure S6. 300 MHz ^{1}H, ^{11}B, and ^{19}F NMR spectra of the [(1,5-COD)Ir($CH_3CN)_2$][1-$MeCB_{11}F_{11}$] in CD_3CN. These spectra are characteristic of 1-$MeCB_{11}F_{11}^{1-}$.[18]

[18] Ivanov, S. V.; Rockwell, J. J.; Polyakov, O. G.; Gaudinski, C. M.; Anderson, O. P.; Solntsev, K. A.; Strauss, S. H. *J. Am. Chem. Soc.* **1998**, *120*, 4224.

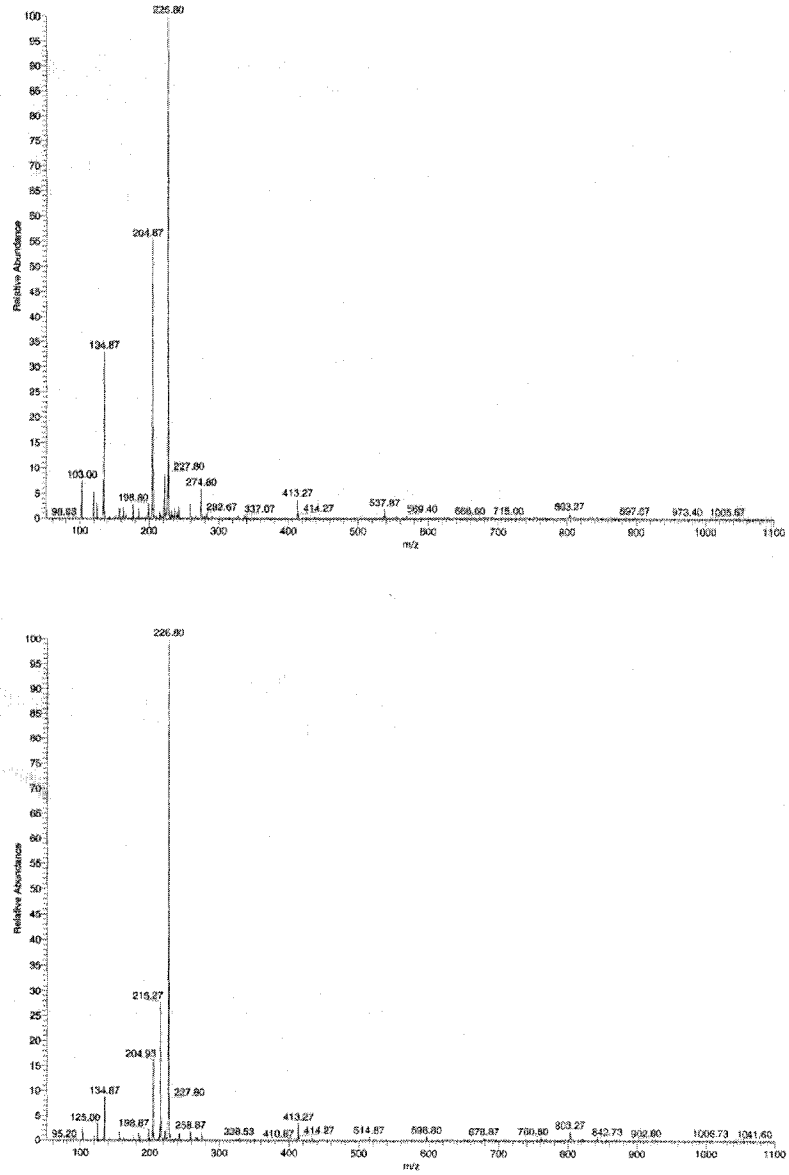

Figure S7. ESI-MS spectra of a solution of neat propylene carbonate (top) and the reaction solution of nanoclusters in propylene carbonate (bottom). Propylene carbonate peaks have a m/z=102.09. Hence, the peak at m/z=204.87 is a dimer, and m/z=226.80 is a dimer with an adventitious sodium ion. Both spectra show a peak at m/z=134.87, which is attributed to a propylene carbonate molecule with the incorporation of MeOH from the injection solution. The m/z=215.27 peak in the reaction solution spectrum arises from PS™. The lack of large m/z peaks indicates that poly(propylene carbonate) is not being formed under our nanocluster synthesis reaction conditions.

How Does BF_4^- Compare to the "Gold Standard" $Ir(0)_n$ Nanocluster Stabilizer $P_2W_{15}Nb_3O_{62}^{9-}$?

Table S1. The 5 criteria Evaluated for $Ir(0)_n$ Nanoclusters in Five Solvents with added $P_2W_{15}Nb_3O_{62}^{9-}$.

	solvent	ε	k_1 (h^{-1})	k_2x10^{-3} ($h^{-1}M^{-1}$) [a]	k_2/k_1x10^{-5} (M^{-1})	d_m (Å)	appearance	redisp?	cat. act.[b]	TTO
1	NMA	165	0.36(4)	7.2(3)	0.30(4)	19 ± 4	clear, blue	yes	0.32(5)	43,600
2	PC	69	0.009(3)	3.54(3)	6(2)	18 ± 4	clear, blue	yes	0.19(5)	19,000
3	CH_3CN	39	0.25(7)	1.9(4)	0.11(2)	---	blue, metal	---	---	23,000
4	NMP	36	0.0036(1)	1.41(1)	5.5(2)	18 ± 4	clear, brown	yes	0.27(1)	58,500
5	acetone	20	0.016(1)	4.6(1)	2.9(2)	21 ± 4	clear, blue	yes	0.19(5)	51,000

(a) The values for k_2/k_1 have been corrected by the mathematically required stoichiometry factor of 1400 as detailed elsewhere.[19] (b) mmol H_2/h.

Evaluating entries 4-8 in Table 1 of the main text in comparison with entries 1-5 in Table S1 reveals that nanoclusters stabilized by BF_4^- and high ε solvents have far inferior stabilization, and much poorer kinetic control, in the formation reaction to those prepared with added $P_2W_{15}Nb_3O_{62}^{9-}$. For example, Figure S8 illustrates the difference in kinetic control[20] of the nanocluster formation reaction in propylene carbonate for nanoclusters prepared with and without added $P_2W_{15}Nb_3O_{62}^{9-}$. The dramatic increase in kinetic control with added $P_2W_{15}Nb_3O_{62}^{9-}$ is reflected in the preparation of 18 ± 4 Å Ir(0) nanoclusters in the presence of $P_2W_{15}Nb_3O_{62}^{9-}$ vs. aggregated nanoclusters (shown in Figure 1 of the main text) in the presence of BF_4^-. Additionally, added $P_2W_{15}Nb_3O_{62}^{9-}$ imparts long-term solution stability, isolability, redissolvability, and increased catalytic lifetimes to the $Ir(0)_n$ nanoclusters that can be scaled up to ~1g quatities.[21] Hence, added strongly coordinating anions such as $P_2W_{15}Nb_3O_{62}^{9-}$ and hydrogen phosphate[22] are preferred for both the formation and stabilization of prototype $Ir(0)_n$ (and hence presumably other transition-metal) nanoclusters.

[19] Watzky, M. A.; Finke, R. G. *J. Am. Chem. Soc.* **1997**, *119*, 10382.

[20] Formation and stabilization of nanoclusters are tightly interlinked issues, as has been illustrated for the case of Pt(0) nanoclusters. See also Besson, C.; Finney, E. E.; Finke, R. G. *Chem. Mater.* **2005**, *17*, 4925.

[21] Hornstein, B. J.; Finke, R. G. *Chem. Mater.* **2003**, *15*, 899.

[22] Özkar, S.; Finke, R. G. *Langmuir* **2003**, *19*, 6247.

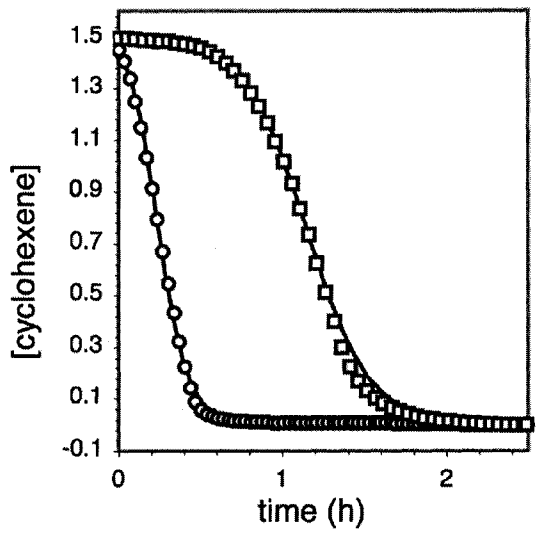

Figure S8. A comparison of the kinetics of nanocluster formation from [(1,5-COD)Ir(CH_3CN)$_2$][BF_4] and PS™ in propylene carbonate with (circles) and without (squares) added [Bu_4N]$_9$[$P_2W_{15}Nb_3O_{62}$].[23] The fit to the autocatalytic nanocluster formation mechanism[19] is shown as a line for both datasets. The nanocluster formation reaction in the presence of $P_2W_{15}Nb_3O_{62}^{9-}$ has a high k_2/k_1 ratio, 1.29(3)x10^5 M^{-1}. The kinetics of the nanocluster formation reaction in the presence of BF_4^- display kinetic control that is two orders of magnitude smaller, k_2/k_1=7.0(4)x10^3 M^{-1}.

[23] The y-axis in Figure 2 has been converted to cyclohexene concentration using the 1:1 stoichiometry between H_2 and cyclohexene and the established cyclohexene reporter reaction.[19]

Further Tests of DLVO Theory: Do Increasingly High ε Solvents Increase the Stability of $Ir(0)_n$ Nanoclusters in the Presence of $P_2W_{15}Nb_3O_{62}^{9-}$? We examined the five solvents shown in Table 1 of the main text for the reaction in Scheme 3 of the main text. The purpose of these experiments was twofold: (1) the direct comparison of the 5 criteria in each solvent in the presence of BF_4^- or $P_2W_{15}Nb_3O_{62}^{9-}$, and (2) the examination of the DLVO theory prediction that, all other factors being equal, increasing the ε of the solvent will increase the stability of the system.

The results of the 5 criteria experiments with added $P_2W_{15}Nb_3O_{62}^{9-}$ in each of the five solvents are presented as entries 1-5 in Table S1. Coordinating solvents such as acetonitrile proved unsuitable for nanocluster synthesis (vide infra),[24] although acetonitrile is suitable for re-dispersing nanoclusters previously prepared in other solvents.[24] Three of the 5 criteria are similar for the remaining four solvents (entries 1, 2, 4, and 5): by TEM, all nanoclusters are near-monodisperse and their sizes are within experimental error of each other (18±4 to 21±4 nm), all four solvents yield nanoclusters that are *isolable and redissolvable without the formation of bulk metal*, and all redissolved nanoclusters are active for further hydrogenation catalysis (0.19(5)-0.32(5) mmol H_2/h). Each of the nanocluster systems displays high total turnovers for cyclohexene hydrogenation (19,000-43,600 turnovers) without the formation of bulk metal. Hence, nanoclusters prepared in the presence of $P_2W_{15}Nb_3O_{62}^{9-}$ and either NMA, PC, NMP, or acetone are well stabilized as measured by the 5 criteria.

One difference between the five solvents is the kinetic control of the nanocluster *formation* reaction. The k_2/k_1 ratio is high for all five solvents (on the order of 10^5 for PC, NMP, and acetone), but the k_2/k_1 ratio is approximately an order of magnitude lower for NMA and acetonitrile. In the case of acetonitrile, the lowered kinetic control could be due to acetonitrile displacing the stabilizing $P_2W_{15}Nb_3O_{62}^{9-}$ anions during the nucleation phase of nanocluster growth. This displacement would lead to a larger-than-expected value for k_1, as observed in Table S1; in turn, $P_2W_{15}Nb_3O_{62}^{9-}$-stabilized nanoclusters prepared in acetonitrile have an overall lower value of k_2/k_1. At this point, the reason(s) for the lowered kinetic control of the nanocluster formation reaction in NMA are unclear: however, near-monodisperse (19 ± 4 Å), isolable and redissolvable nanoclusters are still

[24] Lin, Y.; Finke, R. G. *J. Am. Chem. Soc.* **1994**, *116*, 8335.

formed in NMA in the presence of $P_2W_{15}Nb_3O_{62}^{9-}$. Therefore, NMA, PC, NMP, and acetone are all reasonable (but not exactly equivalent) solvents for the formation of $Ir(0)_n$ nanoclusters in the presence of $P_2W_{15}Nb_3O_{62}^{9-}$.

Considering entries 1, 2, 4, and 5 in Table S1, there is no apparent trend in the 5 criteria with respect to solvent ε in the presence of the strongly coordinating $P_2W_{15}Nb_3O_{62}^{9-}$ anion. All solvents examined (with ε changing by a factor of >8) yield near-monodisperse nanoclusters that are isolable and redissolvable, display high catalytic activity, and yield high total turnover numbers. The DLVO theory prediction that increasing solvent ε will lead to increasing nanocluster stability is apparently not supported for the specific case of $P_2W_{15}Nb_3O_{62}^{9-}$-stabilization of $Ir(0)_n$ nanoclusters. Several alternative hypotheses[25] can be formed with respect to this apparent inconsistency with DLVO theory. One hypothesis is that our 5 criteria method is not sensitive enough to reflect differences in nanocluster stability based on solvent ε influences in this highly stabilized system: that is, the hypothesis here is that the anion is so strongly stabilizing that the effects of the anion may "trump" the comparatively more subtle effects of the solvent ε. An additional hypothesis is that DLVO theory is not strictly applicable to this system (with a sterically bulky 9^- anion in organic solvents), as DLVO theory was originally designed to describe stabilization by point, unit charge ions (i.e., ±1) in water.[26] Given the evidence herein which indicates that $Ir(0)_n$ nanoclusters prepared in organic solvents in the presence of BF_4^- follow the predictions of DLVO theory, we tenatively conclude that the 5 criteria method is not sensitive enough to pick up differences in stability due to solvent ε in this otherwise highly stabilized system.

---

[25] Platt, J. *Science* **1965**, *146*, 347.

[26] Verwey, E. J. W.; Overbeek, J. T. G. *Theory of the Stability of Lyophobic Colloids*; 2nd ed.; Dover Publications, Inc.: Mineola, New York, 1999.

CHAPTER IV

A TEST OF THE TRANSITION-METAL NANOCLUSTER FORMATION AND STABILIZATION ABILITY OF THE MOST COMMON POLYMERIC STABILIZER, POLY(VINYLPYRROLIDONE), AS WELL AS FOUR OTHER POLYMERIC PROTECTANTS

This dissertation chapter contains the manuscript of a full paper in press in *Langmuir*, and describes the evaluation of five polymers for their efficacy in the formation and stabilization of catalytically active Ir(0) nanoclusters. This documents the first application of the 5 criteria method to sterically stabilized systems. Poly(vinyl pyrrolidone) was carefully examined, both with and without added anionic stabilizers. The remaining four polymers were tested exclusively as stand-alone stabilizers. Anionic stabilization, and again the importance of the traditionally weakly coordinating anion BF_4^-, was emphasized in the formation and stabilization of the nanoclusters.

The initial survey experiments reported in this chapter (including the TGA experiment and experiments with PVP and $P_2W_{15}Nb_3O_{62}^{9-}$) were performed by Dr. Brooks Hornstein (BJH). The remainder (and majority) of the experiments were performed by LSO. The manuscript was prepared by LSO, with assistance and editing by BJH and RGF.

Abstract.

Following an introduction to the nanocluster stabilization literature and DLVO (Derjaugin-Landau-Verwey-Overbeek) theory of colloidal stability, the most common steric stabilizer of transition-metal nanoclusters, poly(vinylpyrrolidone) (PVP), has been examined for its efficacy in the formation, stabilization, and subsequent catalytic activity of prototype, test case $Ir(0)_n$ nanoclusters. First, the 5 criteria established previously for ranking nanocluster protectants for their nanocluster formation and stabilization ability were evaluated for 1 equiv 10,000 MW_{ave} PVP in the absence, and then presence, of the traditionally weakly coordinating anion BF_4^- as well as the absence and presence of the strongly coordinating, superior anionic stabilizer, $P_2W_{15}Nb_3O_{62}^{9-}$, all in propylene carbonate solvent. It is found that 1 equiv of BF_4^- in propylene carbonate is equivalent to 1 equiv of (dried) PVP alone, but that neither of these systems allows for isolable and redissolvable nanoclusters without bulk $Ir(0)_n$ metal formation. Careful predrying of the PVP, and by implication other polymers, is shown to be necessary for the formation and stabilization of the nanoclusters. Next, 40 equiv of 10,000 MW_{ave} PVP and 1 equiv BF_4^- are shown to allow isolable, redissolvable nanoclusters. Control experiments reveal little effect on nanocluster stabilization by 3,500 or 55,000 MW_{ave} PVP, but yielded interesting effects on nanocluster nucleation by the 3,500 MW_{ave} PVP (as well as by the polymer PBEP, *vide infra*). Four other key polymers reported in the literature to be nanocluster stabilizers are tested by the 5 criteria method for their efficacy in the formation and stabilization of $Ir(0)_n$ nanoclusters (now in acetone due to the polymers' solubility) and in comparison to each other, specifically, poly(methyl methacrylate) (PMMA), poly(styrene) (PS), poly(methylhydrosilane) (PMHS), and poly(bis(ethoxy)phosphazene)

(PBEP). Only PMMA allows isolable and redissolvable nanoclusters in acetone. Control / reference point experiments show that the electrostatic stabilizer $P_2W_{15}Nb_3O_{62}^{9-}$ is superior to each of the five polymeric stabilizers studied herein in both acetone and propylene carbonate, at least for the test case of $Ir(0)_n$ nanoclusters. Further controls show that 40 equiv of PVP added to $P_2W_{15}Nb_3O_{62}^{9-}$ stabilized nanoclusters has no discernable effect on the 5 criteria other than to *reduce* by ~50% the nanocluster catalytic activity and total catalytic lifetime for cyclohexene hydrogenation. The main finding of this work is that DLVO theory as applied to nanocluster stabilization is fully supported—that is, surface-bound anions in high dielectric constant solvents provide superior stabilization. The importance of even traditionally weakly coordinating anions such as BF_4^- in nanocluster stabilization is a second, important finding of this work. The fact that HPO_4^{2-} has been shown to be a simple, cheap, commercially available, thermally robust and ^{31}P NMR-handle-containing analog of the more esoteric $P_2W_{15}Nb_3O_{62}^{9-}$ stabilizer is also discussed as part of (xiv) total conclusions listed in the Conclusions section from this first study ranking polymeric stabilizers of transition-metal nanoclusters.

Introduction

Poly(vinylpyrrolidone) (PVP) is the most common polymer protectant of transition-metal nanoclusters.[1,2] PVP is widely represented as a superior steric stabilizer[3] of metal nanoclusters, the term "PVP-stabilized..." often appearing in the titles of papers employing PVP as an additive[1] to nanocluster or nanocolloid solutions.[4] However, there is no modern test of the true relative ability of PVP, or any other polymer additive for that matter, to stabilize transition-metal nanoclusters, despite the wide use of these putative

stabilizers.[5] Additionally, a survey of the literature reveals that little is truly known about *how* polymers stabilize nanoclusters.[5]

A 1966 study of 40 polymers employed to protect Co colloids represents early work investigating the colloid/polymer interaction.[6] These authors also make several interesting points: (i) "Little is known about the mechanism of colloid stabilization in media of low dielectric constant"; and (ii) "For each dispersant polymer there is an optimum solvent system which...should be less polar than the most polar constituent of the polymer".[6] The unsurprising implication here is that the polymer must coordinate to the nanocluster's surface to be an effective stabilizer. This early work raises the question of if polymers are really necessary in solvents of suitably high dielectric constant, a point examined herein.

A primary reason for the paucity of knowledge concerning the true nanocluster stabilizing effects of polymer (and other, *vide infra*) additives in various solvents has been the *lack of modern methodology* to assay the stabilizing abilities of the possible combinations of additives and solvents. The prior "gold number" and "protectant value" methods are 41 and 105 years old, respectively, at this time.[7] These historical methods, which rank protectants by their ability to prevent nanocluster precipitation observed by eye, are qualitative, only apply to Au colloids in H_2O, do not separate the effects of anions, cations, solvents, or polymer stabilizers, and do not separate the effects on nanocluster *formation* from those on nanocluster *stabilization.* Additionally, these prior methods are not even applicable to modern transition-metal nanoclusters prepared in organic solvents, rather than the common solvent for classical colloids,[4] H_2O.

Ideally, a kinetic method measuring nanocluster stability *based on the relative rates of nanocluster agglomeration*—a quantitative, general method applicable to all metal nanoclusters in all solvents—would be available. Efforts are underway in our laboratories to develop the needed kinetic methods, but a generally applicable method is not on the immediate horizon.[8] Noteworthy here is that complex process of nanocluster agglomeration[9] is expected to be a complex interplay of kinetic steps such as ligand dissociation, metal-metal bond formation, structural reorganization, and re-ligation.

However, a method for ranking the formation and stabilization of nanoclusters employing 5 criteria is available, having been reported in 2002.[10,11] We have, therefore, embarked on a program to apply the 5 criteria method to rank the relative abilities of anions, cations, solvents and polymers for, first, their ability to allow the kinetically controlled formation of narrow size dispersions of nanoclusters and, second, their ability to stabilize the resulting nanoclusters sufficiently to allow isolable, "bottleable" and ideally subsequently fully redissolvable nanoclusters.[10,11] The 5 criteria[10] (4 of which are quantitative, *vide infra*) are: (i) a high level of kinetic control during the nanocluster formation reaction, as reflected by a large value of the k_2/k_1 ratio for autocatalytic surface-growth (k_2) to nucleation (k_1) of the nanoclusters, the first two steps of Scheme 1 which follows;[12,13] (ii) the degree to which near-monodisperse nanoclusters are formed as verified by TEM (near-monodisperse nanoclusters are defined elsewhere as those with a size distribution of $\leq \pm 10$–15%[1c]); (iii) the degree to which the nanoclusters can be isolated from solution, bottled for future use and fully redissolved on demand for subsequent use; (iv) the relative catalytic hydrogenation activity of the isolated

nanoclusters once redissolved in solution with fresh cyclohexene substrate; and (v) the total catalytic lifetime for cyclohexene hydrogenation of the nanoclusters in solution.

Scheme 1. The 3-step mechanism for nanocluster nucleation, growth, and agglomeration. **A** is the organometallic nanocluster precursor, **B** is the active $Ir(0)_n$ in the nanocluster hydrogenation catalyst, and **C** is larger, bulk-type metal. The 2-step mechanism for nucleation and growth is simply the first two steps below.

$$A \xrightarrow{k_1} B$$

$$A + B \xrightarrow{k_2} 2B$$

$$B + B \xrightarrow{k_3} C$$

Application of these 5 criteria has previously led to an "anion series" (listed below) that ranks polyoxoanions as well as seven common anions for their ability to stabilize prototype $Ir(0)_n$ nanoclusters in acetone solvent with Bu_4N^+ counter ions in the presence of the proton scavenger Proton Sponge™:[10,11,14] $[P_2W_{15}Nb_3O_{62}]^{9-} \sim [(P_2W_{15}Nb_3O_{61})_2O]^{16-} \sim [SiW_9Nb_3O_{40}]^{7-} \sim ([P_2W_{15}(TiOH)_3O_{\sim 59}]^{9-})_n$ (n = 1, 2) > HPO_4^{2-} > $C_6H_5O_7^{3-}$ > $[-CH_2-CH(CO_2^-)-]_n^{n-} \sim OAc^- \sim P_3O_9^{3-} \sim Cl^- \sim OH^-$. Proton Sponge™ ($PS^{TM}$) is added for nanocluster formation under H_2 in the presence of anions since without Proton Sponge™, the conjugate acid of the anion (e.g., H^+Y^-, Scheme 1) is formed which is not a stabilizer in comparison to the unprotonated anion (e.g., Y^- PS^{TM}–H^+, Scheme 1)[11] and as the results to follow will verify.

The general nanocluster formation reaction employed herein is shown in Scheme 2.[15] Hydrogen uptake curves are converted to cyclohexene consumption curves using the known 1:1 H_2 to cyclohexene stoichiometry and following the previously established cyclohexene reporter-reaction kinetic method.[16]

Scheme 2. The generalized $Ir(0)_n$ nanocluster formation reaction in the presence of added anions, $(Bu_4N^+)_nY^{n-}$.

Nanocluster Formation Reaction

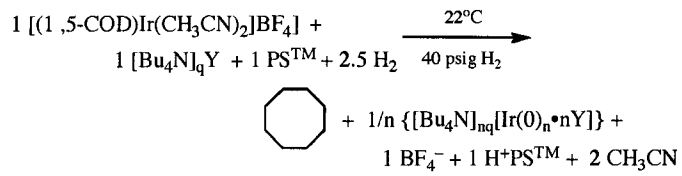

Cyclohexene Reporter Reaction

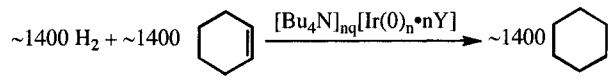

The study of nanocluster stabilizing *anions* was undertaken first in a prior study[10,11] given that DLVO (Derjaugin-Landau-Verwey-Overbeek) theory[17] of colloidal stability predicts that anions adsorbed to the nanocluster surface are in general a key to

$$1/\kappa = ((\varepsilon_0 \times \varepsilon_R \times k \times T)/\sum_i (z_i e)^2 \times c_{i_0}))^{0.5} \quad (1)$$

nanocluster stability. In addition, anions beyond those that can be adsorbed onto the nanocluster surface comprise the diffuse layer of ions which further surround the nanoclusters; this diffuse layer is referred to as the Debye layer (denoted by $1/\kappa$; values are typically in nm) as shown in eq. 1 below.

Above, ε_0 is the permittivity of free space, ε_R is the dielectric constant of the medium (the solvent), k is the Boltzman constant, T is the temperature, z_i is the ion valency, e is the charge on an electron, and c_{i0} is the concentration of the ion, *i*, in the bulk solution.[18] One prediction of eq. 1 is especially important for the studies herein: a thicker Debye layer of ions will be formed in a high dielectric constant solvent, that thickening of the diffuse layer resulting in nanoclusters that are further apart and hence more stable to agglomeration. This predicted solvent dielectric constant effect is tested in detail elsewhere.[19]

Herein we undertake the fifth stage[10,11,14,28] of our fundamental studies aimed at clarifying the additives and solvents that best stabilize transition-metal nanoclusters, especially for their use as soluble catalysts. We address herein the question of the advantages, or disadvantages, of adding PVP or other polymeric protectants[20] in comparison to the presence of BF_4^- (derived from the organometallic precursor, Scheme 2) in the high dielectric constant (ε_R=69) propylene carbonate solvent. Propylene carbonate was chosen as a solvent due to its proven ability to aid in the stabilization of transition-metal nanoclusters and colloids.[18,21] In addition, PVP is completely soluble in propylene carbonate and remains soluble throughout the course of the nanocluster formation and hydrogenation catalysis reactions. This is not the case for acetone, the solvent used in our previous studies,[10,11] but in which three of the polymeric protectants employed in the literature (and hence herein) *are insoluble*. The nanocluster formation reaction utilized herein is identical to that in Scheme 1, except that 1-40 equivalents of the polymer under investigation are added.

In what follows we first evaluate the most common polymer protectant and steric stabilizer, poly(vinylpyrrolidone), of 3,500, 10,000 and 55,000 MW_{ave} g/mol, both as received and after drying, by the 5 criteria method. The test system is the ability of each, individual additive to allow the kinetically controlled formation and then stabilization of prototype $Ir(0)_n$ nanoclusters in propylene carbonate. Second, four other polymers[22] were also evaluated, specifically: poly(methyl methacrylate) (PMMA),[23] poly(styrene) (PS),[24] poly(methylhydrosilane) (PMHS),[25] and poly(bis(ethoxy)-phosphazene) (PBEP),[26] all of which have been implied to be excellent nanocluster stabilizers,[23,24,25,26] but none of which have been explicitly tested for their stabilizing ability compared to (a) each other,

or (b) the "Gold Standard" polyoxoanon stabilizer $P_2W_{15}Nb_3O_{62}^{9-}$.[10,11] Hence, each of these four putative stabilizing polymers were also evaluated by the 5 criteria method, but now in acetone due to the insolubility of the PS and PBEP polymers in propylene carbonate. The studies that follow evaluate the five polymers as nanocluster stabilizers for the first time in the absence of otherwise commonly present, coordinating anions such as Cl^-.[27] The overall goal of these and our prior studies[10,11,14,28] is to simplify the "dizzying variety"[2f] of claimed nanocluster stabilizers by ranking them into a shorter list of preferred stabilizers fortified by as much fundamental understanding as possible. The broader goal of this and our earlier work[10,11,14,28] is to establish a deeper understanding of how nanocluster stabilization is both best and most simply accomplished.

Experimental Section

Analytical Instrumentation. ^1H and ^{31}P NMR experiments were carried out on a Varian Inova 300 spectrometer and referenced to TMS ($\delta = 0$) or 85% H_3PO_4 ($\delta = 0$ ppm) for ^1H and ^{31}P NMR, respectively. Spectra were obtained in 5.0 mm o.d. oven dried NMR tubes at 22 °C in either CD_2Cl_2 or CD_3CN. TGA studies were carried out under a N_2 atmosphere on 5-15 mg of polymer with a TA Instruments 2050 TGA equipped with a Balzers Thermo-Star quadrupole mass spectrometer. TGA samples were heated from 26 °C to 600 °C at a rate of 5 °C/min. Gas chromatography (GC) was performed using a Hewlett-Packard 5890 Series II GC equipped with either a Supelcowax 10 or a Supelco SPB-1 capillary column and a FID detector coupled to a Hewlett-Packard 3395 integrator. All analyses were carried out in at least duplicate.

Materials. All commercially obtained reagents were used as received unless otherwise noted. All solvents were stored in the drybox prior to use. Propylene carbonate (Aldrich, 99.7%) was evacuated for ≥3 hours and dried by storage over activated 4 Å molecular sieves. Cyclohexene (Aldrich, 99%) was freshly distilled over sodium metal under argon and stored in a pre-dried glass bottle. The crystalline iridium solvate complex, $[(1,5\text{-COD})Ir(CH_3CN)_2]BF_4$, used as a precursor to the nanoclusters (eq. 1, vide supra) was prepared following the procedure for the corresponding hexafluorophosphate salt.[29] The purity of the product was verified by ^1H NMR (CD_2Cl_2: δ 1.8(m), 2.3(m), 2.6(s), 4.3(s)). Proton Sponge™ (1,8-bis(dimethylamino)-naphthalene, Aldrich, 99%) was used as received and stored in the drybox prior to use. The polyoxoanion $[Bu_4N]_9[P_2W_{15}Nb_3O_{62}]$ was prepared according to our most recent literature procedure.[30] The purity of the polyoxoanion was checked by ^{31}P NMR and is ≥90% purity (CD_3CN: δ –6.5, –13.6 relative to 85% H_3PO_4, with small impurity peaks at -8.7 and -13.2). This polyoxoanion was then used to prepare the supported organometallic compound $[Bu_4N]_5Na_3(1,5\text{-COD})Ir{\bullet}P_2W_{15}Nb_3O_{62}$ according to our most recent literature procedure, with the only modification being that crystalline $[(1,5\text{-COD})Ir(CH_3CN)_2][BF_4]$ was used as the Ir source.[31] Poly(vinylpyrrolidone) was purchased from Aldrich (10,000 and 55,000 g/mol MW_{ave}) and Acros Organics (3,500 g/mol MW_{ave}). Poly(methyl methacrylate) (15,000 g/mol MW_{ave}), poly(styrene) (13,000 g/mol MW_{ave}), poly(methylhydrosilane) (400,000-800,000 g/mol MW_{ave}), and poly(bis(ethoxy)phos-phazene) (no average molecular weight given) were purchased from Aldrich. For the undried samples, the white powders were used as received. The dried samples were prepared as 1.26 M solutions in dried propylene carbonate and then

stored over activated 4 Å molecular sieves at least overnight. CD_2Cl_2 (99.9%) and CD_3CN (99.9%) were purchased from Cambridge Isotope Laboratories in 1g prescored individual ampoules and used as received. TEM samples were prepared on silicon monoxide grids (Ted Pella, Inc.); see "Preparation of TEM Grids", vide infra.

Hydrogenation Apparatus. Hydrogenation experiments were carried out in a previously described[12,32] apparatus designed to continuously monitor hydrogen pressure loss. This apparatus consists of a Fisher-Porter (F-P) bottle, connected *via* Swagelok quick-connects to both a H_2 line and an Omega PX621 pressure transducer. The pressure transducer is interfaced with a PC by means of an Omega D1131 5V A/D converter with a RS-232 connection. The pressure uptake data was collected using LabView 7.1, and hydrogen uptake curves were initially fit to the analytical equations for autocatalytic nanocluster formation, A→B, rate constant k_1, plus A+B→2B, rate constant k_2 (see Scheme 1),[12,13] using Origin 7.0. The hydrogen uptake curves were converted to cyclohexene consumption curves using the known 1:1 H_2 to cyclohexene stoichiometry and following the previously established cyclohexene reporter-reaction kinetic method.[16]

MacKinetics Numerical Integration Curve Fitting. When a cyclohexene hydrogenation curve displayed sigmoidal kinetics plus a tailing (slowing) characteristic of nanocluster agglomeration,[33] and when TEM confirmed agglomerated nanoclusters as products, then the kinetic curves were fit using a 3-step mechanism (Scheme 1) for nanocluster nucleation, growth, and agglomeration.[33] First, k_1 and k_2 rate constants were determined by fitting the first half of the hydrogen uptake data[13] with Origin. Next, the k_1 and k_2 values from Origin were entered into MacKinetics as fixed values and a *gridsearch* was performed to find an initial value for the bimolecular agglomeration rate

constant k_3. Then, these three values (k_1 and k_2 from Origin, k_3 from MacKinetics) were used as initial values for the rate constants, and numerical integration was initiated using MacKinetics. Iterations were carried out until the visual fit was good, the residual was minimized (≤0.01), and the kinetic parameters were self-consistent (i.e., the program returned as final parameters exactly the initial entered parameters). Next, and as a check, fitting was carried out using random guesses for all three initial rate constants. This second technique was employed to ensure the avoidance of local minima, to search a maximum amount of parameter space, and to estimate the error bars on each parameter. Using this second fitting technique, each dataset was fit ≥3 times with a different set of initial parameters for each fitting session. Again, iterations were carried out until the visual fit was good, the residual was minimized (≤0.01), and the returned kinetic parameters were self-consistent. The reported k_1, k_2, and k_3 values herein are an average of the parameters garnered using both techniques (≥ 5 fitting trials per dataset).

The Reference Point of Nanoclusters Prepared from $[Bu_4N]_5Na_3$(1,5-COD)Ir•$P_2W_{15}Nb_3O_{62}$ With and Without Added PVP. In the drybox, $[Bu_4N]_5Na_3$(1,5-COD)Ir•$P_2W_{15}Nb_3O_{62}$ (20 mg, 3.6 μmol) was weighed into a 2-dram pre-dried glass vial. In experiments with added *undried* PVP, the polymer (40 equivalents, 144 μmol) was added to the vial. In experiments with added *dried* PVP, the polymer (0.1 mL of a 1.26 M solution, 144 μmol) was added at this point. Then, propylene carbonate (2.5 mL for the polyoxoanion-only and undried PVP experiments; 2.4 mL for dried PVP experiments) was added with a 2.5 mL gas-tight syringe. The solution was agitated with a disposable polyethylene pipette until the solution was clear, bright yellow (without PVP) or bright orange (with PVP), and homogeneous. Then, the

polyethylene pipette was used to transfer the reaction solution into a new borosilicate culture tube (22 x 175 mm) with a new 5/8" x 5/16" Teflon-coated octagon shaped spin bar. Then, cyclohexene (0.5 mL) was added to the culture tube with a 1.0 mL gas-tight syringe. The culture tube was then sealed in the F-P bottle, removed from the drybox, and attached to the H_2 line. To initiate each reaction, the F-P bottle was purged 13 times with H_2 (40 ± 1 psig, 15 s/purge). Five min after the first purge, the pressure was set at 40 ± 1 psig, $t = 0$ was noted, and pressure *vs.* time data was collected at 2.5 min intervals. The complete formation of Ir(0) nanoclusters was confirmed in a separate experiment by the production of 1.0 equivalent of cyclooctane as measured by quantitative GLC (as described elsewhere[13]).

Nanocluster Preparation from [(1,5-COD)Ir(CH_3CN)$_2$][BF_4] With and Without Added PVP. These experiments were carried out as described above in the section titled "The Reference Point of Nanoclusters Prepared from $[Bu_4N]_5Na_3$(1,5-COD)Ir•$P_2W_{15}Nb_3O_{62}$ With and Without Added PVP" with the following exceptions. The nanocluster precursor [(1,5-COD)Ir(CH_3CN)$_2$][BF_4] (5.0 mg, 10.6 μmol) was chosen instead of $[Bu_4N]_5Na_3$(1,5-COD)Ir•$P_2W_{15}Nb_3O_{62}$ to separate the effects of the strongly coordinating anion $P_2W_{15}Nb_3O_{62}^{9-}$ vs. that of the polymer. This larger amount of [(1,5-COD)Ir(CH_3CN)$_2$][BF_4] (10.6 μmol vs. 3.6 μmol used with the $[Bu_4N]_5Na_3$(1,5-COD)Ir•$P_2W_{15}Nb_3O_{62}$ precursor) was used to minimize weighing and balance errors. The 5 criteria were evaluated at both concentrations to ensure that this higher concentration system was not affecting the stability and thus the comparison of stabilizing abilities. The results and discussion of these controls, which indicate that the 5 criteria for the two systems at different concentrations are equivalent within error, are

reported in the Supporting Information. In some of these experiments, one equivalent of Proton Sponge™ was also added to test for the effects of scavenging H^+ generated in the reduction of Ir(I) to Ir(0) by 0.5 H_2 (vide supra, Scheme 2). Additionally, experiments were performed with either 1 or 40 equiv of PVP.

Nanocluster Preparation from [(1,5-COD)Ir(CH_3CN)$_2$][BF_4] With Varying Average Molecular Weights (MW_{ave}) PVP. These experiments were carried out in the same manner as described above with the following modifications: [(1,5-COD)Ir(CH_3CN)$_2$][BF_4] (5.0 mg, 10.6 μmol) was used as the nanocluster precursor, and one equivalent of Proton Sponge™ (2.3 mg, 10.6 μmol) was added. All three MW_{ave} polymers were pre-dried over activated molecular sieves in the manner described earlier. In these experiments, 40 equivalents (0.1 mL of a 1.26 M solution, 144 μmol) of PVP were added.

Nanocluster Preparation from [(1,5-COD)Ir(CH_3CN)$_2$][BF_4] With PMMA, PS, PMHS, and PBEP. These four polymers were evaluated in acetone since PS and PBEP are not soluble in propylene carbonate. These experiments were otherwise carried out in the same manner as described above in the section titled "Nanocluster Preparation from [(1,5-COD)Ir(CH_3CN)$_2$][BF_4] With and Without Added PVP" with the following modifications: [(1,5-COD)Ir(CH_3CN)$_2$][BF_4] (5.0 mg, 10.6 μmol) was used as the nanocluster precursor, and one equivalent of Proton Sponge™ (2.3 mg, 10.6 μmol) was added. PMMA and PS polymers were tested both as-received and tested after being dried over activated molecular sieves in the manner described in the section titled "The Reference Point of Nanoclusters... " When tested as received, they were each added as a white powder (40 equiv; 27.0 mg PMMA or 15.1 mg PS). When tested as pre-dried

solutions, each was added as a solution in acetone (0.058M, 40 equiv each 2.5 mL). PMHS is a clear and colorless liquid and was used as received (40 equiv monomer, 36.5 μL). PBEP was received as a red-orange oil. The oil (~250 mg, ~2.3 mmol) was diluted with 40 mL pre-dried acetone, yielding approximately 40 equiv PBEP monomer per 2.5 mL solution.

^{1}H NMR Spectroscopic Investigation of the Interaction between [(1,5-COD)Ir(CH_3CN)$_2$][BF_4] and PMHS. In the drybox, a pre-dried 5 mm o.d. NMR tube was loaded with [(1,5-COD)Ir(CH_3CN)$_2$][BF_4] (1.7 mg, 3.6 μmol) in acetone-d_6 (0.6 mL). The tube was sealed with a rubber septa and removed from the drybox. An initial ^{1}H NMR spectrum was acquired using the parameters outlined in the "Analytical Instrumentation" section. A peak characteristic of the vinylic protons on the COD ligand was observed at δ=2.5 relative to TMS. Then, PMHS was added (36.5 μL, 144 μmol) by injecting the polymer through the rubber septa capping the NMR tube with a 50 μL gas-tight syringe. A second ^{1}H NMR spectrum was then acquired. Both spectra appear as Figure S5 of the Supporting Information.

Preparation of TEM grids. Since propylene carbonate is difficult to remove completely, and since any residual propylene carbonate charges in the TEM electron beam, it is an unsuitable solvent for TEM analysis.[21b] Hence, preparation of the TEM grids was carried out using our previously established method.[21b] Briefly, after nanocluster formation was complete (as judged by a separate cyclooctane evolution experiment monitored by GLC), the F-P bottle was vented, brought into the drybox, and opened. There, an aliquot (0.5 mL) of the nanocluster solution was diluted with 10 mL anhydrous diethyl ether in a pre-dried scintillation vial (the nanocluster solutions were

brown if no $P_2W_{15}Nb_3O_{62}^{9-}$ was present, or a blue solution if $P_2W_{15}Nb_3O_{62}^{9-}$ was present due to the well-known formation of a reduced, W^V containing, heteropoly blue[12] during the hydrogenation reaction). This resulted in a cloudy light brown solution (indicative of $Ir(0)_n$ nanocluster solutions[34]) for reactions without added $P_2W_{15}Nb_3O_{62}^{9-}$ or a light-blue solution for the reactions with added $P_2W_{15}Nb_3O_{62}^{9-}$. The scintillation vial was closed, sealed with Parafilm, and brought out of the drybox. Next, the nanoclusters were separated by centrifugation (1h at 1200 rpm in a swinging-bucket centrifuge with a radius of 20 cm). In well-stabilized solutions, this resulted in the formation of a dark–brown film of nanoclusters on the bottom of the vial. For poorly stabilized systems, centrifugation of the material yielded non-redispersable bulk metal particles. This material was discarded and the presence of bulk metal was noted. For the well-stabilized systems, the scintillation vial was transferred back into the drybox, opened, and the ether decanted. The brown film was redispersed in 1.0 mL acetonitrile resulting in an apparently homogeneous dark brown solution, and again the solution was diluted with 10 mL anhydrous diethyl ether. The centrifugation program was then repeated exactly as described above. Finally, the ether/acetonitrile solution was decanted from the brown nanocluster film, and the film was dried overnight under vacuum. The nanoclusters were sent as a solid for TEM analysis with the expert assistance of Dr. JoAn Hudson at the University of Oregon (and later, but still with the assistance of Dr. Hudson, at Clemson University). An accelerating voltage of 120 kV was employed, and magnification ranged from 120,000 to 580,000. For micrographs that showed well-separated nanoclusters, the size distribution was determined by measuring the diameters of $\geq$ 200 nanoclusters using enlarged images of the micrographs.

Testing the Catalytic Activity of the *in situ* Nanoclusters. Once nanocluster formation was judged complete by a separate cyclooctane evolution experiment, the F-P bottle was vented, brought into the drybox, and opened. Then, an aliquot (0.5 mL) of the nanocluster solution was placed in a new culture tube with a new stir bar. Next, propylene carbonate (2.0 mL) was added with a 2.5 mL gas-tight syringe, and the culture tube was agitated gently to ensure dissolution of the nanocluster solution in the fresh propylene carbonate. Finally, cyclohexene (0.5 mL) was added with a 1.0 mL gas-tight syringe, and the culture tube was sealed into the F-P bottle. The F-P bottle was removed from the drybox and attached to the H_2 line. There, hydrogenation was initiated exactly as described above in the section titled "Nanocluster Preparation from $[Bu_4N]_5Na_3(1,5\text{-}COD)Ir{\bullet}P_2W_{15}Nb_3O_{62}$ With and Without Added PVP". Hydrogenation of cyclohexene proceeded without an induction period, as expected for a fully formed nanocluster catalyst. The initial rate was calculated from the pressure vs. time data (calculated from the maximum slope past the induction period, fit to a 2nd order polynomial in which the second term of the polynomial is the initial rate[35]). This initial rate calculation was accomplished with Microsoft Excel Version 11.1 for Macintosh as described previously.[10]

Testing the Catalytic Activity of the Redispersed Nanoclusters. The nanoclusters were isolated from propylene carbonate exactly as described above in the section titled "Preparation of TEM grids." If the precipitation method resulted in non-redispersable bulk metal, tests of catalytic activity were not possible and the presence of bulk metal was noted. If the precipitation method resulted in a homogeneous brown film of nanoclusters, then the film was redispersed in propylene carbonate (2.5 mL) to yield a

brown solution. The solution was gently agitated with a polyethylene pipette to ensure complete dissolution of the nanoclusters. Then, the polyethylene pipette was used to transfer the nanocluster solution from the scintillation vial to a new culture tube with a new stir bar. Finally, cyclohexene (0.5 mL) was added with a 1.0 mL gas-tight syringe, and the culture tube was sealed in the F-P bottle. The F-P bottle was removed from the drybox and attached to the hydrogenation line. There, hydrogenation was initiated exactly as described above in the section titled "Nanocluster Preparation from $[Bu_4N]_5Na_3(1,5\text{-COD})Ir\bullet P_2W_{15}Nb_3O_{62}$ With and Without Added PVP". Hydrogenation of cyclohexene proceeded without an induction period, as expected for a fully formed nanocluster catalyst and the initial rate was calculated as described above.

Testing the Catalytic Lifetime of the Nanoclusters (Total Turnover Experiments). In the drybox, a reaction solution was prepared exactly as described above in the section titled "Nanocluster Preparation from $[Bu_4N]_5Na_3(1,5\text{-COD})Ir\bullet P_2W_{15}Nb_3O_{62}$ With and Without Added PVP". Next, an aliquot of this reaction solution (0.5 mL) was removed from the 2- dram vial with a 1.0 mL gas-tight syringe and added to a new culture tube with a new stir bar. To this bright-orange solution, propylene carbonate (4.0 mL) was added, resulting in a clear, light orange solution. Cyclohexene (4.5 mL; corresponding to 63,000 possible total turnovers) was then added to the culture tube with a 5.0 mL gas-tight syringe, and the culture tube was sealed inside the F-P bottle. The F-P bottle was removed from the drybox, attached to the H_2 line, and hydrogenation was initiated exactly as described above in the section titled "Nanocluster Preparation from $[Bu_4N]_5Na_3(1,5\text{-COD})Ir\bullet P_2W_{15}Nb_3O_{62}$ With and Without Added PVP". Approximately every 24 hours, the cyclohexene conversion was monitored by ^1H NMR

spectroscopy as follows: aliquots of the reaction solution were obtained by disconnecting the F-P bottle from the hydrogenation line, venting the bottle, and bringing it into the drybox. Using a 50 μL gas-tight syringe, a ca. 10 μL aliquot was removed and added to 1 g of CD_2Cl_2 in an individual glass ampoule. The solution in CD_2Cl_2 was then transferred with a polyethylene pipette to a pre-dried 5 mm o.d. NMR tube, which was subsequently capped. ^1H NMR spectroscopy of the reaction solution gave the conversion of cyclohexene to cyclohexane. The culture tube was resealed in the F-P bottle, and both the NMR tube and the F-P bottle were brought out of the drybox. The F-P bottle was reconnected to the H_2 line, and hydrogenation was initiated exactly as described above in the section titled "Nanocluster Preparation from $[Bu_4N]_5Na_3(1,5\text{-COD})Ir{\bullet}P_2W_{15}Nb_3O_{62}$ With and Without Added PVP". During the time that the F-P bottle was in the drybox, the hydrogenation apparatus was evacuated for at least 25 minutes. This procedure takes ca. 30 minutes, but does not introduce significant error in the catalytic lifetime experiments which took ≥100 hours.

Results and Discussion

Controls Preparing $Ir(0)_n$ Nanoclusters in the Absence of PVP and Strongly Stabilizing Anions. Experiments were performed evaluating the 5 criteria for two systems beginning with the known nanocluster precursor[10] $[(1,5\text{-COD})Ir(CH_3CN)_2][BF_4]$ in the absence and then presence of Proton Sponge™, entries 1 and 2 of Table 1. These control experiments were performed in order to assess the contribution to nanocluster stability from BF_4^-,[19] which is present in its deprotonated form in the presence of Proton Sponge™ (but present as the non-ligating $H^+BF_4^-$, pK_a = ~0 in propylene carbonate,[36] in

the absence of Proton Sponge™). Reduction of $[(1,5\text{-COD})Ir(CH_3CN)_2][BF_4]$ in propylene carbonate without Proton Sponge™ results in *non-redissolvable bulk metal.* However, with 1 equiv Proton Sponge™ added, a brown solution indicative of $Ir(0)_n$ nanoclusters[34] was observed, although agglomerated nanoclusters are still seen by TEM (see Figure 1 elsewhere[19]). Neither system produced isolable and redissolvable nanoclusters, and bulk metal was formed during the course of each TTO experiment, entries 1 and 2, Table 1. The take-home message from these control experiments and our work elsewhere[19] is that even the weakly coordinating BF_4^- anion plus high dielectric constant solvent provides meta-stable $Ir(0)_n$ nanoclusters, albeit ones that are not isolable and which are agglomerated according to TEM. The reasons BF_4^- appears to be serving as a better nanocluster-bound, anionic stabilizer than one might at first suspect include (as discussed more elsewhere[19]) that: (a) BF_4^- presumably can be a tridentate ligand on the nanocluster surface,[28] and (ii) metal-ligand bond energies in nanoclusters can be up to factor of 2 stronger than those involving the corresponding bulk metal.[37,38] The latter is an important point for nanocluster catalysis as discussed elsewhere.[37]

Table 1. Compilation of Data Examining the Effects of PVP, H_2O, and Proton Sponge™, with Controls Examining the Effects of $P_2W_{15}Nb_3O_{62}^{9-}$ and BF_4^-, on $Ir(0)_n$ Nanoclusters in Propylene Carbonate.

	Precursor	PVP	1 Equiv Proton Sponge?	k_2/k_1[a] (M^{-1})	Size (Å)	Redissolvable?	Cat. Act.[b]	TTO[c]
	With no added stabilizer							
1	[(1,5-COD)Ir(CH_3CN)$_2$][BF_4]	none	no	poor fit[d]	---	no	---	[3,700]
2	[(1,5-COD)Ir(CH_3CN)$_2$][BF_4]	none	yes	$7.0(5)\times10^3$	agg.[e]	no	---	[51,000]
	With added PVP							
3	[(1,5-COD)Ir(CH_3CN)$_2$][BF_4]	1 equiv undried 10k	no	$4.5(2)\times10^3$	---	no	---	[2,200]
4	[(1,5-COD)Ir(CH_3CN)$_2$][BF_4]	1 equiv dried 10k	no	poor fit[d]	---	no	---	[2,100]
5	[(1,5-COD)Ir(CH_3CN)$_2$][BF_4]	1 equiv dried 10k	yes	$4.1(5)\times10^3$	---	no	---	[4,200]
6	[(1,5-COD)Ir(CH_3CN)$_2$][BF_4]	40 equiv dried, 10k	no	$1.9(3)\times10^3$	agg.[e]	no	---	[14,000]
7	[(1,5-COD)Ir(CH_3CN)$_2$][BF_4]	40 equiv dried, 10k	yes	$6.7(5)\times10^3$	agg.[e]	yes	$6.0(3)\times10^5$	[12,000]
8	[(1,5-COD)Ir(CH_3CN)$_2$][BF_4]	40 equiv dried, 3.5k	yes	poor fit[d]	agg.[e]	yes	$9.3(5)\times10^5$	[92,000]
9	[(1,5-COD)Ir(CH_3CN)$_2$][BF_4]	40 equiv dried, 55k	yes	$4.1(6)\times10^3$	agg.[e]	yes	$1.00(5)\times10^6$	[9,600]
	With added $P_2W_{15}Nb_3O_{62}^{9-}$							
10	$[Bu_4N]_5Na_3$(1,5-COD)Ir•$P_2W_{15}Nb_3O_{62}$	none	yes	$1.0(2)\times10^5$	21 ± 3	yes	$2.2(1)\times10^6$	56,000
11	$[Bu_4N]_5Na_3$(1,5-COD)Ir•$P_2W_{15}Nb_3O_{62}$	40 equiv dried, 10k	no	$1.2(1)\times10^5$	18 ± 3	yes	$1.3(1)\times10^6$	22,800
12	$[Bu_4N]_5Na_3$(1,5-COD)Ir•$P_2W_{15}Nb_3O_{62}$	40 equiv undried, 10k	no	poor fit[d]	24 ± 7	yes	$4.3(2)\times10^5$	[20,300]

(a) The values for k_2/k_1 have been corrected by the mathematically required stoichiometry factor of 1400 as detailed elsewhere.[12] (b) mmol H_2/h•mol Ir (c) total turnovers of cyclohexene hydrogenation (mol product/mol catalyst); square brackets indicated that *bulk metal* was formed during the course of these experiments, so these values are necessarily an upper limit on the true nanoparticle TTOs. (d) A poor fit to the 2-step mechanism was observed for the indicated data. (e) agg = agglomerated nanoclusters observed by TEM.

Testing the Stabilizing Ability of 1 equiv of PVP in the Absence of Strongly Stabilizing Anions. These studies were carried out under the conditions outlined in Scheme 1. An issue that arises here is the amount of water in commercially available PVP and its effect on the nanocluster formation reaction (see Table 2, p. 4901 elsewhere[12] for data showing that H_2O influences the kinetics of $Ir(0)_n$ nanocluster formation as well as bulk metal formation, even in the presence of the highly stabilizing $P_2W_{15}Nb_3O_{62}^{9-}$ anion). As-received PVP was shown by thermal gravimetric analysis (TGA) to contain up to 2.2 weight percent water (see Figure S1 in the Supporting

Information). Hence, we hypothesized that the water contained in *undried* PVP would negatively influence nanocluster formation and stabilization.

In a control experiment to test the effects of adventitious water, 1 equiv of *undried* PVP also *without* added Proton Sponge™, (which yields $H^+BF_4^-$, so there is effectively no coordinating anion), was examined, entry 3 of Table 1. Reduction of the organometallic precursor did yield a brown solution indicative of $Ir(0)_n$ nanoclusters, but bulk metal was visible to the naked eye. TEM images of the reaction solution were not obtained since they would not be representative of the entire sample. Criteria (iii) and (iv) (i.e., of the 5 criteria) are also unavailable due to the formation of bulk metal; additional formation of bulk metal was observed during the course of the total turnover experiment, Table 1 entry 3. In a second control experiment with 1 equiv *dried* PVP, but again deliberately with no Proton Sponge™, evaluation of the 5 criteria showed that *1 equiv of dried PVP alone (i.e., in the absence of even the weakly coordinating* BF_4^- *anion) is also not a good* $Ir(0)_n$ *nanocluster stabilizer*, entry 4 of Table 1. The results are clear in showing that 1 equiv dried PVP does not permit the formation and stabilization of $Ir(0)_n$ nanoclusters, even in the high ε solvent propylene carbonate.

Next, the 5 criteria were evaluated with 1 equiv PVP *plus 1 equiv Proton Sponge ™* added to the reaction solution, entry 5 in Table 1, so that the potential stabilizers present are BF_4^- / Proton Sponge™–H^+ and the 1 equiv PVP. This time a brown solution of $Ir(0)_n$ nanoclusters[34] is produced, although non-redissolvable bulk metal precipitates from the solution upon standing overnight. This experiment shows that 1 equiv PVP plus 1 equiv BF_4^- is superior for the *formation* of nanoclusters when compared to 1 equiv PVP alone. Also notable here is a comparison between entries 2 and

5 in Table 1: 1 equiv dried PVP certainly does not improve the level of kinetic control of the nanocluster formation reaction and may actually hinder it some as judged by the apparently lower k_2/k_1 ratio (7.0×10^3 for entry 2 vs. 4.1×10^3 for entry 5, Table 1; however, these numbers are probably close to being the same within experimental error). In short, 1 equiv PVP plus 1 equiv BF_4^- is not a preferred system for the formation, stabilization, and subsequent catalytic activity of prototype $Ir(0)_n$ nanoclusters as measured by the 5 criteria method. The findings of others[27] are consistent with this, specifically that a PVP:Ir ratio greater than 1 is necessary for the formation of small, well-separated, spherical $Pt(0)_n$ particles.

Testing the Stabilizing Ability of 40 Equiv PVP in the Absence of Strongly Stabilizing Anions: Further Evidence for the Importance of Anionic Stabilization by Even BF_4^-. A PVP:Ir ratio of 40:1 is commonly used in the literature to stabilize nanoclusters,[3,39] consistent with our findings above that a 1:1 ratio is insufficient. Again we began with a strict evaluation of 40 equiv of PVP in the absence of Proton Sponge™ so that only $H^+BF_4^-$ (i.e., and no anionic BF_4^- stabilizer) should be present[11] (entry 6 Table 1); after that, the reaction with 1 equiv Proton Sponge™ was studied (entry 7, Table 1). A comparison of the results for entries 6 and 7 makes clear that nanoclusters prepared in the presence 40 equiv dried PVP, but in the absence of 1 equiv of Proton Sponge™, have a lower k_2/k_1 ratio, and thus poorer kinetic control in their formation, and are not redissolvable as they are when BF_4^- is present. These data re-emphasize the importance of adding Proton Sponge™ to all nanocluster reactions that produce H^+Y^- by

reduction of MY_x nanocluster precursors under H_2 so that the anionic stabilizer, Y^-, is produced rather than the much weaker to non-stabilizer, H^+Y^-.[11]

A comparison of the 5 criteria measured in entries 5 and 7 in Table 1 does show that, when 1 equiv BF_4^- is also present, 40 equivs PVP provides redissolvable, and thus superior, nanoclusters compared to when 1 equiv of PVP alone is present or vs. when 1 equiv BF_4^- alone is present (entry 2, Table 1). Figure 1 shows a TEM image of the resultant $Ir(0)_n$ nanoclusters prepared with 40 equivalents PVP plus 1 equiv BF_4^-.

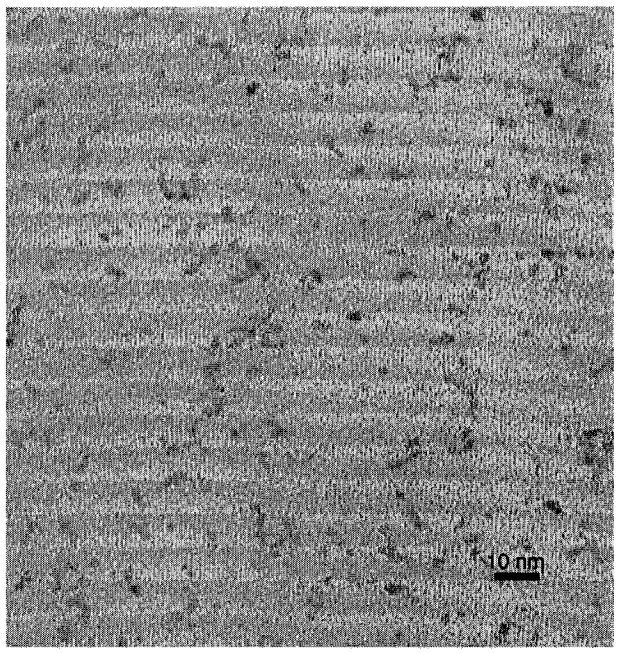

Figure 1. TEM image (580k magnification) of $Ir(0)_n$ nanoclusters stabilized by 40 equiv dried MW_{ave}=10,000 g/mol PVP plus 1 equiv BF_4^-. Non-optimum, agglomerated nanoclusters are seem by TEM following precipitation of the nanoclusters from solution (as detailed in the Experimental Section).

The micrograph in Figure 1, while visually helpful, cannot be used to quantitate the size or size distribution of the nanoclusters due to the extensive agglomeration present. Overall, three conclusions are apparent for at least the test case of $Ir(0)_n$ nanoclusters: PVP alone is not a superior stabilizer; even 40 equiv of PVP is not a sufficient stabilizer to yield redissolvable nanoclusters *unless an anionic stabilizer is also present*; moreover, even 1 equiv of the traditionally weakly coordinating BF_4^- is a

reasonably good anion for use with 40 equiv PVP. It would seem that the broad belief of superior stabilization of nanoclusters by polymeric additives such as PVP *alone* needs to be rethought.

PVP Molecular Weight (MW_{ave}) Dependence on Stability. Previous studies have indicated that the stability of a nanocluster/nanocolloid system may depend on the MW_{ave} of the polymer employed.[40] Consequently, we tested three different average molecular weights of PVP: 3,500, 10,000, and 55,000 g/mol. All polymers were predried over molecular sieves before use. Additionally, all experiments were performed with added Proton Sponge™ so that 1 equiv BF_4^- is present in all cases (i.e, and since the presence of at least some anionic stabilization is representative of how polymeric protectants are used in the literature).

Comparison of the three different MW_{ave} PVP polymers in entries 7, 8, and 9 of Table 1 shows that there is no apparent difference in the level of *stabilization* provided by any of the three different molecular weight polymers. Nanoclusters prepared with all three MW_{ave} polymers and 1 equiv BF_4^- are strikingly similar. For example, TEM images of nanoclusters prepared in the presence of 40 equivs of dried 3,500, 10,000, and 55,000 g/mol MW_{ave} PVP all show agglomerated nanoclusters which are, however, isolable and redissolvable in fresh propylene carbonate in each instance. Their catalytic activity once redispersed is in the same range ($0.6\text{-}1.0 \times 10^6$ mmol h^{-1} mol Ir^{-1}). In addition, nanoclusters stabilized by each MW_{ave} polymer yielded bulk metal during the course of the TTO experiment. Consequently, the average molecular weight of PVP has

no discernable effect on the resultant stability of $Ir(0)_n$ nanoclusters, at least in the 3,500-55,000 g/mol MW_{ave} range and by the 5 criteria.

However, there are significant differences in the kinetics of nanocluster *formation* with the MW_{ave} polymers: while the 10,000 and 55,000 g/mol MW_{ave} polymers appear to have similar kinetics of formation (well fit by the established 2-step autocatalytic nanocluster formation mechanism[13]), the kinetics of nanocluster formation with 3,500 MW_{ave} PVP cannot be fit by this standard mechanism. There is essentially no induction period in the nanocluster formation kinetic curve with 3,500 MW_{ave} PVP, Figure S2 of the Supporting Information. It is as if the nucleation process is especially stabilized in the presence of the low MW PVP,[41] although further studies will be needed to understand this initial, repeatable observation (repeated 4 times).

Control Experiments Determining the 5 Criteria for $P_2W_{15}Nb_3O_{62}^{9-}$-Stabilized Nanoclusters. The best stabilizer examined thus far (for at least $Ir(0)_n$ nanoclusters in acetone) according to the 5 criteria is the polyoxoanion, $P_2W_{15}Nb_3O_{62}^{9-}$.[10,11] This anion therefore serves as a reference point (or so-called "Gold Standard")[10,11] for ranking other stabilizers. Hence, the 5 criteria for the $P_2W_{15}Nb_3O_{62}^{9-}$ anion *in propylene carbonate* were measured and are shown as entry 10 of Table 1. Comparison of this data to our previous work in acetone[10,11] shows that $P_2W_{15}Nb_3O_{62}^{9-}$ is an equally effective stabilizer in both acetone and propylene carbonate as measured by the 5 criteria. Comparison of the $P_2W_{15}Nb_3O_{62}^{9-}$ data in entry 10 to the best 40 equiv PVP / 1 BF_4^- data in entry 7 shows the polyoxoanion has a 15 fold higher level of kinetic control (i.e., a 15 fold higher k_2/k_1 ratio) in its nanocluster formation reaction, yields 21±3 Å, near-monodisperse

nanoclusters by TEM (vs. agglomerated one for the PVP system), yields fully redissolvable nanoclusters (vs. non-redissolvable for the PVP system), yields a ~2.6 higher catalytic rate for the nanoclusters, and yields a 4.6 fold longer catalytic lifetime. Clearly, 40 equiv PVP even with help from 1 equiv BF_4^- is not near as good a stabilizer as is the polyanionic, tridentate,[28] strong electrostatic, and sterically bulky $P_2W_{15}Nb_3O_{62}^{9-}$ stabilizer plus its 9 Bu_4N^+ countercations.

Testing the Effects of PVP on $P_2W_{15}Nb_3O_{62}^{9-}$-Stabilized Nanoclusters. Two reports from other groups suggest that PVP acts as a secondary stabilizer in the presence of anions.[27,39c] To test if added PVP is capable of any stabilizing effect over and above that of the strong electrostatic stabilization provided by $P_2W_{15}Nb_3O_{62}^{9-}$ in polar solvent, a control was done testing the effect of 40 equiv of dried PVP on $P_2W_{15}Nb_3O_{62}^{9-}$ stabilized $Ir(0)_n$ nanoclusters in the polar but not strongly coordinating solvent, propylene carbonate. Entries 10 and 11 in Table 1 show that the addition of 40 equiv of pre-dried MW_{ave}=10,000 g/mol PVP has *no detectable positive influence* on any of the 5 parameters, even when the Proton Sponge™ was deliberately omitted, the polybasic polyoxoanion being known to serve as its own H^+ scavenger.[10,11,12] (Figure S3 of the Supporting Information presents a TEM image of nanoclusters prepared under the conditions of entry 11 for the interested reader.) In short, 40 equiv of PVP has no detectable secondary stabilizing effect in comparison to $P_2W_{15}Nb_3O_{62}^{9-}$ in propylene carbonate.

There is, however, a measurable *negative effect* on the catalytic activity and lifetime. As entry 10 vs. 11 shows, a ~40% lower catalytic rate and a ~60% lower TTO

catalytic lifetime are seen as a result of adding the 40 equiv of PVP, values that are probably equivalent within experimental error (i.e., a ca. 50±10% reduction in both criteria). These data show that PVP does interact with the surface of the nanocluster, primarily serving as a weak poison of nanocluster catalytic activity. This decrease in activity is also observed in a control experiment in which 40 equivs dried PVP were added to pre-formed, isolated, and redispersed $P_2W_{15}Nb_3O_{62}^{9-}$ stabilized $Ir(0)_n$ nanoclusters: the reaction rate for cyclohexene hydrogenation decreased by 80% compared to isolated and redispersed $P_2W_{15}Nb_3O_{62}^{9-}$ stabilized nanoclusters without any added PVP.

Further Characterization of PVP as a Weak Binder to, and Poison of, Nanocluster Catalysts when $P_2W_{15}Nb_3O_{62}^{9-}$ is Present. We can interpret the PVP poisoning effect a bit further given an earlier study which showed that only 0.015 equivalents of an efficient catalyst poison, CS_2, reduced the catalytic activity of in that case $Rh(0)_n$ nanoclusters by roughly the same, ~80 percentage.[42] Hence, a >2,600 fold higher concentration of PVP has approximately the same effect as 1 equiv of the strong catalyst poison, CS_2, when $P_2W_{15}Nb_3O_{62}^{9-}$ is present and if the respective Rh vs. Ir, 40±6 Å vs. 18±3 Å , differences in the size and thus number of surface sites atop the nanoclusters are neglected for the purposes of this approximate, but first such, comparison. El-Sayed et al. provide further evidence that PVP is a weak catalyst poison in the presence of Cl^- by demonstrating that $Pt(0)_n$ nanoclusters can still perform Suzuki coupling reactions in the presence of 20 equiv PVP.[43] However, the above values are the first semi-quantitative estimate of how many surface sites a 10,000 MW_{ave} PVP polymer chain might occupy—a small fraction. The concept or hypothesis which emerges for further testing would seem to be that much

smaller amounts of specifically designed, better coordinating, oligomeric or polymeric ligands might well provide superior nanocluster stabilization in comparison to classic polymeric stabilizers of compositionally and structurally ill-characterized colloids.[4]

Control Experiments Determining the Effects of H_2O in Commercially Available PVP on $P_2W_{15}Nb_3O_{62}^{9-}$–Stabilized Nanoclusters. Given the observed negative effects of adventitious water on PVP-stabilized nanoclusters, we wanted to examine the effects of water from PVP on otherwise highly electrostatically stabilized nanoclusters. Consequently, the 5 criteria were evaluated beginning with $[Bu_4N]_5Na_3$(1,5-COD)Ir•$P_2W_{15}Nb_3O_{62}$ and 40 equiv *undried* PVP. The effects of water from the undried PVP (ca. 11 equiv H_2O with respect to the nanocluster precursor when 40 equiv PVP are present), entry 12 of Table 1, are evident in the kinetics of formation, the size distribution, and the catalytic activity of the nanoclusters in comparison to nanoclusters prepared in the absence of PVP, entry 10 of Table 1. The kinetics of nanocluster formation cannot be fit with the 2-step mechanism for autocatalytic nanocluster formation,[13] the data deviating from the normal sigmoidal curve, Figure 2a. The observed slowing of the observed cyclohexene hydrogenation catalysis is indicative of nanocluster agglomeration.[33] Indeed, TEM shows that the nanoclusters prepared with $P_2W_{15}Nb_3O_{62}^{9-}$ and wet PVP are somewhat larger with a wider size distribution (24 ± 7 Å for nanocluster stabilized by $P_2W_{15}Nb_3O_{62}^{9-}$ with undried PVP as shown in Figure S4 of the Supporting Information *vs.* 21 ± 3 Å for nanoclusters stabilized by $P_2W_{15}Nb_3O_{62}^{9-}$ alone). Moreover, the kinetics of formation in the presence of *undried* PVP are well-fit

by the 3-step mechanism for nanocluster nucleation, growth, *and agglomeration*,[33] Figure 2b.

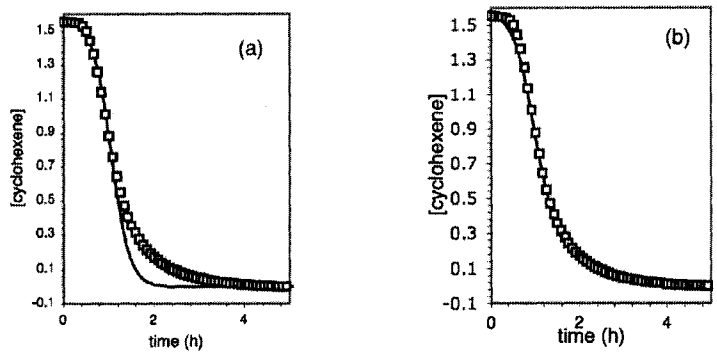

Figure 2. Kinetic curves for the hydrogenation of cyclohexene in propylene carbonate beginning with 1.2mM $[(Bu_4N)_5Na_3]Ir{\bullet}P_2W_{15}Nb_3O_{62}$ and 40 equivalents *undried* 10k PVP. Curve (a) shows that the kinetics are not well fit by the 2-step mechanism for nanocluster formation and growth, A→B, A+B→2B.[13] Nanocluster agglomeration is indicated by the tailing of the curve vs. its expected sigmoidal shape.[33] Curve (b) shows the fit to the 3-step agglomeration mechanism (Scheme 1) A→B, A+B→2B, *B+B→C* which includes the last, third step of bimolecular agglomeration B+B→C (MacKinetics numerical integration curve fitting; k_1=0.045(3) h^{-1}, k_2=4.2(1)x10^3 h^{-1} M^{-1}, k_3=1.30(5) h^{-1} M^{-1}).

Although the nanoclusters prepared in the presence of undried PVP are redissolvable in fresh propylene carbonate, the catalytic activity once redispersed is decreased by 5 fold in comparison to nanoclusters prepared in the presence of $P_2W_{15}Nb_3O_{62}^{9-}$ without added, wet PVP. Moreover, bulk metal is formed during the course of the TTO experiment when undried PVP is used. Clearly, it is important to begin with dried polymer: the effects of uncontrolled water on the formation and stabilization of nanoclusters is dramatic even with otherwise *highly* $P_2W_{15}Nb_3O_{62}^{9-}$*–stabilized* nanoclusters. It seems probable, therefore and based on our results, that two major effects of adding (undried) polymers to nanoclusters syntheses in organic solvents are (a) the undesired effects of H_2O, as well as (b) the slowing of catalytic activity.

Testing the Stabilizing Ability of Four Other Polymeric Protectants, PMMA, PS, PMHS, and PBEP, in the Presence of BF_4^-. Table 2 reports the 5 criteria for 40 equiv of the polymers PMMA,[23] PS,[24] PMHS,[25] and PBEP[26] with 1 equiv Proton Sponge™ so that BF_4^- is also present. A key difference of these studies and those discussed with PVP above is the *solvent* used is necessarily *acetone* (ε_R=20), since PS and PBEP are insoluble in propylene carbonate. Of these four polymers, only PMMA (predried) afforded a brown solution characteristic of $Ir(0)_n$ nanoclusters.[34] However, TEM images showed that these nanoclusters are agglomerated, Figure 3. The *in situ* nanoclusters are active for the hydrogenation of cyclohexene in the presence of dried PMMA, but bulk metal is formed during the course of the TTO experiment. Comparison of entries 1, 2, and 3 of Table 2 reveals that the stabilization provided by PVP and PMMA is similar, but both are inferior to nanoclusters stabilized by $P_2W_{15}Nb_3O_{62}^{9-}$.

Table 2. Evaluation of the 5 Criteria for PMMA, PS, PMHS, and PBEP in Acetone and with 1 equiv BF_4^- present.

	Precursor	Polymer	1 Equiv Added Proton Sponge™ ?	k_2/k_1[a] (M^{-1})	Size (Å)	Redissolve?	Cat. Act.[b]	TTO[c]
	With added $P_2W_{15}Nb_3O_{62}^{9-}$							
1	$[Bu_4N]_5Na_3(1,5\text{-COD})Ir{\bullet}P_2W_{15}Nb_3O_{62}$	none	yes	$4.4(5)\times10^5$	21 ± 4	yes	$3.1(2)\times10^6$	68,000
	With added polymer							
2	$[(1,5\text{-COD})Ir(CH_3CN)_2][BF_4]$	40 equiv dried 10k PVP	yes	$6.7(5)\times10^3$	agg.[d]	yes	$6.0(3)\times10^5$	[12,000]
3	$[(1,5\text{-COD})Ir(CH_3CN)_2][BF_4]$	40 equiv dried PMMA	yes	$2.9(1)\times10^4$	agg.[d]	yes	$6.9(3)\times10^5$	[21,700]
4	$[(1,5\text{-COD})Ir(CH_3CN)_2][BF_4]$	40 equiv undried PMMA	yes	$3.5(1)\times10^3$	agg.[d]	no	---	[20,900]
5	$[(1,5\text{-COD})Ir(CH_3CN)_2][BF_4]$	40 equiv undried PS	yes	$8.1(4)\times10^5$	---	no	---	---
6	$[(1,5\text{-COD})Ir(CH_3CN)_2][BF_4]$	40 equiv dried PS	yes	$3.9(1)\times10^3$	---	no	---	---
7	$[(1,5\text{-COD})Ir(CH_3CN)_2][BF_4]$	40 equiv PMHS	yes	---	---	no	---	---
8	$[(1,5\text{-COD})Ir(CH_3CN)_2][BF_4]$	40 equiv PBEP	yes	$6.2(2)\times10^{13}$	---	no	---	---

(a) The values for k_2/k_1 have been corrected by the mathematically required stoichiometry factor of 1400 as detailed elsewhere.[13] (b) mmol H_2/h•mol Ir (c) total turnovers of cyclohexene hydrogenation (mol product/mol catalyst); square brackets indicated that bulk metal was formed during the course of these experiments, so these values are necessarily an upper limit on the true nanoparticle TTOs. (d) agg=agglomerated nanoclusters.

The importance of trace water in nanocluster stabilization is again emphasized in the case of PMMA. Nanoclusters prepared in the presence of dried PMMA were isolable and redissolvable without the formation of bulk metal, while nanoclusters prepared in the presence of undried PMMA formed bulk metal during the isolation procedure, entry 4 Table 2. The hydrolysis of the ester group in PMMA in the presence of H_2O to form the corresponding carboxylic acid is another, known issue in the use of PMMA as a stabilizer.[23]

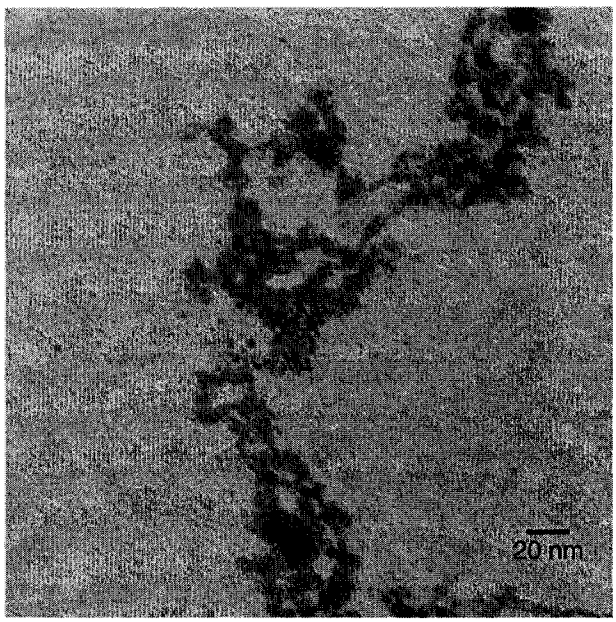

Figure 3. TEM image (580k magnification) of agglomerated $Ir(0)_n$ nanoclusters stabilized by 40 equiv dried PMMA plus the BF_4^- anion.

Neither PS nor PMHS are suitable protectants for the formation and stabilization of $Ir(0)_n$ nanoclusters. Reduction of the organometallic precursor in the presence of PS yielded a clear solution (i.e., few to no nanoclusters appear to be present) with bulk metal formation visible to the naked eye. In the presence of PMHS, reduction of the organometallic precursor did not occur; instead, a yellow solution slightly lighter than the

characteristic color of the precursor persisted under 40 psig H_2 for trials lasting >48 hours. Evidence that PMHS is reacting with the nanocluster precursor [(1,5-COD)Ir($CH_3CN)_2$][BF_4] was obtained by ^1H NMR spectroscopy: the complete disappearance of the signal for the vinylic protons of the COD ligand is observed on the addition of PMHS (see Figure S5 of the Supporting Information). In short, neither PS nor PMHS are preferred additives for the formation and stabilization of $Ir(0)_n$ nanoclusters. There is no compelling evidence that they are superior stabilizers for other transition-metal nanoclusters, either.[24,25]

The final polymer evaluated herein, PBEP, appears to exhibit extremely high kinetic control, with a k_2/k_1 ratio on the order of 10^{13} M^{-1}, see Figure 4, one of the highest *apparent* k_2/k_1 ratios we have ever observed. For PBEP, the k_2 rate constant is similar to those observed for nanoclusters prepared in the presence of $P_2W_{15}Nb_3O_{62}^{9-}$, on the order of 10^3 M^{-1} h^{-1}. *However*, the value of k_1 is extremely small, on the order of 10^{-11} h^{-1}, indicating that PBEP slows nucleation of the nanoclusters. Although the kinetic control on the nanocluster nucleation and growth is impressive for PBEP, the final reaction solution was clear with a bulk metal film on the side of the reaction vessel—that is, PBEP is a relatively poor stabilizer.

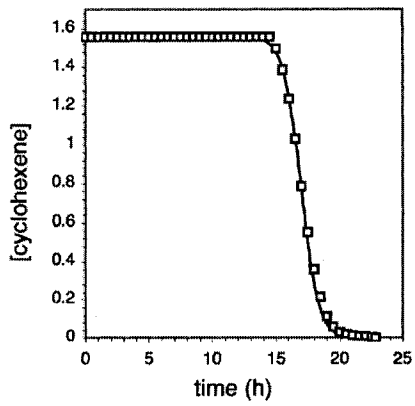

Figure 4. Kinetic curve for the hydrogenation of cyclohexene in acetone beginning with 1.2mM [(1,5-COD)Ir(CH_3CN)$_2$][BF_4] and 40 equivalents PBEP. This data (squares) is well fit by the 2-step mechanism for autocatalytic nanocluster formation (line). For clarity, only one out of every ten data points actually collected is shown.

To summarize, the studies of PMMA, PS, PMHS, and PBEP in acetone with 1 equiv BF_4^- present show that the stabilizing efficacy of 40 equiv PVP plus 1 equiv BF_4^- in propylene carbonate and 40 equiv PMMA plus 1 equiv BF_4^- in acetone are equal within experimental error as measured by the 5 criteria. PS, PMHS, and PBEP (each with 1 equiv BF_4^-) are not preferred stabilizers of at least $Ir(0)_n$ nanoclusters.

Conclusions

Herein, we have shown that:

(i) Using dried polymers is important for preparing transition-metal nanoclusters in (dry) organic solvents. When used as received, PVP contains H_2O that changes the nanocluster formation mechanism and decreases the stability of the resultant nanoclusters, even in the presence of the otherwise highly stabilizing anion $P_2W_{15}Nb_3O_{62}^{9-}$;

(ii) 1 equiv of BF_4^- plus the high dielectric constant, but not strongly coordinating, solvent propylene carbonate provides at least as much nanocluster formation and stabilization ability as does 1 equiv of dried PVP. It follows that previous claims of high nanocluster stability due to PVP are at least in part likely be due to the presence of co-stabilizing entities such as halides or even traditionally weakly coordinating anions such as BF_4^- and any high dielectric constant solvent present;[19]

(iii) The DLVO theory prediction[17,18] that anions in high dielectric constant solvents are one key for nanocluster stability is supported. The present work reveals that *even the traditionally weakly coordinating anion BF_4^- qualifies as a stabilizing anion in the high dielectric constant solvent propylene carbonate;*

(v) Adding 40 equivs of dried PVP plus having 1 equiv BF_4^- present is necessary to achieve isolable and redissolvable $Ir(0)_n$ nanoclusters;

(v) The chain length of the polymer does not appear to affect the *stability* of the system in the range of 3,500-55,000 g/mol;

(vi) The smaller, 3,500 MW_{ave} PVP polymer does, however, influence the nanocluster nucleation kinetics as does PBEP. Both low MW PVP and PBEP are hereby identified as interesting additives to study further as nanocluster nucleation modifiers with the implications of nanocluster size control that come from controlling the k_2/k_1 ratio;[32]

(viii) 40 equiv dried MW_{ave}=10,000 g/mol PVP plus 1 equiv BF_4^- is inferior for *both* nanocluster *formation and stabilization* when compared to then current "Gold Standard"[10] (poly)anion of 1 equiv $P_2W_{15}Nb_3O_{62}^{9-}$, at least for $Ir(0)_n$ nanoclusters;

(vii) 40 equiv dried PVP added to nanoclusters stabilized by 1 equiv $P_2W_{15}Nb_3O_{62}^{9-}$ have little effect except to *slow* the catalytic activity and total catalytic lifetime by ca. 50%;

(ix) Of the four other polymers studied herein, PMMA was the most similar to PVP in providing a modest level of stabilization as measured by the 5 criteria. The three other polymers studied, PS, PMHS, and PBEP, were all found to be ineffective additives for the formation and stabilization of catalytically active $Ir(0)_n$ nanoclusters;

(x) Adding Proton Sponge™ increases the stability of the system by allowing for the formation of BF_4^- rather than the conjugate acid $H^+BF_4^-$—hence, and as pointed out first elsewhere,[11] Proton Sponge™ or an equivalent, sterically bulky / non-coordinating base should be added to *all* nanocluster syntheses prepared by reduction of metal salts under H_2;

(xi) Evaluating Tables 1 and 2 shows that $P_2W_{15}Nb_3O_{62}^{9-}$ in propylene carbonate is superior to the five polymeric protectants evaluated herein for the formation, stabilization, and catalytic activity of prototype $Ir(0)_n$ nanoclusters. Again, the predictions of DLVO theory are fully supported, namely the importance of surface coordinated anions and the resultant Coulombic repulsion of nanoparticles in opposition to their van der Waals attractions;

(xii) Also important here is the cheaper, commercially available, tridentate, thermally robust, and ^{31}P NMR handle-containing substitute for $P_2W_{15}Nb_3O_{62}^{9-}$ that has been reported, namely HPO_4^{2-}.[11] Simple HPO_4^{2-} merits considerably greater use in transition-metal formation, stabilization and catalysis studies than presently reported;

(xiii) These studies show that the 5 criteria method for ranking nanocluster stabilizers can be employed with steric stabilizers as well as the previously studied electrostatic stabilizers, thereby furthering the utility of the 5 criteria method;[10]

(xiv) A hypothesis to emerge from these studies and which merits future study is that the investigation of low MW oligomers / polymers may well provide many of the benefits of traditional polymeric stabilizers, while also providing greater levels of kinetic control over nanocluster size (and possibly shape). Nanoclusters with simpler, better defined compositions would also result, an important goal of modern nanocluster science as discussed elsewhere.[1c]

Acknowledgements. Dr. Y. Kou is thanked for supplying poly[(*N*-vinyl-2-pyrrolidone)-co-(1-vinyl-3-butylimidazolium chloride)],[22] and Dr. M. Antonietti for supplying polystyrene-*b*-poly-4-vinylpyridine block copolymers.[20] Professor E. Y.-X. Chen at Colorado State University is thanked for his insightful comments in footnote 41. Financial support was provided by DOE grant DE-FG02-03ER15453.

Supporting Information Available: Figure S1, TGA of as-received MW_{ave}=10,000 g/mol PVP; Figure S2, Cyclohexene hydrogenation in the presence of MW_{ave}=3500 g/mol PVP; Figure S3, TEM of $Ir(0)_n$ nanoclusters formed under the conditions in entry 11 of Table 1; Figure S4, TEM of Ir(0) nanoclusters formed under the conditions in entry 12, Table 1; Figure S5, ^1H NMR spectroscopy of $[(1,5\text{-COD})Ir(CH_3CN)_2][BF_4]$ before and after the addition of 40 equiv PMHS.

References

[1] (a) Aiken, J. D. III, Finke, R. G. *J. Mol. Cat. A: Chem.* **1999**, *145*, 1. (b) Aiken III, J. D.; Lin, Y.; Finke, R. G. *J. Mol. Catal. A: Chem.* **1996**, *114*, 29-51. (c) Finke, R. G. in "Metal Nanoparticles: Synthesis, Characterization and Applications", Feldheim, D. L.; Foss Jr., C. A., Eds.; Marcel Dekker, Inc.: New York, 2002, Chapter 2, p. 17-54 ("Transition-Metal Nanoclusters: Solution-Phase Synthesis, then Characterization and Mechanism of Formation, of Polyoxoanion- and Tetrabutylammonium-Stabilized Nanoclusters").

[2] Reviews of nanoclusters (see also elsewhere[1]): (a) Astruc, D.; Lu, F.; Aranzes, J. R. *Angew Chem. Int. Ed.* **2005**, *44*, 7852. (b) Burda, C.; Chen, X.; Narayanan, R.; El-Sayed, M. A. *Chem. Rev.* **2005**, *105*, 1025. (c) Murphy, C. J.; Sau, T. K.; Gole, A. M.; Orendorff, C. J.; Gao, J.; Gou, L.; Hunyadi, S. E.; Li, T. *J. Phys. Chem. B* **2005**, *109*, 13857. (d) Green, M. *Chem. Commuun.* **2005**, *24*, 3002. (e) Narayanan, R.; El-Sayed, M. A. *J. Phys. Chem. B* **2005**, *109*, 12663. (f) Cushing, B. L.; Kolesnichenko, V. L.; O'Connor, C. J. *Chem. Rev.* **2004**, *104*, 3893. (g) Shenhar, R.; Rotello, V. M. *Acc. Chem. Res.* **2003**, *36*, 549. (h) Roucoux, A.; Schulz, J.; Patin, H. *Chem. Rev.* **2002**, *102*, 3757. (i) Králik, M.; Biffis, A. *J. Mol. Cat. A* **2001**, *177*, 113. (j) Rao, C. N. R.; Kulkarni, G. U.; Thomas, P. J.; Edwards, P. P. *Chem. Soc. Rev.* **2000**, *29*, 27. (k) Schmid, G.; Baumle, M.; Geerkens, M.; Heim, I.; Osemann, C.; Sawitowski, T. *Chem. Soc. Rev.* **1999**, *28*, 179. (l) Schmid, G.; Chi, L. F. *Adv. Mater.* **1998**, *10*, 515. (m) Fendler, J. H., Ed. *Nanoparticles and Nanostructured Films*; Wiley-VCH: Weinheim, 1998. (n) Fürstner, A., Ed. *Active Metals: Preparation, Characterization, and Applications*, VCH: Weinheim, 1996. (o) Bradley, J. S. in *Clusters and Colloids. From Theory to Applications*; Schmid, G., Ed.; VCH: New York, 1994; p. 459-544. (p) Schmid, G. *Chem. Rev.* **1992**, *92*, 1709. (q) A superb series of papers, complete with a record of the insightful comments by the experts attending the conference, is available in: *Faraday Discussions* **1991**, *92*, 1-300. (r) Schmid, G. in *Aspects of Homogeneous Catalysis*; Ugo, R., Ed.; Kluwer: Dordrecht, 1990; Chapter 1. (s) Andres, R. P.; Averback, R. S.; Brown, W. L.; Brus, L. E.; Goddard, W. A. III; Kaldor, A.; Louie S. G.; Moscovits, M.; Peercy, P. S.; Riley, S. J.; Siegel, R. W.; Spaepen, F.; Wang, Y.; *J. Mater. Res.* **1989**, *4*, 704. (t) Henglein, A. *Chem. Rev.* **1989**, *89*, 1861. (u) Thomas, J. M. *Pure Appl. Chem.* **1988**, *60*, 1517. (v) Jena, P.; Rao B. K.; Khanna, S. N; *Physics and Chemistry of Small Clusters*; Plenum: New York, 1987.

[3] Lead references to the extensive literature of PVP stabilization of colloids and nanoclusters are: (a) El-Sayed, M. A.; Narayanan, R. *J. Phys. Chem. B* **2004**, *108*, 8572-8580. (b) Huang, Y.; Chen, J.; Chen, H.; Li, R.; Li, Y.; Min, L.; Li, X. *J. Mol. Catal. A: Chemical* **2001**, *170*, 143. (c) Köhler, J. U.; Bradley, J. S. *Langmuir*, **2000**, *14*, 2730. (d) Shiraishi, Y.; Nakayama, M.; Takagi, E.; Tominaga, T.; Toshima, N. *Inorg. Chim. Acta.* **2000**, *300-302*, 964. (e) Li, Y.; Hong, X. M.; Collard, D. M.; El-Sayed, M. A. *Organic Letters* **2000**, *2*, 2385. (f) Hiria, H.; Yakura, N.; Seta, Y.; Hodoshima, S.; *Reactive and Functional Polymers* **1998**, *37*, 121. (g) Yu, W.-Y.; Liu, M.; Liu, H.; Zheng, J. *J. Colloid Interf. Sci.* **1999**, *210*, 218. (h) Yu, W.-Y.; Liu, H.; Liu, M.; Tao, Q. *J. Mol. Catal. A: Chemical* **1999**, *138*, 273. (i) Toshima, N.; Yonezawa, T. *New J. Chem.* **1998**, 1179-1201. (j) Hashimoto, T.; Saijo, K.; Harada,

M.; Toshima, N. *J. Chem. Phys.* **1998**, *109*, 5627. (k) Wan, B.-S. Liao, S.-J.; Xu, Y.; Yu, D.-R. *J. Mol. Catal. A: Chemical* **1998**, *136*, 263. (l) Yu, W.; Wang, Y.; Liu, H.; Zheng, W. *J. Mol. Catal. A: Chemical* **1996**, *112*, 105. (m) Yu, W.-Y.; Liu, H.-F.; Tao, Q. *Chem. Comm.* **1996**, 1773. (n) Pd/Cu, PVP-protected bimetallic nanoclusters: Bradley, J. S.; Hill, E. W.; Klein, C.; Chaudret, B.; Duteil, A. *Chem. Mater.* **1993**, *5*, 254. (o) Harada, M.; Asakura, K.; Ueki, Y.; Toshima, N. *J. Phys. Chem.* **1992**, *96*, 9730. (p) Toshima, N.; Harada, M.; Yonezawa, T.; Kushihashi, K.; Asakura, K. *J. Phys. Chem.* **1991**, *95*, 7448. (q) Toshima, N.; Kushihashi, K.; Yonezawa, T.; Kirai, H. *Chem. Let.* **1989**, 1769. (r) Hiria, H.; Chawanya, H.; Toshima, N. *Makromol. Chem., Rapid Comm.* **1981**, *2*, 99. (s) Kim, F.; Connor, S.; Song, H.; Kuykendall, T.; Yang, P. *Angew. Chem. Int. Ed.* **2004**, *43*, 3673. (t) Song, H.; Kim, F.; Connor, S.; Somorjai, G. A.; Yang, P. *J. Phys. Chem. B* **2005**, *109*, 188.

[4] For definitions of modern nanoclusters vs. classical colloids, including the distinctions between them, see reference 1c.

[5] Ott, L. S.; Finke, R. G. "Transition-Metal Nanocluster Stabilization: A Critical Review of Ranking Methods and Putative Stabilizers." *Coord. Chem. Rev.*, accepted pending revisions. (Part V in the series of nanocluster formation and stabilization fundamental studies.)

[6] Key earlier work on polymer stabilization of colloidal metal particles includes the following references as well as the references elsewhere[7]: Hess, P.H. Parker, P. H. Jr. *J. Appl. Poly. Sci.* **1966**, *10*, 1915. In this classic paper, Hess and co-workers test 41 polymers for their ability to allow decent size dispersion, and then to stabilize, Co colloids formed from $Co_2(CO)_8$ thermolysis (probably Co_xO_y colloids, since the studies were done in O_2) with interesting magnetic properties. They also test solvent polarity effects, and conclude for the maximum effect of the polymer, the solvent should be "less polar than the most polar group in the polymer." The authors did find that polymers (plus other anions such as OH^- that are very likely present) afford nanoparticle stabilization, although their criteria for nanocluster formation are neither as extensive nor as quantitative as those we have developed; also, the resultant materials are compositionally ill-defined "$Co_aC_bO_cOH_d(polymer)_e^{n+/-}$" colloids and not modern nanoclusters[1] with well-established stoichiometries.

[7] (a) Historically, the "gold number"[7b] or "protective value"[7c] were used as rough estimates of the ability of a given agent to stabilize an aqueous gold colloid against aggregation or flocculation by a NaCl solution. Note that both these classical tests are only for Au colloids, and then only in aqueous solution. (b) The "gold number" is defined as the weight in mgs of the protecting agent which is just insufficient to prevent 10 ml of a red sol from changing to violet upon the addition of 1 ml of a 10% aqueous NaCl solution: Zsigmondy, R. Z.; *Anal. Chem.* **1901**, *40*, 697. (c) The "protective value" is defined as the number of grams of a red sol that is just protected against (visual) flocculation by 1% NaCl by 1 gm of the protective agent for ~ 3 min: Thiele, H.; Van Levern, H. S. *J. Coll. Sci.* **1965**, *20*, 679. Even this more recent test suffers from problems with the compositionally ill-defined, somewhat irreproducible, large (ca. 250 Å), aqueous Au colloids it employs—materials rather different than compositionally well defined, reproducible, smaller and organic-solvent soluble modern nanoclusters studied herein.[1]

[8] Ott, L. S. Finke, R. G. "Nanocluster Formation, Stabilization, and Agglomeration Fundamental Studies: Can the Catalytic Reporter Reaction Method be Used As A Quantitative, Kinetic, Agglomeration-Based Way to Assay Transition-Metal Nanocluster/Nanocolloid Stabilizers?" *J. Coll. Int. Sci.*, Manuscript in preparation.

[9] Meakin, P. *Adv. Coll. Int. Sci.* **1988**, *28*, 249.

[10] Özkar, S.; Finke, R. G. *J. Am. Chem. Soc.* **2002**, *124*, 5796-5810.

[11] Özkar, S.; Finke, R. G. *Langmuir* **2002**, *18*, 7653.

[12] Lin, Y.; Finke, R. G. *J. Am. Chem. Soc.* **1994**, *116*, 8335.

[13] Watzky, M. A.; Finke, R. G. *J. Am. Chem. Soc.* **1997**, *119*, 10382.

[14] Özkar, S.; Finke, R. G. *Langmuir* **2003**, *19*, 6247.

[15] For control experiments with the strongly stabilizing $P_2W_{15}Nb_3O_{62}^{9-}$ anion[10,11] the supported Ir precursor $[Bu_4N]_5Na_3(1,5\text{-COD})Ir{\bullet}P_2W_{15}Nb_3O_{62}$ was used for the Ir source. See reference 10 and references therein.

[16] Widegren, J. A.; Aiken, J. D., III; Özkar, S.; Finke, R. G. *Chem. Mater.* **2001**, *13*, 312.

[17] Verwey, E. J. W.; Overbeek, J. T. G. *Theory of the Stability of Lyophobic Colloids*; 2 ed.; Dover Publications, Inc.: Mineola, New York, 1999.

[18] Evans, D. F.; Wennerström, H. *The Colloidal Domain*, 2nd ed.; Wiley-VCH: New York, 1999.

[19] Ott, L. S.; Finke, R. G. "Nanocluster Formation and Stabilization Fundamental Studies:[a] Investigating "Solvent-Only" Stabilization En Route to Discovering Stabilization by the Traditionally Weakly Coordinating Anion BF_4^- Plus High Dielectric Constant Solvents." *Inorg. Chem.*, submitted (Part VII in the series of nanocluster formation and stabilization fundamental studies.)

[20] We also attempted to study polystyrene-*b*-poly-4-vinylpyridine block copolymers (generously supplied by Dr. M. Antonietti) as well as commercial poly(propylene imine) and poly(amidoamine) dendrimers as part of this study. However, these three protectants are all insoluble in both acetone and propylene carbonate and, hence, could not be examined as part of this work.

[21] (a) Reetz, M. T.; Lohmer, G. *Chem. Commun.* **1996**, *16*, 1921. (b) Widegren, J. A.; Finke, R. G. *Inorg. Chem.* **2002**, *41*, 1558. (c) Hornstein, B. J.; Finke, R. G. *Chem. Mater.* **2003**, *15*, 899.

[22] We also attempted to study the novel ionic copolymer poly[(*N*-vinyl-2-pyrrolidone)-co-(1-vinyl-3-alkylimidazolium chloride)], but it was insoluble in acetone. In propylene carbonate, 40 equiv of the polymer became soluble after 12 hours in a solution that also contained 3.6 μmol $[(1,5\text{-COD})Ir(CH_3CN)_2][BF_2]$ and 1 equiv Proton Sponge™; no hydrogen uptake was observed after 20 hours in an attempted hydrogenation reaction. The ionic copolymer preparation appears in Mu, X.-d.; Meng, J.-q.; Li, Z.-C.; Kou, Y. *J. Am. Chem. Soc.* **2005**, *127*, 9694.

[23] King, S.; Hyunh, K.; Tannenbaum, R. *J. Phys. Chem. B* **2003**, *107*, 12097.

[24] Tadd, E.; Zeno, A.; Zubris, M.; Dan, R.; Tannenbaum, R. *Macromolecules* **2003**, *36*, 6497.

[25] Chauhan, B. P. S.; Rathore, J. S.; Chauhan, M.; Krawicz, A. *J. Am. Chem. Soc.* **2003**, *125*, 2876.

[26] Supported Ru nanoparticles were recently prepared with polyorganophosphazenes: Spitaleri, A.; Pertici, P.; Scalera, N.; Vitulli. G.; Hoang, M.; Turney, T. W.; Gleria, M. *Inorg. Chem. Acta.* **2003**, *352*, 61.

[27] Duff, D. G.; Edwards, P. P.; Johnson, F. G. *J. Phys. Chem.* **1995**, *99*, 15934-15944.

[28] Özkar, S.; Finke, R. G. *Coord. Chem. Rev.* **2004**, *248*, 135.

[29] Day, V. W.; Klemperer, W. G.; Main, D. J. *Inorg. Chem.* **1990**, *29*, 2345.

[30] Hornstein, B. J., Finke, R. G. *Inorg. Chem.* **2002**, *41*, 2720.

[31] Pohl, M.; Lyon, D. K.; Mizuno, N.; Nomiya, K.; Finke. R. G. *Inorg. Chem.* **1995**, *34*, 1413.

[32] Watzky, M. A.; Finke, R.G. *Chem. Mater.* **1997**, *9*, 3083.

[33] Hornstein, B. J.; Finke, R. G. *Chem. Mater.* **2004**, *16*, 139.

[34] Creighton, J. A.; Eadon, D. G. *J. Chem. Soc., Faraday Trans.* **1991**, *87*, 3881.

[35] Wilkins, R. G. *Kinetics and Mechanism of Reactions of Transition Metal Complexes*, 2nd ed; VCH: New York, 1991; p. 4.

[36] The pK_a of HBF_4 in this solvent is calculated as -0.01 from the following equation: $pK_a = (180.59/\varepsilon)-2.74$ according to Sudakova, T. N.; Krasnoshchekov, V. V. *Zhurnal Neorganicheskoi Khimii* **1978**, *23*, 1506-1508.

[37] Besson, C.; Finney, E. E.; Finke, R. G. *J. Am. Chem. Soc.* **2005**, *127*, 8179.

[38] Parks, E. K.; Nieman, G. C.; Kerns, K. P.; Riley, S. J. *J. Chem. Phys.* **1998**, *108*, 3731.

[39] (a) Ma, H.; Yin, B.; Wang, S.; Jiao, Y.; Pan, W.; Huang, S.; Chen, S.; Meng, F. *ChemPhysChem.* **2004**, *5*, 68-75. (b) Uemura, T.; Ohba, M.; Kitagawa, S. *Inorg. Chem.* **2004**, *43*, 7339-7345. (c) Chou, K.-S.; Lai, Y.-S. *Mater. Chem. Phys.* **2004**, *83*, 82-88. (d) Shin, H. S.; Yang, H. J.; Kim, S. B.; Lee, M. S. *J. Colloid Interface Sci.* **2004**, *274*, 89-94. (e) Narayanan, R.; El-Sayed, M. *J. Am. Chem. Soc.* **2003**, *125*, 8340-8347. (f) Tan, Y.; Dai, X.; Li, Y.; Zhu, D. *J. Mater. Chem.* **2003**, *13*, 1069-1075. (g) Kapoor, S.; Mukherjee, T. *Chem. Phys. Lett.* **2003**, *370*, 83-87. (h) Choo, H. P.; Liew, K. Y.; Liu, H. *J. Mater. Chem.* **2002**, *12*, 934-937. (i) Zhang, Z.; Zhao, B.; Hu, L. *J. Colloid Solid State Chem.* **1996**, *121*, 105-110.

[40] (a) Narayanan, R.; El-Sayed, M. A. *Langmuir* **2005**, *21*, 2027-2033. (b) Junior, A. M.; de Oliveira, H. P. M.; Gehlen, M. H. *Photochem. Photobiol, Sci.*, **2003**, *2*, 921-25. (c) Pastoriza-Santos, I.; Liz-Marzán, L. M. *Langmuir* **2002**, *18*, 2888-2894. (d) Teranishi, T.; Hosoe, M.; Tanaka, T.; Miyake, M. *J. Phys. Chem. B* **1999**, *103*, 3818-3827. (e) Hoogsteen, W.; Fokkink, L. G. J. *J. Colloid Interface Sci.* **1995**, *175*, 12-26.

[41] The caveat here, one pointed out by our polymer chemistry colleague Prof. Eugene Chen, is that there are likely broad distributions for each of the three average MW PVP polymers used, so that until narrower distributions are studied, it is impossible to know for sure if a small MW component is really promoting the nucleation step. Additional studies are in progress.

[42] Hornstein, B. H.; Aiken, J. D., III; Finke, R. G. *Inorg. Chem.* **2002**, *41*, 1625-1638.

[43] Li, Y.; Boone, E.; El-Sayed, M. A. *Langmuir* **2002**, *18*, 4921-49.

SUPPORTING INFORMATION

A Test of the Transition-Metal Nanocluster Formation and Stabilization Ability of the Most Common Polymeric Stabilizer, Poly(vinylpyrrolidone), As Well As Four Other Polymeric Protectants

Lisa Starkey Ott, Brooks J. Hornstein, and Richard G. Finke*

Department of Chemistry, Colorado State University, Ft. Collins, CO 80523

Nanocluster Preparation from $[(1,5\text{-COD})Ir(CH_3CN)_2][BF_4]$ With and Without Added PVP at Higher Concentrations. As noted in the main text, these experiments were carried out at higher concentrations (3.5 mM instead of the 1.2 mM concentration used for the reactions run with $[Bu_4N]_5Na_3(1,5\text{-COD})Ir{\bullet}P_2W_{15}Nb_3O_{62}$), to avoid signficant weighing and balance errors. In order to be sure that the 5 criteria were within error for both concentrations (and therefore the 3.5 mM dataset would be comparable to the 1.2 mM data for reactions with the $[Bu_4N]_5Na_3(1,5\text{-COD})Ir{\bullet}P_2W_{15}Nb_3O_{62}$ precursor), the 5 criteria were evaluated for with 40 equivalents of dried MW_{ave}=10,000 g/mol PVP at both 1.2 mM and 3.5 mM.

Table S1. Compilation of the data for 1.2 and 3.5 mM.

Precursor	Polymer	Conc. (mM)	k_2/k_1[a]	Size (Å)	Redisp ?	Catalytic Activity[b]	TTO[c]
$[(1,5\text{-COD})Ir(CH_3CN)_2][BF_4]$	dried, 10k	1.2	$6.7(5)\times10^3$	agg.	yes	$6.0(3)\times10^5$	[12,000]
$[(1,5\text{-COD})Ir(CH_3CN)_2][BF_4]$	dried, 10k	3.5	$8.6(4)\times10^3$	agg.	yes	$6.2(3)\times10^5$	[13,000]

(a) The k_2 values are corrected by the mathematically required stoichiometry factor of 1400 as detailed elsewhere.[1] (b) mmol h^{-1} mol Ir^{-1}. (c) Due to the formation of bulk metal, the values in [ ] brackets are upper limits to the true nanoparticle TTOs.

As shown in Table S1, the two concentrations are within error of each other with regard to nanocluster formation and stabilization as measured by the 5 criteria. Consequently, an accurate comparison may be made between the $[Bu_4N]_5Na_3(1,5\text{-COD})Ir{\bullet}P_2W_{15}Nb_3O_{62}$ systems with initial concentrations of 1.2 mM and the $[(1,5\text{-COD})Ir(CH_3CN)_2][BF_4]$ plus PVP systems with initial concentrations of 3.5 mM.

[1] Watzky, M. A.; Finke, R. G. *J. Am. Chem. Soc.* **1997**, *119*, 10382.

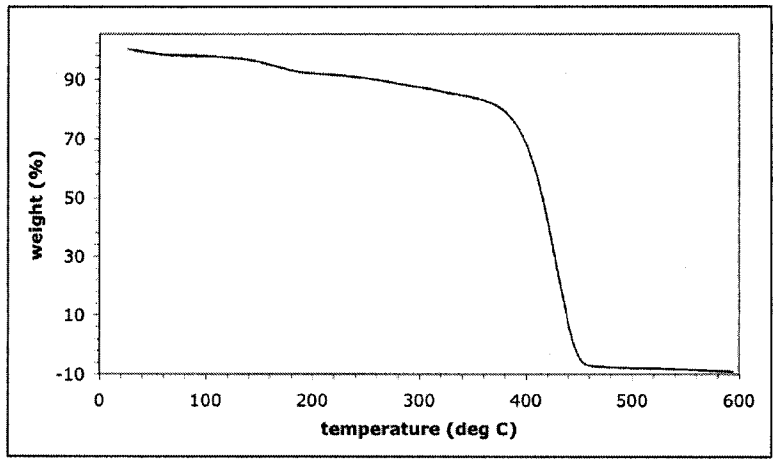

Figure S1. Thermal gravimetric analysis (TGA) of as-received MW_{ave}=10,000 g/mol PVP. A 2.2% weight loss is observed at 100 °C, corresponding to 0.14 mol H_2O per mol PVP. This, in turn, corresponds to 11 equivalents H_2O per Ir atom when 40 eqv of MW_{ave}=10,000 g/mol PVP per eqv Ir is used. This and the evidence in the main text shows that commercially obtained PVP should be dried before use in nanocluster syntheses.

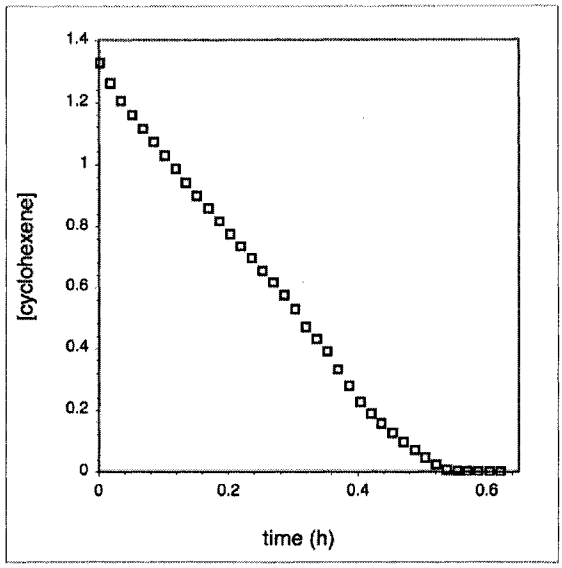

Figure S2. Kinetic curve for hydrogenation of cyclohexene in propylene carbonate by $[(1,5\text{-COD})Ir(CH_3CN)_2][BF_4]$ in the presence of 40 equivalents of dried MW_{ave}=3,500 g/mol PVP. This curve cannot be fit to the established autocatalytic nanocluster formation mechanism, A→B, then A+B→2B. A significant, nucleation-rate-increasing effect appears to be present as indicated by the loss of the induction period (i.e., the apparent increase in k_1.

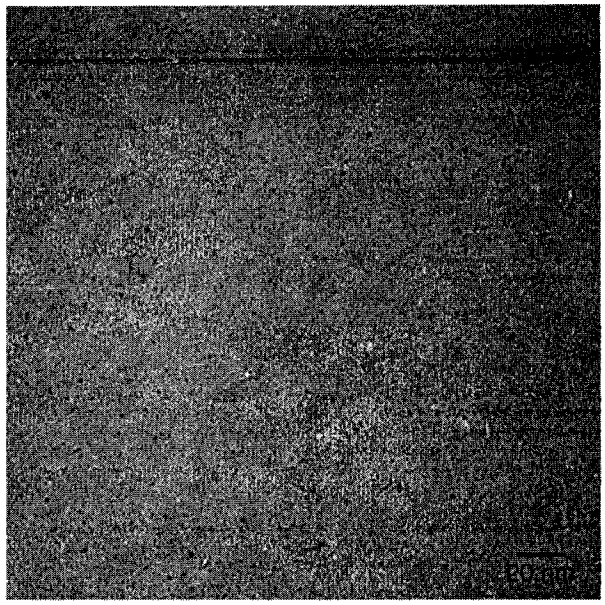

Figure S3. TEM of Ir(0) nanoclusters formed under the conditions in entry 9 of Table 1. $[Bu_4N]_5Na_3(1,5\text{-COD})Ir{\bullet}P_2W_{15}Nb_3O_{62}$ under 40 psig H_2 in the presence of dried 10,000 g/mol PVP. These nanoclusters are well separated and show a near-monodisperse size distribution of ±14%.

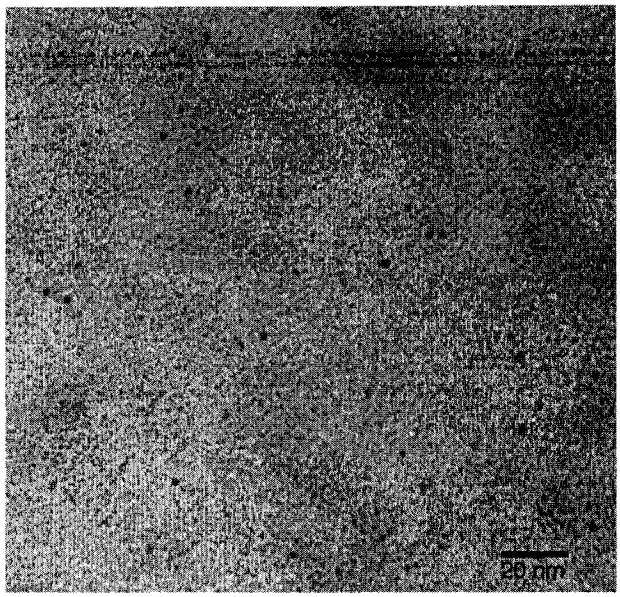

Figure S4. TEM of Ir(0) nanoclusters formed under the conditions in entry 10 of Table 1, namely $[Bu_4N]_5Na_3(1,5\text{-COD})Ir{\bullet}P_2W_{15}Nb_3O_{62}$ under 40 psig H_2 in the presence of undried 10,000 g/mol PVP. The nanoclusters display a larger, ± 29% size distribution.

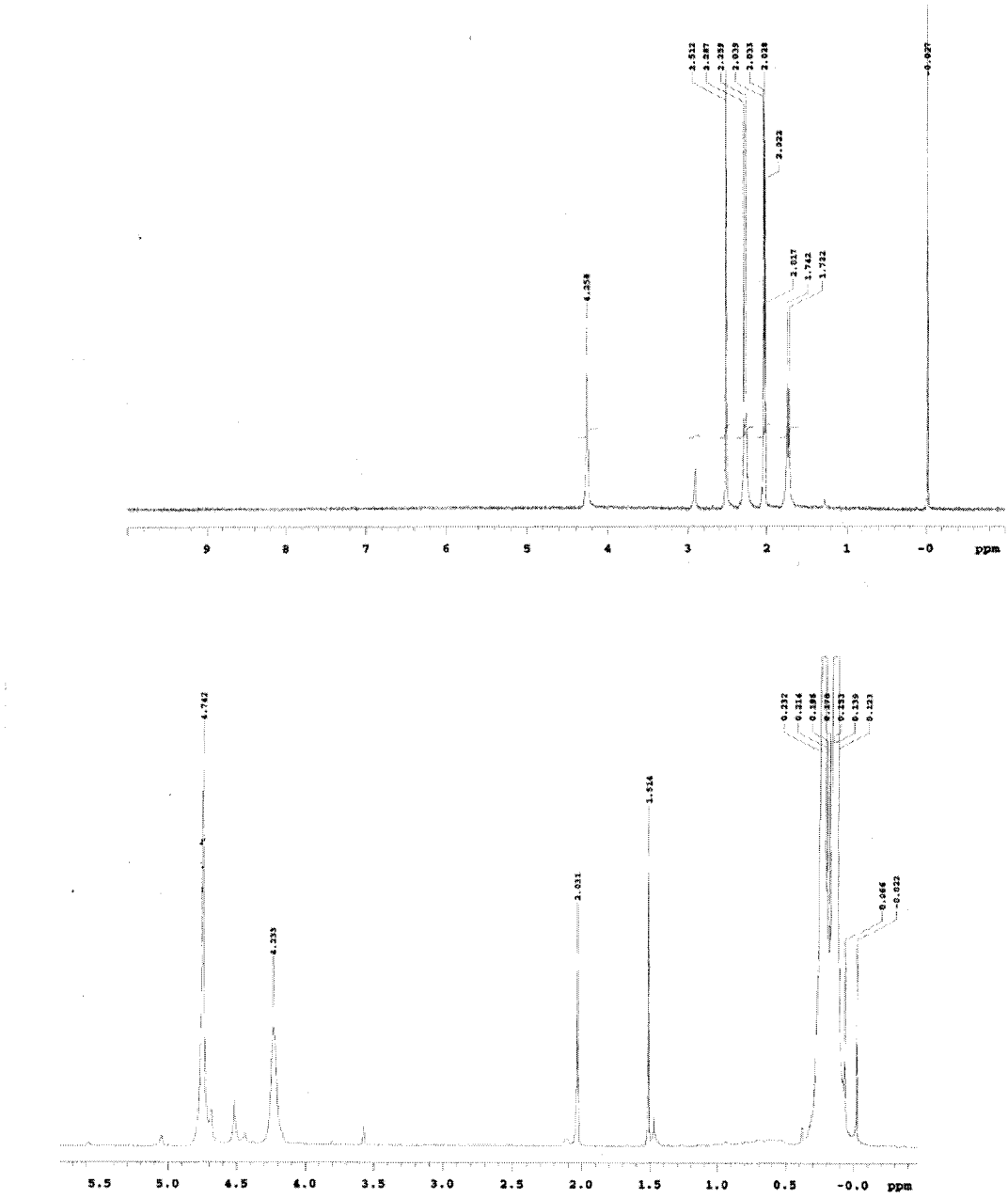

Figure S5. ^{1}H NMR spectra of $[(1,5\text{-COD})Ir(CH_3CN)_2][BF_4]$ before (top) and after (bottom) the addition of 40 equivalents of undried PMHS. Among other changes, the vinylic protons present at δ=2.5 in the top spectrum are not present in the bottom spectrum. This indicates a reaction between $[(1,5\text{-COD})Ir(CH_3CN)_2][BF_4]$ and the 40 equivalents of undried PMHS.

CHAPTER V

NANOCLUSTER FORMATION AND STABILIZATION FUNDAMENTAL STUDIES: RANKING THE NANOCLUSTER STABILIZING ABILITY OF HALIDES

This dissertation chapter contains the manuscript of an article submitted to *Journal of Nanoscience and Nanotechnology*; this chapter tests transition-metal nanocluster formation and stabilization efficacy of the halide series (F^-, Cl^-, Br^-, I^-) for prototype $Ir(0)_n$ nanoclusters. These studies (i) assess the contribution to stability by each individual halide in a prototype nanocluster synthesis (and in the presence of BF_4^-), (ii) compare the stabilizing abilities of each of the four halides to one another and to BF_4^-, and (iii) add the stabilizing abilities of all halides to the previously established anion stabilization series for prototype $Ir(0)_n$ nanoclusters.

The initial survey experiments in this chapter were performed by Morgan Cline (MLC), an undergraduate student working under the direction of LSO. The remaining experiments in this chapter were performed by LSO. The manuscript was prepared by LSO with assistance and editing by RGF.

Abstract.

Following a brief introduction to the nanocluster stabilization literature and DLVO (Derjaugin-Landau-Verwey-Overbeek) theory of colloidal stability, F^-, Cl^-, Br^-, and I^- are evaluated for their efficacy in the formation and stabilization of prototype $Ir(0)_n$ nanoclusters prepared from a $[(1,5\text{-COD})Ir(CH_3CN)_2][BF_4]$ precursor in both acetone and propylene carbonate solvent. First, under conditions utilized previously for establishing an anion stabilization series ("Standard Conditions"; 1.2 mM Ir precursor concentration at 22 °C in acetone solvent), the 5 criteria developed in 2002 for ranking nanocluster stabilizers are evaluated for each halide (each with 1 equiv BF_4^- present from the Ir precursor). Under Standard Conditions, bulk metal is the final product (i.e., no stable nanoclusters) in the presence of each of the four halides, as well as for BF_4^- in the absence of any halide. Next, each halide, again in the presence of 1 equiv BF_4^-, is evaluated under "Improved Conditions" (0.24 mM Ir precursor concentration at 60 °C in propylene carbonate solvent), propylene carbonate being known to be a preferred nanocluster solvent in the presence of anionic (electrostatic) stabilizers. Nanocluster syntheses under the Improved Conditions did, as expected, yield $Ir(0)_n$ nanoclusters for each of the four halide plus BF_4^- systems as well as BF_4^- alone, although none of these nanoclusters are isolable from solution. Importantly, even the traditionally weakly coordinating BF_4^- is shown to contribute significantly to nanocluster stability in the high dielectric constant solvent propylene carbonate. Hence, the importance of anions in conjunction with a high dielectric constant solvent for nanocluster formation and stabilization is illustrated.

Introduction.

Nanocluster chemistry is of enormous current interest[1,2,3,4,5,6,7] for applications as wide and varied as quantum dots,[8] chemical sensors,[9] components in industrial lithography,[10] and catalysis.[11] In the literature, a myriad of anions,[12,13,14] solvents,[15,16,17] polymers,[18,19,20] dendrimers,[21,22,23] siloxanes,[24] and other entities (including, as a few more examples, reverse micelles,[25] ionic liquids,[26,27,28] and resorcinarene molecules[29,30]) are all often explicitly or implicitly claimed to be superior stabilizers of nanoclusters, but typically never tested in any rigorous way. It is not surprising, then, that the myriad of stabilizing additives reported in the literature was recently referred to as a "dizzying variety."[5] Due to the lack of a precise, much less operational, definition for nanocluster stability, in most cases it is not possible to distinguish which among this "dizzying variety"[5] is the best nanocluster stabilizer—or even a useful stabilizer in solution. A survey of the literature reveals that stability is often claimed based on a (ex situ, solid state) transmission electron microscopy (TEM) image alone, and stability is claimed even if the nanoclusters appear agglomerated by TEM.

Developed in the 1940s, the DLVO (Derjaugin-Landau-Verwey-Overbeek) theory of colloidal stability[31] remains the most important and accurate predictor of colloidal/nanocluster solution stability.[32] A central concept behind DLVO theory is that nanocluster stabilization is achieved through a delicate balance of interparticle Columbic repulsion opposing van der Waals attraction. Hence, DLVO theory predicts that *anions* adsorbed on the coordinatively unsaturated, electrophilic nanocluster surface are a key to stability, providing the Coloumbic repulsion component (accordingly, DLVO-type stabilization is also commonly referred to as "electrostatic" stabilization).[7] In addition,

anions are a component of the diffuse layer of ions surrounding nanoclusters. This diffuse layer is known as the Debye layer (denoted by $1/\kappa$; values are typically in nm) and is a function of several variables, as Equation 1 below shows (ε_0 is the permittivity of free space, ε_R is the dielectric constant of the medium (the solvent), k is the Boltzman constant, T is the temperature, z_i is the ion valency, e is the charge on an electron, and c_{i0} is the concentration of the ion species, *i*, in the bulk solution[33]).

$$1/\kappa = ((\varepsilon_0 \times \varepsilon_R \times k \times T) / \sum_i (z_i e)^2 \times c_{i_0}))^{0.5} \quad (1)$$

Despite this predicted importance of anions as part of DLVO-type stabilization,[34,35] the stabilizing effects of halides, the most common anions present when nanoclusters are prepared by the reduction of metal salts, have not previously been ranked among themselves, or versus other anionic stabilizers, for their nanocluster formation and stabilization ability. Additionally, *the effect of halides derived from the nanocluster precursor on the stability of resultant nanocluster is frequently ignored.*[36,37] Hence, it is important to rank all four halides as nanocluster stabilizers.

A relatively new, general method for ranking putative nanocluster stabilizers (such as halides) was developed in 2002,[12] employing 5 criteria to rank the formation and stabilization efficacy of a given additive. The 5 criteria are: (i) the level of kinetic control during the nanocluster formation reaction as measured by the k_2/k_1 ratio of autocatalytic surface-growth (k_2) to nucleation (k_1)—larger values indicating a high level of kinetic control;[12,38] (ii) the nanoclusters' size distribution as determined by TEM ($\leq \pm 15\%$ having been defined elsewhere as "near-monodisperse"[3] nanoclusters); (iii) the ability to isolate from solution and ideally bottle the nanoclusters for future use without agglomeration to

bulk metal; (iv) the catalytic activity of the isolated nanoclusters once redissolved in solution with fresh cyclohexene substrate; and (v) the total turnovers (TTOs) for cyclohexene hydrogenation observed for the in situ generated nanoclusters in solution.[39] The single most important and stringent test of claimed nanocluster stabilizers is criteria (iii), namely, can the nanoclusters be isolated and subsequently redissolved without the formation of bulk metal? The 5 criteria method improves upon past *qualitative* literature methods for ranking Au colloidal stabilizers in water,[40,41] and at present is the only method for ranking modern transition-metal nanocluster stabilizers in organic solvents.

Using this 5 criteria method, the first "anion stabilization series"—really a *formation and stabilization* series—for prototype $Ir(0)_n$ nanocluster stabilizers was constructed,[12] allowing the rational choice of transition-metal nanocluster stabilizing anions for the first time, at least for Ir nanoclusters (and probably other metal nanoclusters such as those of Rh, Pt, Au, and Cu).[42] The current anion stabilization series (with Bu_4N^+ countercations) for prototype $Ir(0)_n$ nanoclusters in acetone solvent is: $P_2W_{15}Nb_3O_{62}^{9-} \sim [(P_2W_{15}Nb_3O_{61})_2O]^{16-} \sim ([P_2W_{15}(TiOH)_3O_{\sim 59}]^{9-})_n$ (n = 1, 2) ~ $SiW_9Nb_3O_{40}^{7-} > HPO_4^{2-} \sim C_6H_5O_7^{3-} > > [\text{-}CH_2CH(CO_2^-)\text{-}]_n^{n-} \sim OAc^- \sim P_3O_9^{3-} \sim OH^- \sim Cl^-$.[12,13] Additionally, application of the 5 criteria method has afforded several important insights, including: (a) the value of added Proton Sponge™ as one preferred scavenger for the H^+ generated during the nanocluster syntheses under H_2;[13] (b) the discovery of HPO_4^{2-} as a simple, effective, readily available, robust, and previously unappreciated nanocluster stabilizer;[43] (c) molecular insights for how preferred tridentate oxoanions are hypothesized to bind to and stabilize transition-metal nanoclusters;[42] (d) evidence for contributions to nanocluster stability by the traditionally weakly coordinating anion BF_4^-

in high dielectric constant (ε) solvents;[44] and (e) evidence that BF_4^- is a significant component of the observed nanocluster stabilization even in the presence of the common steric stabilizer poly(vinylpyrrolidone) (PVP).[45]

Herein, we examine the full halide series, F^-, Cl^-, Br^-, and I^-, for their individual roles in the formation and stabilization of prototype $Ir(0)_n$ nanoclusters. The nanoclusters were prepared from the known precursor $[(1,5\text{-COD})Ir(CH_3CN)_2][BF_4]$ with the Bu_4N^+ salts of F^-, Cl^-, Br^-, and I^-. Controls were performed without any added halides (i.e., with only the traditionally weakly coordinating anion[46] BF_4^- present from the organometallic precursor) and versus the added "Gold Standard"[12] stabilizing anion $P_2W_{15}Nb_3O_{62}^{9-}$ as reference points. Overall, we find (i) that the lower temperature, higher concentration "Standard Conditions" of 22 °C and 1.2 mM Ir precursor in acetone solvent yield only bulk metal (i.e., no stable nanoclusters) for all four halide plus BF_4^- systems and for BF_4^- alone, but (ii) that application of the "Improved Conditions"[47,48] of 60 °C, 0.24 mM Ir precursor, and the higher dielectric constant solvent propylene carbonate, do yield $Ir(0)_n$ nanoclusters with halide plus BF_4^- stabilizers or BF_4^- alone (see Table 1 for a summary of the two sets of synthetic conditions). Even those nanoclusters are only meta-stable, however, and are not isolable and redispersable in solution without the formation of bulk metal. Control / reference point experiments show that added $P_2W_{15}Nb_3O_{62}^{9-}$ permits superior $Ir(0)_n$ nanocluster formation and stabilization under Standard Conditions but, surprisingly, is *detrimental* under the Improved Conditions, for reasons that are discussed and are instructive regarding the subtleties of nanocluster formation and subsequent stabilization.

Table 1. A summary of the two sets of nanocluster synthesis conditions employed herein.

	Ir concentration	Temperature	Sovlent
Standard Conditions	1.2 mM	22 °C	acetone
Improved Conditions	0.24 mM	60 °C	propylene carbonate

Results and Discussion

Standard Conditions Nanocluster Syntheses in Acetone.

To start, the Standard Conditions were applied to the full halide series, $X=F^-$, Cl^-, Br^-, and I^-, so that each halide could then be accurately compared to the eleven anions studied previously.[43] Hence, we initially evaluated the four halides under the conditions of 1.2 mM $[(1,5\text{-COD})Ir(CH_3CN)_2][BF_4]$ and $[Bu_4N][X]$ in acetone solvent in the presence of Proton Sponge™ (PS™; added as a scavenger for the H^+ produced in nanocluster syntheses under H_2),[13] Scheme 1. The nanocluster formation reaction is monitored by the cyclohexene hydrogenation reporter reaction method, which has been described in detail.[38]

Scheme 1. A generalized nanocluster formation reaction with 1.2 mM Ir precursor in acetone in the presence of added anions, $[Bu_4N]_xY$.

Nanocluster Formation Reaction

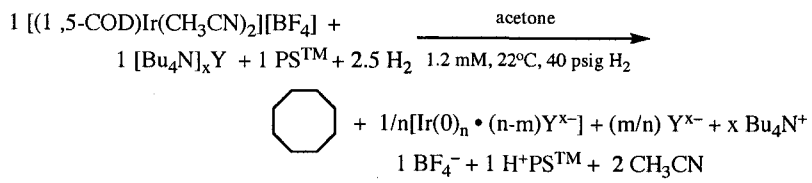

Cyclohexene Reporter Reaction

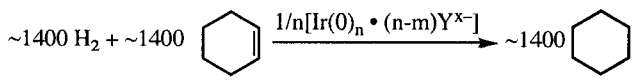

Reference Point of BF_4^- Alone Under the Standard Conditions in Acetone. A control experiment was performed to assess the contribution to stability by the

traditionally weakly coordinating anion BF_4^- derived from the nanocluster precursor in the low dielectric constant solvent acetone (ε=20), entry 1 in Table 2. Examination of the 5 criteria reveals that the BF_4^- anion alone in acetone *yields a bulk metal product and a clear and colorless solution* (i.e., no stable nanoclusters). However, a brown solution characteristic of $Ir(0)_n$ nanoclusters[49] is observed during the course of the nanocluster formation/cyclohexene hydrogenation reaction; hence, we presume that nanoclusters are intermediates en route to the bulk metal product. The key result from this experiment is that BF_4^- alone is not sufficient to allow for well-stabilized nanoclusters under Standard Conditions.

Table 2. The 5 Criteria for BF_4^-, F^-, Cl^-, Br^-, I^- and $P_2W_{15}Nb_3O_{62}^{9-}$ Under the Standard Conditions of 1.2 mM [(1,5-COD)Ir($CH_3CN)_2$][BF_4] in acetone solvent at 22 °C. Entries 1 and 6 are control experiments testing the effects of (entry 1) the traditionally weakly coordinating BF_4 and (entry 6) the current "Gold Standard" stabilizing anion $P_2W_{15}Nb_3O_{62}^{9-}$.

	Anion (with Bu_4N^+ countercation)	Solvent	Ir Conc. (mM)	k_2/k_1 (M^{-1})[a]	TEM (Å)	Appearance?	Redisp?	Rate[c]	TTOs[d]
1	BF_4^-	acetone	1.2	$2.4(2)\times10^5$	---	bulk metal	no	---	---
2	F^- plus BF_4^-	acetone	1.2	$4.4(2)\times10^3$	---	bulk metal	no	---	---
3	Cl^- plus BF_4^-	acetone	1.2	$1.9(1)\times10^4$	---	bulk metal	no	---	---
4	Br^- plus BF_4^-	acetone	1.2	$5.4(3)\times10^4$	---	bulk metal	no	---	---
5	I^- plus BF_4^-	acetone	1.2	$7.0(5)\times10^4$	---	bulk metal	no	---	---
6	$P_2W_{15}Nb_3O_{62}^{9-}$	acetone	1.2	$1.9(1)\times10^5$	22(3)	clear, blue[b]	yes	$2.6(3)\times10^6$	40,000

(a) The values for k_2/k_1 have been corrected by the mathematically required stoichiometry factor of 1400 (the ratio of cyclohexene to Ir as shown in Scheme 1) and as detailed elsewhere.[52] (b) The blue color is due to the well-established formation of a two-electron reduced W^V heteropoly blue.[11] (c) Cyclohexene hydrogenation rate in mmol H_2/h•mol Ir (d) Total turnovers of cyclohexene hydrogenation (mol product/mol catalyst) for nanoclusters prepared in situ according to Scheme 1.

Evaluation of the Halide plus BF_4^- Systems in Under the Standard Conditions in Acetone. Entries 2-5 in Table 2 give the results of the 5 criteria for reaction shown in

Scheme 1 with each of the four halides. *Bulk metal and a clear and colorless acetone solution resulted in all four cases*, indicating the absence of nanoclusters. Since bulk metal is the final product of the reaction with all four halides plus 1 equiv BF_4^-, 4 of the 5 criteria in Table 2 cannot be obtained. The only, but interesting, other result is that the k_2/k_1 ratio can be used to compare the halide plus BF_4^- systems to each other for the relative ability to allow the *formation* of $Ir(0)_n$ nanoclusters, again assuming nanoclusters are intermediates to bulk metal. The k_2/k_1 values in entries 1-5 of Table 2 show that the kinetic control (the k_2/k_1 ratio) for the nanocluster formation reaction is $F^- < Cl^- \sim Br^- \sim I^-$, with a factor of approximately 10 between F^- and $Cl^- \sim I^- \sim Br^- < BF_4^-$ (with 1 equiv BF_4^- present as well for the four halides). Hence, *BF_4^- alone allows better nanocluster formation kinetics under Standard Conditions than do halides plus BF_4^-*. Although the relative ranking of the formation kinetics is interesting, the key result from this section is that none of the halide plus 1 equiv BF_4^-stabilizers are sufficient, at least in the low dielectric constant solvent acetone, to allow for well-stabilized nanoclusters.

Reference Point of $P_2W_{15}Nb_3O_{62}^{9-}$ Under the Standard Conditions in Acetone. The $P_2W_{15}Nb_3O_{62}^{9-}$ anion, along with other Brønsted basic polyoxoanions, was previously ranked at the top of the anion formation and stabilization series for prototype $Ir(0)_n$ nanoclusters and for each of the 5 criteria.[12,13] In a control experiment, $P_2W_{15}Nb_3O_{62}^{9-}$ (entry 6 in Table 2) led to: (i) nanocluster formation kinetics exhibiting a high degree of kinetic control of 10^5 M^{-1}; (ii) near-monodisperse nanoclusters which are isolable and redissolvable without the formation of bulk metal; (iii) activity for hydrogenation with preformed, isolated, and then redispersed nanoclusters; and (iv) a high total turnover number for cyclohexene hydrogenation (see Table 2). Note that

$P_2W_{15}Nb_3O_{62}^{9-}$ provides high stabilization even in the low ε solvent acetone. In short, $P_2W_{15}Nb_3O_{62}^{9-}$ is far better than BF_4^- alone or all four halides (each in the presence of BF_4^-) for the formation and stabilization of $Ir(0)_n$ nanoclusters under Standard Conditions in acetone.

Improved Nanocluster Syntheses Conditions in Propylene Carbonate.

Recently, a new double autocatalytic mechanism for the 4-step nucleation, growth, and agglomeration of transition-metal nanoclusters was elucidated (see Scheme 2).[47,48] Using insights from this work, we predicted "Improved Conditions" for the syntheses of nanoclusters falling under the general guidelines of this mechanism by raising the reaction temperature and lowering the nanocluster precursor concentration. These predictions were, in a $Pt(0)_n$ nanocluster system, *apparently* experimentally verified,[50] the higher temperature and lower concentration conditions *apparently* favoring the unimolecular nucleation step over the two bimolecular aggregation steps.[50]

Scheme 2. The 4-step mechanism for nanocluster formation and agglomeration. **A** is the organometallic nanocluster precursor, **B** is nanocluster metal$(0)_n$, and **C** is kinetically distinguishable bulk-type metal. The formation reaction is monitored by the much much faster cyclohexene reporter reaction,[51] rate constant k_h.

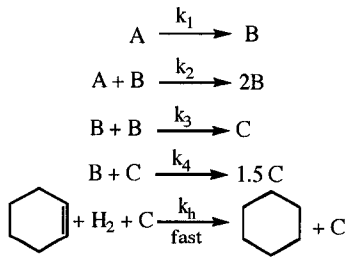

However, under Improved Conditions the solvent was necessarily changed from acetone to propylene carbonate (Table 1) because the 60 °C reaction temperature

desired[47,48] and used is above the 56 °C boiling point of acetone. DLVO theory predicts that the change to propylene carbonate (PC) will also increase nanocluster stabilization by virtue of PC's higher dielectric constant (see eq. 1, where solvent ε is in the numerator[31]). Hence, the change from acetone (ε=20) to propylene carbonate (ε=69) is almost surely another reason for the improved stability of the nanoclusters.[50c] Given the formation of bulk metal under Standard Conditions, it is important, then, to examine herein the predicted-to-be Improved Conditions (Table 1) of 60 °C temperature and 0.24 mM Ir precursor concentration in propylene carbonate for the halide-stabilized systems and via the generalized reaction conditions shown in Scheme 3.

Scheme 3. The generalized nanocluster formation reaction with 0.24 mM Ir precursor in propylene carbonate in the presence of added halides, $[Bu_4N]X$.

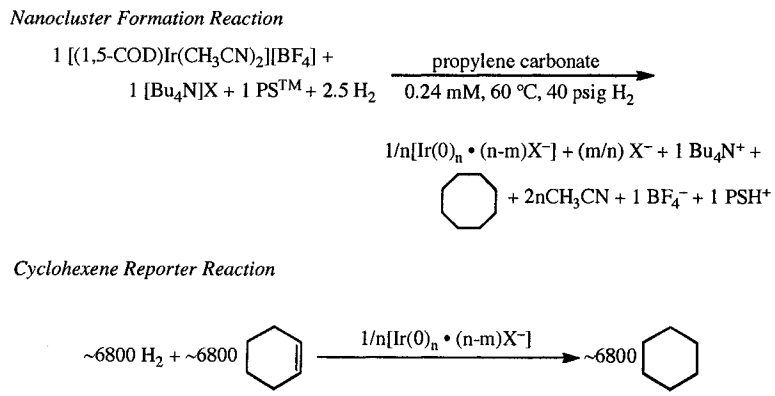

Examining the Influence of BF_4^- under Improved Conditions in Propylene Carbonate. An initial control experiment was performed under the Improved Conditions in the absence of Proton Sponge™, that is, so that $H^+BF_4^-$ is formed instead of (PS™–H^+)/BF_4^-, Scheme 3, (i.e., not even free BF_4^- is present as a potential nanocluster stabilizer). Entry 1 in Table 3 shows that bulk metal and a clear and colorless propylene carbonate solution resulted—that is, stable nanoclusters are not formed if BF_4^- is tied up

as $H^+BF_4^-$. This confirms our earlier findings[44,45] that nanoclusters require anionic, electrostatic stabilization (i.e., free BF_4^-) even in high dielectric constant or high donor number solvents.[44]

Table 3. The 5 Criteria for BF_4^-, F^-, Cl^-, Br^-, I^-, and $P_2W_{15}Nb_3O_{62}^{9-}$ Under the Improved Conditions of 0.24 mM [(1,5-COD)Ir($CH_3CN)_2$][BF_4] in propylene carbonate solvent at 60 °C. Entries 1, 2, and 7 are control experiments testing the effects of the absence (entry 1) or presence (entry 2) of the traditionally weakly coordinating BF_4^- present from the precursor and (entry 7) the current "Gold Standard" stabilizing anion $P_2W_{15}Nb_3O_{62}^{9-}$.

	Anion (with Bu_4N^+ countercation)	Solvent	Ir Conc. (mM)	k_2/k_1[a] (M^{-1})	TEM (Å)	Appearance?[b]	Redisp?	Rates[c]	TTOs[d]
1	$H^+BF_4^-$	PC	0.24	---[e]	---	clear, metal	no	---	---
2	BF_4^-	PC	0.24	$2.8(2)\times10^4$	40(20)	clear, brown	no	---	16,500
3	F^- plus BF_4^-	PC	0.24	---[e]	60(20)	clear, brown	no	---	43,400[f]
4	Cl^- plus BF_4^-	PC	0.24	$8(5)\times10^4$	23(7)	clear, brown	no	---	48,000
5	Br^- plus BF_4^-	PC	0.24	$6(3)\times10^4$	21(6)	clear, brown	no	---	32,700
6	I^- plus BF_4^-	PC	0.24	$6(3)\times10^4$	26(9)	clear, brown	no	---	25,700
7	$P_2W_{15}Nb_3O_{62}^{9-}$	PC	0.24	---[e]	50(20)	clear, blue	no	---	7,300

(a) The values for k_2/k_1 have been corrected by the mathematically required stoichiometry factor of 6800 (the ratio of cyclohexene to Ir as shown in Scheme 3) as detailed elsewhere.[52] (b) The blue color is due to the well-established formation of a two-electron reduced W^V heteropoly blue.[11] (c) Cyclohexene hydrogenation rate in mmol H_2/h•mol Ir (d) Total turnovers of cyclohexene hydrogenation (mol product/mol catalyst) for nanoclusters prepared in situ according to Scheme 2. (e) The kinetic data for this reaction could not be fit by the A→B (rate constant k_1), A+B→2B (rate constant k_2) mechanism (an induction period, indicative of k_1, was not observed). (f) In two separate repeats of this experiment, the TTO number varied by 20,000: (see the Supporting Information for further details about the effects of F^-).

Next, a second control experiment was performed as before in the presence of PS™, Scheme 3, so that BF_4^- (plus (PS™–H^+)) becomes the anionic stabilizer, entry 2 in Table 3. *A brown solution characteristic of $Ir(0)_n$ nanoclusters*[49] *is observed*; TEM confirms that nanoclusters are in fact formed. That is, the Improved Conditions do, indeed, lead to $Ir(0)_n$ nanoclusters (vs. bulk metal as the final product under Standard Conditions) even with just a BF_4^- stabilizer. These nanoclusters are solution-stable only, however; the nanoclusters cannot be isolated and redissolved without the formation of bulk metal.

Also of interest is the kinetic control (i.e., the k_2/k_1 ratio) of the nanocluster formation reaction, under Improved Conditions in the presence of BF_4^- alone, is on the order of 10^4, approximately an order of magnitude smaller—that is, worse—than the kinetic control of BF_4^- alone under Standard Conditions.[12,13] A check by TEM (after complete nanocluster formation as measured by evolution of 1 equiv cyclooctane by gas-liquid chromatography (GLC))[38] reveals a ±50% size distribution, thereby confirming the low kinetic control of the nanocluster formation reaction under Improved Conditions in the presence of BF_4^-.

Evaluation of the Halide plus BF_4^- Systems Under Improved Conditions in Propylene Carbonate. Entries 3-6 in Table 3 give the results of the 5 criteria for reaction shown in Scheme 3 with each of the four halides and under Improved Conditions. Like the nanoclusters prepared in the presence of BF_4^- alone, brown solutions indicative of $Ir(0)_n$ nanoclusters are formed in the presence of each of the four halides (plus 1 equiv BF_4^-), Scheme 3.

The 5 criteria are within experimental error for Cl^-, Br^-, and I^- (plus 1 equiv BF_4^-) under the Improved Conditions in propylene carbonate, entries 4-6 of Table 3. All three systems (i) can be fit with the 2-step nanocluster formation mechanism[38] and display kinetic control on the order of 10^4 M^{-1} for the formation reaction; (ii) provide polydisperse nanoclusters, ~20±10 Å by TEM after complete nanocluster formation as measured by the evolution of 1 equiv cyclooctane by GLC (see Figure 1 for a representative image of nanoclusters prepared in the presence of $[Bu_4N][Cl]$); and (iii) have total turnover numbers for cyclohexene hydrogenation within a factor of 2 of each other. Additionally, these three halide plus BF_4^- systems are solution stable under an N_2

atmosphere for *>1.5 years*, demonstrating a remarkable solution stability. However, the three nanocluster systems are *still not isolable* or redissolvable from solution—a key failure in this stringent test of nanocluster stability. Overall, Cl^-, Br^-, and I^- (plus 1 equiv BF_4^-) are approximately equal additives for the formation and stabilization of $Ir(0)_n$ nanoclusters under the Improved Conditions in propylene carbonate.

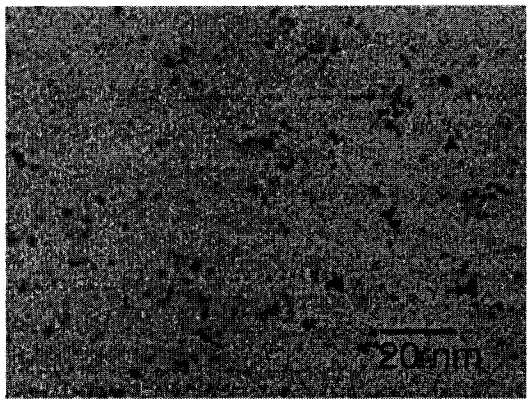

Figure 1. A representative TEM image of $Ir(0)_n$ nanoclusters prepared under the Improved Conditions in propylene carbonate in the presence of $[Bu_4N][Cl]$. Note that, while nanoclusters are formed, they are polydisperse / somewhat aggregated (23 ± 7 Å).

Comparison of the BF_4^- Alone System to the Cl^-, Br^-, and I^- plus BF_4^- Systems. Comparing entry 2 with entries 4-6 in Table 3 shows that: the kinetic control of each of these four nanocluster formation reactions is on the order of 10^4 M^{-1}, polydisperse nanoclusters are formed as measured by TEM, and none of the four systems are isolable or redissolvable without the formation of bulk metal. An important, take-home message, then, is that *the BF_4^- alone system is within experimental error of the three halide plus BF_4^- systems for the formation and stabilization of $Ir(0)_n$ nanoclusters under the Improved Conditions in propylene carbonate solvent.* That is, we again find[44,45] that even the traditionally weakly coordinating anion BF_4^- contributes significantly to prototype $Ir(0)_n$ nanocluster stability in the high dielectric constant solvent propylene carbonate.

Comparison of F^- to the BF_4^- Alone and Cl^-, Br^-, and I^- Stabilizer Systems. The results for the 5 criteria are somewhat different for F^-, entry 3 of Table 3. First, the kinetics of nanocluster formation cannot be fit with either the 2-step mechanism for nanocluster nucleation and growth, nor by either the established 3-step nor 4-step mechanisms for nanocluster nucleation, growth, and agglomeration.[47,48,51] The lack of an induction period in reactions in the presence of $[Bu_4N][F]$ (see Figure S1 of the Supporting Information) indicates an uncontrolled nucleation step. Additionally, the nanoclusters are larger (60 ± 20 Å) by TEM than nanoclusters prepared in the presence of Cl^-, Br^-, and I^- (20 ± 10 Å). The system does show activity in the cyclohexene hydrogenation total turnover (TTO) reaction, presumably because small, highly active—but unstable—nanoclusters are formed, then agglomerate to the larger nanoclusters observed by TEM. The key result here is that F^- is inferior and ranks below the other three halides (the interested reader is referred to the Supporting Information for some additional experiments and discussion).

Evaluation of $P_2W_{15}Nb_3O_{62}^{9-}$ Under the Improved Conditions in Propylene Carbonate. Comparison of entries 2 and 4-7 in Table 3 reveals two important surprises: first, three of the halide plus BF_4^- stabilizers and BF_4^- alone are *preferred to the previous "Gold Standard"*[12] *stabilizer $P_2W_{15}Nb_3O_{62}^{9-}$* under the Improved (for halides) Conditions. Second, and for the first time, the kinetic control of the nanocluster formation reaction with added $P_2W_{15}Nb_3O_{62}^{9-}$ cannot be modeled by the 2-step, 3-step, or 4-step mechanisms for nanocluster nucleation, growth, and agglomeration,[38,47,48,,51] despite the fact that $[Bu_4N]_5Na_3[(1,5\text{-COD})Ir{\bullet}P_2W_{15}Nb_3O_{62}]$ is the nanocluster precursor from which the 2- and 3-step mechanisms were developed,[38,51] as well as a system for

which the 4-step mechanism has also been shown to apply![52] TEM images show that large, polydisperse, 50±20 Å nanoclusters are formed (Figure 2). Moreover, and in contrast to $P_2W_{15}Nb_3O_{62}^{9-}$–stabilized nanoclusters prepared under Standard Conditions, $P_2W_{15}Nb_3O_{62}^{9-}$–stabilized nanoclusters prepared under Improved Conditions (i.e., in the normally preferred solvent of propylene carbonate) are *not* redispersable once taken to dryness. Additionally, the cyclohexene hydrogenation TTO value for $P_2W_{15}Nb_3O_{62}^{9-}$–stabilized nanoclusters is lower than (i) all four halide plus BF_4^- systems, (ii) the BF_4^- alone system and (iii) the $P_2W_{15}Nb_3O_{62}^{9-}$-stabilized nanoclusters under Standard Conditions.

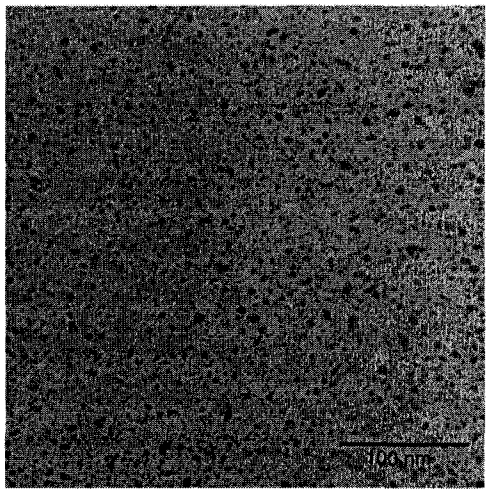

Figure 2. Nanoclusters prepared in the presence of $P_2W_{15}Nb_3O_{62}^{9-}$ under the Improved Conditions in propylene carbonate. These nanoclusters are larger and more polydisperse (50±20 Å) than nanoclusters prepared in the presence of $P_2W_{15}Nb_3O_{62}^{9-}$ under the Standard Conditions in acetone (22±3 Å).

These unexpected results rather dramatically reveal that the "Improved Conditions" for halides are *not* Improved Conditions for $P_2W_{15}Nb_3O_{62}^{9-}$. The important finding here is that the change to the higher ε solvent propylene carbonate, along with the lower concentration and higher temperature, are seemingly small/subtle—but actually very important changes—in determining the kinetics of formation in transition-metal

nanoclusters. The danger in extrapolating the nanocluster formation and stabilization ability of a given additive over different concentrations, temperatures, and solvents is apparent. We are examining, and will present elsewhere, why the previous "Gold Standard" $P_2W_{15}Nb_3O_{62}^{9-}$ anion is not a preferred stabilizer under Improved Conditions, studies which are focusing on the rapid dissociation of (and hence uncontrolled nucleation from) (1,5-COD)Ir^+ off its $P_2W_{15}Nb_3O_{62}^{9-}$anionic ligand ((1,5-COD)Ir•$P_2W_{15}Nb_3O_{62}^{8-}$ ⇆ (1,5-COD)Ir(solvate)$_2^+$ + $P_2W_{15}Nb_3O_{62}^{9-}$). Facile H_2 reduction and uncontrolled nucleation of the resultant, easily reduced[11] (1,5-COD)Ir(solvate)$_2^+$ then leads to the formation of large, polydisperse nanoclusters.[53] It seems likely that too much (1,5-COD)Ir(solvate)$_2^+$ is also a problem in the F^- stabilized system, with the added implication being that the equilibrium (1,5-COD)Ir(solvate)$_2^+$ + X^- ⇆ ½[(1,5-COD)IrX]$_2$ + BF_4^- lies at least somewhat to the right for the other halides.

Summary and Conclusions

Overall, the significant findings herein are as follows:

- Even the traditionally weakly coordinating anion BF_4^- contributes to nanocluster stability in high dielectric constant solvents—that is, BF_4^- is a rather unexpected, "hidden" stabilizer.[44,45]
- High dielectric constant solvents like propylene carbonate[54] are preferred for nanocluster stability and have a large if not dominant[50c] effect so long as even traditionally weakly coordinating anions such as BF_4^- are present.
- Solution-stable (≥1.5 years), polydisperse $Ir(0)_n$ nanoclusters were prepared under the Improved Conditions in *propylene carbonate* for each of the four halide plus BF_4^-

systems, as well as BF_4^- alone. However, none of these nanoclusters are isolable and redissolvable without the formation of bulk metal, a key failure in this stringent test of nanocluster stability.

- By the 5 criteria method, Cl^-, Br^-, I^- (plus 1 equiv BF_4^-) or BF_4^- alone are approximately equal additives for the formation and stabilization of prototype $Ir(0)_n$ nanoclusters under the Improved Conditions. F^- (plus 1 equiv BF_4^-) is inferior for the preparation and stabilization of $Ir(0)_n$ nanoclusters.
- However, each of the four halides (plus 1 equiv BF_4^-) and BF_4^- alone under Standard Conditions yields bulk metal as the final product of the reaction. Hence, none of the four halide plus BF_4^- systems, nor BF_4^- alone, are sufficient for the formation and stabilization of prototype $Ir(0)_n$ nanoclusters. Under the Standard Conditions in acetone, $P_2W_{15}Nb_3O_{62}^{9-}$ is a far superior stabilizer in comparison to each of the four halides and also to BF_4^- alone.
- The finding herein of poor control for nanocluster formation and stabilization by all four halides under Standard Conditions is consistent with our previous anion formation and stabilization series, which placed Cl^- eleventh of eleven anions (each with Bu_4N^+ cations) studied in terms of stabilizing efficacy for prototype $Ir(0)_n$ nanoclusters. The updated anion stabilization series (under Standard Conditions in acetone for prototype $Ir(0)_n$ nanoclusters) can now be expanded to be: $P_2W_{15}Nb_3O_{62}^{9-} \sim [(P_2W_{15}Nb_3O_{61})_2O]^{16-} \sim ([P_2W_{15}(TiOH)_3O_{\sim 59}]^{9-})_n$ (n = 1, 2) $\sim SiW_9Nb_3O_{40}^{7-} > HPO_4^{2-} \sim C_6H_5O_7^{3-} >> BF_4^- \sim [-CH_2CH(CO_2^-)-]_n^{n-} \sim OAc^- \sim P_3O_9^{3-} \sim OH^- \sim Cl^- \sim Br^- \sim I^- > F^-$.

- Surprisingly, but interestingly, $P_2W_{15}Nb_3O_{62}^{9-}$, which is ranked first in the anion stabilization series under the Standard Conditions *in acetone*, is not a preferred stabilizer under Improved Conditions *in propylene carbonate*, instead leading to the formation of large, polydisperse nanoclusters that are not isolable and/or redissolvable.[53] Further details and the underlying reason, which appears to be tied to the solvent-dependent equilibrium (1,5-COD)Ir•$P_2W_{15}Nb_3O_{62}^{8-}$ ⇆ (1,5-COD)Ir(solvate)$_2^+$ + $P_2W_{15}Nb_3O_{62}^{9-}$, will be presented elsewhere.[53]

Experimental Section

Materials. All commercially obtained reagents were used as received unless otherwise noted. All solvents and compounds used for nanocluster syntheses were stored in a drybox prior to use. Propylene carbonate (Aldrich, 99.7%) was evacuated under vacuum for at least four hours and stored over activated 4Å molecular sieves to remove H_2O. Acetone (Burdick and Jackson, 99.9+% by GC) was purged with argon for a minimum of 20 minutes. Cyclohexene (Aldrich, 99%) was freshly distilled over Na metal under argon. The crystalline iridium solvate complex [(1,5-COD)Ir$(CH_3CN)_2$][BF_4], was prepared following the procedure for the corresponding hexafluorophosphate salt.[55] The purity of the resultant crystalline solvate complex was verified by ^{1}H NMR (CD_2Cl_2: s(δ 4.3), s(δ 2.6), m(δ 2.3), m(δ 1.8)). Proton Sponge™ (1,8-bis(dimethylamino)naphthalene, Aldrich, 99%) was used as received. The polyoxoanion $[Bu_4N]_9[P_2W_{15}Nb_3O_{62}]$ was prepared according to our most recent literature procedure.[56] The purity of the polyoxoanion was checked by ^{31}P NMR (CD_3CN: δ -6.5, -13.6 relative to 85% H_3PO_4, with small impurity peaks at -8.7 and -

13.2). $[Bu_4N]_5Na_3[(1,5\text{-COD})Ir{\bullet}P_2W_{15}Nb_3O_{62}]$ was prepared following literature procedure with the exception that crystalline $[(1,5\text{-COD})Ir(CH_3CN)_2][BF_4]$, prepared as above, was used as the Ir source.[57] $[Bu_4N][Cl]$, $[Bu_4N][Br]$, and $[Bu_4N][I]$ (Aldrich, ≥99%) were used as received. $[Bu_4N][F]{\cdot}xH_2O$ (Aldrich, 98%; TGA analysis showed that x=2 for our specific bottle) was dissolved in acetone or propylene carbonate and dried overnight over activated 4 Å mol sieves to produce a 1.2 mM solution in acetone or propylene carbonate. Control experiments of taking the ^1H NMR of the resultant propylene carbonate solution revealed no change in the propylene carbonate resonances (i.e., $[Bu_4N][F]$ is not catalytically decomposing the solvent). CD_2Cl_2 (Cambridge Isotope Laboratories, 99.9%) was purchased in prescored 1g amber glass vials.

Instrumentation. Gas chromatography was performed using a Hewlett-Packard 5890 Series II GC with a FID detector equipped with a Supelcowax SPB-1 capillary column. Parameters were as follows: T_1=50 °C, t_1=3 min, ramp=10 °C/min, T_2=160 °C, t_2=10 min, injection volume 2 μL. Data were acquired and analyzed with Galaxie Chromatography Data System v1.7 from Varian, Inc. TGA studies were carried out under a N_2 atmosphere on 5-15 mg $[Bu_4N][F]{\bullet}xH_2O$ with a TA Instruments 2050 TGA. TGA samples were heated from 25 °C to 500 °C at a rate of 5 °C/min. Nuclear magnetic resonance (NMR) spectra were obtained at 22 °C on a Varian Inova 300 MHz instrument. Spectral parameters for ^1H NMR: tip angle, 38.9°; acquisition time, 2.372 s; relaxation delay, 1.000 s; sweep width, 6000.6 Hz; total acquisition time, 67 s. Spectral parameters for ^{31}P: tip angle, 88.2°; acquisition time, 1.600 s; sweep width, 10000.0 Hz.

Hydrogenation Apparatus. Hydrogenation experiments were carried out in a previously fully described[11,58,59] in-house constructed apparatus designed to continuously

monitor pressure loss. This apparatus consists of a Fisher-Porter (F-P) bottle, which connects *via* Swagelok quick-connects to both a H_2 line and an Omega PX621 pressure transducer. The pressure transducer is interfaced with a PC by means of an Omega D1131 5V A/D converter with a RS-232 connection. The pressure uptake data was collected using LabView 7.1; these hydrogen uptake curves were converted to cyclohexene hydrogenation curves using the known 1:1 H_2 to cyclohexene stoichiometry and following the previously established cyclohexene reporter-reaction kinetic method.[38] Cyclohexene hydrogenation curves were fitted to the analytical equations[38,58] for A→B, plus A+B→2B using Origin 7.0.

During the hydrogenation reactions, the F-P bottle was immersed in a 500 mL jacketed reaction flask (Ace Glass, Inc.) filled with dimethyl silicon fluid (Thomas Scientific). The temperature of the flask was regulated with a thermostatted recirculating water bath (see Figure I in the Supporting Information elsewhere[59]). For reactions under the Improved Conditions run at 60 °C, this apparatus is not optimally designed, as there is a significant temperature gradient between the bottom of the F-P bottle, immersed in the oil-filled jacketed reaction flask (60 °C), and the pressure transducer (22 °C). However, this apparatus was sufficient for the reactions performed herein, as the observed kinetics for each anion were within error for ≥3 repeats of the same reaction. Additionally, we are looking for large, order-of-magnitude-type changes in rate constants, which are easily detected by even this non-optimized system at 60 °C.

Nanocluster Formation in the Presence of Halides or BF_4^- Alone Under Standard Conditions in Acetone. These conditions were modeled after the Standard Conditions in our previous papers.[43] For each experiment, $[(1,5\text{-COD})Ir(CH_3CN)_2][BF_4]$

(1.7 mg; 3.6 μmol) was weighed into a pre-dried (160 °C for ≥12h) 2 dram glass vial in a drybox. Next, Proton Sponge™ (0.8 mg; 3.6 μmol) was added to the vial. For the experiments with added Cl^-, Br^-, or I^-, one equivalent (3.6 μmol) of the Bu_4N^+ salt of the halide under study was added ([Bu_4N][Cl], 1.0 mg; [Bu_4N][Br], 1.2 mg; [Bu_4N][I], 1.3 mg). Then, acetone (2.5 mL) was added with a 1.0 mL gas-tight syringe, yielding a clear brilliant-yellow solution for Cl^-, Br^-, and BF_4^-, and a clear orange solution for I^-. For the experiments with F^-, 2.5 mL of a 1.2mM [Bu_4N][F] solution in acetone was added with a 1.0 mL gas-tight syringe. The solution was agitated with a polyethylene pipet until the solution was homogeneous. The reaction solution was transferred to a new borosilicate culture tube (22 x 175 mm) with a new 5/8" x 5/16" Teflon-coated octagon shaped spin bar. Freshly distilled cyclohexene (0.5 mL) was added to the culture tube with a 1.0 mL gas-tight syringe. The culture tube was placed in the F-P bottle, and the F-P bottle was sealed, brought out of the drybox, and attached to the H_2 line via its Quick-Connects. To begin each reaction, the F-P bottle was purged 13 times with H_2 (40 ± 1 psig, 15 s/purge). Five min after the first purge, the pressure was set at 40 ± 1 psig, $t = 0$ was noted, and pressure *vs.* time data was collected at 2.5 min intervals.

Nanocluster Formation in the Presence of $P_2W_{15}Nb_3O_{62}^{9-}$ Under Standard Conditions in Acetone. For each experiment, [Bu_4N]$_5$Na$_3$[(1,5-COD)Ir•$P_2W_{15}Nb_3O_{62}$] (20.0 mg; 3.6 μmol) was weighed into a pre-dried 2 dram glass vial in the drybox. Next, Proton Sponge™ (0.8 mg; 3.6 μmol) was added to the vial. Then, acetone (2.5 mL) was added to the vial, yielding a clear, brilliant-yellow solution. This solution was agitated until homogeneity using a polyethylene pipet, and the same pipet was used to transfer the solution into the culture tube. Cyclohexene (0.5 mL) was added with a 1.0 mL gas-tight

syringe. The remainder of the procedure was carried out exactly as described in the preceding section.

Nanocluster Formation in the Presence of Halides or BF_4^- Alone Under the Improved Conditions in Propylene Carbonate. For each experiment, [(1,5-COD)Ir($CH_3CN)_2$][BF_4] (1.7 mg; 3.6 μmol) was weighed into a pre-dried 2 dram glass vial in the drybox. Next, Proton Sponge™ (0.8 mg; 3.6 μmol) was added to the vial. For the experiments with added Cl^-, Br^-, or I^-, one equivalent (3.6 μmol) of the Bu_4N^+ salt of the halide under study was added ([Bu_4N][Cl], 1.0 mg; [Bu_4N][Br], 1.2 mg; [Bu_4N][I], 1.3 mg). Then, propylene carbonate (2.5 mL) was added with a 2.5 mL gas-tight syringe, yielding a clear brilliant-yellow solution for Cl^-, Br^-, and BF_4^-, and a clear orange solution for I^-. For the experiments with added F^-, 2.5 mL of a 1.2 mM [Bu_4N][F] solution in propylene carbonate was added with a 1.0 mL gas-tight syringe. The solution was agitated with a polyethylene pipet until the solution was homogeneous. Then, an aliquot (0.5 mL) of the reaction solution was removed with a 1.0 mL disposable polyethylene syringe and placed in a new borosilicate culture tube (22 x 175 mm) with a new 5/8" x 5/16" Teflon-coated octagon shaped spin bar. Next, propylene carbonate (2.0 mL) was added to the culture tube with a 2.5 mL gas-tight syringe, resulting in a final volume of 2.5 mL and a final molarity of 0.24 mM. Last, freshly distilled cyclohexene (0.5 mL) was added with a 1.0 mL gas-tight syringe. The culture tube was sealed in the F-P bottle and brought out of the drybox. The F-P bottle was attached to the H_2 line via its Quick-Connects and placed in a 60 °C oil-filled jacketed reaction flask. There, the reaction solution was stirred for ≥10 minutes before being exposed to H_2 to attain the desired 60 °C reaction temperature. To begin each reaction, the F-P bottle was purged 13

times with H_2 (40 ± 1 psig, 15 s/purge). Five min after the first purge, the pressure was set at 40 ± 1 psig, $t = 0$ was noted, and pressure *vs.* time data was collected at 2.5 min intervals.

Nanocluster Formation in the Presence of $P_2W_{15}Nb_3O_{62}^{9-}$ Under the Improved Conditions the Improved Conditions. For each experiment, $[Bu_4N]_5Na_3[(1,5\text{-COD})Ir{\bullet}P_2W_{15}Nb_3O_{62}]$ (20.0 mg; 3.6 μmol) was weighed into a pre-dried 2 dram glass vial in the drybox. Next, Proton Sponge™ (0.8 mg; 3.6 μmol) was added to the vial. Then, propylene carbonate (2.5 mL) was added with a 2.5 mL gas-tight syringe, yielding a clear brilliant-yellow solution. The solution was agitated with a polyethylene pipet until the solution was homogeneous. Then, an aliquot (0.5 mL) of the reaction solution was removed with a 1.0 mL disposable polyethylene syringe and placed in a new borosilicate culture tube (22 x 175 mm) with a new 5/8" x 5/16" Teflon-coated octagon shaped spin bar. Next, propylene carbonate (2.0 mL) was added to the culture tube with a 2.5 mL gas-tight syringe, resulting in a final volume of 2.5 mL and a final concentration of 0.24 mM. Last, freshly distilled cyclohexene (0.5 mL) was added with a 1.0 mL gas-tight syringe. The rest of the hydrogenation procedure was carried out exactly as described in the preceding section.

Cyclooctane Evolution Under the Improved Conditions in Propylene Carbonate. Gas-liquid chromatography (GLC) was carried out to monitor the evolution of 1 equivalent of cyclooctane and thus complete nanocluster formation for each reaction. In the drybox, a reaction was prepared exactly as described in the section above titled "Nanocluster Formation in the Presence of Halides or BF_4^- Alone Under the Improved Conditions in Propylene Carbonate" or "Nanocluster Formation in the Presence of

$P_2W_{15}Nb_3O_{62}^{9-}$ Under the Improved Conditions in Propylene Carbonate", with the exception that 2.5 mL of cyclohexene was used, for a total reaction volume of 5.0 mL. The F-P bottle was attached to the hydrogenation apparatus as described above, stirred for ≥10 minutes, but after the purging cycle the valve to the H_2 line was left open. This allows a constant pressure of 40 ± 1 psig H_2. Periodically, the reaction solution was sampled to monitor cyclooctane evolution. For each sampling event, the stir bar was turned off and the solution was allowed to settle for 30 s to allow the immiscible propylene carbonate and cyclohexene/cyclohexane/cyclooctane layers to separate. Then, the top valve to the F-P bottle was opened and a 0.50 mL gas-tight syringe equipped with a 45 cm stainless steel needle was introduced through the top valve for sampling. An aliquot (≤ 0.1 mL) of the top cyclohexene/cyclohexane/cyclooctane layer was removed with the syringe. Next, the syringe was removed from the F-P bottle, the top valve was sealed, and stirring was re-initiated. The aliquot was placed in a 0.5 dram glass vial with a screw-cap top and sealed. The F-P bottle was purged three times in 15 s intervals, beginning 15 s after the top valve was closed. The whole sampling procedure, including the 30 s settling time and purging cycle, takes approximately 1.5 min. Between samplings, the stainless steel needle was rinsed four times with acetone and thoroughly dried. Cyclooctane evolutions were compared to a calibration curve created with authentic cyclooctane.

Transmission Electron Microscopy (TEM) for Samples Prepared under Improved Conditions in Propylene Carbonate. Identical procedures were carried out for the halide-stabilized nanoclusters as well as the control solutions with $P_2W_{15}Nb_3O_{62}^{9-}$ stabilized nanoclusters. After the nanocluster formation reaction was complete as judged

by a separate cyclooctane evolution experiment (vide supra), the F-P bottle was brought into the drybox and TEM grids were prepared. Since propylene carbonate charges in the electron beam (and, hence, does not provide suitable TEMs[60] if the grids are prepared by placing two drops of the diluted reaction solution on TEM grids), the reaction solutions were sprayed onto 300 mesh silicon monoxide grids using an asthmatic's nebulizer (PulmoAide, model 5610D). In the drybox, the reaction solution (0.5 mL) was decanted into a new disposable medicine cup. Silicon monoxide TEM grids (Ted Pella, Inc.) were carefully held with tweezers in front of the nebulizer mouthpiece while the reaction solution was nebulized. It was determined empirically that 5 s exposure to the nebulized reaction solution was sufficient to visualize the nanoparticles. TEM analysis was carried out with the expert assistance of Dr. JoAn Hudson at the University of Oregon and later at Clemson University. Micrographs were obtained with a Phillips CM-12 microscope operating at 100 keV. Size measurements were obtained from micrographs with 430k magnification or higher (some lower magnification images were also obtained to visually survey a larger area of each grid to ensure representative micrographs were being obtained, but not used for size measurements), and size distributions of nanoclusters were determined by counting >300 nanoclusters. TEM images were enlarged using Adobe Photoshop 7.0.

Nanocluster Isolation Attempts and *in situ* Hydrogenation for all Nanoclusters Prepared Under Improved Conditions in Propylene Carbonate. After the nanocluster formation reaction was judged complete by a separate cyclooctane evolution experiment, the F-P bottle was vented, sealed, and brought into the drybox. There, two aliquots of the reaction solution (0.5 mL each) were taken with a 1.0 mL

disposable polyethylene syringe. One of the aliquots was used to test the hydrogenation activity of the preformed nanoclusters. This aliquot was placed in a new borosilicate culture tube (22 x 175 mm) with a new 5/8" x 5/16" Teflon-coated octagon shaped spin bar. Then, fresh propylene carbonate (2.0 mL) was added with a 2.5 mL gas-tight syringe. The resulting solution was light brown and apparently homogeneous. Next, freshly distilled cyclohexene (0.5 mL) was added with a 1.0 mL gas-tight syringe. The culture tube was sealed in the F-P bottle and hydrogenation was initiated exactly as described above in the section titled "Nanocluster Formation in the Presence of Halides or BF_4^- Alone Under the Improved Conditions in Propylene Carbonate."

The second aliquot of the nanocluster reaction solution was placed in a pre-dried glass scintillation vial. There, following our earlier procedure,[60] approximately 10 mL of anhydrous diethyl ether was added to the light–brown nanocluster solution. The vial was swirled, resulting in a nearly colorless, clear solution. Next, the vial was capped and sealed with Parafilm, and brought out of the drybox. The vial was then subjected to centrifugation (1 h at 1200 rpm in a swinging-bucket centrifuge with a radius of 20 cm). After centrifugation, the vial, still sealed, was brought back into the drybox. After decanting the solvent, non-redispersable bulk metal was the product. Attempts to isolate the nanoclusters using the same general procedure, but a CH_3CN solvent, also resulted in the formation of bulk metal.

Total Turnover Experiments. The cyclohexene hydrogenation total turnover experiments under Standard Conditions in acetone were carried out exactly as detailed our earlier report.[12] The total turnover experiments under Improved Conditions in propylene carbonate were also carried out as detailed in our earlier report,[12] with the

exception that each reaction was stirred in the oil-filled jacketed reaction flask for ≥10 minutes before H_2 introduction to attain the desired 60 °C temperature.

Acknowledgements. This work was funded by DOE grant DE-FG02-03ER15453.

Supporting Information Available. Figure S1, a sample cyclohexene hydrogenation curve in the presence of F^- (plus 1 equiv BF_4^-) under Improved Conditions; further investigation of the F^- stabilizer system; Table S1, total cyclohexene hydrogenation reaction times in the presence of F^- (plus 1 equiv BF_4^-) under Improved Conditions.

References

[1] G. Schmid and L. Chi, Adv. Mater. 10, 515 (1998).
[2] G. Schmid, M. Baumle, M. Geerkens, I. Heim, C. Osemann, and T. Sawitowski, Chem. Soc. Rev. 28, 179 (1999).
[3] J. D. Aiken, III and R. G. Finke, J. Mol. Cat. A 145, 1 (1999).
[4] A. Roucoux, J. Schulz, and H. Patin, Chem. Rev. 102, 3757 (2002).
[5] B. L. Cushing, V. L. Kolesnichenko, and C. J. O'Connor, Chem. Rev. 104, 3893 (2004).
[6] D. Astruc, F. Lu, and J. R. Aranzes, Angew. Chem. Int. Ed. 44, 7852 (2005).
[7] L. S. Ott and R. G. Finke, "Transition-Metal Nanocluster Stabilization: A Critical Review of Ranking Methods and Putative Stabilizers." Coord. Chem. Rev. 2006, accepted pending minor revisions.
[8] U. Simon, G. Schön, and G. Schmid, Angew. Chem. Int. Ed. 32, 250 (1993).
[9] R. Elghanian, J. J. Storhoff, R. C. Mucic, R. L. Letsinger, and C. A. Mirkin, Science 277, 1078 (1997).
[10] M. T. Reetz, M. Winter, G. Dumpich, J. Lohau, and S. Friedrichowski, J. Am. Chem. Soc. 199, 4539 (1997).
[11] Y. Lin, and R. G. Finke, J. Am. Chem. Soc. 116, 8335 (1994).
[12] S. Özkar and R. G. Finke, J. Am. Chem. Soc. 124, 5796 (2002).
[13] S. Özkar and R. G. Finke, Langmuir 18, 7653 (2002).
[14] J. Turkevich and G. Kim, Science 169, 873 (1970).
[15] B. Chaudret, O. Vidoni, K. Philippot, C. Amiens, O. Balmes, J.-O. Malm, J.-O. Bovin, F. Senocq, and M.-J. Casanove, Angew. Chem. Int. Ed. 38, 3736 (1999).
[16] P. J. Collier, J. A. Iggo, and R. Whyman, J. Mol. Cat. A 146, 149 (1999).
[17] Y. Shiraishi, D. Arakawa, and N. Toshima, Eur. Phys. J. E. 8, 377 (2002).

[18] M. S. Romero-Cano, A. Martin-Rodriguez, and F. J. de las Nieves, Langmuir 17, 3505 (2001).
[19] A. Y. Kim and J. C. Berg, Langmuir 18, 3418 (2002).
[20] G. Fritz, V. Schadler, N. Willenbacher, and N. J. Wagner, Langmuir 18, 6381 (2002).
[21] R. M. Crooks, M. Zhao, L. Sun, V. Chechik, and L. K. Yeung, Acc. Chem. Res. 34, 181 (2001).
[22] R. Dagani, Chem. Eng. News 77, 33 (1999).
[23] L. Balogh and D. A. Tomalia, J. Am. Chem. Soc. 120, 7355 (1998).
[24] B. P. S. Chauhan, J. S. Rathore, M. Chauhan, and A. Krawichz, J. Am. Chem. Soc. 125, 2876 (2003).
[25] C. Petit, P. Lixon, and M. P. Pileni, J. Phys. Chem. 97, 12974 (1993).
[26] J. Dupont, G. S. Fonseca, A. P. Umpierre, P. F. P. Fichtner, and S. R. Teixeira, J. Am. Chem. Soc. 124, 4228 (2002).
[27] H. Itoh, K. Naka, Y. Chujo, J. Am. Chem. Soc. 126, 3026 (2004).
[28] C. C. Cassol, A. P. Umpierre, G. Machado, S. I. Wolke, and J. Dupont, J. Am. Chem. Soc., 127, 3298 (2005).
[29] R. Balasubramanian, K. Beomseok, S. L. Tripp, X. Wang, M. Lieberman, and A. Wei, Langmuir 18, 3676 (2002).
[30] S. L. Tripp, S. V. Pusztay, A. E. Ribbe, and A. Wei, J. Am. Chem. Soc. 124, 7914 (2002).
[31] E. J. W. Verwey and J. T. G. Overbeek, *Theory of the Stability of Lyophobic Colloids*; 2 ed.; Dover Publications, Inc.: Mineola, New York (1999).
[32] B. W. Ninham, Adv. Coll. Int. Sci. 83, 1 (1999).
[33] D. F. Evans and H. Wennerström, *The Colloidal Domain*, 2nd ed.; Wiley-VCH: New York, (1999).
[34] It has been shown in the literature that chloride serves as a competent nanocluster stabilizer for metals such as Pt (J. U. Köhler and J. S. Bradley, Catal. Lett. 45, 203 (1997)). Separately, it was reported for Rh nanoclusters that the nature of the halide counter-ion (Cl^-, Br^-, or I^-) in a surfactant stabilizer had a significant effect on the nanoclusters' catalytic activity for arene hydrogenation (A. Roucoux, J. Schulz, and H. Patin, Adv. Synth. Catal. 345, 222 (2003)).
[35] J. D. Aiken, III, Y. Lin, and R. G. Finke, J. Mol. Cat. A. 114, 29 (1996).
[36] W. Bönnemann, W. Brijoux, R. Brinkmann, E. Dinjus, T. Joußen, and B. Korall, Angew. Chem. Int. Ed. 30, 1312 (1991).
[37] M. T. Reetz, W. Helbig, S. A. Quaiser, U. Stimming, N. Breur, and R. Vogel, Science 267, 367 (1995).
[38] M. A. Watzky and R. G. Finke, J. Am. Chem. Soc. 119, 10382 (1997).
[39] The total turnover (TTO) number is actually a measurement of catalytic activity which reflects both nanocluster formation and stabilization, as the TTO experiment begins with the organometallic nanocluster precursor $[(1,5\text{-COD})Ir(solvent)_2]^+[anion]^-$. Accordingly, less stable nanoclusters can have a high TTO number if small, highly reactive yet poorly stabilized nanoclusters are formed en route to agglomerated nanoclusters or bulk metal. Conversely, some very stable nanoclusters might have a lower TTO number if highly stabilized, less reactive nanoclusters are formed.
[40] R. Zsigmondy, Z. Anal. Chem., p.697 (1901).

[41] H. Thiele and H. S. von Levern, J. Coll. Sci. 20, 679 (1965).
[42] R. G. Finke and S. Özkar, Coord. Chem. Rev. 248, 135 (2004).
[43] S. Özkar and R. G. Finke, Langmuir 19, 6247 (2003).
[44] L. S. Ott and R. G. Finke, "Nanocluster Formation and Stabilization Fundamental Studies: Investigating "Solvent-Only" Stabilization En Route to Discovering Stabilization by the Traditionally Weakly Coordinating Anion BF_4^- Plus High Dielectric Constant Solvents." Inorg. Chem., in press (2006).
[45] L. S. Ott, B. J. Hornstein and R. G. Finke, "A Test of the Transition-Metal Nanocluster Formation and Stabilization Ability of the Most Common Polymeric Stabilizer, Poly(vinylpyrrolidone), As Well As Four Other Polymeric Protectants." Langmuir, in press (2006).
[46] S. H. Strauss, Chem. Rev. 93, 927 (1993).
[47] C. Besson, E. E. Finney, and R. G. Finke, J. Am. Chem. Soc. 127, 8179 (2005).
[48] C. Besson, E. E. Finney, and R. G. Finke, Chem. Mater. 17, 4925 (2005).
[49] J. A. Creighton and D. G. Eadon, J. Chem. Soc., Faraday Trans. 87, 3881 (1991).
[50] (a) Actually, we now know that the first step has a higher molecularity, nA→B,[50b] which in turn changes slightly mechanism used to predict the "Improved Conditions". Hence, the observed improvement in the formation of $Pt(0)_n$ nanoclusters seen elsewhere[47,48] appears in significant part to be due to the solvent change from acetone to propylene carbonate, a point under investigation in a separate study.[50c] (b) E. E. Finney, L. S. Ott and R. G. Finke, "A New Mechanism for the Nucleation of Transition-Metal Nanoclusters." Manuscript in preparation. (c) E. E. Finney and R. G. Finke, "The Four-Step, Double-Autocatalytic Mechanism for Transition-Metal Nanocluster Nucleation, Growth, and Then Agglomeration: Metal, Ligand, Concentration, Temperature, and Stirring Rate Dependency Studies." Manuscript in preparation, intended for Chem. Mater.
[51] B. J. Hornstein and R. G. Finke, Chem. Mater. 16, 139 (2004).
[52] L. S. Ott and R. G. Finke, "Nanocluster Formation, Stabilization, and Agglomeration Fundamental Studies: Can the Kinetics of Agglomeration, as a Preferred, Quantitative Way to Assay Transition-Metal Nanocluster Stabilizers, Be Measured by the Catalytic Reporter Reaction Method?" Manuscript in preparation.
[53] C. R. Graham, L. S. Ott and R. G. Finke, Manuscript in preparation.
[54] M. T. Reetz and W. Helbig, J. Am. Chem. Soc. 116, 7401(1994).
[55] V. W. Day, W. G. Klemperer and D. J. Mann, Inorg. Chem. 29, 2345 (1990).
[56] B. J. Hornstein and R. G. Finke, Inorg. Chem. 41, 2720 (2002).
[57] M. Pohl, D. K. Lyon, N. Mizuno, K. Nomiya, and R. G. Finke, Inorg. Chem. 34, 1413 (1995).
[58] M. A. Watzky and R.G. Finke, Chem. Mater. 9, 3083 (1997).
[59] J. D. Aiken, III and R. G. Finke, Chem. Mater. 11, 1035 (1999).
[60] J. A. Widegren and R. G. Finke, Inorg. Chem. 41, 1558 (2002).

SUPPORTING INFORMATION

Nanocluster Formation and Stabilization Fundamental Studies:

Ranking the Nanocluster Stabilizing Ability of Halides

Lisa Starkey Ott, Morgan L. Cline, and Richard G. Finke*

Department of Chemistry, Colorado State University, Fort Collins, Colorado 80523

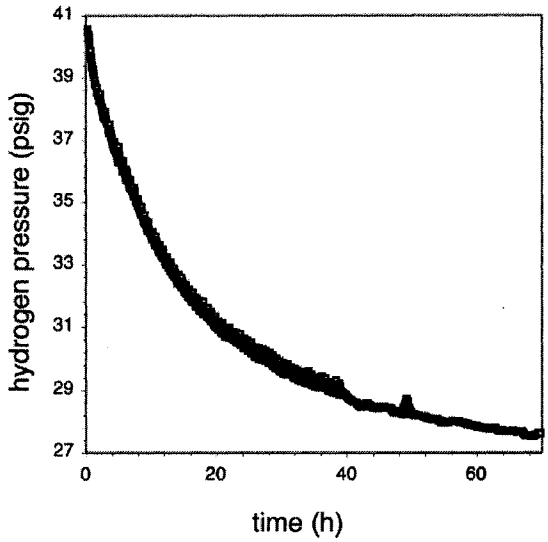

Figure S1. Sample cyclohexene hydrogenation curve in the presence of $[Bu_4N][F]$ under the Improved Conditions of 0.24 mM Ir precursor at 60 °C in propylene carbonate solvent with 0.50 mL cyclohexene. Note that, despite the use of the Improved Conditions which did yield nanoclusters for all four halides, there is a lack of an induction period in the presence of $[Bu_4N][F]$ leading to rapid, uncontrolled nucleation and, overall, polydisperse nanoclusters (60 ± 20 Å).

Further Investigation of the F^- Stabilizer System. The fact that the nanocluster formation kinetics in the presence of F^- are unusual in that they cannot be fit by the known 2-, 3-, or 4-step nanocluster formation mechanisms suggested that either: (i) F^- coordinates less to the (1,5-COD)Ir^+ precursor, so it slows nucleation less; (ii) F^- poisoning of the cyclohexene hydrogenation reporter reaction is occurring; or (iii) some other explanation. To test hypothesis (ii), we carried out two additional nanocluster formation reactions under the Improved Conditions in propylene carbonate in the presence of $[Bu_4N][F]$, but changing the volume of cyclohexene to one half or one quarter of the amount originally used to determine whether or not the nanocluster formation kinetics change as a function of cyclohexene concentration—they should not if the cyclohexene reporter reaction is working properly.[1] The kinetics of these three hydrogenations could not be fit to any of the 2-, 3-, or 4-step mechanisms for nanocluster nucleation, growth, and agglomeration; in addition, the timescale for complete hydrogenation was a strong function of the amount of cyclohexene (see Table S1). Hence, at least one problem appears to be that the cyclohexene reporter reaction is not reliable under Improved Conditions in the presence of F^-, for reasons which remain obscure. Because of the overall poor properties of the F^- system, further investigations were deemed unwarranted.

[1] M. A. Watzky and R. G. Finke, J. Am. Chem. Soc. 119, 10382 (1997); see Figure 6 therein.

Table S1. Total cyclohexene hydrogenation reaction times in the presence of $[Bu_4N][F]$ under the Improved Conditions of 0.24 mM Ir precursor at 60 °C in propylene carbonate solvent. For entries 1, 3, and 4, the reaction time refers to the complete consumption of cyclohexene; in entry 2, incomplete consumption of cyclohexene was observed (approx. 70 % hydrogenation) but hydrogenation activity ceased. Had the reaction continued until completion, extrapolation of the reaction time indicates that the reaction would have been complete in ~30 h. In short, these results show that the cyclohexene hydrogenation times are a strong function of amount of cyclohexene, indicating that the catalytic reporter reaction cannot be trusted in the case of F^-.[1]

	volume cyclohexene	reaction time
1	0.50 mL	70 h
2	0.50 mL	20 h
3	0.25 mL	1.6 h
4	0.13 mL	1.2 h

CHAPTER VI

NANOCLUSTER STABILIZATION IN IONIC LIQUIDS: EVIDENCE FOR *N*-HETEROCYCLIC CARBENE FORMATION FROM IMIDAZOLIUM-BASED IONIC LIQUIDS DETECTED BY ^{2}H NMR

This dissertation chapter contains the manuscript of a communication with extensive Supporting Information published in *Journal of the American Chemical Society*, and describes an investigation into the true source of nanocluster stabilization observed in ionic liquids. Kinetic and D labeling studies imply that nanoclusters catalyze the formation of *N*-hereocyclic carbenes from the imidazolium component of the ionic liquid. These carbenes are then predicted to be the source of the stabilization observed in ionic liquids.

Dr. Maggel Deetlefs (MD) prepared the ionic liquids used in this study, and MLC (an undergraduate student working under the direction of LSO) performed the initial survey experiments in neat ionic liquids. Dr. Ken Seddon (KRS) read the manuscript and suggested minor revisions. The manuscript was prepared by LSO, with assistance and editing from RGF.

Abstract

The mystery of how imidazolium-based ionic liquids (ILs) can provide high stabilization for transition-metal(0) nanoclusters—that is, in the absence of the usual strongly coordinating anions—has been probed. ^2H NMR product and kinetic studies of imidazolium ILs under D_2 reveal that nanocluster-catalyzed H/D exchange occurs at the 2- (as well as at the 4-, 5- and 8-) C-H positions of the imidazolium cation. The results (i) provide compelling evidence that N-heterocyclic carbene formation and ligation of nanoclusters is occurring in ILs; and (ii) argue that N-heterocyclic carbenes merit further investigation as heretofore unappreciated stabilizers of transition-metal nanoclusters.

Introduction

Ionic liquids (ILs) are very good *apparent* stabilizers of transition-metal nanoclusters / nano-colloids.[1,2,3,4,5,6,7] However, *precisely how* ILs stabilize transition-metal nanoclusters has remained a mystery, since only anions such as $[BF_4]^-$, $[PF_6]^-$, or $[N(SO_2CF_3)_2]^-$, Scheme 1, are typically present—albeit in high concentrations in neat ILs. Can even such non-basic, weakly coordinating anions bind tightly to nanocluster surfaces to provide classic, anion-based, DLVO (Dergaugin-Landau-Verwey-Overbeek) type Coulombic repulsion between, and thus stabilization of, (nano)colloidal particles?[8] Or, is there some other source of nanocluster stabilization in ILs?

Scheme 1. Three 1-butyl-3-methylimidazolium, $[bmim]^+$, based ILs utilized in the present studies. The $[N(SO_2CF_3)_2]^-$ anion is abbreviated, as in the literature, as $[NTf_2]^-$.

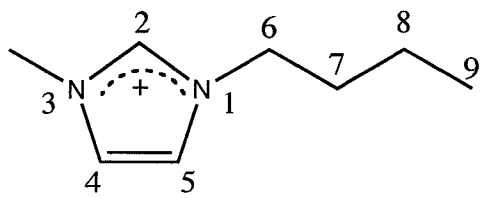

Herein, after confirming that ILs provide high nanocluster stabilization in our hands as in the literature,[1-7] we tested five alternative hypotheses as to the source(s) of this high stabilization. Our results: (i) provide compelling D labeling and ^2H NMR evidence for *the formation of N-heterocyclic carbenes from imidazolium-based ILs*; (ii) provide, thereby, the first evidence for a *N*-heterocyclic carbene ligated to a nanocluster; (iii) contribute to the growing literature implicating some ILs as non-innocent solvents,[9,10,11,12,13] and (iv) illustrate an easily implemented ^2H NMR-based technique[14] for the detection of H/D exchange reactions on reactive nanocluster surfaces. The latter is significant in its own right since nanoclusters hold considerable potential to serve as well defined, easily studied, soluble analogs of the commercially important heterogeneous catalysts.[15]

Results and Discussion

We chose the $Ir(0)_n$ nanoclusters in Scheme 2 for our studies based on a series of papers,[16] especially key papers which rate the relative efficacy of transition-metal nanocluster stabilizers using $Ir(0)_n$ as the prototype system.[17] Scheme 2 illustrates the synthesis of the $Ir(0)_n$ nanoclusters via the reduction of $[(1,5\text{-COD})Ir(CH_3CN)_2]BF_4$ (**1**)

under H_2 in the presence of Proton Sponge™ (PS™) *in acetone*, with predetermined but variable amounts (*x* eqvs, Scheme 2) of the IL [bmim][NTf_2].

Scheme 2. The $Ir(0)_n$ nanocluster system employed herein.

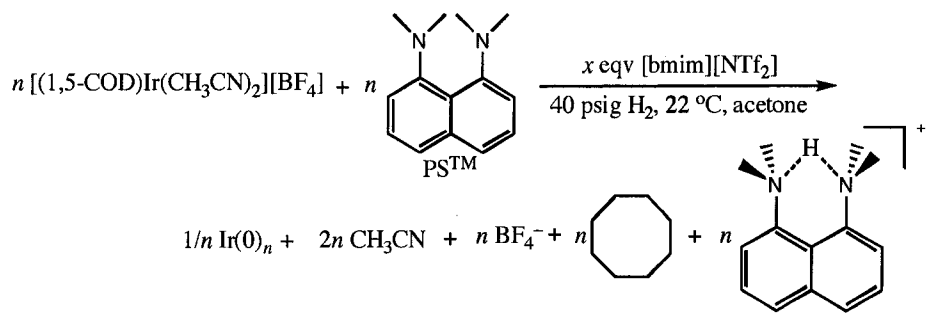

First, control experiments were performed to confirm that the IL is the source of a high degree of stabilization of the Ir(0) nanoclusters. With *no* added IL, a colorless, clear reaction solution plus bulk metal (only) results. However, increasing the [bmim][NTf_2] to 10 equivs yields a stable, dark-brown Ir(0) nanocluster[18] solution (no bulk metal was observed) containing 2.1±0.6 nm nanoclusters by transmission electron microscopy (TEM; 201 particles counted). A TEM control consisting of the precursor alone in the IL did not yield nanoclusters; that is, the observed nanoclusters are not an artifact of precursor reduction in the energetic TEM beam.[19] With higher, 100, 250, and 480 equivalents of IL (the latter equaling neat [bmim][NTf_2]), stable, dark-brown nanocluster solutions are formed that are stable against agglomeration for >1 year. Ir(0) nanoclusters in [bmim][NTf_2] IL are, therefore, highly stabilized.

Next, we experimentally excluded trace Cl^-, H_2O, coordination by CH_3CN or Proton Sponge™ as sources of the observed high stabilization (see the Supporting Information for details). We were forced, therefore, to the alternative hypothesis that the

cationic, imidazolium component of ILs might—surprisingly and unprecedentedly—be interacting or reacting with the nanocluster surface by either: (i) a little precedented, seemingly unlikely, but conceivable,[20] η^5-coordination of the imidazolium *cation* to the *electron deficient* metal(0) surface; or more likely by (ii) C-H oxidative addition of the acidic, p*Ka*≈24 C-H bond[21] in the 2-H position of the imidazolium cation, resulting in *N*-

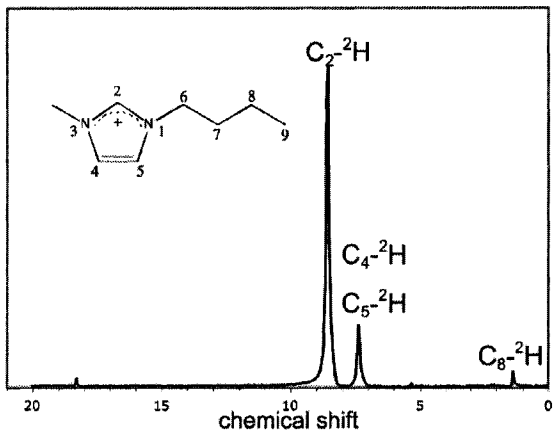

heterocyclic carbene formation atop the nanocluster's metal(0) surface.

Figure 1. ^{2}H NMR spectroscopy showing deuterium incorporation in the 2, 4, 5, and 8 positions of the imidazolium cation, $[bmim]^+$. The rate of D incorporation is faster for the 2, 4, and 5 positions; incorporation at the 8position of the alkyl chain is slower (>8 h) as discussed in the Supporting Information.

The crucial experiments detecting surface-ligand-coordinated *N*-heterocyclic carbene formation in ILs were accomplished using D_2 plus ^{2}H NMR spectroscopy, Figure 1. *Deuterium incorporation is apparent at the 2-H, 4-H, 5-H and 8-H positions of the imidazolium cation.* ^{1}H NMR spectra of the same reaction solution confirmed the expected decreased intensity of the 2-, 4-, and 5-H hydrogens in the $[bmim][NTf_2]$ (see Table S3 of the Supporting Information). A control experiment shows that if the nanocluster precursor **1** is omitted from the reaction, no D-incorporation into the

imidazolium cation occurs; this rules out carbene formation by base deprotonation of the weak, (aqueous) pK_a≈24 imidazolium acid 2-H site,[9,10,13,22,23,24,25,26,27,28] by the (aqueous) pK_a≈12.4 base Proton Sponge™ (DpK_a = 11.6).

Instead, a sequence of *N*-heterocyclic carbene formation by oxidative addition[11,29,30] of the imidazolium cation, H/D scrambling atop the nanocluster surface, then reductive elimination of a C-D bond, is implicated. However, since precedent exits for the oxidative addition of imidazolium salts to iridium organometallic complexes,[31,32] the kinetics of deuterium incorporation as a function of time were studied to distinguish the nanocluster vs. iridium organometallic complex H/D exchange mechanisms. If the Ir(0) nanoclusters are the true catalyst (and must be formed before H/D exchange can occur), then an induction period plus sigmoidal, autocatalytic kinetics diagnostic of nanocluster formation[33,34] (A → B, then A + B → 2B) should be observed. On the other hand, if **1** is the key H/D exchange catalyst, then *no induction period* and smooth, presumably second-order kinetics should be observed.

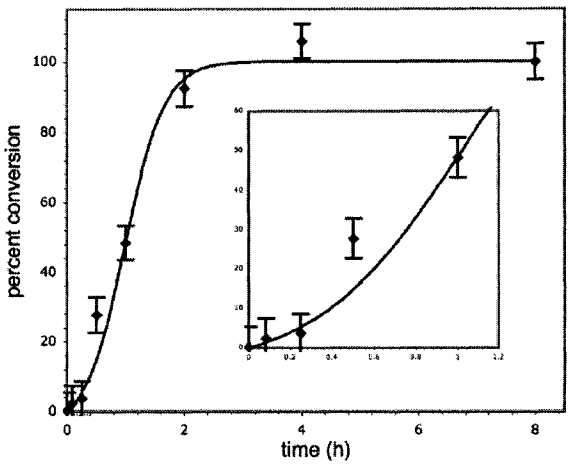

Figure 2. Deuterium incorporation kinetics into the 2-H position of $[bmim]^+$. The curve-fit is to the A → B (rate constant k_1), then A + B → 2B (rate constant k_2) mechanism diagnostic of transition-metal nanocluster nucleation and autocatalytic surface-growth.[33,34] The data were fit with MacKinetics, yielding the rate constants k_1=0.078(2) and k_2=0.038(1).

Figure 2 shows the results of eight separate, time-dependent NMR experiments (one for each data point shown), under D_2 with 3.6 mM (10 equivalents) of $[bmim][NTf_2]$ in acetone at 22 °C. As predicted for the nanocluster as the true H/D exchange catalyst, deuterium incorporation in the 2-H and 4-H (Figure S1) positions occurs *only after an induction period.* Moreover, the kinetics are well-fit by the analytic equations corresponding to the A —> B, plus A + B —> 2B mechanism diagnostic of nanocluster formation,[33,34] Figure 2. The coordinatively unsaturated surface of the nanocluster is clearly implicated as the true catalyst.

Conclusion

In conclusion, Ir(0) nanoclusters react with imidazolium-based ILs to form surface-attached carbenes, at least transiently. This contributes to the growing literature

implicating some ILs as non-innocent solvents[9-13] and raises a new hypothesis—*carbene-ligand-stabilized* nanoclusters.[35]—as to how imidazolium-based ILs could be providing some stabilization to transition-metal nanoclusters:[1,36] via The present studies provide the first example of a carbene ligating a nanocluster surface, and suggest that *N*-heterocyclic carbene ligation and stabilization of nanoclusters is a topic which merits further investigation. Note that some p bound, h^5-imidazolium cation atop the nanocluster surface is still conceivable, although there is presently no evidence for it. In addition, DLVO-type stabilization by coordination of even anions such as $[BF_4]^-$, $[PF_6]^-$ or $[N(SO_2CF_3)_2]^-$ to electron-deficient nanocluster surfaces under neat IL (i.e., high concentration, no co-solvent) conditions is still possible if not probable in our opinion.

Acknowledgments: Dr. C. Rithner assisted with the ^2H NMR. This work was funded by DOE grant DE-FG02-03ER15453.

Supporting Information Available: the additional materials referred to in the text as well as additional experiments, data, evidence, discussion and additional references.

References

[1] Dupont, J.; Fonseca, G. S.; Umpierre, A. P.; Fichtner, P. F. P.; Teixeira, S. R. *J. Am. Chem. Soc.* **2002**, *124*, 4228.
[2] Scheeren, C. W.; Machado, G.; Dupont, J.; Fichtner, P. F. P.; Texeira, S. R. *Inorg. Chem.* **2003**, *42*, 4738.
[3] Fonseca, G. S.; Umpierre, A. P.; Fichtner, P. F. P.; Teixeira, S. R.; Dupont, J. *Chem. Eur. J.* **2003**, *9*, 3263.
[4] Caló, V.; Nacci, A.; Monopoli, A.; Laera, S.; Cioffi, N. *J. Org. Chem.* **2003**, *68*, 2929.
[5] Huang, J.; Jiang, B.; Gao, H.; Chang, Y.; Zhao, G.; Wu, W. *Chem. Commun.* **2003**, *14*, 1654.
[6] Kim, K.-S.; Demberelnyamba, D.; Lee, H. *Langmuir* **2004**, *20*, 556.

[7] Huang, J.; Jiang, T.; Gao, H.; Han, B.; Liu, Z.; Weize, W.; Chang, Y.; Zhao, G. *Angew. Chem. Int. Ed.* **2004**, *43*, 1397.
[8] Verwey, E. W. J.; Overbeek, J. Th. G. *Theory of the Stability of Lyophobic Colloids*; 2nd ed,; Dover Publications, Inc.: Mineola, New York, 1999.
[9] Carmicheal, A. J.; Earle, M. J.; Holbrey, J. D.; McCormac, P. B.; Seddon, K. R. *Org. Lett.* **1999**, *1*, 997.
[10] Xu, L.; Chen, W.; Xiao, J. *Organometallics* **2000**, *19*, 1123.
[11] McGuiness, D. S.; Cavell, K. J.; Yates, B. F.; Skelton, B. W.; White, A. H. *J. Am. Chem. Soc.* **2001**, *123*, 8317.
[12] Peris, E.; Crabtree, R. H. *C. R. Chemie* **2003**, *6*, 33.
[13] Nyce, G. W.; Glauser, T.; Connor, E. F.; Möck, A.; Waymouth, R. W.; Hedrick, J. L. *J. Am. Chem. Soc.* **2003**, *125*, 3046.
[14] A SciFinder search returned 7446 hits for "H/D exchange". For a recent example see: Yung, C. M.; Skaddan, M. B.; Bergman, R. G. *J. Am. Chem. Soc.* **2004**, *126*, 13033 and others in the Supporting Information.
[15] Finke, R. G. In *Metal Nanoparticles: Synthesis, Characterization, and Applications*; Feldheim, D. L.; Foss, C. A., Jr., Eds.; Marcel Dekker: New York, 2001.
[16] Hornstein, B. J.; Finke, R. G. *Chem. Mater.* **2004**, *16*, 139.
[17] Özkar, S.; Finke, R. G. *Langmuir* **2003**, *19*, 6247 and references therein.
[18] Creighton, J. A.; Eadon, D. G. *J. Chem. Soc., Farad. Trans.* **1991**, *87*, 3881.
[19] Jaska, C. A.; Manners, I. *J. Am. Chem. Soc.* **2004**, *126*, 9776.
[20] Collman, J. P.; Hegedus, L. P.; Norton, J. R.; Finke, R. G. *Principles and Applications of Organotransition Metal Chemistry*; University Science Books: Mill Valley, CA, 1987.
[21] Herrmann, W. A.; Köcher, C. *Angew. Chem. Int. Ed. Engl.* **1997**, *36*, 2162.
[22] Zhang, C.; Huang, J.; Trudell, M. L.; Nolan, S. P. *J. Org. Chem.* **1999**, *64*, 3804.
[23] Deshmukh, R. R.; Rajagopal, R.; Srinivasan, K. V. *Chem. Commun.* **2001**, *17*, 1544.
[24] Lee, H. M.; Jiang, T.; Stevens, E. D.; Nolan, S. P. *Organometallics* **2001**, *20* 1255.
[25] Vásquez-Serrano, L. D.; Owens, B. T.; Buriak, J. M. *Chem. Commun.* **2002**, *21*, 2518.
[26] Poyatos, M.; Uriz, P.; Mata, J. A.; Claver, C.; Fernandez, E.; Peris, E. *Organometallics* **2003**, *22*, 440.
[27] Mas-Marzá, E.; Poyatos, M.; Sanaú, M.; Peris, E. *Inorg. Chem.* **2004**, *43*, 2213.
[28] Earle, M.J. and Seddon, K.R., World Pat., WO 01 77081 (2001).
[29] McGuiness, D. S.; Mueller, W.; Wasserscheid, P.; Cavell, K. J.; Skelton, B. W.; White, A. H.; Englert, U. *Organometallics* **2002**, *21*, 175.
[30] Clement, N. D.; Cavell, K. J.; Jones, C.; Elsevier, C. J. *Angew. Chem. Int. Ed.* **2004**, *43*, 1277.
[31] Prinz, M.; Grosche, M.; Herdtweck, E.; Herrmann, W. A. *Organometallics* **2000**, *19*, 1692.
[32] Danopoulos, A. A.; Winston, S.; Hursthouse, M. B. *J. Chem. Soc., Dalton Trans.* **2002**, *16*, 3090.
[33] Watzky, M. A.; Finke, R. G. *J. Am. Chem. Soc.* **1997**, *119*, 10382.
[34] Widegren, J. A.; Aiken, J. D. III; Özkar, S.; Finke, R. G. *Chem. Mater.* **2001**, *13*, 312.
[35] Schmid, G. *Chem. Rev.* **1992**, *92*, 1709.
[36] Fonseca, G. S.; Scholten, J. D. Dupont, J. *Syn. Lett* **2004**, No. 9, 1525 and earlier papers from their 2002 paper[1] to this 2004 paper

SUPPORTING INFORMATION

Nanocluster Stabilization in Ionic Liquids: Evidence for *N*-Heterocyclic Carbene Formation from Imidazolium-Based Ionic Liquids Detected by ^{2}H NMR

Lisa Starkey Ott, Morgan L. Cline, Maggel Deetlefs, Kenneth R. Seddon, and Richard G. Finke

Additional Experimental Details.

Hydrogenation Apparatus. Hydrogenation experiments were carried out in a previously well-described[1,2,3] in-house constructed apparatus designed to continuously monitor pressure loss. This apparatus consists of a Fisher-Porter (F-P) bottle, which connects *via* Swagelok quick-connects to both a dihydrogen line and an Omega PX621 pressure transducer. The pressure transducer is interfaced with a PC by means of an Omega D1131 5V A/D converter with a RS-232 connection. The pressure uptake data was collected using LabView 7.1, and hydrogen uptake curves were fitted to the analytical equations for A→B, plus A+B→2B[2,4] using Origin 7.0. These hydrogen uptake curves were converted to cyclohexene consumption curves using the known 1:1 H_2 to cyclohexene stoichiometry and following the previously established cyclohexene reporter-reaction kinetic method.[5]

Nanocluster Formation *in Acetone* with Varying Equivalents of IL. These conditions were modeled after the Standard Conditions in many of our previous papers[6] with some modifications. For each experiment, $[(1,5\text{-COD})Ir(CH_3CN)_2][BF_4]$ (5.0 mg; 0.011 mmol) was weighed into a pre-dried 2 dram glass vial in the drybox. Next, Proton Sponge™ (2.3 mg; 0.011 mmol) was added to the vial. Then, acetone (1.5 mL) was added with a 1.0 mL gas-tight syringe. To this mixture, a predetermined amount of IL (0, 5, 10, 100, 250 or 480 (corresponding to neat IL; no acetone was added in this last experiment) equivalents *vs.* $[(1,5\text{-COD})Ir(CH_3CN)_2][BF_4]$) were added with a gas-tight syringe. For the kinetic studies, the IL used was $[bmim][NTf_2]$ due to its lower viscosity (η=12.0 cP[7]; this leads to ease of sample preparation and permits efficient stirring). The

solution was agitated with a polyethylene pipette until the solution was homogeneous (both the $[(1,5\text{-COD})Ir(CH_3CN)_2][BF_4]$ and the IL are readily soluble in acetone). The yellow-orange solution was transferred to a new borosilicate culture tube (22 x 175 mm) with a new 5/8" x 5/16" Teflon-coated octagon shaped spin bar. Freshly distilled cyclohexene (1.0 mL) was added to the culture tube with a 1.0 mL gas-tight syringe. The culture tube was placed in the F-P bottle, the F-P bottle was sealed and brought out of the drybox, and hydrogenation was initiated. To begin each reaction, the F-P bottle was purged 13 times with H_2 (40 ± 1 psig, 15 s/purge). Five min after the first purge, the pressure was set at 40 ± 1 psig, $t = 0$ was noted, and pressure *vs.* time data was collected at 2.5 min intervals.

Hydrogen uptake curves from these hydrogenations are shown and discussed below in the section titled "Studies of the Kinetics of Nanocluster Formation *vs.* Equivalents of Added IL." Transmission Electron Microscopy (TEM) from these studies is discussed in the section titled "Transmission Electron Microscopy (TEM) of the Nanoclusters Prepared in Acetone with Varying Equivalents of IL."

Fitting of the Resultant Kinetic Data. MacKinetics (version 0.9, available from http://members.dca.net/leipold/mk/advert.html, equipped with a numerical integration package and a data fitting routine) was used to fit the percent conversion *vs.* time data. Since the data are sigmoidal, they were fitted to the autocatalytic model A → B (rate constant k_1), A + B → 2B (rate constant k_2).[4] Since the fit values obtained from MacKinetics can often be very sensitive to the initial parameters, and since converging on local (rather than the desired global) minima is always a possibility one must strive to

avoid, each data set was fit ≥ 3 times with different initial parameters for each fitting session. Iterations of the fitting program were carried out until the kinetic parameters proved self-consistent — that is, until the program returned the exact values entered as the initial guesses.

Studies of the Kinetics of Nanocluster Formation *vs.* Equivalents of Added IL. Transition-metal nanoclusters form under H_2 via an autocatalytic A→B, A+B→2B mechanism.[4] The kinetics of nanocluster formation under the conditions described above in the section titled "Nanocluster Formation in Acetone with Varying Equivalents of IL" deviate significantly from this now well-precedented autocatalytic mechanism. Qualitatively, they deviatiate from this autocatalytic formation, as illustrated below in Figure S1, by a slowed rate of cyclohexene catalytic hydrogenation near the end of the reaction. Note that increasing equivalents of IL magnify the slowing of the hydrogenation.

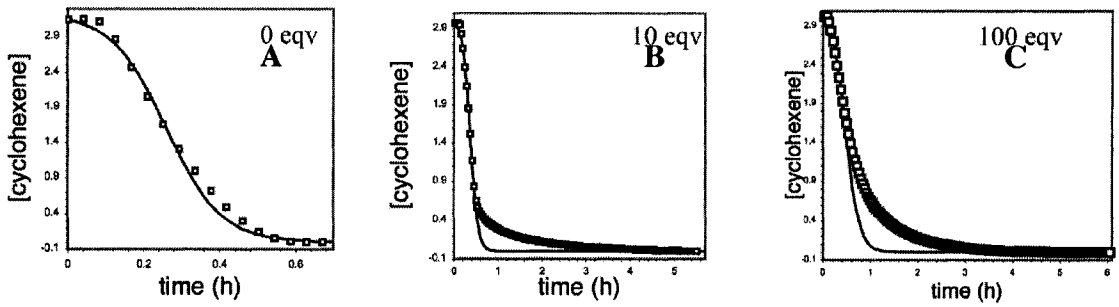

Figure S1 A-C. Hydrogenations in acetone with added IL.

In the three cyclohexene hydrogenation curves S1A-S1C shown above, the experimental data is shown as squares and the fit to the A→B, A+B→2B mechanism is

shown as a line. With 0 equivalents of added IL in acetone, the experimental data is well fit by this mechanism. However, when the equivalents of [bmim][NTf_2] are increased (as shown for 10 (**B**) and 100 equivalents (**C**) above), there is a significant deviation from the autocatalytic mechanism near the end of the hydrogenation. This slowed cyclohexene hydrogenation is plausibly due to carbene coordination to the nanocluster surface and its resultant fewer coordinatively unsaturated, catalytically active surface atoms.

We attempted to fit all hydrogenation curves in acetone with added IL with a new kinetic method developed to monitor nanocluster nucleation, growth, and agglomeration.[8] This mechanism consists of the two steps for nanocluster nucleation and growth described earlier (A→B, rate constant k_1; A+B→2B, rate constant k_2) plus a third step describing the bimolecular agglomeration of two active nanocluster surface atoms (B) to an agglomerated product, C (i.e., B+B→C, rate constant k_3). The data were fit with the numerical integration program MacKinetics (for further discussion of MacKinetics, see the section titled "Fitting of the Resultant Kinetic Data"). Fitting with this three-step mechanism improved the visual fit of the curve to the data. However, the observed error bars associated with this three-parameter fit[9] proved too large to quantitate the agglomeration step (i.e., the k_3 rate constant) as a function of varying the equivalents of IL.

Transmission Electron Microscopy (TEM) of the Nanoclusters Prepared in Acetone with Varying Equivalents of IL. After the nanocluster formation reaction was judged complete by cyclooctane evolution,[4] the F-P bottle was vented, sealed, brought into the drybox, and opened. An aliquot of the dark brown reaction solution (0.5 mL) was

removed with a 1.0 mL gas-tight syringe and placed in an oven-dried scintillation vial. The aliquot was then diluted 15:1 with acetone, resulting in a clear, light brown solution. A silicon monoxide grid (Ted Pella, Inc.) was dipped into the nanocluster solution for 2 s, and allowed to air dry. The grids were sealed in borosilicate, large-opening autosampler vials (1.8 mL) sealed with aluminum crimp-top closures with PTFE/silicon linings. The samples were sent to the University of Oregon where TEM was carried out by Dr. JoAn Hudson and her staff. TEM of these samples show polydisperse, but well-separated, nanoclusters: 2.4 ± 0.6 nm nanoclusters (197 particles counted), for example, for a sample prepared in acetone in the presence of 10 equivalents [bmim][NTf_2].

Control Demonstrating that Nanoclusters Are Not Formed in the TEM Beam in Acetone with Varying Equivalents IL. Recently, it has been shown that it is possible to form metal nanoclusters from organometallic precursors in the energetic TEM beam.[10,11] Consequently, it was important to rule out nanocluster formation in the TEM beam for our system. Therefore, a TEM grid was prepared with the organometallic precursor prior to reduction to determine whether or not nanoclusters were being formed under TEM conditions with an accelerating voltage of 120 kV.

In the drybox, [(1,5-COD)Ir($CH_3CN)_2$][BF_4] (5.0 mg; 0.011 mmol) was weighed into a pre-dried 2 dram glass vial. Next, Proton Sponge™ (2.3 mg; 0.011 mmol) was added to the vial. Then, acetone (1.5 mL) was added with a 1.0 mL gas-tight syringe. To this mixture, a predetermined amount of IL (0, 5, 10, 100, or 250 equivalents *vs.* [(1,5-COD)Ir($CH_3CN)_2$][BF_4]) was added with a gas-tight syringe. The solution was agitated with a polyethylene pipette until the solution was homogeneous (both the

[(1,5-COD)Ir($CH_3CN)_2$][BF_4] and the IL are readily soluble in acetone). An aliquot (0.5 mL) of this yellow-orange solution was removed with a 1.0 mL gas-tight syringe and placed in a separate pre-dried glass scintillation vial. The aliquot was then diluted 15:1 with acetone, resulting in a clear, light yellow-orange solution. A silicon monoxide grid (Ted Pella, Inc.) was dipped into the nanocluster solution for 2 s, and allowed to air dry. Finally, the grid was sealed in a borosilicate, large-opening autosampler vial (1.8 mL) sealed with aluminum crimp-top closures with PTFE/silicon linings. The sample was sent to the University of Oregon where TEM was carried out by Dr. JoAn Hudson and her staff.

Six images were taken of this precursor-only grid with an accelerating voltage of 120 kV. These images showed no nanocluster formation: either the blank grid was imaged, or some feature of the grid (for example, a tear) was imaged. Consequently, we can conclude that no nanocluster formation is taking place under the conditions of the TEM imaging. Therefore, the nanoclusters we observed above in the section titled "Transmission Electron Microscopy (TEM) of the Nanoclusters Prepared in Acetone with Varying Equivalents of IL" do not contain such artifacts.

Alternative Hypotheses for the True Source of Nanocluster Stabilization in Ionic Liquids. Hypothesis #1: Trace Cl^- and/or H_2O. One initial hypothesis was that trace Cl^- and/or water present in the ILs might be stabilizing the nanoclusters in the absence of any superior stabilizing entity. Accordingly, we tested the ILs for Cl^- and H_2O to determine if we could correlate an increase in stability with an increase in either Cl^- or H_2O content. The results of these tests for both commercially obtained (Fluka) and

independently prepared (at the Queen's University Ionic Liquid Laboratories, QUILL) ILs are reported as Table S1.

Table S1.

IL	Cl^- content[a] (ppm)	LoQ[b] (ppm)	Water content before drying[a] (%)	Water content after drying overnight (*ca.* 15 h) @ 65 °C[a] (%)
Fluka [bmim][PF_6]	7.9	7.1	0.19896	0.03298
Fluka [bmim][BF_4]	228	4.5	0.16166	0.050387
QUILL [bmim][PF_6]	< 7	7.1	0.012452	0.009903
QUILL [bmim][BF_4]	12.6	4.5	0.039984	0.029594
QUILL [bmim][NTf_2]	-[c]	-[c]	0.009038	0.006854

[a]All values are reported as mass substance/mass IL.
[b]LoQ= Limit of Quantitation (the lowest concentration at which quantitative measurements can be made, usually 10 standard deviations from the blank signal).
[c]No halide determination method currently exists for this class of IL.

The ILs were tested for H_2O and Cl^- using previously published methods. Specifically, the H_2O content was determined by Karl-Fischer titration,[5] and the Cl^- content was determined by ion chromatography.[12] In the above table, it can easily be seen that the H_2O content, and more dramatically the Cl^- content, vary according to the source of the IL and the IL anion.

Initially, we attempted to use the five criteria for ranking modern transition metal nanocluster stabilizers published earlier[6] as a means for evaluating the contribution to stability by Cl^- and H_2O. These parameters are: the kinetic control exhibited during the nanocluster formation reaction as measured by the k_2/k_1 ratio, TEM probing the level of disperesity of the nanoclusters, the nanocluster isolability and redissolvability, the catalytic activityof the nanoclusters once redispersed in fresh solvent, and the total

catalytic turnovers (TTOs).[6] For the H_2O and Cl^- tests, the hydrogenations were carried out in the presence of 480 eqv IL (this corresponds to neat IL) in order to maximize the amount of H_2O and/or Cl^- present and therefore maximize the effect (if any) of these impurities.

However, we encountered several difficulties in evaluating the five criteria for nanocluster formation in neat IL. First, the kinetics of nanocluster formation in ILs could be fit for only about the first hour of cyclohexene hydrogenation (after this time catalysis is significantly slowed, as discussed in the section titled "Nanocluster Formation in Neat IL"), negating the acquisition of accurate values for the rate constants k_1 and k_2. Second, the impossibility of isolating the nanoclusters from IL (see the section titled "Attempts to Isolate Nanoclusters Prepared in Neat ILs") eliminates the study of the size dispersity of the nanoclusters. Additionally, since isolation is not possible, one cannot evaluate the isolability, redissolvability, or catalytic activity once redispersed. Consequently, it is not possible to use three of the five criteria of the only modern means at present[13] to rank the stabilization of transition-metal nanoclusters.

However, comparing the Cl^- and H_2O content results with the results for TEM (see the section below titled "TEM of the Nanoclusters in Neat IL"), the solution stability, and the isolation attempts proved informative. Table S2 examines [bmim][BF_4] ILs which differ by a factor of >18 in chloride content and a factor of almost 2 in the water content of even the "dried" samples.

Table S2. A comparison of some of the properties of nanoclusters prepared in [bmim][BF_4].

Source	Dried?[a]	TEM (nm)	Solution stability?[b]	Isolable?	Kinetics Visually Similar?
Fluka	No	2.5 ± 0.8	yes, >6 months	No	Yes
Fluka	Yes	2.8 ± 0.7	yes, >6 months	No	Yes
QUILL	Yes	3.6 ± 0.9	yes, >6 months	No	Yes

[a] ILs were dried as above in Table S1.
[b] Nanocluster solutions were stored in 1.5 mL polyethylene centrifuge tubes and kept in a drybox maintained at <2 ppm O_2.

As limited as the comparison in Table S2 is, the similarity of the nanocluster size, long-term solution stability, and non-isolability while the Cl^- and H_2O are variable indicate that some factor *other* than either Cl^- or H_2O (or their combination) is very likely the source of the stabilization. Additionally, the kinetics of nanocluster formation in each of the ILs are visually *qualitatively* the same regardless of IL source, IL anion, or drying as Table S2 notes (i.e., and even though the k_2/k_1 kinetic control parameter could not be quantitated due to the apparent change in mechanism). These data argue against the "Cl^- and/or H_2O" effects as the key to the nanocluster stabilization.

Alternative Hypotheses for the True Source of Nanocluster Stabilization in Ionic Liquids. Hypothesis #2: CH_3CN Coordination. One potential source of stabilization might be the coordinating CH_3CN ligand, present in 2 equivalents per Ir in the [(1,5-COD)Ir(CH_3CN)$_2$][BF_4] nanocluster precursor. However, coordinating solvents such as pyridine[14,15] often actually *destabilize* nanoclusters. Nevertheless, in order to test this alternative hypothesis, we reduced the above nanocluster precursor under H_2 in neat acetonitrile. If the CH_3CN ligand is the source of the stabilization, then using pure

CH_3CN should lead to highly stabilized nanoclusters. Experimentally, only non-redispersable bulk metal plus a clear, colorless solution (i.e.., one devoid of any Ir(0) nanoclusters) resulted from the reduction of $[(1,5\text{-COD})Ir(CH_3CN)_2][BF_4]$ in CH_3CN. This provides compelling evidence against the alternative hypothesis that CH_3CN is the source of stabilization for nanoclusters formed in ILs.

Alternative Hypotheses for the True Source of Nanocluster Stabilization in Ionic Liquids. Hypothesis #3: Proton Sponge™ Coordination. Another hypothesis was that Proton Sponge™ could conceivably be coordinating with its two nitrogen lone pairs to the coordinatively unsaturated, electrophilic nanocluster surface. This is unlikely, as steric crowding by the two methyl groups is why Proton Sponge™ finds the uses it does– it is a strong H^+ scavenger but a poorly coordinating ligand. Nevertheless, two separate reactions were carried out *in acetone only* (i.e., without any IL present) with either 1 or 10 equivalents of Proton Sponge™ to probe this alternative hypothesis. Both formed non-redispersable bulk metal plus a clear and colorless reaction solution. Consequently, this disproves the alternative hypothesis that Proton Sponge™ is the source of stabilization for the nanoclusters formed in acetone.

Alternative Hypotheses for the True Source of Nanocluster Stabilization in Ionic Liquids. Hypothesis #4: Coordination by the Weakly Coordinating Anions. We continue to suspect that even weakly coordinating anions,[16] such as $[BF_4]^-$, can coordinate to electrophilic nanocluster surfaces, thereby lending some level of DLVO-type stabilization[17] to the nanoclusters, especially in neat ILs where the concentration of $[BF_4]^-$

is very high and where coordinating co-solvents are absent. We are continuing to investigate this possibility.

The one case where we at present do have evidence against $[BF_4]^-$ coordination is from a study carried out in *propylene carbonate* (a polar, weakly-coordinating solvent) with the $[(1,5\text{-COD})Ir(CH_3CN)_2][BF_4]$ precursor, work performed initially as part of another study.[18] In this case, ^{19}F NMR spectroscopy should be able to detect the Ir-F bond, which is expected to appear downfield (in a homogeneous compound containing and Ir-F bond, the signal was observed at δ–219.3 ppm[19]). This First, the ^{19}F NMR spectra of $[Bu_4N][BF_4]$ in propylene carbonate was examined as a reference, and the signal for "free" $[BF_4]^-$ was found at δ –152.4(2) ppm. The ^{19}F NMR spectrum of the reaction solution after complete nanocluster formation had a signal for $[BF_4]^-$ at δ –152.8(2) ppm. *These two values are within experimental error of each other* and the reaction solution does not show any peaks further downfield as would be expected for an Ir-F bond.[19] Consequently, and *at least in propylene carbonate and at concentrations of $[BF_4]^-$ much lower than present in neat ILs*, there is no detectable coordination of the weakly coordinating $[BF_4]^-$ anion to the nanocluster surface. We are in the process of repeating these studies for the specific case of neat ILs to test whether or not there is any DLVO-type stabilization due to even weakly coordinating anions such as $[BF_4]^-$, $[PF_6]^-$, and $[NTf_2]^-$ under neat IL conditions.

Nanocluster Formation in Acetone with Varying Equivalents of IL under Deuterium. These experiments were carried out exactly as reported in the section titled "Nanocluster Formation in Acetone with Varying Equivalents of IL", except the

dihydrogen gas was replaced by dideuterium gas. Based on the results of the experiments performed with varying amounts of IL under H_2, it was determined that 100 equivalents of IL were optimum for studying the kinetics of deuterium incorporation. This was based on the volume of IL used (0.31 mL, enough to isolate easily and use for subsequent NMR spectroscopy) and reproducibility of the timescale of cyclohexene hydrogenation.

For the initial experiment investigating deuterium incorporation, the reaction solution was stirred under D_2 for 22 hours to ensure complete nanocluster formation. Then, the F-P was disconnected from the dideuterium line, vented, sealed, brought into the drybox, and opened. The reaction solution was decanted into a pre-dried 2 dram screw-capped vial, and the volatiles were removed under vacuum for $\geq$ 4 h. The dark brown, oily nanocluster solution in IL that remained was diluted with 600 μL dichloromethane and agitated with a polyethylene pipette until the solution was light brown and homogenous. Then, the same pipette was used to transfer the solution into a pre-dried 5 mm o.d. NMR tube. The tube was capped, brought out of the drybox, and subjected to ^{2}H NMR spectroscopy.

^{2}H NMR spectra recorded on a Varian Inova 400 MHz instrument verified deuterium incorporation in the imidazolium cation, with the spectral parameters: pulse width, 90.0 degrees; acquisition time, 2.666 s; sweep width, 3001.2 Hz; scan repetitions, 432; and total acquisition time, 19 min 25 s. This spectrum is shown as Figure 1 in the main text. An ^{1}H NMR spectrum was also taken of this solution to monitor the decrease of the 2-H, 4-H, 5-H, and 8-H proton signals (spectral parameters: pulse width, 90.0 degrees; acquisition time, 2.291 s; sweep width, 6982.6 Hz; scan repetitions, 1; total

acquisition time, 2 s). Tabulated values for the ^{1}H signal intensities are shown below in Table S3.

Table S3.

Imidazolium Hydrogen	**2**	**4 and 5[a]**	**8**
Expected Relative Intensity	1.00	2.00	2.00
Observed Intensity in Neat IL	0.99	2.00	2.01
Observed Intensity Post IL Reaction	0.26	1.82	1.96

[a]The 4- and 5-H signals overlap as a single, $\Delta\nu_{1/2}\approx$50 Hz peak (Figure 1 in the main text).

As expected, the proton signal decreased as the deuterium signal increased. The 2-H is the most dramatically reduced, as expected for significant carbene formation at the 2 position.

Control Showing No D Incorporation if the [(1,5-COD)Ir(CH_3CN)$_2$][BF_4] Precursor is Omitted. This experiment was carried out exactly as described in the section titled "Nanocluster Formation in Acetone with Varying Equivalents of IL under Deuterium" with 100 equivalents [bmim][NTf_2] except [(1,5-COD)Ir(CH_3CN)$_2$][BF_4] was omitted. The solution was stirred for 22 h under D_2, and then prepared for ^{2}H NMR spectroscopy exactly as described above in the section titled "Kinetic Experiments Under Deuterium Gas to Determine the True H/D Exchange Catalyst". No discernable signals above the noise were observed in the resultant ^{2}H NMR spectra, and the ^{1}H NMR signal intensities were identical to those of neat [bmim][NTf_2] (that is, there was no decrease in signal intensity as a result of deuterium substitution). Hence, one can conclude that a metal catalyst is necessary for D incorporation in the [bmim]$^+$.

Control Confirming None of the Peaks Attributed to D Incorporation are Seen If H_2 Is Employed. This simple control experiment was carried out exactly as described in the section titled "Nanocluster Formation in Acetone with Varying Equivalents of IL." After the reaction was complete, the F-P was vented, brought into the drybox, and opened. Then, the IL was isolated and dried, and an NMR sample was prepared exactly as reported above in the section titled "Nanocluster Formation in Acetone with Varying Equivalents of IL under Deuterium." ^{2}H NMR spectroscopy of the IL showed no discernable signal above the noise, as expected, but was still useful to confirm, thereby providing additional confidence in the D-incorporation studies and their (artifact-free) assignments.

Kinetic Experiments Under Deuterium Gas to Determine the True H/D Exchange Catalyst. These eight experiments were carried out exactly as reported in the section titled "Nanocluster Formation in Acetone with Varying Equivalents of IL under Deuterium" with 100 equivalents of added [bmim][NTf_2]. However, each of the 8 separate reactions was stopped after a predetermined amount of time after $t = 0$ (specifically, $t = 0$, 5 min, 15 min, 30 min, 1 h, 2 h, 4 h, and 8 h). After each stoppage, the dideuterium gas was vented and the F-P bottle sealed, brought into the drybox, and opened. The reaction solution was decanted into a pre-dried 2 dram screw-capped vial, and the volatiles were removed under vacuum for $\geq$ 4 h. The dark brown, oily nanocluster solution in IL that remained was capped, sealed with Parafilm, and stored in the drybox (to avoid contamination by adventitious water) until all of the kinetic runs were complete ($\leq$ 2 weeks).

^{2}H NMR Experiments to Determine the Kinetics of Deuterium Incorporation. In the drybox, each of the eight nanocluster solutions prepared above was diluted with dichloromethane (600 μL). Each diluted solution was then placed in a pre-dried 5 mm o.d. NMR tube, capped, and brought out of the drybox. ^{2}H NMR spectra were recorded on a Varian Inova 500 MHz NMR. Spectral parameters employed were: pulse width, 90.0 degrees; acquisition time, 0.652 s; relaxation delay, 0.0 s; sweep width, 1533.9 Hz; scan repetitions, 2048; and total acquisition time, 22 min 39 sec. A ^{2}H NMR spectrum of the solution that had been exposed to D_2 for 8 hours was taken first. The peaks corresponding to deuteration in the 2-, 4-, and 5-H positions were integrated, and values for these integrals were set and saved. The integral values for these peaks then set a scale for the remaining samples, with the 8 h peak areas and associated integrals corresponding to the maximum values. For the seven remaining ^{2}H NMR experiments, the integration scale remained as it was for the 8 h experiment. Consequently, all integrated values could be referenced to the intensity of the 8 h peaks and, thus, the percent conversion over time could be determined. The results are presented in Figure 2 of the main text for the 2-H position and Figure S2 herein for the 4-H and 5-H positions in the section titled "Kinetics for Deuterium Incorporation in the 4- and 5-H Positions of $[bmim]^+$".

Kinetics for Deuterium Incorporation in the 4-, 5- and 8-H Positions of $[bmim]^+$.

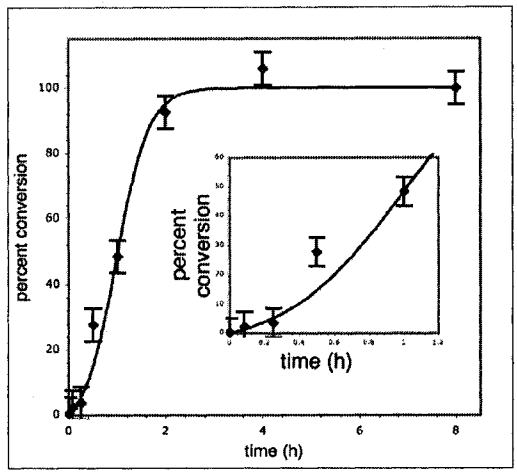

Figure S2. Deuterium incorporation as a function of time in the 4- and 5-H positions of $[bmim]^+$. The curve-fit is to the A → B, then A + B → 2B mechanism diagnostic of transition-metal nanocluster nucleation and autocatalytic surface-growth.[4] The data were fit with MacKinetics 0.9b, yielding the rate constants k_1=0.15(1) and k_2=0.028(3).

As in the case for the 2-H position, the quantitative fit to the A → B, then A + B → 2B mechanism and sigmoidal kinetic curve for deuterium incorporation into the 4- and 5- positions demand that the nanocluster, B, is the active catalyst, [(1,5-COD)Ir(CH_3CN)$_2$][BF_4], A: the kinetics are saying that A must be converted to B (the true catalyst) before H/D exchange can occur. The timescale for deuterium addition into the 4-and 5-H positions is similar to that for the 2-H position (approximately four hours for complete substitution). The mechanism for exchange in the 4- and 5-H positions has good precedent in the oxidative addition of the carbene vinylic C-H bonds to Ir as observed by Crabtree and coworkers ("abnormal" bonding of the imidazolium to Ir),[20,21] although in our case the kinetic results require that B (the nanoclusters) and not A (the [(1,5-COD)Ir(CH_3CN)$_2$][BF_4] precursor) must be the H/D exchange catalyst.

The timescale for deuterium substitution into the 8-H position is longer than for the 2-, 4- or 5-H positions: even after eight hours, there is no substitution in this position,

but after 17 h, substitution in the 8-H position is apparent (see Figure 1 of the main text). It is highly likely that the H/D exchange into the 8-H position follows established H/D pathways in heterogeneous catalysis.[22] The task remains, however, to examine H/D scrambling—as well as the underlying fundamental reactions (such as ligand substitution, oxidative addition, and reductive elimination remain; some ligand substitution studies on Au nanocluster surfaces[23,24] do exist, however)—with well-defined nanoclusters in order to support or refute the precedented heterogeneous catalysis mechanism[22] for the specific case of soluble nanoclusters in media such as ionic liquids.

Attempted Detection of an Ir-C or η^5-Imidazolium Bonds by ^{13}C NMR. A hydrogenation experiment was performed as detailed above in the section titled "Nanocluster Formation in Neat ILs" in [bmim][BF_4]. After stirring under H_2 for 70 h, the F-P bottle was vented, sealed, brought into the drybox, and opened. The dark brown reaction solution was placed in a 10 mm o.d. pre-dried NMR tube with d_6 acetone (0.25 mL) added for instrument locking purposes. ^{13}C NMR spectroscopy was carried out on a Varian Inova 500 MHz NMR with spectral parameters: pulse width, 33.8 degrees; relaxation delay, 5.000 s; acquisition time, 0.667 s; sweep width, 36003.6 Hz; scan repetitions, 1372. A signal appearing at approximately δ174-202 ppm is expected for an Ir-C bond in a homogeneous complex.[25] Approximately the same chemical shift should be expected in for carbon bound to an Ir nanocluster as Ir has a very small Knight shift.[26] No signals were observed between δ150-280 ppm, save the signal from the carbonyl carbon of the acetone internal standard at δ208.4(1). Our inability to observe the Ir-C signal is not surprising, given the low natural abundance of ^{13}C nuclei and the unknown number of

carbenes coordinated to the nanocluster surface. There are also no detectable signals assignable to any η^5-imidazolium ligation of the nanocluster surface (i.e., there is negative evidence against the η^5-imidazolium ligation alternative hypothesis for nanocluster stabilization raised in the main text).

We also performed a control attempting to detect whether or not the imidazolium cation can oxidatively add to the Ir(I) precursor, $[(1,5\text{-COD})Ir(CH_3CN)_2][BF_4]$. In this control, $[(1,5\text{-COD})Ir(CH_3CN)_2][BF_4]$ (5.0 mg, 1.06 μmol) and Proton Sponge™ (2.3 mg, 1.06 μmol) were dissolved in $[bmim][BF_4]$ (2.5 mL) . This solution was agitated thoroughly with a polyethylene pipet and placed in a 10 mm o.d. pre-dried NMR tube. The bright yellow solution was diluted with 0.25 mL d_6 acetone, capped, and brought out of the drybox. ^{13}C NMR spectroscopy was carried out under the exact same conditions and spectral parameters as above. Again, there were no observable peaks in the region of Ir-C bonds. There was also, as expected, no ^{13}C NMR signal in the δ240-255 ppm region characteristic of the C_2 position of a "free" imidazolium carbene[27] nor any other discernable signals (e.g., due to a carbene dimer).

Additional, Initial Background Experiments in Neat ILs

The conditions employed in the main text which utilize primarily ILs *in acetone,* rather than neat ILs, resulted from a battery of experiments done initially which revealed that the combined IL / acetone system is preferred to neat ILs for the majority of the studies reported in the main text. This preference derives from primarily two factors: (i) the homogeneity of the acetone / IL / cyclohexene / cyclohexane (product) and cyclooctane (product) system (vs the biphasic nature of the neat IL / cyclohexene /

cyclohexane (product) and cyclooctane (product) system); and (ii) the easier, more reliable stirring possible for the less viscous acetone / IL system (neat ILs are up to 50 times more viscous than acetone[7]), as vortex stirring of immiscible neat IL / cyclohexene layers proved very difficult. These additional, initial background experiments are summarized next, as they contain useful information for others interested in nanoclusters in ILs.

Controls Ruling Out Mass-Transfer Limitation (MTL) Effects Under Our Reaction and Stirring Conditions in Neat ILs. The solubility of dihydrogen gas in the ILs employed is known to be fairly small, estimated to be $8.8x10^{-4}$ mol L^{-1} atm^{-1} for [bmim][BF_4] and $3.0x10^{-3}$ mol L^{-1} atm^{-1} for [bmim][PF_6][28] (however, there is some debate over the accuracy of these values[29]). In addition, due to the high viscosity of ILs, it was important to determine whether or not the observed kinetics are due to the chemical system itself rather than a reflection of H_2 gas-to-liquid MTL conditions.[30] We chose to carry out these MTL studies in [bmim][PF_6], the most viscous of the ILs studied here with η=48.9 cP,[7] studies that should, therefore, expose any extant MTL effects.

First, we determined the *in situ* hydrogenation rate of fully formed nanoclusters prepared as reported in the section titled "Nanocluster Formation in Neat IL" as a function of stirring speed (see the section titled "TEM of the Nanoclusters in Neat IL" for a discussion of fully formed nanoclusters). After the nanoclusters were fully formed and the F-P bottle had been vented, sealed, brought back into the drybox, and opened, the cyclohexane was removed with a Pasteur pipette. The 1.5 mL solution of nanoclusters remained in the culture tube as a dark-brown, apparently homogeneous solution. An

aliquot of fresh cyclohexene (1.0 mL) was added, and the culture tube was re-sealed in the F-P bottle. Next, the F-P bottle was removed from the drybox and attached to the hydrogenation apparatus. The F-P bottle was pressurized to 40 ± 1 psig, and hydrogenation was initiated at a stirring speed of 650 rpm. After two hours, the F-P bottle was repressurized to 40 ± 1 psig and the stirring speed was lowered to 450 rpm. This repressurization procedure was repeated until five stirring speeds has been tested. These results are shown below as Figure S3.

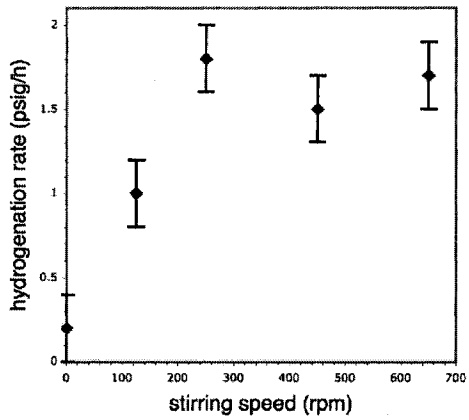

Figure S3. Hydrogenation rate as a function of stirring speed in the neat IL, [bmim][PF_6].

From Figure S3, it is evident that hydrogenation is slowed at stirring speeds ≤ 250 rpm; that is, H_2 gas-to-solution MTL effects are present at ≤250 rpm. Consequently, all hydrogenations performed in this study were stirred at speeds ≥ 650 rpm to ensure we were operating well above the MTL regime. Since the remaining two ILs under study are less viscous than [bmim][PF_6] ([bmim][BF_4] and [bmim][NTf_2] have viscosities of 15.4 cP and 12.0 cP, respectively[7]), stirring at speeds above 650 rpm should be sufficient to avoid MTL conditions in these ILs as well as in the less viscous acetone / IL mixtures emphasized in the main text.

Nevertheless, we performed two additional hydrogenation experiments with different concentrations of the precatalyst [(1,5-COD)Ir(CH_3CN)$_2$][BF_4] to provide further evidence against MTL effects: one experiment was performed exactly as reported in the section titled "Nanocluster Formation in Neat ILs" (0.011 mmol of both [(1,5-COD)Ir(CH_3CN)$_2$][BF_4] and Proton Sponge™), and one was performed with doubled concentration of both precatalyst and Proton Sponge™ (0.022 mmol each). The experiment with doubled concentration completely hydrogenated the cyclohexene in *half the time* of the Initial Conditions reaction, and the initial rate of hydrogenation was *twice* as fast, within experimental error: 1.8(2) mmol H_2/h for the Initial Conditions reaction *vs.* 3.4(2) mmol H_2/h for the doubled concentration reaction. This experiment clearly indicates that it the catalyst concentration, not the amount of dissolved dihydrogen, that is controlling the rate of the reaction under our specific apparatus, temperature and stirring conditions. In short, our nanocluster formation reaction does not have detectable MTL effects under our reaction conditions and at stirring speeds >>250 rpm.

Other Controls in Neat ILs. Numerous other reactions, controls, and TEMs were performed using the *neat IL* conditions and the three ILs cited in the main text, [bmim][PF_6], [bmim][BF_4], and [bmim][NTf_2]. In a number of cases, these studies were done in an attempt to repeat previous literature reports of nanocluster syntheses and catalysis in ILs.[31,32,33,34,35,36,37]

Nanocluster Formation in Neat ILs. These conditions were modeled after the Standard Conditions in many of our previous papers.[6] For each experiment, [(1,5-

COD)Ir($CH_3CN)_2$][BF_4] (5.0 mg; 0.011 mmol) was weighed into a pre-dried 2 dram glass vial in the drybox. Next, Proton Sponge™ (2.3 mg; 0.011 mmol) was added to the vial. Then, the IL being studied (2.5 mL) was added to the vial with a 1.0 mL gas-tight syringe. The solution was vigorously agitated with a polyethylene pipette for ≥5 min to ensure complete dissolution of the [(1,5-COD)Ir($CH_3CN)_2$][BF_4] (for [bmim][PF_6], this was particularly slow, taking approximately 15 min at room temperature). The yellow-orange solution was transferred to a new borosilicate culture tube (22 x 175 mm) with a new 5/8" x 5/16" Teflon-coated octagon shaped spin bar. Next, freshly distilled cyclohexene (0.5 mL) was added to the culture tube with a 1.0 mL gas-tight syringe. The culture tube was then sealed in a Fisher-Porter bottle and removed from the drybox. To begin each reaction, the F-P bottle was purged 13 times with H_2 (40 ± 1 psig, 15 s/purge). Five min after the first purge, the pressure was set at 40 ± 1 psig, $t = 0$ was noted, and pressure *vs.* time data was collected at 2.5 min intervals. A representative example of hydrogenation in commercially obtained [bmim][BF_4] is shown below in Figure S4.

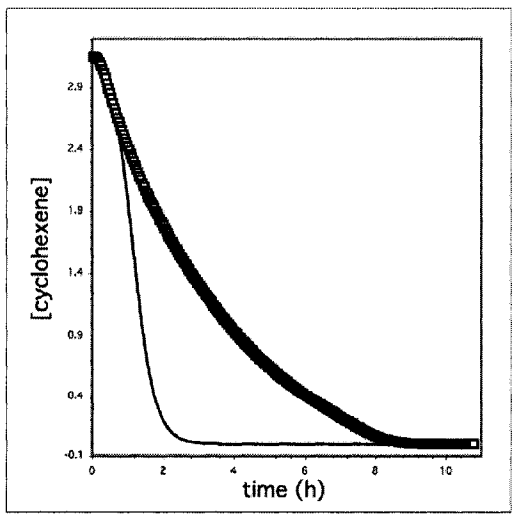

Figure S4. A representative hydrogenation in neat commercial [bmim][PF_6]. The attempted fit to the A→B, A+B→2B mechanism is shown as the thin grey line.

In neat IL, only a very poor fit to the A→B, A+B→2B mechanism of nanocluster formation is seen, Figure S5, the quickly slowed reaction after the induction period looking reminiscent of nanocluster systems which agglomerate. *However*, attempts to fit the nanocluster formation reaction to our published three-step nanocluster formation and then agglomeration mechanism[8] failed (graph not shown). The lack of agglomeration is supported by TEM images of the nanoclusters prepared in neat IL: non-agglomerated, well-separated nanoclusters are observed (see Figure S6 below). We infer, therefore, that N-heterocyclic carbene formation and coordination to the nanocluster surface results in poisoning of the catalyst, an important finding for nanocluster catalysis (i.e., non-catalysis) that merits further investigation and confirmation or refutation.

TEM of Nanoclusters Prepared in Neat IL. In evaluating the size distribution of the nanoclusters formed in neat IL, it is important that the nanoclusters be fully formed to avoid TEM-induced nanocluster formation and resultant artifacts.[10,11] Historically, we have accomplished this by directly monitoring the cyclooctane evolution from the $[Bu_4N]_5Na_3[(1,5\text{-COD})Ir{\bullet}P_2W_{15}Nb_3O_{62}$ precursor by GLC.[4] This valuable technique and organic-product handle built into our Ir systems can, in principle, also be employed with the $[(1,5\text{-COD})Ir(CH_3CN)_2][BF_4]$ precursor used herein. However, the apparent biphasic nature of the neat IL / cyclohexene / cyclohexane (product) and cyclooctane (product) mixture, even when stirred as rapidly as possible and even for the 2.5 mL IL plus 0.5 mL cyclohexene system, made the cyclooctane sampling unreliable. (If one increases the cyclohexene 5 fold to 2.5 mL, the system is clearly biphasic to the naked eye; hence, we

assume that the 0.5 mL cyclohexene conditions are biphasic as well.) In short, accurate sampling the cyclooctane, which partitions into the cyclohexene layer, is not reliable so that the normally useful cyclooctane evolution experiment cannot be employed in this case to determine when the nanoclusters are fully formed.

However, a decent indication of the time after which the nanoclusters are fully formed is available from the cyclohexene reporter reaction.[5] In the past, we have found that cyclooctane evolution takes approximately twice as long as the cyclohexene hydrogenation.[4] For most ILs, the cyclohexene hydrogenation was complete in ~7 h. Consequently, each nanocluster formation reaction was stirred under H_2 for a total reaction time of ≥15 h (i.e., for at least eight hours *after* the cyclohexene hydrogenation was complete) before samples for TEM were collected.

After nanocluster formation in neat IL was judged complete using the criteria above, the F-P bottle was vented, sealed, brought back into the drybox, and opened. An aliquot of the dark brown solution (0.5 mL) was removed with a gas-tight syringe and placed in an oven-dried scintillation vial. The aliquot was then diluted 15:1 with acetone (acetone proving fully miscible with all of the ILs studied), resulting in a clear, light brown solution. A silicon monoxide grid (Ted Pella, Inc.) was dipped into the nanocluster solution for 2 s, and allowed to air dry. The grids were sealed in borosilicate, large-opening autosampler vials (1.8 mL) sealed with aluminum crimp-top closures with PTFE/silicon linings. The samples were sent to the University of Oregon where TEM was carried out by Dr. JoAn Hudson and her staff. A sample TEM showing 3.6 ± 0.9 nm nanoclusters (315 particles counted) prepared in [bmim][BF_4] is shown below in Figure S5.

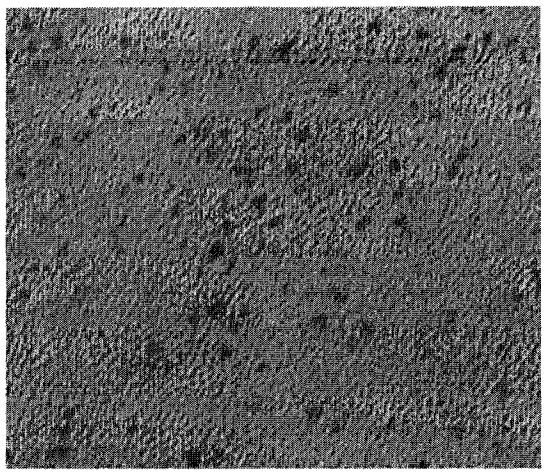

Figure S5. A representative TEM of Ir(0) nanoclusters prepared in neat [bmim][BF_4].

Additional controls confirmed that the [(1,5-COD)Ir(CH_3CN_2)][BF_4] precursor does not forming nanoclusters in the energetic TEM beam. A sample of [(1,5-COD)Ir(CH_3CN_2)][BF_4] (5.0 mg) was dissolved in IL (2.5 mL) and diluted 15:1 with acetone. The rest of the TEM preparation was carried out exactly as reported in the section titled "Transmission Electron Microscopy (TEM) of the Nanoclusters Prepared in Acetone with Varying Equivalents of IL". No nanoclusters were observed in this TEM control experiment. Overall, the TEM controls make it clear that the nanoclusters are fully formed before the TEM analysis.

Finally, TEMs were also obtained for nanocluster solutions that had been used in catalyst recycling experiments which involved even longer times (see the section entitled "Catalyst Recycling Experiments in Neat ILs" below); it was found that there was no change in the size distribution. For example, even after five days of catalyst recycling experiments the nanocluster ize distribution was 3.8 ± 1.1 nm, the same as that seen in

Figure S4 above. Clearly, the nanoclusters in neat ILs are stable against agglomeration for ≥ 1 week under our specific hydrogenation reaction conditions.

Attempts to Isolate Nanoclusters Prepared in Neat ILs. Attempts to isolate the Ir nanoclusters generated in ILs were based on literature reports of successful isolation via centrifugation at 5 minutes at 3,000 rpm.[33] The literature isolations were not repeatable in our hands even after multiple attempts, *vide infra.*

After complete nanocluster formation (≥15 hrs, *vide supra*), the F-P bottle was brought back into the drybox and opened. An aliquot of the dark brown reaction solution (0.5 mL) was removed from the culture tube with a gas-tight syringe, and placed in a polypropylene graduated centrifuge tube (1.5 mL) with a flat-top, snap-cap lid. The lid was sealed with Parafilm, and the tube was transferred out of the drybox. Each sample was centrifuged in an Eppendorf 5415C centrifuge. Each vial was initially centrifuged for 10 min at 5,000 rpm analogous to the literature reports.[33] When this failed, *as it did for the 8 total samples tested,* the vial was further centrifuged for 30 min at 8,000 rpm, then 2x30 min at 12,000 rpm. When this further centrifugation also failed, the centrifuge tube was brought back into the drybox, unsealed, and opened. Acetone (1.0 mL) was added to each sample in order to dilute the solution and reduce the viscosity. The centrifuge vial was re-closed, re-sealed with a new piece of Parafilm, removed from the drybox, and subjected to the same four cycles of centrifugation. *No nanocluster isolation was possible in any of the ILs of conditions tested*; instead, in our hands the nanoclusters remained suspended in solution in every case despite the application of higher centrifugation speeds than those reported in the literature.[33]

Testing the Catalytic Activity of the *in situ* Generated Nanoclusters in Neat ILs. These experiments were carried out in the same fashion and in the same apparatus as in the "Nanocluster Formation in Neat ILs" section above. After complete nanocluster formation, the F-P bottle was brought into the drybox and opened. An aliquot of the dark brown reaction solution (0.5 mL) was removed from the culture tube with a gas-tight syringe and placed in a new culture tube with a new stir bar. Next, the IL under study (2.0 mL) was added to the culture tube, and the tube was gently shaken to mix the nanoclusters into the fresh IL, resulting in a light brown apparently homogeneous solution. To this solution, freshly distilled cyclohexene (0.5 mL) was added. The culture tube was sealed, brought out of the drybox, and hydrogenation was initiated under the conditions reported in the "Initial Conditions for Forming Nanoclusters in Neat ILs" section above. In all cases, we found the *in situ* nanoclusters to be active for further cyclohexene hydrogenation. However, the *in situ* activity was an order of magnitude lower than the activity we have seen for $Ir(0)_n$ nanoclusters stabilized by polyoxoanions (0.16 mmol H_2/h for nanoclusters prepared in [bmim][NTf_2] as part of this study *vs.* 1.9 mmol H_2/h reported for $P_2W_{15}Nb_3O_{62}^{9-}$ stabilized nanoclusters in acetone[38]).

Testing the Catalytic Activity of the Isolated Nanoclusters. These experiments, normally performed as a part of a series of five tests,[38] are designed to determine whether or not the nanoclusters can be taken to dryness and redispersed in fresh solvent without losing catalytic activity. However, since the nanoclusters in ILs were not isolable, this test was not possible.

Testing the "Recyclability" of the *in situ* Nanoclusters in Neat ILs. These experiments were designed to test the claim[31] that nanoclusters prepared in neat ILs were recyclable, reusable hydrogenation catalysts. An aliquot of the nanoclusters (0.5 mL) was taken after complete nanocluster formation and the activity of the *in situ* nanoclusters was assessed as above in the "Testing the Catalytic Activity of the *in situ* Generated Nanoclusters in Neat ILs" section. After 24 h, the dihydrogen pressure was vented and the F-P bottle was sealed, brought into the drybox, and opened. There, the culture tube was removed from the F-P bottle and the organic layer was removed with a Pasteur pipette. An aliquot was taken for ^{1}H NMR analysis to determine the percent conversion of cyclohexene. A fresh aliquot of cyclohexene (0.5 mL) was added to the culture tube, which was re-sealed in the F-P bottle. The bottle was brought out of the drybox and hydrogenation was initiated as detailed above in the "Nanocluster Formation in Neat ILs" section.

For nanoclusters in all three neat ILs, the hydrogenations were slow—the now expected result given that surface-bound carbenes are probably poisoning some of the catalytically active sites. Nanoclusters in IL were recyclable in tests up to five fresh hydrogenations, but the hydrogenation rates decreased significantly during the recycling process. For example, nanoclusters suspended in pre-dried [bmim][BF_4] prepared at QUILL had an initial hydrogenation rate of 0.16(1) mmol H_2/h which decreased 50% to 0.082(4) mmol H_2/h after five consecutive days of recycling.

Attempted Control Experiment Testing the Effect of Added Polyoxoanion in ILs. The current "Gold Standard" anionic stabilizer for at least Ir(0) nanoclusters is $P_2W_{15}Nb_3O_{62}^{9-}$.[39] Consequently, a conceptually important experiment is to examine the effects of this polyoxoanion in ILs in order to determine if an especially high stabilization could result from the combination of the superior anion and the IL.[38] However, addition of $[Bu_4N][P_2W_{15}Nb_3O_{62}]$ to any of the three ILs studied herein results in the immediate formation of a white, insoluble precipitate, almost surely due to the bulky cation of the IL and the $P_2W_{15}Nb_3O_{62}^{9-}$ having a sizable lattice energy thereby driving the formation of an insoluble precipitate. It was, therefore, impossible to perform this otherwise important and interesting control experiment. The incompatibility of at least the imidazolium IL with at least this polyanion, a superior anionic stabilizer of transition-metal nanoclusters,[38] is noteworthy.

Recent Literature on the Non-innocence of ILs as Solvents. The issue of the non-innocence of IL solvents is drawing increasing attention. Recently, a communication titled "On the Noninnocent Nature of 1,3-Dialkylimidazolim Ionic Liquids"[40] has appeared. Additionally, three recent articles document the reactivity of 1,3-subsituted imidazolium cations (whether added as a salt or in IL form) towards oxidative addition to low and/or zero valent metals.[41,42,43] These important references are mentioned here in the Supporting Information, rather then in the main text as we would have preferred, due only to that fact that their inclusion in the main text was ruled out by the 2 page space limitations for communications wherein this text was originally published.

Additional Relevant References

Recent Representative Examples of a Voluminous Literature Using H/D Exchange Reactions to Study Catalysis:

Buskens, P.; Giunta, D.; Leitner, W. *Inorg. Chim. Acta* **2004**, *357*, 1969.
Fox, D. J.; Bergman, R. G. *Organometallics* **2004**, *23*, 1656.
Hunger, M. *Catal. Today* **2004**, *97*, 3.
Daguenet, C.; Scopelliti, R.; Dyson, P. J. *Organometallics*, **2004**, *23*, 4849.

Nanoclusters as Analogs of Heterogeneous Catalysis:

Aiken, J. D., III; Lin, Y.; Finke, R. G. *J. Mol. Cat. A: Chem.* **1996**, *114*, 29.
Aiken, J. D., III; Finke, R. G. *J. Mol. Cat. A: Chem.* **1999**, *145*, 1.

Series of Papers Behind the Choice of the Ir(0) System:

Lin, Y.; Finke, R. G. *J. Am. Chem. Soc.* **1994**, *116*, 8335.
Lin, Y.; Finke, R. G. *Inorg. Chem.* **1994**, *33*, 4891.
Watzky, M. A.; Finke, R. G. *J. Am. Chem. Soc.* **1997**, *119*, 10382.
Watzky, M. A.; Finke, R. G. *Chem. Mater.* **1997**, *9*, 3083.
Widegren, J. A.; Aiken III, J. D.; Özkar, S.; Finke, R. G. *Chem. Mater.* **2001**, *13*, 312.

Efficacy of Nanocluster Stabilizers:

Özkar, S.; Finke, R. G. *J. Am. Chem. Soc.* **2002**, *124*, 5796.
Özkar, S.; Finke, R. G. *Langmuir* **2002**, *18*, 7653.
Hornstein, B. J.; Finke, R. G. *Chem. Mater.* **2003**, *15*, 899.
Özkar, S.; Finke, R. G. *Langmuir* **2003**, *19*, 6247.
Özkar, S.; Finke, R. G. *J. Organomet. Chem.* **2004**, *689*, 493.

Ionic Liquids

Rogers, R. D.; Seddon, K. R. (ed.), *Ionic Liquids IIIB: Transformations and Processes*; American Chemical Society: Washington D.C., 2004; Vol. 902.
Rogers, R. D.; Seddon, K. R. (ed.), *Ionic Liquids IIIA: Properties and Structure*; American Chemical Society: Washington D.C., 2004; Vol. 901.
Wasserscheid, P.; Welton, T. (ed.), *Ionic Liquids in Synthesis*; Wiley-VCH: Weinheim, 2003.
Rogers, R. D.; Seddon, K. R. (ed.), *Ionic Liquids as Green Solvents: Progress and Prospects*; American Chemical Society: Washington D.C., 2003; Vol. 856.
Rogers, R. D.; Seddon, K. R.; Volkov, S. (ed.), *Green Industrial Applications of Ionic*

Liquids; Kluwer: Dordrecht, 2002; Vol. 92.
Rogers, R. D.; Seddon, K. R. (ed.), *Ionic Liquids: Industrial Applications for Green Chemistry*; American Chemical Society: Washington D.C., 2002; Vol. 818.

---

[1] Lin, Y.; Finke, R. G. *J. Am. Chem. Soc.* **1994**, *116*, 8335.
[2] Watzky, M. A.; Finke, R.G. *Chem. Mater.* **1997**, *9*, 3083.
[3] Aiken, J. D., III; Finke, R. G. *Chem. Mater.* **1999**, *11*, 1035.
[4] Watzky, M. A.; Finke, R. G. *J. Am. Chem. Soc.* **1997**, *119*, 10382.
[5] Widegren, J. A.; Aiken, J. D., III; Özkar, S.; Finke, R. G. *Chem. Mater.* **2001**, *13*, 312.
[6] Özkar, S.; Finke, R. G. *Langmuir* **2003**, *19*, 6247 and references therein.
[7] Anderson, K.; Goodrich, P.; Hardacre, C.; Rooney, D. W. *Green Chem.* **2003**, *5*, 448.
[8] Hornstein, B. J.; Finke, R. G. *Chem. Mater.* **2004**, *1*, 139.
[9] Besson, C.; Finney, E. E.; Finke, R. G. Unpublished results.
[10] Hagen, C. M; Widegren, J. A.; Maitlis, P. M.; Finke, R. G. "Is it Homogeous or Heterogeneous Catalysis? Compelling Evidence for Both Types of Catalyts Derived from $[Rh(\eta^5\text{-}C_5Me_5)Cl_2]_2$ as a Function of Temperature and Hydrogen Pressure" *J. Am. Chem. Soc.*, **2005**, in press.
[11] Jaska, C. A.; Manners, I. *J. Am. Chem. Soc.* **2004**, *126*, 9776.
[12] Villagran, C.; Deetlefs, M.; Pitner, W. R.; Hardacre, C. *Anal. Chem.* **2004**, *76*, 2118.
[13] Historical methods of ranking stabilizers are antiquated, qualitative, and applicable only to Au colloids in water: (a) Zsigmondy, R. *Z. Anal. Chem.* **1901**, *60*, 697. (b) Thiele, H.; von Levern, H. S. *J. Coll. Sci.* **1965**, *20*, 679..
[14] Weitz, D. A.; Huang, J. S.; Lin, M. Y.; Sung, J. *Phys. Rev. Lett.* **1985**, *54*, 1416.
[15] Blatchford, C. G.; Campbell, J. R.; Creighton, J. a. *Surf. Sci.* **1982**, *120*, 435.
[16] Strauss, S. H. *Chem. Rev.* **1993**, *93*, 927.
[17] Verwey, E. W. J.; Overbeek, J. Th. G. *Theory of the Stability of Lyophobic Colloids*; 2nd ed,; Dover Publications, Inc.: Mineola, New York, 1999.
[18] Ott, Lisa S.; Finke, R. G. Experiments in progress.
[19] Gorol, M.; Mösch-Zaetti, N. C.; Roesky, H. W.; Noltemeyer, M.; Schmidt, H.-D. *Eur. J. Inorg. Chem.* **2004**, *13*, 2678.
[20] Gründeman, S.; Kovacevic, A.; Albrecht, M.; Faller, J. W.; Crabtree, R. H. *Chem. Commun.* **2001**, *21*, 2274.
[21] Chianese, A. R.; Kovacevic, A.; Zeglis, B. M.; Faller, J. W.; Crabtree, R. H. *Organometallics* **2004**, *23*, 2461.
[22] The literature contains many examples of H/D exchange by heterogeneous catalysts. For a review, see: Burwell, R. L., Jr. *Catalysis Reviews* **1972**, *7*, 25.
[23] Warner, M. G.; Reed, S. M.; Hutchison, J. E. *Chem. Mater.* **2000**, *12*, 3316.
[24] Woehrle, G. H.; Warner, M. G.; Hutchison, J. E. *J. Phys. Chem. B.* **2002**, *106*, 9979.
[25] Mas-Marzá, E.; Poyatos, M.; Sanaú, M.; Peris, E. *Inorg. Chem.* **2004**, *43*, 2213.
[26] Carter, G. C.; Bennett, L. H.; Kahan, D. J. *Metallic Shifts in NMR*. Pergamon Press: New York, 1977.
[27] Arduengo, A. J., III. *Acc. Chem. Res.* **1999**, *32*, 913.
[28] Berger, A.; de Souza, R. F.; Delgado, M. R.; Dupont, J. *Tetrahedron: Asymmetry* **2001**, *12*, 1825.
[29] Anthony, J. L.; Maginn, E. J.; Brennecke, J. F. *J. Phys. Chem. B.* **2002**, *106*, 7315.

[30] Aiken, J. D., III; Finke, R. G. *J. Am. Chem. Soc.* **1998**, *120*, 9545 and references therein.
[31] Dupont, J.; Fonseca, G. S.; Umpierre, A. P.; Fichtner, P. F. P.; Teixeira, S. R. *J. Am. Chem. Soc.* **2002**, *124*, 4228.
[32] Scheeren, C. W.; Machado, G.; Dupont, J.; Fichtner, P. F. P.; Texeira, S. R. *Inorg. Chem.* **2003**, *42*, 4738.
[33] Fonseca, G. S.; Umpierre, A. P.; Fichtner, P. F. P.; Teixeira, S. R.; Dupont, J. *Chem. Eur. J.* **2003**, *9*, 3263.
[34] Caló, V.; Nacci, A.; Monopoli, A.; Laera, S.; Cioffi, N. *J. Org. Chem.* **2003**, *68*, 2929.
[35] Huang, J.; Jiang, B.; Gao, H.; Chang, Y.; Zhao, G.; Wu, W. *Chem. Commun.* **2003**, *14*, 1654.
[36] Kim, K.-S.; Demberelnyamba, D.; Lee, H. *Langmuir* **2004**, *20*, 556.
[37] Huang, J.; Jiang, T.; Gao, H.; Han, B.; Liu, Z.; Weize, W.; Chang, Y.; Zhao, G. *Angew. Chem. Int. Ed.* **2004**, *43*, 1397.
[38] Özkar, S.; Finke, R. G. *J. Am. Chem. Soc.* **2002**, *124*, 5789.
[39] See reference 5 and additional references at the end of this text.
[40] Dupont, J.; Spencer, J. *Angew. Chem. Int. Ed.* **2004**, *43*, 5296.
[41] Lebel, H.; Janes, M. K.; Charette, A. B.; Nolan, S. P. *J. Am. Chem. Soc.* **2004**, *126*, 5046.
[42] Clement, N. D.; Cavell, K. J.; Jones, C.; Elsevier, C. J. *Angew. Chem. Int. Ed.* **2004**, *43*, 1277.
[43] Clement, N. D.; Cavell, K. J. *Angew. Chem. Int. Ed.* **2004**, *43*, 3845.

CHAPTER VII

ARE IMIDAZOLIUM-BASED IONIC LIQUIDS A PREFERRED MEDIUM AND STABILIZER FOR NANOCLUSTER CATALYSTS? THE TEST CASE OF ACETONE HYDROGENATION BY $Ir(0)_n$ NANOCLUSTERS.

This dissertation chapter contains the manuscript of a full paper submitted to *Inorganic Chemistry*, and examines the effects of added IL on catalytic acetone hydrogenation by $Ir(0)_n$ nanoclusters. Specifically, the nature of the catalyst in the absence and presence of IL was investigated, along with observed poisoning effects of added IL on acetone hydrogenation catalysis. Additionally, a brief investigation was performed to ascertain whether or not *N*-heterocyclic carbenes were also formed under the specific conditions employed therein.

Sarah Campbell (SC) prepared the ionic liquids used in this study. SC and KRS read the manuscript and suggested minor revisions. The manuscript was prepared by LSO with assistance and editing by RGF.

Abstract.

The question of whether or not ionic liquids (ILs) are preferred stabilizers for transition-metal catalysts, or actually catalyst poisons at least at lower temperatures and H_2 pressures, is probed for the specific case of acetone hydrogenation. Acetone hydrogenation is significant in applications such as heat pumps and fuel cells, as well as for the production of 2-propanol. Two recent, separate studies have reported the $Ir(0)_n$ nanocluster catalyzed hydrogenation of acetone beginning with the identical precursor, $[(1,5\text{-COD})IrCl]_2$ (**1**). One study prepared the nanoclusters and carried out the reaction in neat acetone; the second study first prepared the nanoclusters in an ionic liquid and then used this pre-generated "colloidal suspension" to catalyze acetone hydrogenation. A comparison of the reaction conditions and catalytic results in the two papers shows that both reactions go to 95% completion after 2 hours, despite the fact that the IL-prepared nanoclusters employed the more vigorous catalysis conditions of 53 °C higher temperature, 18.7 psig higher H_2 pressure, and a 14.4-fold higher $[(1,5\text{-COD})IrCl]_2$ concentration. This observation strongly suggests that the IL is detrimental for nanocluster formation and/or subsequent acetone hydrogenation catalysis, the hypothesis tested herein. Indeed, we have found that even 1 eqv added IL (i) inhibits the formation of $Ir(0)_n$ nanoclusters, and (ii) poisons previously active nanoclusters *under the specific conditions of 3.6 mM* ***1****, 22 °C, and 40 psig* H_2. Interestingly, under the more forcing conditions of 52 mM **1**, 75 °C, and 58.7 psig H_2, the catalyst preformed in ionic liquid does lead to a catalytically active system for acetone hydrogenation, albeit one that is poorly defined since precursor, nanoclusters, and bulk metal are all present. Kinetic studies testing the literature claim that nanoclusters are the true / sole catalyst reveal that,

in fact, bulk metal is a fast catalyst, one kinetically competent to account for all the observed catalysis. Hence, another important finding of this work is that bulk metal can out perform nanocluster catalysts when strongly coordinating ligands are present.

Introduction

Over the last decade, interest in the field of ionic liquids has grown enormously.[1,2] Ionic liquids (ILs) possess a wide range of properties, which can be tailored to suit their applications; as a result they have been dubbed "designer solvents".[3] Among key properties of ILs are their negligible vapour pressure at RT,[4] their wide range of viscosities, their high stability in many cases, and their ability to assume a vast number of unique combinations of cations and anions (there are at least one million possible ionic liquids). They are often considered as "green alternatives" to volatile organic solvents, although their toxicity and biodegradability are yet to be fully determined. Ionic liquids are currently being investigated for use in several fields, including but not limited to solvents for catalysis,[5] biocatalysis,[6,7] and analytical applications,[1a] including chromatography, extraction, and spectrometry.[8]

Also of considerable current interest is catalysis by nanoclusters,[9] as well as high selectivity and mild temperature acetone hydrogenation[10] for use in heat pumps, H_2 storage schemes, fuel cells, and due to the general demand for the end product, 2-propanol.[10]

Two recent literature reports detail the $Ir(0)_n$ nanocluster catalyzed hydrogenation of acetone.[10,11] Both studies use the identical nanocluster precursor, $[(1,5\text{-COD})IrCl]_2$ (**1**). However, one nanocluster formation reaction and subsequent acetone hydrogenation was

carried out in neat acetone,[10] while the other study pre-generated what was called a "colloidal suspension" of nanoclusters in the ionic liquid (hereafter IL) 1-butyl-3-methylimidazolium hexafluorophosphate, [bmim][PF_6], Figure 1. The second study then employed this pre-generated "colloidal suspension" for acetone hydrogenation.[11] The nanocluster formation reaction and subsequent acetone hydrogenation is shown below in Scheme 1.

Figure 1. The ionic liquid 1-butyl 3-methyl imidazolium hexafluorophosphate, [bmim][PF_6], used previously[11] as well as herein.

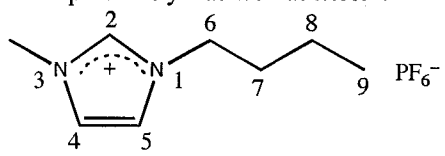

Scheme 1. The reactions established in study[10] #1 of Table 1 and which are important to the present studies.

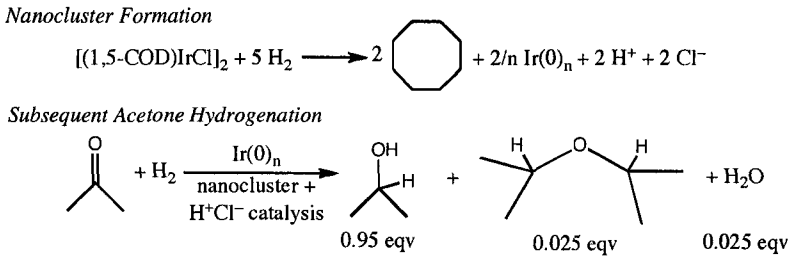

Table 1 outlines the nanocluster formation and subsequent acetone hydrogenation conditions previously reported in the literature. The 53 °C higher temperature, 18.7 psig higher H_2 pressure, and 14.4-fold higher concentration of **1**—*yet slower TOF*—in the IL system suggests that either the added IL inhibits catalysis or the *nature* of the catalyst in the two systems is different (or both), despite the claim of nanocluster catalysis in each case. [10,11] Especially important is that the above data demand a test of the implied,

repeated claim—one rigorously untested previously—that ILs are a superior medium for nanocluster catalysis.[12,13,14,15,16,17,18] The results in Table 1 imply, instead, that an important hypothesis to be tested *is that ILs can be potent poisons of nanocluster catalysts*, at least at lower temperatures. This is not unexpected since ILs with hydrogens in the 2-position (see Figure 1) have recently been shown to form *N*-heterocyclic carbenes (NHCs) atop $Ir(0)_n$ nanoclusters,[19] and since NHCs are well known to be strongly coordinating ligands for transition-metal centers.[20,21,22,23,24]

Table 1. The reported literature conditions[10,11] and results for the two studies of acetone hydrogenation.

Study	**#1**[10]	**#2**[11]
Solvent	Acetone	[bmim][PF_6]
Reaction time	2h	2h
Yield	95%	95%
T (°C)	22	**75**
P (psig)	40	**58.7**
Conc. of **1** (mM)	3.6	**52**
average TOF [a]	1.92 [b]	**0.033**
Selectivity	95%	not reported

[a] Turn-over frequency, (mol product)/[(mol total catalyst loading)•s]. [b] Note that if corrected for the number of active surface Ir atoms, the true initial TOF for the nanocluster can be as much as 11-fold larger.[10]

Herein, we test the hypothesis of whether or not prototype 1,3-substituted imidazolium-based IL, [bmim][PF_6], is a help or hindrance to $Ir(0)_n$ catalyzed acetone hydrogenation. We find that (i) 1 eqv of added IL *poisons* the formation of nanoclusters from the precursor, $[(1,5\text{-COD})IrCl]_2$, **1**, (i.e., including poisoning any forming critical nuclei[25]) and that 1 eqv of added IL also *poisons* preformed, active nanoclusters under the conditions of 3.6 mM **1**, 22 °C, and 40 psig H_2. Interestingly, however, we also (ii) reproduce the literature result[11] that even neat IL (i.e., 92 eqv of IL/eqv **1**) *does not poison* catalysis derived from **1** *under the more forcing conditions of 52 mM 1, 75 °C and*

58.7 psig H_2. These observations in turn (iii) imply that either the poisoning effect is reversed at higher temperature and higher H_2 pressure, or the nature of the catalyst is different in the two systems, or both. Studies addressing the true nature of the catalyst under the different conditions are, therefore, also reported even though the primary goal of this work is to provide the first definitive test case of whether or not added IL a help or hindrance to nanocluster catalysis.

Experimental Section

Materials. All reaction solutions were prepared under oxygen- and moisture-free conditions in a Vacuum Atmospheres drybox (≤5 ppm O_2 as continuously monitored by a Vacuum Atmospheres O_2 monitor). $[(1,5\text{-COD})IrCl]_2$ (**1**; Strem, 99%) was stored in the drybox and used as received. Acetone (Burdick and Jackson, 0.26% H_2O) was purged with Ar for 30 minutes and transferred into the drybox. The IL 1-butyl-3-methylimidazolium hexafluorophosphate ([bmim][PF_6]) was prepared at the Queen's University Ionic Liquid Laboratories (QUILL).[26] The IL was dried under vacuum (≤100 mmHg) at 60 °C for ≥5 h and stored in the drybox. [Bu_4N][PF_6] (Aldrich, 98%) was dried under vacuum (≤100 mmHg) at 22 °C for ≥12 h and stored in the drybox. ^1H NMR spectroscopy was performed on a Varian Inova 300 spectrometer. Spectra were obtained in CD_2Cl_2 (Cambridge Isotope Laboratories, 99%) in pre-dried (≥160 °C for ≥24 h) 5 mm o.d. NMR tubes. Spectra were referenced to the residual solvent impurity. ^2H NMR spectroscopy was performed on a Varian Inova 400 spectrometer; spectra were obtained in CH_2Cl_2 (Aldrich, 99+%). XPS spectra were collected using a Physical Electronics (PHI) Model 5800XPS system equipped with a monochromator (Al Kα

source operating at 1486.8 eV; system pressure $\leq 1x10^{-8}$ Torr) and a hemispherical analyzer to detect the ejected electrons. An Eppendorf 5415c 18-well centrifuge was used for nanocluster isolation.

Hydrogenation Apparatus. Hydrogenation experiments were carried out in a previously described[10,27,28] apparatus designed to continuously monitor H_2 pressure loss. This apparatus consists of a Fisher-Porter (FP) bottle, which connects *via* Swagelok quick-connects to both a dihydrogen line and an Omega PX621 pressure transducer. The pressure transducer is interfaced with a PC by means of an Omega D1131 5V A/D converter with a RS-232 connection. The pressure uptake data is collected using LabView 7.1. The FP bottle is placed in a jacketed reaction flask with temperature control by means of a recirculating water bath. The reaction solution is stirred by a Fisher Jumbo Magnetic Stirrer with a 5/8" x 5/16" Teflon-coated octagon shaped spin bar at speeds ≥600 rpm so as to avoid H_2 gas-to-solution mass transfer limitations.[29]

Nanocluster Formation Under 52 mM 1, 75 °C, 58.7 psig H_2 Conditions in Neat [bmim][PF_6], Studies Repeating the Literature Conditions as Exactly as Possible.[11] In the drybox, **1** (35.0 mg, 0.052 mmol) was weighed into a pre-dried 2 dram glass vial. Since this complex is insoluble at room temperature in the stated literature[11] ionic liquid [bmim][PF_6], the red crystalline complex was transferred as a solid into a new borosilicate culture tube (22 x 175 mm) with a new 5/8" x 5/16" Teflon-coated octagon shaped spin bar. Next, [bmim][PF_6] (1.0 mL) was added to the culture tube with a 1.0 mL gas-tight syringe. The culture tube was placed in the FP bottle, and the FP bottle was sealed and brought out of the drybox. the reaction solution was stirred in the water bath at 75 °C for ≥10 minutes before being exposed to H_2 in order to raise the reaction solution

temperature to the reported literature temperature of 75 °C (a necessary step albeit one not reported in the prior study[11]). At the end of the ≥10 minutes of stirring, **1** had dissolved resulting in a clear yellow-orange solution.

Next, the reaction solution was exposed to 58.7 psig (4 atm) H_2 for 10 minutes. After approximately 2 minutes, the reaction solution turned brown. At the end of the 10 minute exposure, the reaction solution was opaque and black, with *bulk metal* visible to the naked eye on the sides of the culture tube [this mixture is, apparently, the "colloidal suspension"[11] cited in the literature, namely both a brown[30] $Ir(0)_n$ nanocluster solution (as judged by TEM, *vide infra*) plus bulk metal]. The FP bottle was disconnected from the H_2 line, vented, sealed, and brought back into the drybox. Once the FP bottle was opened in the drybox,, visual examination of the stir bar revealed that it was also coated with bulk metal.

To the same culture tube used for the nanocluster formation reaction (i.e., and which had the nanocluster solution in 1.0 mL IL and bulk metal present both on the sides of the culture tube and on the stir bar), acetone was added (1.0 mL, 13 mmol) for a total volume of 2.0 mL. The culture tube was sealed in the FP bottle, and then the FP bottle was brought out of the drybox. The FP bottle was attached via its Swagelok quick-connects to the H_2 line, and again stirred for 10 minutes in the water bath and under N_2 to raise the temperature of the reaction solution. To initiate the acetone hydrogenation reaction, the FP bottle was purged 13 times with H_2 (58 ± 1 psig, 15 s/purge). Five min after the first purge, the pressure was set at 58 ± 1 psig, $t = 0$ was noted, and pressure *vs.* time data was collected at 2.5 min intervals.

Separately, attempts to isolate the nanoclusters were carried out as closely as possible to prior literature reports.[11] After the 10 minute reaction time, the FP bottle was vented, sealed, and brought back into the drybox. The 1.0 mL solution of nanoclusters in IL was decanted into a 1.5 mL snap-cap centrifuge tube. Acetone (0.5 mL) was added with a polyethylene pipet, and the brown-black solution was shaken vigorously. The tube was sealed with Parafilm and brought out of the drybox. Next, the tube was centrifuged for 10 min at 10,000 rpm and brought back into the drybox. The bright yellow supernatant (a color characteristic of **1** in acetone) was removed with a new polyethylene pipet, leaving a brown-black powder at the bottom of the vial. Acetone (1.5 mL) was added to the powder at the bottom of the vial. The solution was shaken vigorously, producing a brown-black solution. This cycle of centrifugation and adding fresh acetone was repeated twice more, after which the brown-black powder was dried under vacuum overnight.

Nanocluster Formation Under 52 mM 1, 75 °C Conditions in Neat [bmim][PF_6] But Employing D_2 in Place of H_2.[11] This reaction was carried out exactly as described, except D_2 was used in place of H_2.

X-ray Photoelectron Spectroscopy (XPS) of the Reaction Vessel from 52 mM 1, 75 °C, 58.7 psig H_2 Conditions in Neat [bmim][PF_6]. A nanocluster formation reaction was carried out exactly as described in the section titled "Nanocluster Formation Under 52 mM **1**, 75 °C, 58.7 psig H_2 Conditions in Neat [bmim][PF_6]." After the 10 minute reaction time, there was bulk metal visible to the naked eye on the sides of the culture tube. The FP bottle was vented, re-sealed, and brought into the drybox. In the drybox, the FP bottle was opened and the culture tube removed. After decanting the IL from the

culture tube into a beaker, the culture tube was rinsed with acetone to remove any remaining IL/nanocluster solution. Next, the culture tube was broken with a hammer. A piece of the culture tube with the metal film visible to the naked eye was sealed in an oven-dried glass scintillation vial, and the vial was sealed with electrical tape. The vial was removed from the drybox. Under flowing N_2, the metal-coated glass was mounted onto a XPS sample holder with Scotch tape. After thoroughly evacuating the sample chamber ($\leq 10^{-9}$ Torr), sample analysis was initiated.

Testing the Kinetic Competence of the Bulk-metal Film Produced from 52 mM 1, 75 °C, 58.7 psig H_2 Conditions in Neat [bmim][PF_6]. A nanocluster formation reaction was carried out exactly as described above. The resultant "colloidal suspension" was decanted and the bulk-metal film inside of the culture tube was washed with acetone exactly as described above with the exception that the stir bar was kept in the culture tube. (Washing the culture tube to remove any remaining IL following the decanting procedure is necessary to avoid an ill-determined, variable amount of remaining IL between experiments, especially since we find that even 1 equiv. IL is a catalyst poison, *vide infra*). Next, acetone (1.0 mL) was added to the culture tube. The culture tube was sealed in the F-P bottle and hydrogenation was initiated exactly as described in the section titled "Nanocluster Formation Under 52 mM **1**, 75 °C, 58.7 psig H_2 Conditions in Neat [bmim][PF_6]."

Acetone/IL Stock Solutions. Stock solutions of IL in acetone were prepared for both 1 and 5 equivalents IL in pre-dried 25 mL volumetric flasks. For the each solution, approximately half the acetone was transferred into the flask with a disposable polyethylene pipet. The needed volume of IL (7.5 μL for 1 eqv, 37.6 μL for 5 eqv) was

added next with a 10 or 50 μL gas-tight syringe. The solution was swirled, and the remaining acetone was added with the same polyethylene pipet to reach 25 mL. The volumetric flask was capped with a lightly greased ground glass stopper and sealed with Parafilm. All solutions were used within 2 days of being prepared.

Nanocluster Formation Under 3.6 mM 1, 22 °C, 40 psig H_2 Conditions in Neat Acetone. In the drybox, **1** (1.2 mg, 3.6 μmol Ir) was weighed into a pre-dried 2 dram glass vial. Acetone (1.0 mL, 13 mmol) was added with a 1.0 mL gas-tight syringe. The reaction solution was agitated with a disposable polyethylene pipet until the precursor had dissolved (approximately 5 minutes), resulting in a clear, bright-yellow solution. Next, the reaction solution was transferred with the pipet into a new culture tube with a new stir bar. The culture tube was sealed into the FP bottle, brought out of the drybox, and attached to the H_2 line. To initiate the reaction, the FP bottle was purged 13 times with H_2 (40 ± 1 psig, 15 s/purge). Five min after the first purge, the pressure was set at 40 ± 1 psig, $t = 0$ was noted, and pressure *vs.* time data was collected at 2.5 min intervals.

Nanocluster Formation Under 3.6 mM 1, 22 °C, 40 psig H_2 Conditions in Acetone with Added [bmim][PF_6]. These experiments were carried out exactly as described above in the section titled "Nanocluster Formation Under 3.6 mM 1, 22 °C, 40 psig H_2 Conditions in Neat Acetone" with the following exception: instead of neat acetone, a stock solution containing the desired number of equivalents [bmim][PF_6] in acetone was used. **Acetone Hydrogenation with 3.6 mM 1, 22 °C, 40 psig H_2 Conditions in Acetone with [bmim][PF_6] or [Bu_4N][PF_6] Added During Hydrogenation.** These experiments were initiated exactly as described above, except only 0.8 mL acetone was used to dissolve **1**. A hydrogenation experiment was initiated exactly as described in the

section titled "Nanocluster Formation Under 3.6 mM **1**, 22 °C, 40 psig H_2 Conditions in Neat Acetone." After approximately 5 psig of H_2 was taken up, the FP bottle was sealed and removed from the H_2 line. The pressure in the line was adjusted to 35 psig, and the bottle was re-attached to the line. Under 35 psig flowing H_2, 0.2 mL of a solution of [bmim][PF_6] or [Bu_4N][PF_6] in acetone (86 mM, 1 equivalent) was added for a total reaction volume of 1.0 mL. The FP bottle was purged 3 times, and data collection was re-initiated.

Results and Discussion

Initial Control Experiments.

In Acetone:[10] A control experiment was performed for 3.6 mM **1**, 22 °C, and 40 psig H_2 conditions with a volume of 1.0 mL acetone.[10] After an induction period (know to be due to the nucleation and initial growth of a nanoparticle catalyst[31]), acetone hydrogenation took off smoothly with the same general H_2 uptake curve as we previously reported (see Figure 4 herein which is similar to Figure S1 of our prior work[10]). The solution acquired a brown color characteristic of Ir(0) nanoclusters as the catalysis ensued; note also that the kinetics and TEM evidence reveal a nanocluster catalyst (plus some bulk metal catalysis as part of the high, 16,4000 TTOs reported elsewhere[10]). An overall 95% hydrogenation was observed after 2 hours and complete hydrogenation after approximately 10 hours, results comparable to the neat IL conditions (vide infra). As we reported earlier,[10] after the 10 hour period the final reaction solution is clear with non-redispersable bulk metal present as the final metal product.

In Neat IL:[11] The literature nanocluster formation conditions detail an initial "around 10 minute"[11] reaction time for 52 mM **1** at 75 °C and 4 atm H_2 (58.7 psig). After this 10 minute reduction, the sides of the reaction vessel were covered with a *metal film*, the stir bar was coated with appreciable quantities of *bulk metal*, and the dark brown solution contained bulk metal particles visible to the naked eye. (In the course of 6 repetitions generating the "colloidal suspension", a bulk metal film was always formed, although the amount of bulk metal varied somewhat by eye from run to run.) The brown-black suspended material was isolated after the 10 minute reduction following the reported centrifugation method.[11] Shaking the dark-brown reaction solution with 0.5 mL acetone in a centrifuge tube yielded a dark-brown solution. After centrifugation, a brown-black powder collected at the bottom of the tube with a bright-yellow supernatant, the latter characteristic of remaining, unreacted **1** in acetone. Hence, the 10 minute initial reaction conditions employed in the literature[11] *is insufficient to completely reduce the precursor*. After removing the yellow supernatant, the brown-black powder was redissolvable in fresh acetone with shaking, again resulting in a dark-brown solution. Two identical, subsequent centrifugation cycles yielded equivalent results: each time a bright-yellow supernatant of remaining precursor **1** was removed and a dark-brown powder collected at the bottom of the tube. Transmission electron microscopy (TEM) images of the dark-brown power redissolved in acetone and then placed on a TEM grid, Figure 2, reveal that agglomerated, polydisperse colloids (plus bulk metal) are the product of the above synthesis and isolation procedure.

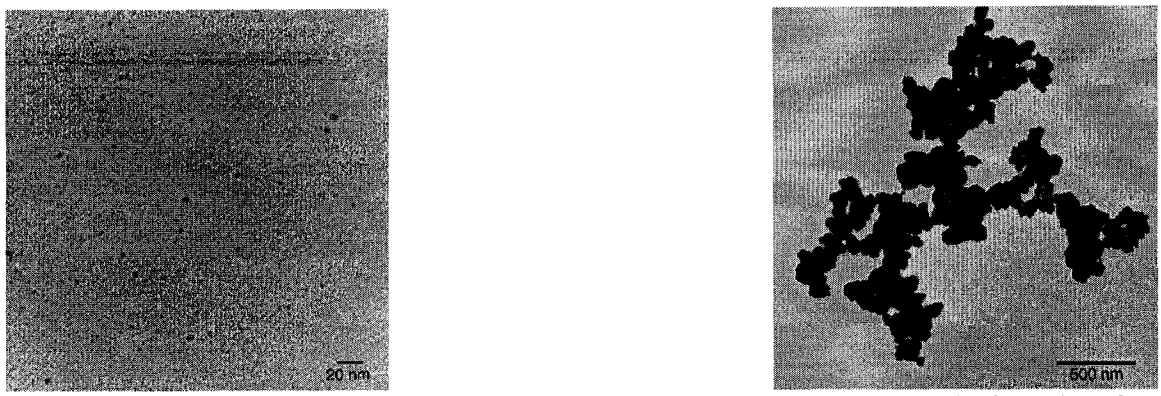

Figure 2. TEM micrographs of the *soluble* portion of the reaction solution revealing the formation of polydisperse plus agglomerated colloids generated from 52 mM **1**, 75 °C, and 58.7 psig H_2 in neat IL. Recall that bulk metal is also observed in these reactions; hence, these micrographs are not representative of the entire sample. Instead, these TEMs are primarily useful only for visualizing the polydisperse, agglomerated colloids which are present.

At this point, we can conclude that the catalyst system derived from the literature conditions of 52 mM **1** at 75 °C under 58.7 psig H_2 contains at least three components: unreacted **1**, colloids, and bulk metal. Hence, its composition is not solely "iridium nanoparticles"[11] as previously claimed.

In a separate experiment, once acetone was added to the culture tube in which the unreacted **1**, the "colloidal suspension" plus bulk metal are all present, an overall 95% hydrogenation was observed after 2 hours and complete hydrogenation after approximately 10 hours, Figure 3, consistent with the literature report. The observation of an induction period in Figure 3, *from even the three component mixture*, is important, suggesting (i) that either bulk metal and/or nanocluster surface-bound ligands must removed before catalysis can begin (vide infra), or (ii) that some other activation or true catalyst generation process[31] must occur prior to catalysis. Neither the presence of bulk metal, nor the kinetics of acetone hydrogenation, were reported previously.[11] The lack of kinetics as a function of added IL, and in comparison to no IL ever present, meant that

the prior work could not possibly have correctly deduced if added IL is good, or bad, for catalysis.

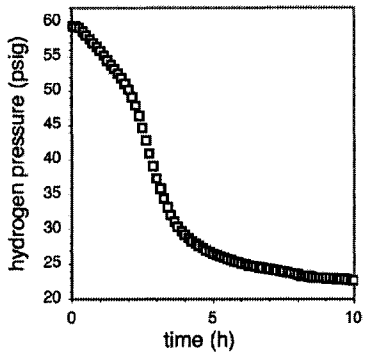

Figure 3. Hydrogen uptake kinetic curve for acetone hydrogenation after the 10 minute reduction of **1** in neat [bmim][PF_6]. This kinetic data is qualitatively reproducible in 3 separate experiments. An induction period of ~20 minutes is observed before catalysis begins, indicating that the true catalyst is being generated during this time and even from the three components that are present, **1**, nanoclusters, and bulk metal.

Poisoning of Nanocluster Formation, at 3.6 mM 1, 22 °C, and 40 psig H_2, by 1 and 5 Eqv IL. In a series of experiments in acetone with 0, 1, and 5 eqv added [bmim][PF_6] we observed that even *1 equivalent* of added IL per Ir atom in **1** poisons ≥90% of the acetone hydrogenation catalysis, Figure 4. Only 10% conversion *after 22 hours* is observed with 1 eqv added IL in comparison to 100% conversion in < 1/2 the time (after 10 hours) in neat acetone without added IL. Five eqvs IL further poisons the hydrogenation activity: even *after 7 fold longer* (70 hours) only a mere 10% conversion is observed. Additionally, the solutions with 1 or 5 eqv added IL remain the brilliant yellow characteristic of **1** in acetone rather than changing to the brown solution characteristic of $Ir(0)_n$ nanoclusters.[30]

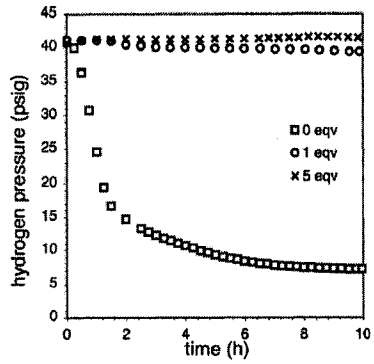

Figure 4. Hydrogen uptake curves for 3.6 mM **1** under 40 psig H_2 in acetone with 0, 1, and 5 eqv added [bmim][PF_6]. The results demonstrate rather convincingly that even 1 eqv [bmim][PF_6] is a strong poison for the acetone hydrogenation catalyst derived from 3.6 mM **1** at 22 °C and 40 psig H_2.

Furthermore, even 0.1 eqv IL added to the precursor solution is a poison: only 26% conversion of acetone is observed after 24h. In short, *1,3-substituted imidazolium-based ILs are a poison for at least Ir(0)$_n$ nanocluster catalysis of acetone hydrogenation* beginning with **1** and under the specific conditions of 22 °C and 40 psig H_2.

Poisoning of the Previously Active Nanocluster Catalyst by 1 Eqv IL at 22 °C and 40 psig H_2. Next, we hypothesized that added IL would also poison the active nanocluster catalyst (i.e., and since the simplest interpretation of the poisoning data back in Figure 4 is that the added IL is poisoning the forming critical nuclei[25] which are precursors to the lager nanoclusters). To test this hypothesis, a nanocluster formation and subsequent acetone hydrogenation experiment was initiated *in neat acetone* (i.e., without any IL present) using 3.6 mM **1** as precatalyst. After the solution became catalytically active, 1 eqv [bmim][PF_6] was added. As Figure 5 shows, the addition of just 1 eqv IL *completely halted* catalytic activity of preformed nanoclusters at 22 °C and 40 psig H_2 (≤5% activity seen after 24 hours after the IL was added; no bulk metal was visible in this experiment). This result demonstrates unequivocally that *added 1,3-substituted imidazolium-based IL*

is a poison, not a preferred solvent, for $Ir(0)_n$ nanocluster catalysis of acetone hydrogenation, at least at 3.6 mM **1**, 22 °C, and 40 psig H_2. It is also evidence consistent with the interpretation offered above that the poisoning observed when beginning with **1** is due to IL poisoning of the forming critical nuclei (athough poisoning of **1** itself cannot be ruled out).

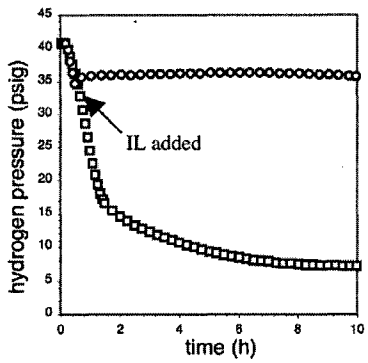

Figure 5. Acetone hydrogenation with no added IL (squares) and then with 1 eqv [bmim][PF_6] added after nanoclusters have formed (circles, IL added where arrow indicates; the slight rise in pressure observed at this point is due to the acetone vapor phase re-equilibration with the post flushing the system with H_2 to restart the reaction.[32]). Hydrogenation at 22 °C and 40 psig H_2 is completely halted by the addition of 1 eqv IL, unequivocally indicating that the IL poisons the previously active nanocluster catalyst.

A sub-hypothesis to be tested here is that the PF_6^- *anion* of the IL is what is really poisoning the active catalyst. Anions are known to coordinate strongly to electrophilic nanocluster surfaces,[33] and it was recently shown that even the traditionally weakly coordinating PF_6^- is present on the surface of dried $Pd(0)_n$ nanoclusters prepared in [bmim][PF_6].[34] Hence, we carried out an experiment identical to the one described above, except in which 1 eqv [Bu_4N][PF_6] was added in place of 1 eqv [bmim][PF_6]. Unlike the poisoning shown in Figure 5, acetone hydrogenation continued uninhibited to completion (Figure S1 of the Supporting Information).[35] Given that added [bmim][PF_6] poisons catalysis (Figure 5) but PF_6^- does not (Figure S1), it follows that the poisoning is due somehow to the $[bmim]^+$ counterion. Given or recent work showing that $Ir(0)_n$

nanoclusters oxidatively add the cationic component of ILs such as $[bmim]^+$ to form surface-coordinated *N*-heterocyclic carbenes (NHCs),[19] Scheme 2, it is highly likely that the true poison is a surface-coordinated NHC. Hence, this possibility is examined in the next section for the case of the literature, higher pressure and temperature system.

Scheme 2. Precedented *N*-heterocyclic carbene formation $Ir(0)_n$ nanoclusters.

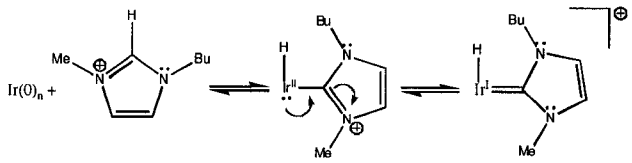

Noteworthy here is that in our previous study of $Ir(0)_n$ nanocluster reactions with ILs we also observed that increasing the number of equivalents of added IL *slowed the catalysis,* in that case of cyclohexene hydrogenation—further indication of the poisoning effect of increasing amounts of ILs.

D_2 Labeling Evidence for the Formation of Surface Coordinated *N*-Heterocyclic Carbenes in the Higher Temperature and Pressure Literature Acetone Hydrogenation System. The NHC formation shown above in Scheme 2 was uncovered by D_2 labeling experiments which revealed D incorporation into several positions of the $[bmim]^+$ counter-ion of the IL, but most importantly into the C_2-H position[19] (as seen herein, Figure 6, vide infra). Also, kinetic studies showed that the $Ir(0)_n$ nanoclusters (i.e., and not the precursor **1**) are the H/D exchange catalyst in our prior study.[19]

To investigate whether or not NHCs are also formed under 52 mM **1**, 75 °C, and 58.7 psig H_2 (D_2) conditions, we performed an identical acetone hydrogenation reaction in neat IL[11] except that we substituted D_2 for H_2. The key result from the ^2H NMR shown

in Figure 6 is the incorporation of deuterium into the C_2 position (as well as at the other positions of the $[bmim]^+$ counter-ion exactly as seen previously[19]), indicating the reversible formation of NHCs under the literature conditions 52 mM **1**, 75 °C, and 58.7 psig D_2 (H_2)

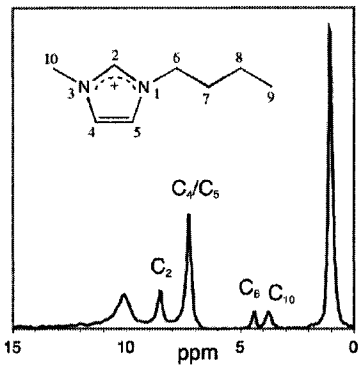

Figure 6. ^2H NMR spectrum of the reaction solution prepared from 52 mM **1**, 75 °C, and 58.7 psig D_2 reaction in neat IL. The peak at δ=8.5 is attributable to substitution at C_2, indicative of NHC formation atop the $Ir(0)_n$ catalyst. The peaks at δ=1.0 and δ=10 are attributable to deuteration of the methyl groups and the alcohol group, respectively, of isopropanol.

Significantly, the following four lines of evidence all strongly suggest that NHCs are the nanocluster poison herein for *both* sets of catalyst conditions examined herein: (i) the formation of NHCs at 52 mM **1**, 75 °C, and 58.7 psig H_2 (D_2) as shown in Figure 6; (ii) our earlier finding[19] the NHCs are both formed, and also slow nanocluster catalysis, under 1.2 mM Ir precursor, 22 °C, and 40 psig H_2 (D_2) conditions, (iii) the poisoning observed with added IL herein under 3.6 mM **1**, 22 °C, and 40 psig H_2 conditions, and (iv) the exclusion of PF_6^- as the only other possible poison derived from $[bmim][PF_6]$. In short, NHCs are the only obvious, as well as simplest (i.e., Ockham's razor), explanation for the observed poisoning of catalysis.

Is Poisoning by 1 Eqv IL Reversible at Higher Temperatures and Pressures? An interesting, apparent dichotomy which remains to be explained is why 1 eqv IL completely poisons acetone hydrogenation at 22 °C and 40 psig H_2, yet the higher temperature and pressure (75 °C, and 58.7 psig H_2) system is active—indeed, why it has any activity at all in the presence of *92 eqvs of IL* (the 92 equiv IL system is slowed ≥58 fold, however, and in comparison to the lower temperature and pressure, 22 °C and 40 psig H_2 system—see the TOFs in Table 1). One plausible answer is suggested by our published poisoning experiments of $Ir(0)_n$ nanoclusters in which we find that complete poisoning at room temperature by the strong poison, CS_2, is reversible at higher temperatures[36,37,38]—as expected and generally found for exothermic poisoning reactions.[39] Hence, one expects that exothermic poisoning by NHC formation, Ir(0) + IL ⇆ H-Ir–NHC + *heat*, will be reversed at least somewhat at higher temperatures (the high H_2 pressure of 58.7 psig vs 40 psig may also facilitate higher surface Ir-H concentration and thus reversal of the NHC formation, oxidative addition reaction[40,41,42]).

This predicted / precedented reversibility of the poisoning process was tested as follows: the literature higher temperature and pressure catalyst was made in the normal way (i.e., in IL), cooled and then subjected to the lower temperature and pressure, 22 °C and 40 psig H_2 conditions, with the expectation that the system might be poisoned at lower temperature. The results (see the Supporting Information for the experimental and other details) show, in opposition to the predicted result, that the IL containing system *is in fact still active*, giving 90% acetone hydrogenation in 24 hrs.

This result, in turn, requires that a second hypothesis be formulated, namely that the system prepared in 92 equivalents of IL and run at 75 °C and 58.7 psig involves a

different catalyst than the established nanocluster catalyst[10] of the 22 °C, 40 psig system which does not contain any IL. Given that we now know that the literature 75 °C, 58.7 psig, IL system contains three components (unreacted **1**, nanoclusters and bulk metal), and given that we know that **1** is not a catalyst,[19] this new, alternative hypothesis becomes that "the bulk metal present in the literature 75 °C, 58.7 psig,, and IL system is hypothesized to be the main catalyst in that system". It is this hypothesis that is addressed next. The published evidence that nanoclusters are the at least initial catalyst in the low temperature system[10] (#1 of Table 1) is summarized in the Supporting Information for the interested reader.

Evidence for the Nature of the Catalysts in the Literature, 52 mM 1 at 75 °C and 58.7 psig H_2 system in neat IL System.

Nanocluster catalysis was assumed—that is, nanocluster catalysis *is the (untested) hypothesis of the literature work at higher temperature and pressures.*[11] Visual observation of a brown "colloidal suspension"[11] and TEM images of nanoclusters, are the only prior evidence that nanoclusters could be the only active catalyst as was hypothesized. Of course, herein, we have shown that unreacted **1**, some nanoclusters (including agglomerated ones, assuming the solid state TEM is at least somewhat reflective of what is actually present in solution), *and bulk metal* are all present as possible catalysts.

The key experiment is to examine the kinetics of acetone hydrogenation for the higher temperature and pressure system, and this is done in Figure S3 of the Supporting Information. The observed kinetics (i.e., when beginning with the 3-component mixture

1, nanoclusters, plus bulk metal that results from the literature preparation) is not well fit (especially in the beginning, Figure S3) by the same 3-step mechanism which fits the data for the lower temperature system in Figure S2. This is not surprising, however, as we already know that substantial bulk metal plus some nanoclusters are already present, and the data in Figure S2 plus the sigmoidal kinetics show that, at least at lower temperature, **1** is not a catalyst, but instead must evolve to nanoclusters and/or bulk metal for acetone hydrogenation catalysis to ensue.

Taking another clue from our recent work, we suspected that bulk metal is a superior catalyst to even nanoclusters *in the presence of ligands such as NHCs* formed from ILs. The relevant literature here is our recent mechanistic investigations revealing that bulk metal catalysis can be favored over nanocluster catalysis *in the presence of excess ligand* (the precedent being specifically for Pt catalyzed hydrogenation of cyclohexene[43,44]). The underlying reason is that there appears to be an up to ca. 2-fold stronger metal-ligand bond energy in small nanoclusters in comparison to the bond energy for the same ligand bound to the same metal, but in large, bulk-metal-like particles.[43,44] This in turn leads to the observation of a particle-size dependence of the fractional coverage of catalyst's surface,[43,44] *something that promises to be very important for nanocluster vs larger particle catalysis as discussed elsewhere.*[43,44] The bottom line effect is that there is more poisoning of smaller nanoclusters vs larger bulk-metal is predicted when IL and its accompanying NHCs are present as they are in the higher temperature and pressure system.[43,44]

To test the hypothesis that bulk metal is an active catalyst when IL is present, we carried out an acetone hydrogenation reaction using only the bulk metal present that is

formed on the sides of the culture tube and stir bar (i.e., after decanting the soluble "colloidal suspension" / nanoclusters and unreacted **1**) but, importantly, after washing the bulk-metal catalyst with acetone to remove any IL present so as to achieve a reproducible experiment in which the amount of IL present is better controlled. If bulk metal is an active catalyst, the hydrogenation is expected to proceed *without an induction period* and *at a kinetically competent rate* (i.e., at the rate seen for the catalysis at the higher temperature and pressure conditions, once one factors in the fact that not all the metal is present as bulk metal). Indeed, acetone hydrogenation commenced *immediately (i.e., without an induction period)*, as Figure 7 demonstrates.

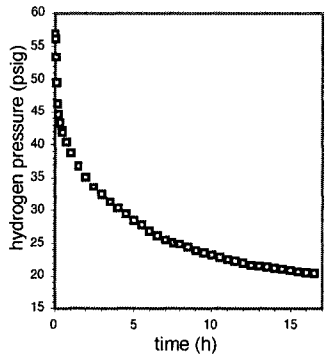

Figure 7. Acetone hydrogenation beginning with the *acetone-washed* bulk metal that is present on the sides of the culture tube and stir bar after decanting the soluble "colloidal suspension" and any unreacted **1** and washing the bulk metal film to remove the remaining (acetone-soluble) IL. Note that there is no discernable induction period; moreover, the initial rate of hydrogenation is 19 fold larger than the initial rate in Figure 3 as discussed in the text.

The observed initial rate in Figure 7 is 65±3 psig H_2/h for *the acetone-washed* bulk metal, a rate *ca. 19 fold higher* than the rate of hydrogenation of 3.5±0.2 psig/h see in Figure S4 of the Supporting Information (i.e., after an induction period)—note that the rate enhancement is actually more than 19 fold since the catalysis in Figure S4 involves all the Ir (i.e., of the 3 components present) whereas that in Figure 7 involves just the Ir(0) bulk-metal. In addition, the rate of 65±3 psig H_2/h is still 5 times faster than the

larger rate of 13.2±0.7 psig H_2/h for the second downturn (the fastest rate) seen in Figure 3 (see Figure S4 of the Supporting Information). In short, bulk metal *is not only a kinetically competent catalyst,*[45] it is fast, powerful catalyst. The prior claim that nanoclusters are the sole catalyst in the IL system is hereby refuted. We cannot, however, rule out some catalysis by the nanoclusters, although the ca. 19 fold higher rate by the *acetone-washed* (i.e., and IL-free) bulk metal indicates that bulk metal is a superior catalyst and that washing the remaining IL off the bulk metal enhances catalysis—*further evidence that the presence of IL leads to catalyst poisoning.* We have also shown that the bulk-metal catalyst does still have P, F, C, and N present, and P and F in the atomic ratio of 1:6 as expected for the presence of the PF_6^- anion; see the Supporting Information for details.

In summary, the important finding from investigating the true nature of the catalyst is a second finding, following our recent work,[43,44] that bulk metal can be a faster catalyst—perhaps more generally—when good coordinating ligands are present.

Conclusions

The main findings of this contribution are:

- Even 1 equivalent of added [bmim][PF_6] poisons both the formation of nanoclusters from [(1,5-COD)IrCl]$_2$ (presumably by poisoning any critical nuclei formed) as well as any previously active nanoclusters, at least in neat acetone at 3.6 mM **1**, 22 °C, and 40 psig H_2.
- However, we also are able to reproduce the literature report that neat IL (corresponding to 92 equivalents of IL) do not irreversibly poison the catalyst derived

from 52 mM **1**, 75 °C, and 58.7 psig H_2 in neat IL. This acetone hydrogenation catalyst system is ≥22 fold slower compared to the reaction in neat acetone so that it requires higher concentrations, temperatures, and pressures to attain the same reaction time and percent conversion in 2 hrs.

- Bulk metal, not the previously claimed nanoclusters,[11] are indicated as the kinetically competent / dominant catalyst in the 52 mM **1**, 75 °C, and 58.7 psig H_2 system in neat IL. It must also be that at least some temperature-dependent reductive elimination / dissociation of NHCs (i.e., the reverse of Ir(0) + IL ⇆ H–Ir–NHC + heat) occurs at higher temperature.

- Although the poisoning effects of even small amounts of added [bmim][PF_6] on at least acetone hydrogenation catalysis by nanoclusters are unequivocally demonstrated herein, it remains to be demonstrate if the poisoning effects of ILs (or of other ILs, such as 2-R-ILs that might be more inert) are more general or not.

- The finding that bulk metal can be a superior catalyst in comparison to smaller nanoclusters is significant.[43,44] This insight stands in direct opposition to the current hypothesis and widely believed assumption that smaller nanoclusters will almost always be the kinetically domanant catalyst.

Supporting Information: Figure S1, kinetics of acetone hydrogenation with added [Bu_4N][PF_6]; Figure S2, kinetics of acetone hydrogenation at 3.6 mM **1**, 22 °C, and 40 psig fit by the 2-step and 3-step mechanisms;[46] Figure S3, kinetics of acetone hydrogenation at 52 mM **1**, 75 °C, and 58.7 psig fit by the 3-step mechanism;[46] Figure S4, a comparison of initial hydrogenation rates in the two systems; Figure S5, XPS spectrum

of the metal film derived from 52 mM **1**, 75 °C, and 58.7 psig; a discussion of attempted nanocluster formation under 3.6 mM **1**, 22 °C, 40 psig H_2 conditions in neat [bmim][PF_6]; an experiment at 22 °C and 58.7 psig with the catalyst system derived from 52 mM **1**, 75 °C, and 58.7 psig; control of 1 eqv added [bmim][PF_6] at 75 °C and 58.7 psig H_2 in neat acetone.

Acknowledgments. Dr. C. Rithner assisted with the ^2H NMR spectroscopy, and Dr. P. McCurdy collected the XPS spectra. This work was supported by DOE grant DE-FG02-03ER15453.

References

[1] Some recent review articles include: (a) Anderson, J. L.; Armstrong, D. W.; Wei, G.-T. *Anal. Chem.* **2006**, *78*, 2892. (b) Deetlefs, M.; Seddon, K. R. *Chem. Today* **2006**, *24*, 16. (c) Dupont, J.; de Souza, R. F.; Suarez, P. A. Z. *Chem. Rev.* **2002**, *102*, 3667. (d) Earle, M. J.; Seddon, K. R. *Pure Appl. Chem.* **2000**, *72*, 1391. (e) Wasserchеid, P.; Keim, W. *Angew. Chem. Int. Ed.* **2000**, *39*, 3772. (f) Welton, T. *Chem. Rev.* **1999**, *99*, 2071.

[2] Endres, F.; Zein El Abedin, S. *Phys. Chem. Chem. Phys.* **2006**, *8*, 2101.

[3] Freemantle, M. *C&E N* **2001**, *79*, 21.

[4] Seddon, K. R. *Kinet. Catal.* **1996**, *37*, 693.

[5] Muzart, J. *Adv. Synth. Catal.* **2006**, *348*, 275.

[6] Zhao, H. *J. Mol. Cat. B: Enz.* **2005**, *37*, 16.

[7] Yang, Z.; Pan, W. B. *Enz. Microb. Tech.* **2005**, *27*, 19.

[8] Pandey, S. *Anal. Chim. Acta.* **2006**, *556*, 38.

[9] Reviews of nanoclusters: (a) Astruc, D.; Lu, F.; Aranzes, J. R. *Angew Chem. Int. Ed.* **2005**, *44*, 7852. (b) Burda, C.; Chen, X.; Narayanan, R.; El-Sayed, M. A. *Chem. Rev.* **2005**, *105*, 1025. (c) Murphy, C. J.; Sau, T. K.; Gole, A. M.; Orendorff, C. J.; Gao, J.; Gou, L.; Hunyadi, S. E.; Li, T. *J. Phys. Chem. B* **2005**, *109*, 13857. (d) Green, M. *Chem. Commuun.* **2005**, *24*, 3002. (e) Narayanan, R.; El-Sayed, M. A. *J. Phys. Chem. B* **2005**, *109*, 12663. (f) Cushing, B. L.; Kolesnichenko, V. L.; O'Connor, C. J. *Chem. Rev.* **2004**, *104*, 3893. (g) Shenhar, R.; Rotello, V. M. *Acc. Chem. Res.* **2003**, *36*, 549. (h) Roucoux, A.; Schulz, J.; Patin, H. *Chem. Rev.* **2002**, *102*, 3757. (i) Králik, M.; Biffis, A. *J. Mol. Cat. A* **2001**, *177*, 113. (j) Rao, C. N. R.; Kulkarni, G. U.; Thomas, P. J.; Edwards, P. P. *Chem. Soc. Rev.* **2000**, *29*, 27. (k) Schmid, G.;

Baumle, M.; Geerkens, M.; Heim, I.; Osemann, C.; Sawitowski, T. *Chem. Soc. Rev.* **1999**, *28*, 179. (l) Schmid, G.; Chi, L. F. *Adv. Mater.* **1998**, *10*, 515. (m) Fendler, J. H., Ed. *Nanoparticles and Nanostructured Films*; Wiley-VCH: Weinheim, 1998. (n) Fürstner, A., Ed. *Active Metals: Preparation, Characterization, and Applications*, VCH: Weinheim, 1996. (o) Bradley, J. S. in *Clusters and Colloids. From Theory to Applications*; Schmid, G., Ed.; VCH: New York, 1994; p. 459-544. (p) Schmid, G. *Chem. Rev.* **1992**, *92*, 1709. (q) A superb series of papers, complete with a record of the insightful comments by the experts attending the conference, is available in: *Faraday Discussions* **1991**, *92*, 1-300. (r) Schmid, G. in *Aspects of Homogeneous Catalysis*; Ugo, R., Ed.; Kluwer: Dordrecht, 1990; Chapter 1. (s) Andres, R. P.; Averback, R. S.; Brown, W. L.; Brus, L. E.; Goddard, W. A. III; Kaldor, A.; Louie S. G.; Moscovits, M.; Peercy, P. S.; Riley, S. J.; Siegel, R. W.; Spaepen, F.; Wang, Y.; *J. Mater. Res.* **1989**, *4*, 704. (t) Henglein, A. *Chem. Rev.* **1989**, *89*, 1861. (u) Thomas, J. M. *Pure Appl. Chem.* **1988**, *60*, 1517. (v) Jena, P.; Rao B. K.; Khanna, S. N; *Physics and Chemistry of Small Clusters*; Plenum: New York, 1987.

[10] Özkar, S.; Finke, R. G. *J. Am. Chem. Soc.* **2005**, *127*, 4800.

[11] Fonseca, G. S.; Scholten, J. D.; Dupont, J. *Syn. Lett.* **2004**, *9*, 1525.

[12] Dupont, J.; Fonseca, G. S.; Umpierre, A. P.; Fichtner, P. F. P.; Teixeira, S. R. *J. Am. Chem. Soc.* **2002**, *124*, 4228.

[13] Scheeren, C. W.; Machado, G.; Dupont, J.; Fichtner, P. F. P.; Teixeira, S. R. *Inorg. Chem.* **2003**, *42*, 4738.

[14] Fonseca, G. S.; Umpierre, A. P.; Fichtner, P. F. P.; Teixeira, S. R.; Dupont, J. *Chem. Eur. J.* **2003**, *9*, 3263.

[15] Caló, V.; Nacci, A.; Monopoli, A.; Laera, S.; Cioffi, N. *J. Org. Chem.* **2003**, *68*, 2929.

[16] Huang, J.; Jiang, B.; Gao, H.; Chang, Y.; Zhao, G.; Wu, W. *Chem. Commun.* **2003**, *14*, 1654.

[17] Kim, K.-S.; Demberelnyamba, D.; Lee, H. *Langmuir* **2004**, *20*, 556.

[18] Huang, J.; Jiang, T.; Gao, H.; Han, B.; Liu, Z.; Weize, W.; Chang, Y.; Zhao, G. *Angew. Chem. Int. Ed.* **2004**, *43*, 1397.

[19] Ott, L. S.; Cline, M. L.; Deetlefs, M.; Seddon, K. R.; Finke, R. G. *J. Am. Chem. Soc.* **2005**, *127*, 5758.

[20] Hermann, R.; Ugi, I. *Angew. Chem. Int. Ed.* **1982**, *21*, 788.

[21] Zhang, C.; Huang, J.; Trudell, M. L.; Nolan, S. P. *J. Org. Chem.* **1999**, *64*, 3804.

[22] Lee, H. M.; Jiang, T.; Stevens, E. D.; Nolan, S. P. *Organometallics* **2001**, *20*, 1255.

[23] Vázquez-Serrano, L. D.; Owens, B. T.; Buriak, J. M. *Chem. Comm.* **2002**, *21*, 2518.

[24] Mas-Marzá, E.; Poyatos, M.; Sanaú, M.; Peris, E. **2004**, *43*, 2213.

[25] Watzky, M. A.; Finke, R.G. *J. Am. Chem. Soc.* **1997**, *119*, 10382.

[26] Seddon, K. R.; Stark, A.; Torres, M.-J. *Pure Appl. Chem.* **2000**, *72*, 2275.

[27] Watzky, M. A.; Finke, R.G. *Chem. Mater.* **1997**, *9*, 3083.

[28] Aiken, J. D., III; Finke, R. G. *Chem. Mater.* **1999**, *11*, 1035.

[29] Aiken, J. D., III; Finke, R. G. *J. Am. Chem. Soc.* **1998**, *120*, 9545.

[30] Creighton, J. A.; Eadon, D. G. *J. Chem. Soc., Faraday Trans.* **1991**, *87*, 3881.

[31] Widegren, J. A.; Finke, R. G. *J. Mol. Cat. A: Chem.* **2003**, *198*, 317.

[32] Widegren, J. A.; Aiken III, J. D.; Özkar, S.; Finke, R. G. *Chem. Mater.* **2001**, *13*, 312.

[33] Finke, R. G. in *Metal Nanoparticles: Synthesis, Characterization, and Applications*; Feldheim, D. L., Foss, C. A., Jr., Eds.; Marcel Dekker: New York, 2002; Chapter 2, p 17-54.

[34] Umpierre, A. P.; Machado, G.; Fecher, G. H.; Morais, J.; Dupont, J. *Adv. Synth. Catal.* **2005**, *347*, 1404.

[35] Complete acetone hydrogenation was observed after the addition of 1 eqv $[Bu_4N][PF_6]$: however, the timescale for complete hydrogenation was increased to 24h as opposed to 10h if $[Bu_4N][PF_6]$ in 0.2 mL acetone was not added during the course of the reaction. A control experiment repeating this reaction, but adding 0.2 mL neat acetone, also increased the hydrogenation timescale to 24h indicating that the longer timescale observed in the added $[Bu_4N][PF_6]$ in 0.2 mL acetone system can be attributed to the added volume of acetone, not the $[Bu_4N][PF_6]$.

[36] Hornstein, B. J.; Aiken, J. D., III; Finke, R. G. *Inorg. Chem.* **2002**, *41*, 1625 and references therein on poisoning studies of traditional heterogeneous catalysts as a function of temperature and other variables.

[37] Hornstein, B. J. ; Finke, R. G. *Chem. Mater.* **2003**, *15*, 899.

[38] Widegren, J. A.; Bennett, M. A., Finke, R. G. *J. Am. Chem. Soc.* **2003**, *125*, 10301 (see the evidence for and discussion of the reversibility at higher temperature of CS_2 poisoning of $Ru(0)_n$ nanocluster catalysis of benzene hydrogenation on p. 10307).

[39] (a) Gonzalez-Tejuca, L.; Aika, K.; Namba, S.; Turkevich, J. *J. Phys. Chem.* **1977**, *81*, 1399. (b) Frety, R.; Da Silva, P. N.; Guenin, M. *Catal. Lett.* **1989**, *3*, 9. (c) Butt, J. B. *Catal. Sci. Technol.* **1987**, *6*, 1.

[40] Lebel, H.; Janes, M. K.; Charette, A. B.; Nolan, S. P. *J. Am. Chem. Soc.* **2004**, *126*, 5046.

[41] Clement, N. D.; Cavell, K. J.; Jones, C.; Elsevier, C. J. *Angew. Chem. Int. Ed.* **2004**, *43*, 1277.

[42] Clement, N. D.; Cavell, K. J. *Angew. Chem. Int. Ed.* **2004**, *43*, 3845.

[43] Besson, C.; Finney, E. E.; Finke, R. G. *J. Am. Chem. Soc.* **2005**, *127*, 8179.

[44] Besson, C.; Finney, E. E.; Finke, R. G. *Chem. Mater.* **2005**, *17*, 4925.

[45] One hypothesis for the slower rate in neat IL is the higher viscosity of $[bmim][PF_6]$ than acetone. However, the viscosity of ILs decreases exponentially with temperature (Harris, K. R.; Woolf, L. A.; Knakubo, M. *J. Chem. Eng. Data* **2005**, *50*, 1777); at 75 °C, the viscosity of neat IL should decrease to less than 18% of its viscosity at 25 °C (271 mPa·s). The addition of a co-solvent is also expected to decrease the viscosity exponentially (Seddon, K. R.; Stark, A.; Torres, M.-J. *Pure Appl. Chem.* **2000**, *72*, 2275; Wang, J.; Tian, Y.; Zhuo, K. *Green Chem.* **2003**, *5*, 618). Back-of-the-envelope calculations, factoring in both the addition of a 1.0 mL aceto and the 75 °C reaction temperature, estimate that the viscosity of the acetone ne /IL solution at 75 °C should be ~0.7 mPa·s, a value in the same ballpark as the 0.324 mPa·s viscosity of neat acetone. Hence, the viscosity of the acetone/IL solution is not expected to significantly slow catalysis.

[46] Hornstein, B. J.; Finke, R. G. *Chem. Mater.* **2004**, *16*, 139.

SUPPORTING INFORMATION

Are Imidazolium-Based Ionic Liquids a Preferred Medium and Stabilizer for Nanocluster Catalysts? The Test Case of Acetone Hydrogenation by $Ir(0)_n$ Nanoclusters.

Lisa Starkey Ott,[‡] Sarah Campbell,[§] Kenneth R. Seddon,[§] and Richard G. Finke[‡]*

Contribution from the [‡]Department of Chemistry, Colorado State University, Fort Collins, CO 80523, USA and the [§]QUILL Centre, The Queen's University of Belfast, Stranmillis Road, Belfast BT9 5AG, Northern Ireland, UK

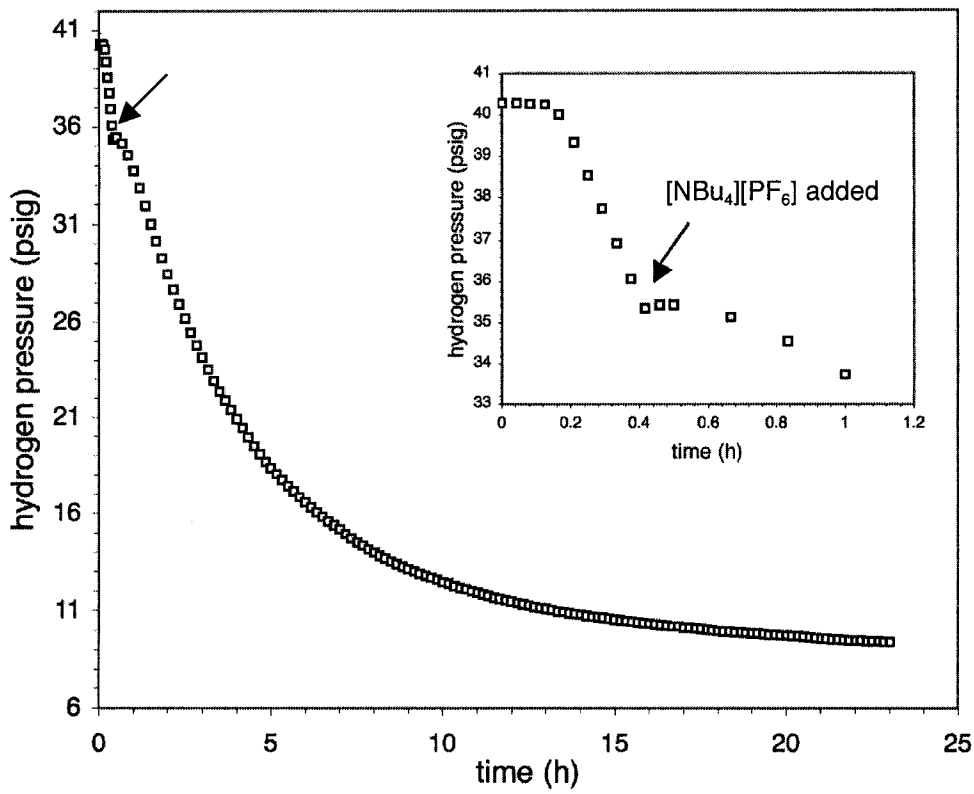

Figure S1. Acetone hydrogenation with 1 eqv $[Bu_4N][PF_6]$ in 0.2 mL acetone added at the time the arrow indicates; the slight rise in pressure observed at the point of addition is due to the acetone vapor phase re-equilibration with the system following the flushing with H_2 to reinitiate the reaction.[1] Complete acetone hydrogenation is observed after ~24 h. As mentioned in the main text, a control experiment reveals that the timescale is also lengthened to ~24 h when 0.2 mL neat acetone is added so that the increased reaction time is due to the added acetone, not the 1 eqv $[Bu_4N][PF_6]$.

[1] Widegren, J. A.; Aiken, J. D., III; Özkar, S.; Finke, R. G. *Chem. Mater.* **2001**, *13*, 312.

Evidence for the true catalyst in *the 3.6 mM 1, 22 °C, and 40 psig H_2 system in neat acetone.* In our previous work, $Ir(0)_n$ nanoclusters are implicated as the at least initial true catalyst for acetone hydrogenation at 3.6 mM **1**, 22 °C, and 40 psig H_2 on the basis with the following pieces of evidence:[2] TEM of the reaction solution shows that 18 ± 5 Å $Ir(0)_n$ nanoclusters are present, the brown color of the solution is characteristic of $Ir(0)_n$ nanoclusters[3] being present, bulk metal is not observed at least initially (i.e., until later in the reaction, typically after 2-4 hrs), and most importantly the kinetics of acetone hydrogenation which reveal the sigmoidal shape characteristic of nanocluster formation.[4] Fortifying the description of $Ir(0)_n$ nanoclusters as the true catalyst at least initially is the good fit to the kinetic data by the 3–step nanocluster formation mechanism of A→B, A+B→2B and B+B→C,[5] Figure S2 below. The tailing of catalytic activity toward the end of the reaction is characteristic of nanocluster agglomeration, B+B→C, as expected if little stabilizer is present (i.e., no anion[6] such as Cl^- from the precursor **1** since the formation of H^+ in reduction of the Ir(I) in **1** ties up the available Cl^- as H^+Cl^-.[7]).

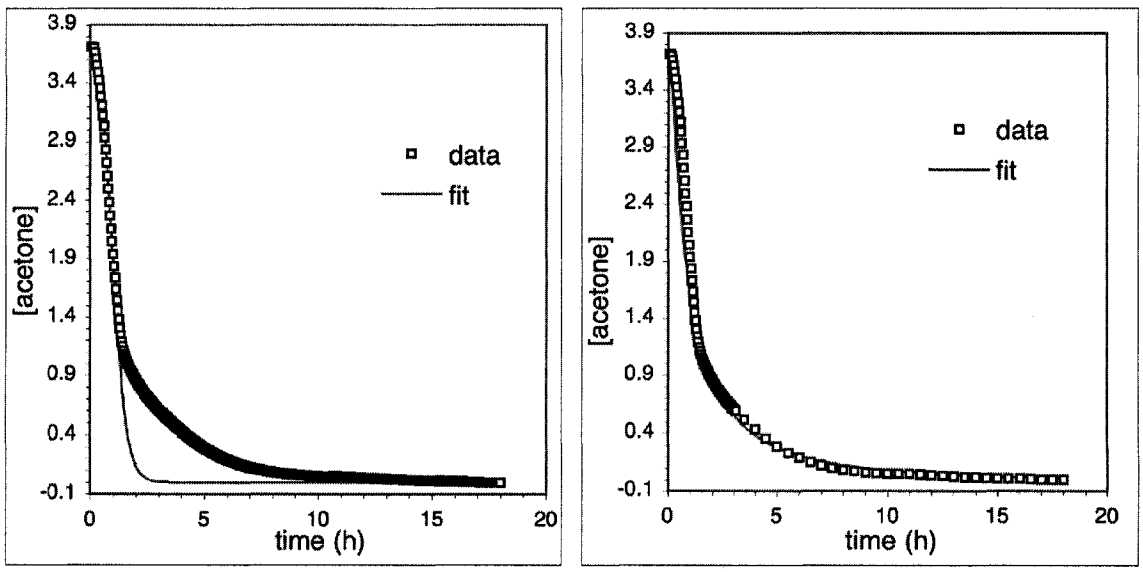

Figure S2. Kinetics for acetone hydrogenation in neat acetone at 3.6 mM **1**, 22 °C, and 40 psig H_2. The first two hours of the data are well-fit by the 2-step mechanism for nanocluster nucleation and growth (left; A→B, A+B→2B). However, the entire dataset is much better fit by the 3-step mechanism for nanocluster nucleation, growth, and agglomeration (right; A→B, A+B→2B, B+B→C),[5] a fact which also accounts for the

---

[2] Özkar, S.; Finke, R. G. *J. Am. Chem. Soc.* **2005**, *127*, 4800.

[3] Creighton, J. A.; Eadon, D. G. *J. Chem. Soc., Faraday Trans.* **1991**, *87*, 3881.

[4] Watzky, M. A.; Finke, R.G. *J. Am. Chem. Soc.* **1997**, *119*, 10382.

[5] Hornstein, B. J.; Finke, R. G. *Chem. Mater.* **2004**, *16*, 139.

[6] Anions have been shown to be key for the stabilization of prototype $Ir(0)_n$ nanoclusters (see, for example: Özkar, S.; Finke, R. G. *Langmuir* **2003**, *19*, 6247 and references therein), as predicted by the Derjaugin-Landau-Verwey-Overbeek (DLVO) theory of colloidal/nanocluster stability: Verwey, E. J. W.; Overbeek, J. T. G. *Theory of the Stability of Lyophobic Colloids*; 2 ed.; Dover Publications, Inc.: Mineola, New York, 1999.

[7] The formation of insoluble bulk metal at the end of the reaction implies a contribution to the total catalytic turnover number from the bulk metal (see footnote 21 on p. 4803 elsewhere[2]).

agglomeration of the unstable nanoclusters into the bulk metal observed at the end of the reaction.

In short, the evidence[2] is good that nanoclusters are the initial acetone hydrogenation catalyst in neat acetone at 22 °C and 40 psig H_2. That said, as pointed out previously bulk metal is known to make a contribution to catalysis at the higher, 16,400 maximum total turnovers for acetone hydrogenation observed.[2]

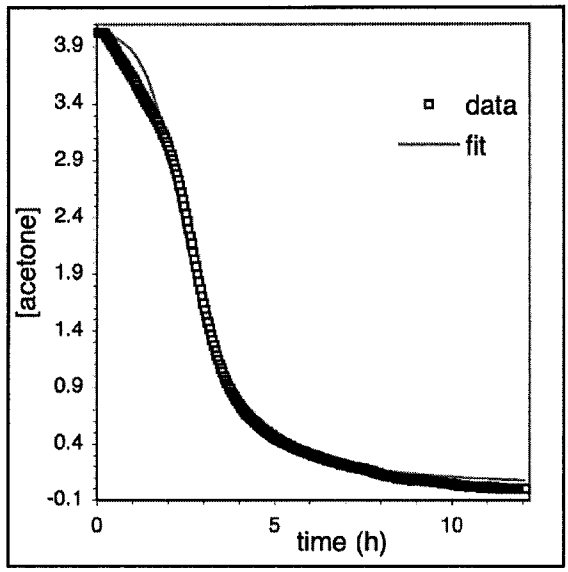

Figure S3. Kinetics of acetone hydrogenation beginning with the "colloidal suspension" derived from 52 mM **1**, 75 °C, and 58.7 psig H_2. The data is poorly fit by the 3-step mechanism for nanocluster nucleation, growth, and agglomeration[5] (A→B, A+B→2B, B+B→C), not unexpectedly since the starting material in this reaction is a mixture of **1,** nanoclusters plus agglomerated nanoclusters, and bulk metal.

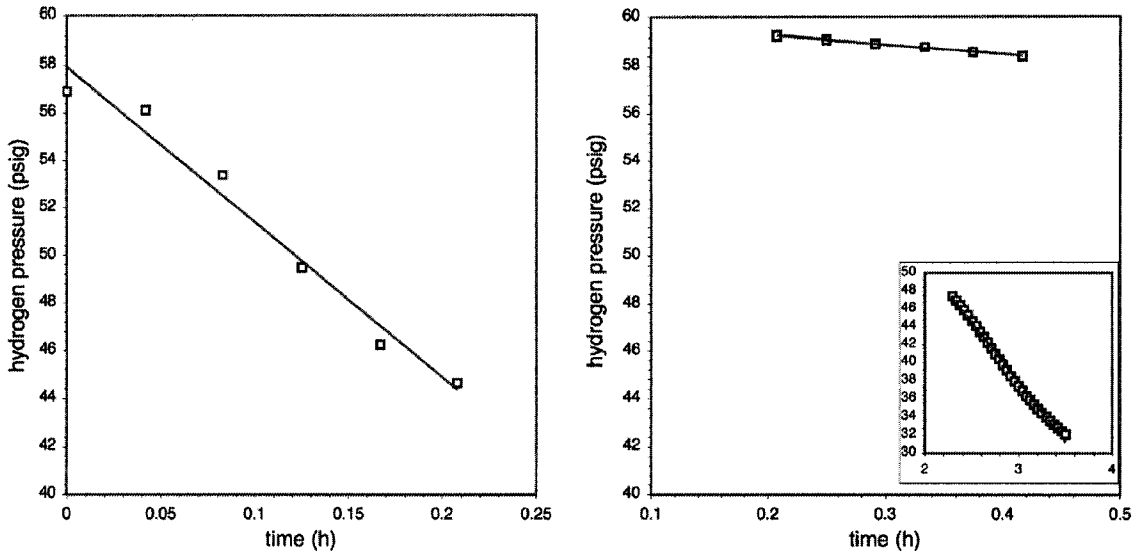

Figure S4. A comparison of the initial rates of cyclohexene hydrogenation by the bulk metal isolated from the 52 mM **1**, 75 °C, 58.7 psig H_2 conditions (left; 65±3 psig/h; data are from Figure 7 in the main text) and the "colloidal suspension" generated from the 52 mM **1**, 75 °C, 58.7 psig H_2 conditions (right; 3.5±0.2 psig/h directly after the induction period; the inset shows the rate of 13.2±0.7 psig/h after the second turndown / faster rate; the data are from Figure 3 in the main text). Note that the y-axes are plotted on the same scale in both cases while the time axis is longer in the right-hand figure.

Investigating The Metal Film and the Reaction Solution Prepared from 52 mM 1, 75 °C, and 58.7 psig H_2 in Neat IL. The bulk metal was investigated by XPS, Figure S5. Importantly, P, F, C, and N were detected. P and F were detected from the PF_6^- anion in the expected atomic ratio of 1:6. *Since the metal film was washed with acetone to remove the readily soluble IL before XPS analysis*, the detection of P and F indicates that intact PF_6^- molecules persist on the metal surface. Our finding of PF_6^- atop the Ir(0) surface is corroborated by XPS evidence that PF_6^- was present on the surface of dried $Pd(0)_n$ nanoclusters prepared in [bmim][PF_6].[8] The presence of PF_6^- on the metal film also (i) supports its role as a ligand, and (ii) supports recent findings which indicate that even weakly coordinating anions will interact with coordinatively unsaturated, electrophilic metal nanocluster surfaces.[9] Additionally, C and N were detected, atoms which may be present simply as the $[bmim]^+$ counterion for adsorbed PF_6^-. Alternatively, some of the C and N present may be due to *N*-heterocyclic carbenes (NHCs) formed from the $[bmim]^+$ counter cation (see Scheme 2 and the discussion in the main text).

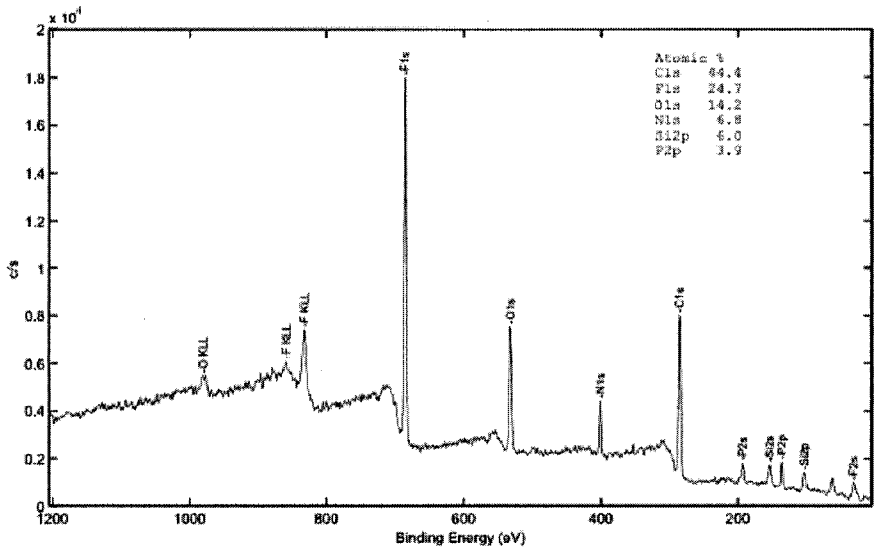

Figure S5. XPS spectrum of the Ir film produced in the 52 mM **1**, 75 °C, and 58.7 psig H_2 reaction in neat IL. Before analysis, the film was washed with acetone once (the IL is readily soluble in acetone). P and F peaks are present in a 1:6 atomic ratio, attributed to intact PF_6^- anions on the bulk metal surface. Peaks for C and N are clearly visible, attributable to either (i) the $[bmim]^+$ counterion to the PF_6^-, or (ii) possibly also some NHC on the metal surface. The O peak is likely a result of oxygen exposure during sample mounting and introduction into the XPS sample chamber. The Ir peak is small but detectable in a high resolution scan, as expected for the metal is under a layer of adsorbed PF_6^- and associated $[bmim]^+$. Also small but detectable in a high resolution scan is a peak for trace Cl, presumably from the $[(1,5\text{-COD})IrCl]_2$ precatalyst.

[8] Umpierre, A. P.; Machado, G.; Fecher, G. H.; Morais, J.; Dupont, J. *Adv. Synth. Catal.* **2005**, *347*, 1404.
[9] Ott, L. S.; Finke, R. G. "Nanocluster Formation and Stabilization Fundamental Studies: An Evaluation of DLVO Theory and Traditionally Weakly Coordinating Anions Plus High Dielectric Constant Solvents as Stabilizers of Prototype, Ir(0)n Transition-Metal Nanoclusters." Manuscript in preparation.

Attempted Nanocluster Formation Under 3.6 mM 1, 22 °C, 40 psig H_2 Conditions in Neat [bmim][PF_6].

To probe the effects of concentration, temperature, and pressure *in neat IL*, an experiment was carried out in an attempt to prepare a nanocluster "suspension" under our less forcing conditions of 3.6 mM **1**, 22 °C, and 40 psig H_2. After the 10 minute reduction under 40 psig H_2, the IL solution remained bright-yellow characteristic of [(1,5-COD)IrCl]$_2$ in [bmim][PF_6]; it did not change to a dark brown solution characteristic of Ir(0) nanoclusters[10] plus bulk metal as observed for the 52 mM **1**, 75 °C, 40 psig H_2 conditions. When acetone (1 mL) was added, the solution appeared somewhat darker. However, after 24 h no H_2 was taken up and ^{1}H NMR spectroscopy showed no conversion of acetone to isopropanol.

In a second, separate experiment, using the same 3.6 mM concentration and 22 °C temperature but changing to the higher 58.7 psig H_2 pressure, was also unsuccessful and did not yield either nanoclusters nor bulk metal; again, after 24 h no H_2 was taken up and ^{1}H NMR spectroscopy showed no acetone conversion.

These experiments: (i) confirm the poisoning of nanocluster formation from **1** in the presence of IL, (ii) attest to the need for "forcing conditions" to induce acetone hydrogenation catalysis in neat IL, and (iii) indicate the need for the combination of higher concentration, temperature, and/or pressure are needed before nanoclusters and/or bulk metal can be formed in neat IL.

[10] Creighton, J. A.; Eadon, D. G. *J. Chem. Soc., Faraday Trans.* **1991**, *87*, 3881.

Investigating the System Derived from 52 mM 1, 75 °C, and 58.7 psig H_2 in neat IL *but at 22 °C.* In order to investigate the possible temperature-dependent reversiblity of poisoning with added IL, the active catalyst system derived from 52 mM **1**, 75 °C, and 58.7 psig H_2 was studied at 22 °C, the prediction being that it might be inactive at lower temperature. Hence, a "colloidal suspension" was generated as described in the main text and following the literature procedure. The entire system, known through the work in the main text to include unreacted **1**, colloids, and bulk metal, was cooled and brought into the drybox. Acetone (1.0 mL) was added, the FP bottle was sealed, removed from the drybox, and re-attached to the H_2 line. The reaction solution was stirred for ≥10 minutes to attain a stable 22 °C temperature. Then, hydrogenation was initiated as described in the main text at 58.7 psig *but now at 22 °C.* Acetone hydrogenation (90% conversion after 24 h) was observed.

Since the evidence in the main text shows that *nanocluster* formation is poisoned by 1 equiv IL at 22 °C, the catalytic activity observed is very likely due to the bulk metal—indeed, we see no alternative explanation. This experiment, then, (i) provides additional evidence for the presence of a bulk-metal catalyst in the literature, higher temperature and pressure system involving precatalyst generation in IL; and (ii) is consistent with and supportive of bulk metal being catalytically active in the presence of *N*-heterocyclic carbenes derived from ILs. The reason for this is discussed in the main text, namely an apparent lower metal-ligand bond dissociation energy and the increased number of active sites on the bulk-metal in comparison to the smaller, more electrophilic, tighter ligand-binding nanoclusters.

Attempted Control of Catalyst Made with 1 Equiv Added [bmim][PF_6] but at 75 °C and 40 psig H_2 in Acetone. This experiment was set up exactly as described in the Experimental section of the main text under the heading "Nanocluster Formation Under 3.6 mM 1, 22 °C, 40 psig H_2 Conditions in Acetone with Added [bmim][PF_6]", with 1 eqv [bmim][PF_6] present in the acetone reaction solution. The FP bottle was attached to the H_2 line and stirred for 10 minutes in the water bath and under N_2 to raise the temperature of the reaction solution to 75 °C. Hydrogenation was initiated exactly as described in the section titled "Nanocluster Formation Under 52 mM **1**, 75 °C, 58.7 psig H_2 Conditions in Neat [bmim][PF_6]."

The yellow precursor solution quickly turned brown, then precipitated out of solution as bulk metal during the first five minutes of exposure to H_2. This finding that an active catalyst formed at the higher temperature and pressures (i.e., and when 1 equivalent of IL poisoned the catalyst as 22 °C and 40 psig H_2) would seem to demand reversal at higher temperatures and pressures of the poisoning effect. However, this experiment is somewhat flawed in that the kinetics of acetone hydrogenation were obfuscated by evaporation of acetone at the 75 °C reaction temperature via (1) acetone loss via venting out of the top of the FP bottle during the H_2 purging cycle, and (2) loss of acetone outside the culture tube placed inside the FP bottle apparatus (the latter of which separates the acetone from the catalyst, thereby shutting down catalysis).

CHAPTER VIII

SUMMARY

This dissertation has focused on the factors which affect the formation, stabilization, and subsequent catalytic activity of prototype $Ir(0)_n$ nanoclusters. A critical review of the extant nanocluster literature pointed out the need for compositionally well-defined nanocluster systems before nanocluster formation and stabilization can be rigorously addressed. Then, five solvents, five polymers, and four halides were thoroughly evaluated for their individual contributions to nanocluster formation, stabilization, and subsequent catalytic activity. The use of multiple alternative hypotheses led to verification of the ~60 year old predictions of DLVO theory, that anions in high dielectric constant solvents are the two most important factors controlling nanocluster stability, of at least catalytically active, $Ir(0)_n$ nanoclusters. Additionally, these three studies all confirmed the importance of the traditionally weakly coordinating anion BF_4^- as a surprisingly effective nanocluster stabilizer in high dielectric constant solvents. Next, the effects of 1,3-substituted imidazolium-based ionic liquids on $Ir(0)_n$ nanoclusters were investigated. The discovery of *N*-heterocyclic carbene formation from the $[bmim]^+$ cation contributed to the growing literature of ionic liquids as non-innocent solvents, and provided one hypothesis for the observed stability of $Ir(0)_n$ nanoclusters in

ionic liquids. Finally, our studies revealed that added ionic liquid could serve as a poison for nanoclusters at lower temperature and pressure for the test case of acetone hydrogenation, while a bulk metal catalyst remains active at higher temperatures and pressures.

There are several potential avenues for future research related to the materials presented herein. For example, useful studies include: (i) investigating the efficacy of other traditionally weakly coordinating anions, such as PF_6^- and $N(SO_2CF_3)_2^-$, for $Ir(0)_n$ nanoclusters and nanoclusters of other important transition-metals (such as Ru, Rh, and Pt); (ii) applying the 5 criteria method to rank the myriad of proposed nanocluster stabilizers in the literature; and (iii) extending the studies on the poisoning effects of ILs to include ILs prepared with other common cations, such as pyridinium and ammonium, to investigate whether or not the finding of nanocluster catalyst poisoning is general or not. Perhaps most importantly, we have recently developed a method for measuring the temperature-induced agglomeration of $P_2W_{15}Nb_3O_{62}^{9-}$–stabilized $Ir(0)_{\sim 2000}$ nanoclusters.[1] This study opens the door to quantitatively rank the "dizzying variety" of nanocluster stabilizers in the literature, and guides future research quantitating nanocluster stability toward using: (i) calorimetry; (ii) UV-visible spectroscopy (for metals with an appreciable plasmon absorbance band); and (iii) X-ray absorption fine structure or small-angle X-ray scattering spectroscopies. These final three topics are being pursued collaboratively.[2]

---

[1] Ott, L. S.; Finke, R. G. "Nanocluster Stabilization and Agglomeration Fundamental Studies: Can the Catalytic Reporter Reaction Method Quantitatively Measure Agglomeration Kinetics with Added Pyridine, Salts Such as $[Bu_4N][BF_4]$, or with Varying Temperature?" *Chem. Mater.*, submitted.

[2] Finke, R. G.; Buhro, W. E. Experiments in progress.

APPENDIX A

GENERAL STATEMENT ON "JOURNALS-FORMAT" THESES

(Written by Professor Richard G. Finke)

The Graduate School at Colorado State University allows, and the Finke Group in particular encourages, so-called journals-format theses. Journals-format theses, such as the present one, consist of a student written and lightly edited literature background section, chapters corresponding (in the limiting, ideal case) to final-form papers either accepted or at least submitted for publication, a summary or conclusions chapter, and short bridge or transition sections between the chapters as needed to make the thesis cohesive and understandable to the reader. The "bridge" sections and summary are crucial so that the thesis fulfills the requirement that the thesis be an entity (an official requirement of most Graduate Schools). All chapters (manuscripts) in a journals-format thesis must of course be written initially by the student, with subsequent (ideally light) editing by the Professor, the student's committee, and even the student's colleagues where appropriate and productive.

The advantages for doing a journals-format thesis are several-fold and compelling. Specifically, some of the major advantages are: the level of science (i.e. of refereed, accepted publications) is at the highest level; the student and Professor must

interact closely and vigorously (i.e. to bring both the science and the writing to their highest level), hence the student is getting the best education possible and is being at least exposed to (if not held to) the highest standards; the needed clean-up or control experiments that invariably come up have all been identified and completed before the student leaves; there are no further time demands once the student has left the University (since all the publications are at least submitted; it is terribly inefficient to try to complete either writing or often specialized experiments once the student has left); and the American tax payers, who ultimately pay the bill for the research, are getting their money's worth since all the research is published and thus widely disseminated in the highest form, as refereed science. Professorial experience teaches that a student who has achieved a journals-format thesis has indeed received a better education and has learned critical thinking and clear writing skills that will serve them well for a lifetime.

Experience also teaches, however, that much more than light editing is often needed in at least some student theses; it follows, then, that considerable professorial writing and editing might be needed for at least the initial chapters of most journals-format thesis. Indeed, a journals-format thesis is not recommended (and may not even be possible) for less strong students. Hence, the issue arises of exactly how much of the science and the writing, in the final (or submittable) chapters, is due to the student vs. the Professor and whether or not this level of contribution constitutes that acceptable of a new Ph.D. and independent investigator. An additional potential problem is that the journals-format thesis does not include unpublished/unpublishable experimental results (i.e., unless they are in footnotes or the Supporting Information), which may have significant value for future members of the research group.

To deal with these issues, several recommendations are made; the recommendations below have been discussed with the committee signing Lisa Starkey Ott's dissertation: (Mrs. Ott's dissertation is the thirteenth such thesis from the Finke Group following Dr. C. Garr's, Dr. Y. Lin's, Dr. M. Pohl's, Dr. J. Sirovatka's, Dr. J. Aiken's, Dr. R. Suto's, Dr. J. Widegren's, Dr. K. Doll's and Dr. C.-X. Yin's dissertations, and Ms. K. Weddle's, Mr. W. White's, and Mr. C. Hagen's Masters theses.) The recommendations are:

(i) That the present pages be enclosed in the thesis until such a time as it is no longer needed;

(ii) That for each chapter it is detailed, and to the satisfaction of the committee and the advisor, who made what contributions, both of intellectual substance and writing. [Substantial contributions of other students or Professors should of course also be acknowledged. In the case of disagreements, the various drafts (i.e. as their electronic files) can be examined by the committee (in light of a knowledge of who wrote which draft) to easily determine who contributed what. In possible borderline or controversial cases it may even be advisable to keep all (electronic) drafts of the papers as a record];

(iii) That it be specifically stated whether or not all the experimental work is the Ph.D. candidate's;

(iv) Furthermore, it is recommended that allowances be made for the expectation that a greater degree of involvement of the professorial advisor is likely in a journals-format thesis than in a traditional thesis. [That this is reasonable follows from the fact that some Professors write 100% of all their papers; this, unfortunately, robs the student

of the valuable experience of participating in the science and the end product as practiced at the highest levels.];

(v) Notwithstanding (iv), there needs to be ideally no more than ca. 40% Professorial writing contribution in a given early chapter in the thesis, and there should be a clear evolution in the thesis of a decreasing professorial involvement to, say, a 10-20% direct contribution in the last chapter or two;

(vi) As a further aid towards separating out the candidate's and the professorial (and other) contributions, it is recommended that the Introductory (usually literature background) chapters(s) and at least the final chapter be lightly edited only, so that authentic examples of the student's contributions are documented in an unambiguous form.

(vii) In order to avoid the loss of useful, but unpublished/unpublishable, experimental work by the student writing a journals format-thesis, the Finke Group requires the following: (1) carefully kept laboratory notebooks; (2) mandatory research reports detailing the results of any unpublished work; and (3) the extensive use of Supporting Information and textual footnotes, where appropriate, in all published work.

APPENDIX B

RESEARCH PROPOSAL

Synthesis of Benzoylthiourea-Modified Carbon Aerogels and Xerogels for Mercury Remediation from Waste Streams

Abstract/Specific Aims

Mercury remediation from the air, water, and soil is a pressing environmental concern. The isolation and sequestration of both Hg^0 and Hg^{2+} are of interest as each form of mercury carries its own environmental and toxicological risks. Consequently, in addition to reducing anthropogenic sources of mercury pollution, the removal of existing mercury from the waste gases and liquids is also important. Many materials have been used for Hg^{2+} remediation from both gaseous and liquid wastes: recently, mesoporous materials have been used for this purpose. Mesoporous materials (defined and having pore sizes of 2-50 nm[1]) are advantageous as remediation materials due to their high surface area. Though mesoporous silicas such as MCM-41[2] and MCM-48[3] functionalized with "mercury-loving" thiol groups have been shown to competently sorb Hg from test solutions, there are also several drawbacks to using siliceous materials.

Aerogels and xerogels (*vide infra*) can be prepared from a variety of different materials, including silica, titiania, alumina, and many others. Organic aerogels are easily prepared with a mild synthesis, and are unique in their pyrolyzed xerogel form as they are capable of conducting electricity. The aim of this work is to develop novel benzoylthiourea-functionalized carbon aerogels and xerogels as materials for Hg^{2+} remediation: their simple preparation, high porosity and surface area, and potential for electrochemical recovery of the adsorbed mercury should make them superior remediation materials. Additionally, the xerogels are expected to have some competence at removing Hg^0 from waste streams by physical adsorption.[4] The hypothesis to be tested herein is that novel benzoylthiourea-functionalized carbon aerogels and xerogels will be superior materials for Hg remediation in terms of ease of synthesis, total mercury sorption, and efficient method for Hg recovery and material recyclability.

Background and Significance

Mercury remediation is a critical environmental and toxicological issue. Mercury is found in the atmosphere, soil, and water in greater than natural abundances due to several anthropogenic sources, including the chloralkali process, coal combustion, discarded laboratory chemical, batteries, broken thermometers, and formerly from lawn fungicides and pharmaceutical products.[5] It is been estimated that anthropogenic sources are responsible for 70% of the mercury deposited in the last 100 years.[6] This increased level of mercury is of concern due to the relatively low ability of the human body to excrete mercury—thus, the metal bio-accumulates.[6] Once in the body, mercury may penetrate the blood-brain barrier causing severe harm. Toxicological effects of mercury

accumulation include but are not limited to "neurological damage, including irritability, paralysis, blindness, or insanity; chromosome breakage, and birth defects."[5] Mercury may enter the body through many pathways, including inhalation of mercury vapors and consumption of contaminated species such as fish (as in the well-known Minimata Bay incident).[7]

Due to these human risks (among others), it is important to remove mercury from contaminated soils, waters, and gases. Many methods have been used for the recovery of mercury-contaminated soils. One common, traditional method involves the excavation and disposal of contaminated soil.[6] However, this just moves the problem, not addressing the isolation of the mercury from the contaminated soils. Two methods under current development are phytoremediation and bioremediation, both of which focus on the concentration and removal of mercury from the soils.[6] Though there have been some promising strides made in this area, neither option is viable for liquid or gaseous waste streams.

For liquid and gaseous wastes, a porous, solid material is desirable so the waste to be treated may be passed through the material. Additionally, the use of a solid material facilitates removal of the material once it has been saturated with mercury. Several solid adsorbents have been used as heavy metal remediation materials, including activated carbon, organic ion exchange polymers, and many thiol-functionalized silica materials.[8] These solid materials allow for simple removal of the metal-loaded material from liquid and gaseous waste streams. Mesoporous solids are desirable as remediation materials due to their high surface area. A mesoporous material is defined as having pores of

widths between 2-50 nm, while macroporous materials have pores exceeding 50 nm and microporous materials have pores not exceeding 2 nm.[1]

Two mesoporous materials receiving current interest in the literature are aerogels and xerogels (porosity >85%).[9] Simply defined, aerogels and xerogels are "dried gels with a very high relative pore volume".[10] Aerogels and xerogels have been prepared from a wide variety of materials, including titania, silica, alumina, other metal oxides, and aromatic organics.[10] The difference between an aerogel and a xerogel depends on the method of gel drying.[11] If the reaction solvent is allowed to simply evaporate from the gel, capillary forces cause the gel skeleton to collapse and a *xerogel* is formed. However, if the solvent is removed under supercritical conditions, the gel skeleton is preserved and an *aerogel* is formed.[12] Since these gels are metastable with respect to their thermodynamic properties, they can undergo chemical transformations easily (i.e., when pyrolyzed).[10] Such chemically transformed gels are also referred to in the literature as xerogels.

There are now many reports of organic aerogels and xerogels. These aerogels have been studied since 1931,[13] but have only recently come into vogue.[14,15,16] The most common preparation for organic aerogels involves the polycondensation of resorcinol with formaldehyde (referred to as RF gels).[12,31] Other precursor include melamine-formaldehyde, phenolic-furfural with poly(dimethylsiloxane), poly(acrylonitrile), or poly-isocyanates.[10] Organic aerogels possess high surface areas (~700 $m^2 g^{-1}$ for simple carbon aerogels,[13] up to ~900 $m^2 g^{-1}$ for a recently prepared thiophene-modified carbon aerogel[17]). Additionally, some unmodified carbon aerogels are now commercially available.[14] Organic aerogels and xerogels have found many widely varied applications,

including architectural and appliance insulation, capacitors, and lightweight optic materials.[18] Functionalized carbon aerogels are also being investigated as hosts for supported metal nanoclusters and for fuel cell electrocatalysts.[19]

In addition to the above applications, some aerogels have been tested as waste-remediation materials for a variety of different substances.[20,21,22] For example, a titania-silica aerogel was used as a photocatalyst in the oxidation and degradation of aqueous cyanide species.[20] This aerogel, which could be reused three times, showed an approximately 60% higher removal of cyanide than colloidal titania tested under the same conditions. In two separate cases, silica aerogels were used as remediation materials for nuclear wastes (Nd_2O_3 was used as a model for actinide oxides[21]) and metal cations such as Cu^{2+}, Ni^{2+}, Co^{2+} and the heavier Cd^{2+}.[22] Both silica aerogels were shown to be competent at removing the desired species, but in one case it was admitted that the metal loading was lower than previous materials due to "low ligand access" in the functionalized silica material.[22]

Thiol-functionalized mesoporous silica materials have been studied in some detail as Hg^{2+} remediation materials.[2,3,23,24,25,26] These thiolated, "mercury-loving" materials offer several benefits. For example, some thiolated silicas have achieved a high loading of Hg, including some materials that are able to absorb more than their own weight in mercury (up to ~1.3 g Hg^{2+} per g adsorbent[26]). Additionally, some of these functionalized silica materials offer simple regeneration processes.[26]

Though they show promise for Hg remediation, mesoporous silica materials also have several drawbacks. For the regeneration mentioned above, the most common procedure (washing with a thiol-containing, acidified solution[2,3]) leads to the generation

of a secondary waste. Additionally, some silicas studied thus far have been thiolated with a two-step "postsynthesis functionalization" to incorporate a benzoylthiourea ligands on the surface.[2,3] This synthesis first functionalizes the silanol surface groups with amine groups (for example, 3-aminopropyltriethoxysilane[2]), then converts these amine groups by reaction with benzoyl isothiocyanate. This method, in addition to being time consuming, leaves some silanol sites unfunctionalized and some with amine functionalities. For instance, functionalization with benzoylthiourea only went to 70% completion with an MCM-41 material[2] and decreased even to 50% for an MCM-48 material.[3] The authors attributed this low functionalization, which normally goes to completion,[27] to the confined geometry of the pre-formed pore structure. This functionalization with both amines and thiol groups leads to a significant decrease of the surface area of the silica materials. For example, one thiol-functionalized material lost over 60% of its surface area post-functionalization.[2] Functionalization likely blocks the channels of the silica material, making the material less useful for applications when the fluid to be treated must be passed through the material for remediation. Thus, it appears that an alternative material needs to be developed for effective Hg adsorption.

Several forms of carbon (including carbon aerogels, *vide infra*) have been studied as mercury remediation materials. Activated carbon was first used as a mercury filter in a breathing apparatus in 1934.[28] Since then, it has been studied as a filter used to remove Hg^{2+} from gas streams.[29] In this study, it was found that without specific "mercury-loving" functionalities, the Hg^{2+} loading was low. While the activated carbon did adsorb some Hg^{2+} from the gas stream, it was found that an activated carbon material functionalized with sulfur (either by functionalization with 8 wt% sulfuric acid or with 11

wt% elemental sulfur) was capable of a higher loading of Hg^{2+} through a chemisorption mechanism.[29] Using the sulfur-impregnated material, the Hg filter lifetime increased 40-fold. This illustrates the importance of incorporating a specific "mercury-loving" functionality into carbonaceous remediation materials. Since the initial study, a wide variety of other forms of carbon such as carbon cloth[4] and sewage sludge carbon[30] have been studied for the removal of both Hg^0 and Hg^{2+}.

Recently, carbon aerogels have been studied as Hg^{2+} remediation materials.[14,15,16] In these studies, the aerogels were purchased from and characterized at Lawrence Livermore National Laboratories. The aerogels were subsequently used in the test reaction of Hg^{2+} remediation from a model wastewater stream prepared from $HgCl_2$. While the carbon aerogels did adsorb some mercury from the simulated wastewater, the maximum loading of 35 mg Hg^{2+} per g of carbon aerogel[14] was more than 38 times lower than reported for a thiol-functionalized silica material.[26] This suggests that a carbon aerogel would benefit from incorporated sulfur. Additionally, no competition studies were performed with the pure carbon aerogel to determine if the material specifically adsorbed Hg, and no recycling studies were performed.

The preparation of a sulfur-functionalized carbon aerogel has been recently reported in the literature.[17] In this synthesis, the sulfur functionality was introduced as a co-condensate (as 3-thiophenecarboxaldehyde) during an RF gel synthesis. After pyrolysis of the aerogel, the presence of the thiophene moiety in the final xerogel was confirmed by XPS. This novel material was used to adsorb pre-formed Pt colloids and subsequently used for oxygen reduction catalysis. The mild synthesis with a high percent incorporation of sulfur indicates that a similar material may be synthetically accessible as

a stable, porous, high-surface area Hg remediation material. Additionally, this synthesis incorporates sulfur in one step (instead of the previously used two-step "post-synthesis functionalization"), saving time and avoiding remaining amine groups in the final material.

The hypothesis to be tested herein is that novel benzoylthiourea-functionalized carbon aerogels and xerogels will be superior materials for Hg remediation in terms of ease of synthesis, total mercury sorption, and efficient method for Hg recovery and material recyclability. The one-pot co-condensation of an aldehyde-modified benzoylthiourea during gel synthesis[31] should lead to a high percent incorporation of sulfur functionality without the need for a prior amine functionalization step.[2,3] Additionally, this novel materials should offer higher levels of Hg^{2+} adsorption using multiple functionalities on the benzoylthiourea ligand, coupled with high accessibility garnered by building the ligand into the gel skeleton. In their pyrolyzed, electrically conductive form, it may be possible to electrochemically remove adsorbed mercury from the xerogel material. If realized, this material should allow for an easily prepared, highly functionalized material with a high sorption capability and a regeneration method with significantly reduced secondary waste generation.

Research Design and Methods

The synthesis of the novel benzoylthiourea-functionalized carbon gel should be fairly straightforward. Benzoylthiourea has been selected for Hg adsorption for two reasons: (i) it has other functional groups (in addition to the thiol) that are "active" toward mercury adsorption, and (ii) the thiourea ligand should bind the mercury less

strongly than a thiol, facilitating removal of the mercury during recycling.[2,3] Before the gel is prepared, formylated benzoylthiourea needs to be prepared. This will be accomplished following literature precedent for the formylation of substituted aromatic compounds,[32] as in Scheme 1 below.

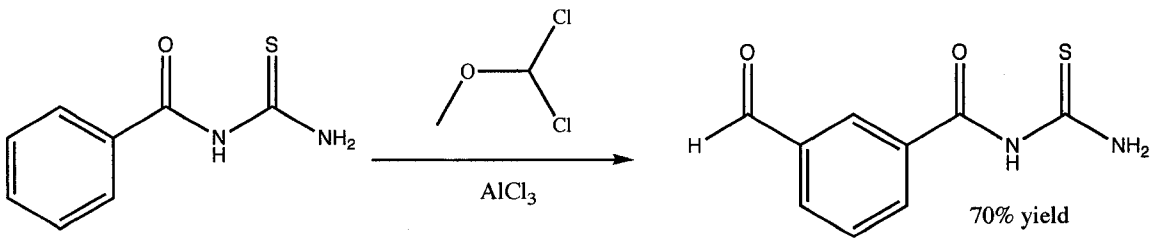

Scheme 1. Synthesis of the formylated benzoylthiourea.

Next, the aerogel will be prepared by the well-known RF method.[12,31] The initial steps of the RF gel preparation will be carried out in water using Na_2CO_3 as a base catalyst (a portion of this sample should be set aside without functionalization for use as a control, *vide infra*). The aldehyde-modified benzoylthiourea ligand will be added before the curing step, as done previously in the preparation of a thiophene-modified aerogel,[17] for co-condensation and incorporation of "mercury-loving" functionality into the gel skeleton. However, at this point, one modification will be made from the previously published method of incorporating a sulfur functionality: the now-functionalized material will be subjected to an acid wash with trifluoroacetic acid in order to remove the sodium salts remaining (from the Na_2CO_3 catalyst) and to promote further cross-linking of the gel.[12] The remaining solvent exchange, curing, and drying steps will be carried out as previously described (see Scheme 2).[17] While this synthesis is mild with a high yield of product, one drawback is the timescale. The complete synthesis, including the modification of the benzoylthiourea ligand, is estimated to take approximately 18 days.

Scheme 2. Synthesis of the novel benzoylthiourea-functionalized carbon aerogel.

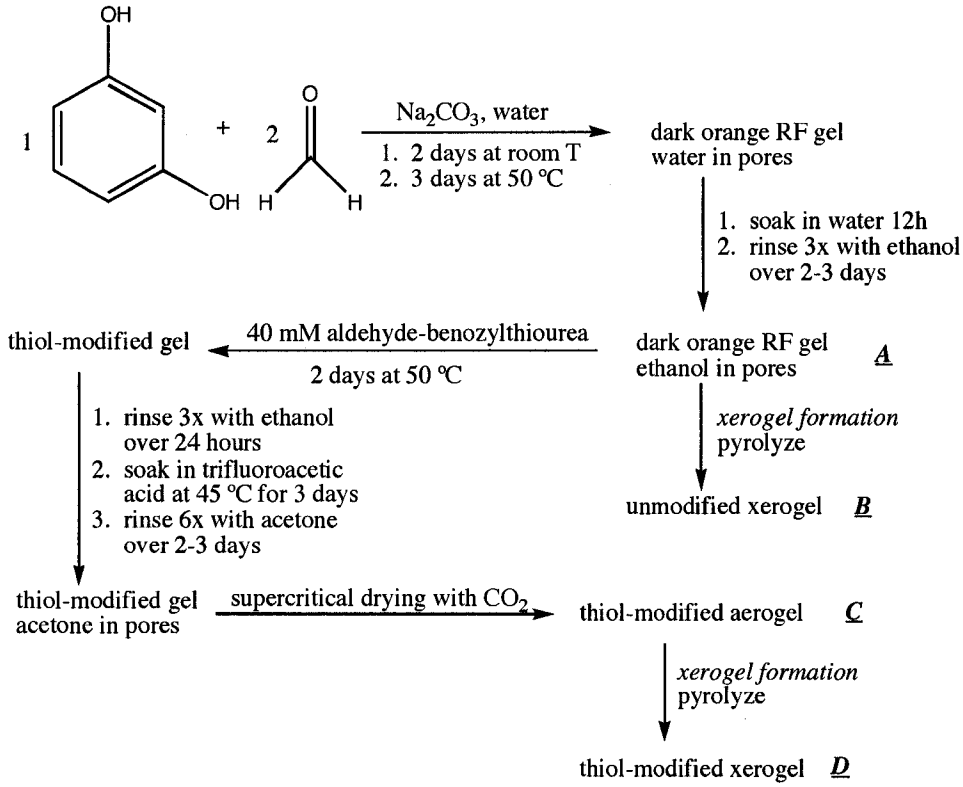

From this synthesis, four materials should first have their physical properties characterized and then their ability to remove mercury from the solution should be studied. First, the portion of the sample that was not functionalized should be examined in both its aerogel (sample A) and xerogel (sample B) form. These samples will be used as controls to examine the influence of the benzoylthiourea group. The as-prepared sulfur-functionalized aerogel (sample C) and its pyrolyzed xerogel form (sample D) should both be examined to ensure that co-condensation was successful. For this, X-ray photoelectron spectroscopy (XPS) can be used to test for the presence of S.[17] These four materials should then be characterized by the following methods.

The three most important characterization techniques for these aerogels and xerogels are determination of the total pore volume, the Brunauer-Emmett-Teller (BET) surface

area, and the primary mesopore diameter. The total pore volume is measured by determining the quantity of an absorbent (usually N_2 at a temperature and pressure near its liquid phase transition), assuming that the pores are then filled with condensed adsorptive.[1] The BET surface area is the most widely used and reported measure of the surface area of a given material.[1] In this test, the number of molecules of a test gas (again, usually N_2) needed to form an absorbed monolayer on the material surface is determined. From this number of molecules, an average surface coverage of each molecule is calculated and the surface area is established.[1] The primary mesopore diameter is measured by first determining the mean hydraulic radius of a group of mesopores (Equation 1) and then, assuming a cylindrical shape for the pores, calculating the mean pore radius (Equation 2),[1]

$$r_h = \left(\frac{V}{A_S}\right)_p \qquad r_p = 2r_h \qquad \textit{equation 2}$$

where r_h is the mean hydraulic radius, V is the volume of the pore walls, A_S is the area of the walls (both V and A at a given pressure p), and r_p is the mean pore radius. After these materials have been thoroughly characterized, their pore volumes, surface areas, and mesopore diameters should be compared to previous literature reports.

The most valuable tests for the new material are Hg^{2+} remediation tests. For this, there are four important tests: batch, kinetic, competition, and regeneration/recyclability tests. First, batch tests should be run to determine the total capacity of the material. In these tests, the material should be stirred with a standard solution of known Hg concentration (for example, prepared with $Hg(NO_3)_2$ as in the literature[24]). The final Hg

concentration remaining in solution can be monitored using inductively coupled plasma-optical emission spectroscopy set to monitor emission at 253 nm for Hg^{2+}.[25] The total amount of Hg adsorbed by the material can then be determined by taking the difference of the total mercury added and the mercury concentration remaining in solution. In the second important test of the novel material, kinetic tests should be performed to determine the timescale for Hg^{2+} adsorption. These tests can be carried out in the same manner as the batch tests, but the Hg content remaining in solution should be examined frequently during the course of the test. These tests will help determine if this material is appropriate for rapid application. Third, competition tests should be performed with other soft heavy metal cations to determine the specific affinity of the novel material for Hg^{2+} in the presence of other cations. This is important for applications for which the removal of Hg in the exclusion of other cations is desired. Additionally, this is important so that the material does not get "saturated" with other cations before it has a chance to adsorb Hg from solution. Controls should also be done with a non-benzoylthiourea modified aerogel (samples A and B) to determine the effects of the new ligand.

Lastly, the fourth important test of the new material involves regeneration/recyclability tests. These should be performed to determine whether or not this material will be reusable. In previous studies, Hg has been removed from mesoporous media by washing with HCl solutions. While this method has been shown to be effective, it does produce a significant quantity of acidic waste contaminated with mercury. Regardless, this method should be tested on all four material in order to compare the recyclability of the novel materials with past materials. One unique method for recovery of the mercury from the xerogel material could exist. Recently, it has been

shown that carbon aerogels can be used as electrodes.[33,34] Additionally, it was recently shown that a carbon cloth used as a Hg^{2+} sorption material could be regenerated by electrochemical stripping.[4] If the xerogel is to be used as an electrode (samples B and D), optimized synthesis conditions and pyrolyzing temperatures have been elucidated to maximize surface area and conductivity.[34] Using the xerogel described herein, it may be possible to electrochemically reduce the adsorbed Hg^{2+} to Hg^0. The Hg^0 can then be removed from solution by deposition on a sacrificial electrode.[4] This will regenerate the unloaded xerogel for further use, and eliminate the generation of acidic secondary waste generated in the commonly used recycling procedure. Additionally, since in the previous case >99% of the mercury was removed from the electrode, this electrochemical regeneration of the xerogel may lead to repeated use without a significant loss of mercury adsorption.

This material described herein are expected to remove Hg^{2+} from waste streams by chemical adsorption with sulfur moiety on the benzoylthiourea ligand. It may be anticipated that the xerogel form of this material may adsorb Hg^0 as well, as activated carbons have frequently been studied as Hg^0 adsorbent materials.[4,30,35,36] Most activated carbons have shown improved performance for Hg^0 adsorption once impregnated with sulfur. However, along with this improved performance increase comes a decrease in surface area with sulfur impregnation and thus a decrease in the total loading capability of the material. The material described herein may be an efficient adsorbent material for Hg^0 given the nature of the xerogel material and the high surface area achieved by building the sulfur functionality into the gel skeleton.

Potential limitations to this approach include incomplete incorporation of the benzoylthiourea ligand into the gel during the curing step and/or loss of the sulfur functionality during the pyrolyzation step. Additionally, the somewhat bulky benzoylthiourea ligand may block some of the channels in the aerogel, reducing both the total capacity of the material and the flow of liquid or gas through the material. In the electrochemical regeneration method, it may be possible that some of the Hg-S bonds are too strong to break electrochemically. However, there is some evidence that Hg-S bonds may be broken this way.[4] An alternative pathway to novel sulfur-functionalized carbon aerogels may be the utilization of different precursors: for example, the melamine-formaldehyde gel may show enhanced mercury sorption through its amine groups.[10] Coupled with a benzoylthiourea functionality, this material may surpass the material described herein in terms of total sorption capacity.

Conclusions

This proposal intends to test the hypothesis that novel carbon aerogels and xerogels with benzoylthiourea groups built into the gel skeleton will be superior materials for mercury remediation. This material should be easily accessible through a polycondensation reaction after the desired benzoylthiourea ligand has been formylated. Incorporating the benzoylthiourea ligand into the gel skeleton should allow for greater ligand access and thus higher loading of mercury into the material. Once prepared and characterized, the novel material should be capable of removing Hg^0 and Hg^{2+} from gaseous and aqueous wastes. After the mercury has been adsorbed, an electrochemical method for removing the mercury and regenerating the material may be possible. This

method should allow for the reuse of the material without the generation of acidic mercuric wastes. Overall, the material herein should provide the current best material for Hg remediation in terms of ease of synthesis, total mercury sorption, and efficient method for Hg recovery and material recyclability.

References

[1] Sing, K. S. W.; Everett, D. H.; Haul, R. A. W.; Moscou, L.; Pierotti, R. A.; Rouquérol, J.; Siemieniewska, T. *Pure Appl. Chem.* **1985**, *57*, 603.
[2] Antochshuk, V.; Olkhovyk, O.; Jaroniec, M.; Park, I.-S.; Ryoo, R. *Langmuir* **2003**, *19*, 3031.
[3] Olkhovyk, O.; Antonchshuk, V.; Jaroniec, M. *Coll. Surf., A: Physiochem. Eng. Aspects* **2004**, *236*, 69.
[4] Bolger, P. T.; Szlag, D. C. *Environ. Sci. Tech.* **2003**, *36*, 4430.
[5] Manahan, S. E. *Environmental Chemistry*, 8th Ed.: CRC Press; Boca Raton, FL, 2005.
[6] Hutchison, A. R.; Atwood, D. A. *J. Chem. Crystal.* **2003**, *33*, 631.
[7] Fellenberg, G. *The Chemistry of Pollution*: John Wiley and Sons, Ltd.; London, 2000.
[8] Schroden, R. C.; Al-Daous, M.; Sokolov, S.; Melde, B. J.; Lytle, J. C.; Stein, A.; Carbajo, M. C.; Fernández, J. T.; Rodriguez, E. E. *J. Mater. Chem.* **2002**, *12*, 3261.
[9] Reichenauer, G. *Part. Part. Syst. Charact.* **2004**, *21*, 117.
[10] Pierre, A. C.; Pajonk, G. M. *Chem. Rev.* **2002**, *102*, 4243.
[11] Pekala, R. W.; Alviso, C. T. Carbon Aerogels and Xerogels. In *MRS Symposium Proceedings*; Renschler, C. L., Pouch, J. J., Cox, D. M., Eds.; Materials Research Society: Pittsburg, PA, 1992; vol. 270, p. 3.
[12] Pekala, R. W. US Patent 4,873,218.
[13] Kistler, S. S. *Nature* **1931**, *127*, 741.
[14] Goel, J.; Kadirvelu, K.; Rajagopal, C.; Garg, V. K. *Carbon* **2005**, *43*, 195.
[15] Goel, J.; Kadirvelu, K.; Rajagopal, C.; Garg, V. K. *J. Chem. Technol. Biotechnol.* **2005**, *80*, 469.
[16] Goel, J.; Kadirvelu, K.; Rajagopal, C.; Garg, V. K. *Ind. Eng. Chem. Res.* **2005**, *44*, 1987.
[17] Baker, W. S.; Long, J. W.; Stroud, R. M.; Rolison, D. R. *J. Non-Crystal. Solids* **2004**, *350*, 80.
[18] Hrubesh, L. W. *J. Non-Crystal. Solids* **1998**, *225*, 335.
[19] Rolison, D. R. *Science* **2003**, *299*, 1698.
[20] Ahmed, M. S.; Attia, Y. A. *J. Non-Crystal. Solids* **1995**, *186*, 402.
[21] Woingnier, T.; Reynes, J.; Phalippou, J.; Dussossoy, J. L.; Jacquet-Francillon, N. *J. Non-Crystal. Solids* **1998**, *225*, 353.
[22] Bois, L.; Bonhommé, A.; Ribes, A.; Pais, B.; Raffin, G.; Tessier, F. *Coll. Surf. A: Physiochem. Eng. Aspects* **2003**, *221*, 221.

[23] Mercier, L.; Pinnavaia, T. J. *Adv. Mater.* **1997**, *9*, 500.
[24] Mercier, L.; Pinnavaia, T. J. *Environ. Sci. Technol.* **1998**, *32*, 2749.
[25] Nooney, R. I.; Kalyanaraman, M.; Kennedy, G.; Maginn, E. J. *Langmuir*, **2001**, *17*, 528.
[26] Olkhovyk, O.; Antonchshuk, V.; Jaroniec, M. *Coll. Surf., A: Physiochem. Eng. Aspects* **2004**, *236*, 69.
[27] *Comprehensive Organic Functional Group Transformations*; Katritzky, A. R., Meth-Cohn, O., Rees, C. W., Eds.; Pergamon: New York, 1995; Vol. 6, Chatper 18.
[28] Pütter, K. E.; Hirsch, M. *Angew. Chem.* **1934**, *47*, 184.
[29] Henning, K.-D.; Keldenich, K.; Knoblauch, K.; Degel, J. *Gas Sep. Pur.* **1988**, *2*, 20.
[30] Zhang, F.-S.; Nriagu, J. O.; Itoh, H. *J. Photochem. Photobio., A* **2004**, *167*, 223.
[31] Saliger, R.; Bock, V.; Petricevic, R.; Tillotson, T.; Geis, S.; Fricke, J. *J. Non-Cryst. Solids* **1997**, *221*, 144.
[32] Yakubov, A. P.; Tsyganov, D. V.; Belen'kil, L. I.; Krayushkin, M. M. *Tetrahedron* **1993**, *49*, 3397.
[33] Pekala, R. W.; Farmer, J. C.; Alviso, C. T.; Tran, T. D.; Mayer, S. T.; Miller, J. M.; Dunn, B. *J. Non-Crystal. Solids* **1998**, *225*, 74.
[34] Kim, S. J.; Hwang, S. W.; Hyun, S. H. *J. Mater. Sci.* **2005**, *40*, 725.
[35] Lee, S.-H.; Park, Y.-O. *Fuel Process. Technol.* **2003**, *84*, 197.
[36] His, H.-C.; Rood, M. J.; Rostam-Abadi, M.; Chen, S.; Chang, R. *J. Environ. Eng.* **2002**, *128*, 1080.